

**INHIBITION OF HEPATITIS B VIRUS
REPLICATION USING SYNTHETIC
ANTIVIRAL RNA INTERFERENCE
ACTIVATORS**

Musa Donald Marimani

A thesis submitted to the Faculty of Health Sciences, University of the Witwatersrand in
fulfilment of the requirements for the degree of Doctor of Philosophy.

Johannesburg 2016

DECLARATION

I, Musa Donald Marimani declare that this thesis is my own work. It is being submitted for the degree of Doctor of Philosophy in the University of the Witwatersrand, Johannesburg. It was not submitted before for any degree or examination at this or any other University.

.....

25 May 2016

DEDICATION

This work is dedicated to members of the Marimani family (Khoza clan) of the Shangaan nation and my friends:

UMagudu lowo kade bamtsho abeNguni bathi:

uMagudu uyakhanya,

ngoba waqinisa inkanyezi ya khanyisa intaba kaMagudu.

Makhonkotha ebusuku, kuvuka abathakathi,

ngoba engu Mabona.

Mabona kude owabona impi igqamuka, ngaphesheya komfula eNkomazi.

Umude kodwa kawumdaka, unjenge zinhlanga zamabele,

uyakhalipha, ngoba usika hlangothi zombili,

njengo mkhonto waseChaimite.

Mlotshwa, Mkhathini, Mlilo, Mabona, Nomageja,

Sokhabase, Skotana, Ntshamase, Ndlandla!

Ripanga raku xeka homu rixeka MaKhosa.

Magudu, Phukwani, tinhlanga ta mavele enkanyini.

Hi vaka Marimani, hi vaka Magigwana, hi vaka Magudu, hi vaka Mavona, hi vaka Khosa.

Hi vaka ntsanda ava tluli, ku tlula Khosa a vonaka. Anga Mavona na Magigwana.

Vaku: Mangatlu ava hungeli, va hungela tuva xingana vutoya. Hi swigwigwigwigwi vafa

vatele! I Maputukezi, vaku: *Obrigado Magigwana, aluta continua, Saudação lenda*

Shangaan! I nghundu ya Magigwana ya ku phazamisa Maputukezi ka Gaza. Wena waka

mkhonto awu goveki, ku goveka xibamu xa Maputukezi. EBileni ka Masiya byi virile. Ka

Magudu eXinavana enkanyini, incambala ya Mavona eKhoseni! Hi vahloti vaku dlaya

tinghala hi thlarhi. UMabona omuhle, namehlo akhe. Lawo khanya nok` bona

ebum`nyameni.

Marimani! Khoza!

Mabona! Khoza!

LIST OF PUBLICATIONS AND PRESENTATIONS

Publications:

1. Jolanta Brzezinska, Jennifer D'Onofrio, Maximilian C.R. Buff, Justin Hean, Abdullah Ely, Musa Marimani, Patrick Arbuthnot, Joachim W. Engels (2012). **Synthesis of 2'-O-guanidinopropyl-modified nucleoside phosphoramidites and their incorporation into siRNAs targeting hepatitis B virus.** *Bioorganic and Medicinal Chemistry* **20**: 1594–1606.
2. Musa D. Marimani, Abdullah Ely, Maximilian C.R. Buff, Stefan Bernhardt, Joachim W. Engels, Patrick Arbuthnot (2013). **Inhibition of hepatitis B virus replication in cultured cells and *in vivo* using 2'-O-guanidinopropyl modified siRNAs.** *Bioorganic and Medicinal Chemistry* **21**: 6145-6155.
3. Musa Marimani, Justin Hean, Kristie Bloom, Abdullah Ely and Patrick Arbuthnot (2013). **Recent advances in developing nucleic acid-based HBV therapy.** *Future Microbiology* **8** (11): 1489-1504 (Invited Review).
4. Maximillian C.R Buff, Stefan Bernhardt, Musa D. Marimani, Abdullah Ely, Joachim W. Engels, Patrick Arbuthnot (2015). **Use of Guanidinopropyl-Modified siRNAs to Silence Gene Expression.** *Methods in Molecular Biology* **1218**: 217-249 (Invited paper).

List of publications and presentations

5. Musa D. Marimani, Abdullah Ely, Maximillian C.R Buff, Stefan Bernhardt, Joachim W. Engels, Daniel Scherman, Virginie Escriou, Patrick Arbuthnot (2015). **Inhibition of replication of hepatitis B virus in transgenic mice following administration of hepatotropic lipoplexes containing guanidinopropyl-modified siRNAs.** *Journal of Controlled Release* **209**: 198-206.

Presentations:

1. **University of the Witwatersrand Biennial Health Sciences Research day and Postgraduate Expo**, 17 September 2014, Wits University, Johannesburg, South Africa. *Poster: Musa D. Marimani, Abdullah Ely, Maximilian CR. Buff, Stefan Bernhardt, Justin Hean, Joachim Engels and Patrick Arbuthnot. Silencing of hepatitis B virus replication using guanidinopropyl modified siRNAs (MCB-P-18)*
2. **European Society of Gene and Cell Therapy (ESGCT)**, 25-28 October 2013, Palacio Municipal de Congresos, Madrid, Spain. *Poster: Musa D. Marimani, Abdullah Ely, Maximilian CR. Buff, Stefan Bernhardt, Justin Hean, Joachim Engels and Patrick Arbuthnot. Inhibition of hepatitis B virus replication using guanidinopropyl modified siRNAs (P004)*
3. **Department of Molecular Medicine and Haematology Presentation**, 23 October 2013, Departmental Audio-visual Seminar Room, Wits University, Johannesburg, South Africa. *Oral: Musa D. Marimani, Abdullah Ely, Maximilian CR. Buff, Stefan Bernhardt, Justin Hean, Joachim Engels and Patrick Arbuthnot. Inhibition of hepatitis*

List of publications and presentations

B virus replication in cultured cells and in vivo using 2'-O-guanidinopropyl modified siRNAs

4. **Wits 5th Cross-Faculty Postgraduate Symposium**, 01 August 2013, Wits University, Johannesburg, South Africa. *Oral: Musa D. Marimani, Abdullah Ely, Maximilian CR. Buff, Stefan Bernhardt, Justin Hean, Joachim Engels and Patrick Arbuthnot. Inhibition of hepatitis B virus replication in cultured cells and in vivo using 2'-O-guanidinopropyl modified siRNAs*

5. **The Molecular Biosciences Research Thrust (MBRT) Research Day**, 05 December 2012, Wits University, Johannesburg, South Africa. *Poster: Musa D. Marimani, Abdullah Ely, Maximilian CR. Buff, Stefan Bernhardt, Justin Hean, Joachim Engels and Patrick Arbuthnot. Silencing of hepatitis B virus replication in vitro using novel 2'-O-guanidinopropyl modified siRNAs*

6. **Wits 4th Cross-Faculty Postgraduate Symposium**, 19 and 22 October 2012, Wits University, Johannesburg, South Africa. *Poster: Musa D. Marimani, Abdullah Ely, Maximilian CR. Buff, Stefan Bernhardt, Justin Hean, Joachim Engels and Patrick Arbuthnot. The use of 2'-O-guanidinopropyl modified siRNAs to silence hepatitis B virus replication in cultured cells*

7. **International Meeting on Molecular Biology of Hepatitis B Viruses**, 22-25 September 2012, Oxford University, Oxford, England. *Poster: Musa D. Marimani, Abdullah Ely, Maximilian CR. Buff, Stefan Bernhardt, Justin Hean, Joachim Engels*

List of publications and presentations

and Patrick Arbuthnot. Inhibition of hepatitis B virus replication using guanidinopropyl modified siRNAs (P-170)

8. **University of the Witwatersrand Biennial Health Sciences Research day and Postgraduate Expo**, 19 September 2012, Wits University, Johannesburg, South Africa. *Poster: Musa D. Marimani, Abdullah Ely, Maximilian CR. Buff, Stefan Bernhardt, Justin Hean, Joachim Engels and Patrick Arbuthnot. Inhibition of hepatitis B virus replication using guanidinopropyl modified siRNAs*
9. **South African Society of Biochemistry and Molecular Biology (SASBMB)/Federation of African Societies of Biochemistry and Molecular Biology (FASBMB)**, 29 January-01 February 2012, Champagne Sports Resort Drakensberg, South Africa. *Poster: Musa D. Marimani, Abdullah Ely, Maximilian CR. Buff, Stefan Bernhardt, Justin Hean, Joachim Engels and Patrick Arbuthnot. Inhibition of hepatitis B virus replication using synthetic anti-viral RNA interference activators*
10. **Molecular Biosciences Research Thrust (MBRT) Research Day**, 07 December 2011, Wits University, Johannesburg, South Africa. *Poster: Musa D. Marimani, Abdullah Ely, Maximilian CR. Buff, Stefan Bernhardt, Justin Hean, Joachim Engels and Patrick Arbuthnot. Silencing of hepatitis B virus replication using 2'-O-guanidinopropyl modified siRNAs*

ABSTRACT

Chronic liver infection by hepatitis B virus (HBV) may lead to devastating clinical conditions that include hepatocellular carcinoma and cirrhosis. Approved antiHBV drugs do not completely eradicate the infection, leading to continued viral persistence in infected individuals. Inhibition of HBV replication using synthetic activators of RNA interference (RNAi) may provide a feasible strategy of developing superior antiviral drugs. The aim of this study was to evaluate the therapeutic utility of novel 2'-*O*-guanidinopropyl (GP) modified synthetic small interfering RNAs (siRNAs) to counter HBV replication in cultured mammalian cells and mice. Initially, single GP moieties were placed at different nucleotide positions of the guide strand of a potent antiHBV siRNA. Some GP-modified siRNAs enhanced antiHBV activity *in vitro* following transient transfection of Human hepatoma 7 (Huh7) cells with siRNAs and pCH-9/3091, a replication competent HBV target plasmid. These siRNAs inhibited the secretion of Hepatitis B surface antigen (HBsAg) by up to 95% in Huh7 cells. The level of knockdown exhibited by some modified siRNAs was statistically significant relative to that displayed by unmodified siRNA3 which achieved HBsAg silencing of 73%. Additionally, modified siRNAs were also capable of reducing RNA containing the X sequence *in vitro* by 88-93%. Impressively, some of these knockdown levels were statistically significant when compared to unmodified siRNA3, which achieved *HBx* knockdown of 83%. Quantitation of interferon (IFN) response genes by reverse transcription quantitative polymerase chain reaction (RT-qPCR) and evaluation of cell viability by 3-(4,5-Dimethylthiazol-2-yl)-2,5-diphenyltetrazolium bromide (MTT) assay revealed no evidence of innate immune stimulation or cytotoxicity in cultured cells, respectively.

Abstract

Modified siRNAs also displayed moderate stability in 80% foetal calf serum (FCS). Target specificity was markedly improved by GP-modified siRNAs, especially those with seed modifications (comprising nucleotide position 2 to 8 from the 5' end of the guide strand). The siRNA-mediated mRNA cleavage product was detected from transfected cells using 5' Rapid Amplification of cDNA ends (5' RACE).

In the hydrodynamic mouse model, co-injection of GP-modified siRNAs and HBV plasmid vector led to HBsAg suppression of approximately 80-92% at day 3 and 77-96% at day 5 post-administration. The HBV knockdown levels observed at day 3 were statistically significant when compared to those displayed by unmodified siRNA3 which achieved HBsAg silencing of 58% during the same time frame. Furthermore, both sets of siRNAs also suppressed the number of circulating viral particle equivalents (VPEs) by 88-90% at day 3 post-injection. HBV silencing efficacy of 70-75% and 65% was achieved by modified and unmodified siRNAs, respectively at day 5 post-administration.

Finally, antiHBV efficacy of GP-modified siRNAs was tested in HBV transgenic mice following delivery of these RNAi effectors using cationic polyglutamate (PG) adjuvant liposomes. Both groups of antiHBV siRNAs effected HBsAg knockdown that ranged from 70-86% at day 3 to 7 post-administration as siRNA lipoplexes in HBV transgenic mice. In contrast to the unmodified siRNA3, GP-containing siRNAs achieved durable HBsAg silencing of 70% at day 14 post-administration, while the unmodified siRNA3 displayed a shorter duration of activity. As with HBsAg data, the GP-modified siRNAs also displayed

Abstract

silencing efficacy that was similar to the unmodified siRNA, reducing the number of circulating VPEs by 95% from day 3 to 7 post-injection. However, the unmodified siRNA3 lost efficacy by day 14 post-administration, while the GP-modified siRNAs displayed prolonged suppression by reducing the number of circulating VPEs by 75% during the same time interval. Intrahepatic RNA levels were also assessed in transgenic mice, in which GP3 siRNA3 significantly suppressed *surface* and *core* RNA levels by 40 and 42%, respectively at day 18 post-injection. The unmodified siRNA3 suppressed *surface* RNA levels by 20% and *core* RNA levels by 25% at day 21 post-administration. Furthermore, GP4 siRNA3 silenced both *surface* and *core* RNA levels by 42% during the same time period. Additionally, intrahepatic RNA quantitation revealed no induction of IFN response genes by either unmodified or GP-modified siRNAs. In contrast to mice that had received GP-modified siRNAs, significant induction of proinflammatory cytokine release was observed in mice treated with unmodified siRNAs. The siRNA-mediated mRNA cleavage product was also detected from liver samples following 5' RACE analysis. Neither GP-modified nor unmodified siRNAs significantly induced toxicity in injected mice. Collectively, our data provide evidence that utilisation of GP-modified siRNAs and an efficient hepatotropic non-viral delivery system may be used as a strategy to counter chronic HBV infection.

ACKNOWLEDGEMENTS

1. I am grateful to my supervisors Prof. Arbuthnot and Dr. Ely for their supervision, patience and visionary leadership.
2. I thankfully acknowledge Prof. Engels and his team for provision of GP-modified siRNAs.
3. I am grateful to Prof. Daniel Scherman and his team for providing the polyglutamate (PG) adjuvant liposomes used for animal studies.
4. I greatly acknowledge Drs Betty Mowa and Carol Crowther for assisting with animal studies.
5. I thankfully acknowledge Ms Patti Kay and Ms Pam Sharp for assisting with flow cytometry and confocal microscopy experiments, respectively.
6. Finally, I am very grateful to the following funding bodies: the National Research Foundation (NRF) of South Africa, the Poliomyelitis Research Foundation (PRF), the Ernst & Ethel Eriksen Trust, as well as the Health and Welfare Sector Education and Training Authority (HWSETA).

TABLE OF CONTENTS

DECLARATION.....	ii
DEDICATION	iii
LIST OF PUBLICATIONS AND PRESENTATIONS	iv
Publications:	iv
Presentations:.....	v
ABSTRACT	viii
ACKNOWLEDGEMENTS	xi
TABLE OF CONTENTS	xii
LIST OF FIGURES	xvi
LIST OF TABLES	xvii
LIST OF ABBREVIATIONS	xviii
LIST OF SYMBOLS.....	xxv
Chapter 1: Introduction and literature review.....	1
1.1. Hepatitis B virus prevalence, transmission and geographical distribution.....	1
1.2. Biology and replication of HBV.....	3
1.3. Current HBV prevention and treatment	9
1.4. RNA interference.....	12
1.5. Expressed RNAi activators.....	15

Table of contents

1.6. Synthetic activators of RNAi and chemical modification of siRNAs	16
1.7. Delivery methods.....	23
1.7.1. Viral delivery methods	23
1.7.2. Non-viral delivery methods	24
1.8. Aims and objectives:	32
Chapter 2: Materials and methods	34
Chapter 3: Recent advances in developing nucleic acid-based HBV therapy.....	35
Chapter 4: Inhibition of hepatitis B virus replication in cultured cells and <i>in vivo</i> using 2'- O-guanidinopropyl modified siRNAs.....	36
Supplementary methods.....	37
4.1. Transfections and antiHBV activity of GP-modified siRNAs <i>in vitro</i> by ELISA and Dual-luciferase assays.....	37
4.2. Assessment of innate immune stimulation of antiHBV siRNAs <i>in vitro</i>	39
4.3. AntiHBV effects of unmodified and GP-modified siRNAs in a hydrodynamic mouse model.....	41
Chapter 5: Inhibition of replication of hepatitis B virus in transgenic mice following administration of hepatotropic lipoplexes containing guanidinopropyl-modified siRNAs.....	43
Supplementary methods.....	44

Table of contents

5.1. Characterisation and biodistribution of PG adjuvant-siRNA lipoplexes in HBV transgenic mice.....	44
5.2. AntiHBV effects and toxicity of PG adjuvant-siRNA lipoplexes in HBV transgenic mice.....	46
5.3. Innate immune stimulation of PG adjuvant-siRNA lipoplexes in HBV transgenic mice.....	49
5.4. Detection of siRNA-mediated mRNA cleavage <i>in vivo</i> by 5' RACE.....	51
5.4.1. Ligation of RNA to GeneRacer™ RNA Oligo.....	51
5.4.2. Reverse transcription of ligated RNA.....	52
5.4.3. Amplification of cDNA by 5' RACE-PCR, cloning and DNA sequencing..	53
Chapter 6: General discussion and conclusion.....	57
Chapter 7: Appendix.....	64
7.1. Animal Ethics Clearance Certificate.....	64
7.2. Particle sizing and zeta potential of siRNA-lipoplexes.....	65
7.2.1. Particle sizing of siRNA3-lipoplexes.....	65
7.2.2. Zeta potential of siRNA3-lipoplexes.....	66
7.2.3. Particle sizing of GP3 siRNA3-lipoplexes.....	67
7.2.4. Zeta potential of GP3 siRNA3-lipoplexes.....	68

Table of contents

7.3. Detection of siRNA-mediated mRNA cleavage product in cultured cells by 5' RACE.....	69
7.3.1. Detection of cleavage product by 5' RACE-PCR and DNA sequencing.....	69
7.3.2. Representative sequencing data of siRNA samples used for the 5' RACE experiment <i>in vitro</i>	70
7.4. Detection of siRNA-mediated mRNA cleavage in mice by 5' RACE.....	74
7.4.1. Detection of cleavage product by 5' RACE-PCR and DNA sequencing.....	74
7.4.2. Representative sequencing data of siRNA samples used for 5' RACE experiment <i>in vivo</i>	75
7.5. List of publications.....	76
Supplementary methods.....	77
7.5.1. Detection of siRNA-mediated HBV cleavage by 5' RACE.....	77
7.5.1.1. Generation of positive control for 5' RACE.....	77
7.5.1.2. Preparation of <i>in vitro</i> transcribed RNA.....	78
7.5.1.3. Detection of siRNA-mediated mRNA cleavage product <i>in vitro</i> by 5' RACE.....	79
7.5.1.4. Amplification of cDNA by 5' RACE-PCR, cloning and DNA sequencing.....	80
Chapter 8: References.....	84

LIST OF FIGURES

Figure 1.1. Genome organisation of HBV.....	5
Figure 1.2. HBV replication cycle.....	8
Figure 1.3. Schematic representation of the RNAi mechanism	14
Figure 1.4. Graphical representation of the siRNA molecule	20
Figure 7.2.1. Particle sizing of PG adjuvant-siRNA3 lipoplexes.....	65
Figure 7.2.2. Zeta potential of PG adjuvant-siRNA3 lipoplexes.....	66
Figure 7.2.3. Particle sizing of PG adjuvant-GP3 siRNA3 lipoplexes.....	67
Figure 7.2.4. Zeta potential of PG adjuvant-GP3 siRNA lipoplexes.....	68
Figure 7.3.1. Detection of siRNA-mediated mRNA cleavage product <i>in vitro</i>	69
Figure 7.4.1. Detection of siRNA-mediated mRNA cleavage product <i>in vivo</i>	74
Figure 7.5A. Generation of positive control for 5' RACE.....	82
Figure 7.5B. Preparation of <i>in vitro</i> transcribed RNA.....	83

LIST OF TABLES

Table 5.1: Experimental groups used for assessing biodistribution of siRNAs in HBV transgenic mice.....	45
Table 5.2: Experimental groups used for assessing activity and toxicity of siRNAs in transgenic mice.....	46
Table 5.3: Experimental groups used for assessing immunostimulatory effects of siRNAs in transgenic mice.....	50
Table 7.1: The siRNAs employed for 5' RACE analysis <i>in vitro</i>	80

LIST OF ABBREVIATIONS

2'-F	-	2'-fluoro
2'-O-Me	-	2'-O-methyl
2'-O-MOE	-	2'-methoxyethyl
5' RACE	-	5' Rapid Amplification of cDNA ends
A	-	Adenosine
AAV	-	Adeno-associated virus
Ad	-	Adenovirus
ALT	-	Alanine aminotransferase
ANA	-	Altritol
AP	-	2'-O-aminopropyl
ASGPr	-	Asialoglycoprotein receptor
AST	-	Aspartate transaminase
BCP	-	Basic core promoter
C	-	Cytidine
CBA	-	Cytometric bead array
cccDNA	-	Covalently closed circular DNA
CPG	-	Controlled-pore-glass

List of Abbreviations

CRISPR	-	Clustered regularly interspaced short palindromic repeat
DAPI	-	4',6-diamidino-2-phenylindole
DC-Chol	-	3 β -[N(N',N'-Dimethylaminoethane) carbamoyl cholesterol]
DEPC	-	Diethylpyrocarbonate
DGCR8	-	DiGeorge syndrome critical region gene 8
DLS	-	Dynamic Light Scattering
DMAPAP	-	2-{3-[Bis-(3-amino-propyl)-amino]-propylamino}-N-dite- tracylcarbamoyl methyl-acetamide
DMEM	-	Dulbecco's modified Eagle medium
DOPE	-	1,2-dioleoyl-sn-Glycero-3-Phosphoethanolamine
DPC	-	Dynamic PolyConjugate
DR1	-	Direct repeat1
DR2	-	Direct repeat2
DTBS	-	Di-tert-butylsilanediyl
EDTA	-	Ethylenediaminetetraacetic acid
EGS	-	External guide sequence
ELISA	-	Enzyme-Linked Immunosorbent Assay
ERI1	-	3'-5' exoribonuclease 1

List of Abbreviations

ESI	-	Electrospray ionisation
F7	-	Factor VII
FCS	-	Foetal calf serum
G	-	Guanosine
GALA	-	Glutamic acid-alanine-leucine-alanine
GAPDH	-	Glyceraldehyde 3-phosphate dehydrogenase
GP	-	2'- <i>O</i> -guanidinopropyl
HA2	-	Haemagglutinin subunit 2
HBcAg	-	Hepatitis B core antigen
HBeAg	-	Hepatitis B e antigen
HBIG	-	Hepatitis B immune globulin
HBsAg	-	Hepatitis B surface antigen
HBV	-	Hepatitis B virus
HBx	-	Hepatitis B X protein
<i>HBx</i> sequence	-	Sequence that codes for HBx
HCC	-	Hepatocellular carcinoma
HD Ad	-	Helper-dependent adenovirus
HDI	-	Hydrodynamic dynamic injection

List of Abbreviations

HDR	-	Homology directed repair
HEK293	-	Human Embryonic Kidney 293
HIV	-	Human immunodeficiency virus
HPLC	-	High performance liquid chromatography
HRMS	-	High resolution-mass spectrometry
Huh7	-	Human hepatoma 7
IFIT1	-	Interferon-induced protein with tetratricopeptide repeats 1
IFN	-	Interferon
IL	-	Interleukin
IPTG	-	Isopropyl β -D-1-thiogalactopyranoside
LAR II	-	Luciferase Assay Reagent II
LNA	-	Locked nucleic acid
LV	-	Lentivirus
MALDI	-	Matrix-assisted laser desorption ionisation
MCP-1	-	Monocyte Chemoattractant Protein-1
miRNA	-	microRNA
MS	-	Mass spectrometry
MTT	-	3-(4,5-Dimethylthiazol-2-yl)-2,5-diphenyltetrazolium bromide
NAG-MLP	-	<i>N</i> -acetylgalactosamine-conjugated melittin-like peptide

List of Abbreviations

NHEJ	-	Non-homologous end joining
NMR	-	Nuclear magnetic resonance
NTCP	-	Sodium taurocholate cotransporting polypeptide
OAS-1	-	Oligoadenylate synthetase-1
ORF	-	Open reading frame
PE	-	Phycoerythrin
PEG	-	Polyethylene glycol
PG	-	Polyglutamate
pgRNA	-	Pre-genomic RNA
Pol	-	Polymerase
PEI	-	Polyethyleneimine
Poly(I:C)	-	Polyinosinic:polycytidylic acid
Pre-miRNA	-	Precursor miRNA
Pri-miRNA	-	Primary miRNA
qPCR	-	Quantitative polymerase chain reaction
rcDNA	-	Relaxed circular DNA
RGEN	-	RNA-guided endonuclease
RISC	-	RNA Induced Silencing Complex

List of Abbreviations

RLM-RACE	-	RNA ligase-mediated amplification of cDNA ends
RNAi	-	RNA interference
RT-qPCR	-	Reverse transcription quantitative polymerase chain reaction
S	-	Surface
SCID	-	Severe combined immunodeficiency
SDS	-	Sodium dodecyl sulphate
shRNA	-	Short hairpin RNA
siRNA	-	Synthetic small interfering RNA
SNALP	-	Stable nucleic acid lipid particle
TALEN	-	Transcription-activator-like effector nuclease
TIPS	-	1,1,3,3-tetraisopropylidisiloxane-1,3-diyl
TLC	-	Thin layer chromatography
TLR	-	Toll-like receptor
TNF	-	Tumour Necrosis Factor
TPS	-	2,4,6-triisopropylbenzenesulfonyl
TRBP	-	Transactivation response RNA binding protein
Tris	-	Tris(hydroxymethyl)aminomethane
U	-	Uridine
UNA	-	Unlocked nucleic acid

List of Abbreviations

uPA-SCID	-	Urokinase plasminogen activator-severe combined immunodeficiency
VPE	-	Viral particle equivalent
X-gal	-	5-bromo-4-chloro-3-indolyl- β -D-galactopyranoside
YMDD	-	Tyrosine-methionine-aspartate-aspartate
ZFN	-	Zinc finger nuclease
ZFP	-	Zinc finger protein

LIST OF SYMBOLS

α	-	Alpha
β	-	Beta
γ	-	Gamma
Δ	-	Delta
ε	-	Epsilon
ζ	-	Zeta

Chapter 1: Introduction and literature review

1.1. Hepatitis B virus prevalence, transmission and geographical distribution

Hepatitis B virus (HBV) is a member of the viral family called *Hepadnaviridae* [1]. This family consists of partially double-stranded DNA viruses capable of infecting the liver of humans [2-4], woodchucks [5], woolly monkeys [6, 7], ducks [8], herons [9] and other animals. Specifically, members of this family infect the liver resulting in chronic or acute liver infection. A patient's acute or chronic HBV state depends mainly on HBV virulence factors and host immune competence [10-14]. Approximately 240 million people worldwide are infected with chronic HBV and a large number of these individuals die annually due to liver complications (<http://www.who.int/mediacentre/factsheets/fs204/en/>). In most adults, acute HBV infection does not usually require treatment as the infection is cleared spontaneously [15]. However, individuals who acquire infection at a young age have a greater risk of developing devastating liver complications [16, 17]. These include hepatocellular carcinoma (HCC) and cirrhosis [18, 19] and the majority of chronically infected individuals are located in East Asia and sub-Saharan Africa (<http://www.who.int/mediacentre/factsheets/fs204/en/>).

In Black Africans, the asymptomatic stage is established during the early years of life [20] and rarely persists until adulthood. As a result, an estimated 1-14% of the adult population remain positive for Hepatitis B e antigen (HBeAg), an indicator of active HBV replication

Chapter 1

in infected individuals. Conversely, about 40% of the Chinese population remain HBeAg-positive during early adulthood [21]. The asymptomatic phase is characterised by absence or low detection of markers of HBV replication and acute inflammation [22]. An increase in the levels of liver enzymes such as alanine aminotransferase (ALT) [22, 23] and aspartate transaminase (AST) [22] may be observed from the necrotic hepatocytes. The virus may be spread from mother to child from about 28 weeks of gestation up to 7 days after birth (perinatal transmission) [24], contact with an infected individual (horizontal transmission) [25], exposure to contaminated blood products or infected fluids (parenteral transmission) [26] or by sexual contact [27]. A patient is described as having chronic HBV infection when hepatitis B surface antigen (HBsAg, an indicator of recent HBV infection) remains detectable in the serum for more than six months.

To date, ten genotypes of HBV have been described. Global distribution of these genotypes is as follows: genotype A is mainly found in central, eastern and southern Africa (reviewed in [28]), genotypes B and C are dominant in Asia [29], D is common in northern Africa, E is widespread in western Africa [29], F is the dominant genotype in Alaska, El Salvador and parts of South America (reviewed in [30]), G is widespread in France, Germany and the United States [29], H dominates central and South America, I has been commonly identified in Laos and Vietnam, while J has been reported in the Ryukyu islands in Japan [29]. Furthermore, subgenotypes have been identified within genotypes A-D, F and I. Coinfections also exist in countries where two different HBV genotypes are prevalent (reviewed in [28]). In countries like Cameroon and Nigeria coinfection with genotypes A and E have been observed in HIV positive patients [31].

Sequence analysis of African genotype A strains revealed that many isolates in this group belong to subgenotype A1 (reviewed in [28]). This HBV subgenotype is prevalent in eastern and southern Africa and includes countries such as Somalia, Tanzania, Democratic Republic of Congo, Uganda, Malawi and South Africa (reviewed in [28]).

1.2. Biology and replication of HBV

HBV consists of a circular, partially double-stranded DNA genome [32] (Fig. 1.1) and replicates in the liver to cause hepatitis B infection [33]. HBV has a compact genome that is composed of a relaxed circular DNA (rcDNA). This rcDNA is produced following reverse transcription of a pre-genomic RNA (pgRNA) replication intermediate [34-36]. In infected hepatocytes, the rcDNA is repaired to produce covalently closed circular DNA (cccDNA). The cccDNA is important for the transcription of viral RNAs, production of pgRNA and is also essential for HBV replication and persistence [32, 37].

The genome of HBV has four overlapping open reading frames (ORFs) namely *precore/core*, *surface* (composed of *pre-S2*, *pre-S1* and *S*), *polymerase (Pol)* and *hepatitis B x (HBx)* [32]. The four RNAs code for seven viral proteins: polymerase, core, Hepatitis B core antigen (HBcAg), HBx and three surface (*pre-S1*, *pre-S2* and *S*) proteins. Viral gene expression is controlled by four separate promoters: the basic core promoter (BCP), *pre-S1*, *pre-S2* and X promoters (Fig. 1.1). In addition to the four promoters, transcription is also controlled by three *cis*-elements, namely: the negative regulatory element, Enhancer

Chapter 1

I and Enhancer II elements. The negative regulatory element is situated upstream of the BCP and serves as an antagonist of BCP function [38]. Enhancer I domain is situated between the X promoter region and S ORF and is involved in recruiting liver-specific transcription factors [39, 40]. Enhancer II overlaps the BCP region and functions in conjunction with the Enhancer I domain to activate transcription in differentiated liver cells [41].

The pgRNA codes for core and polymerase. The *pre C* RNA has the same nucleotide sequence as the pgRNA, but its 5' end is longer compared to pgRNA [42, 43] and codes for precore/core protein. The *precore/core* gene codes for HBeAg [44]. The HBeAg is produced by liver cells following HBV infection [45]. The upstream start codon of *pre C* sequence results in the incorporation of a secretory signal peptide in the synthesised protein. This secreted HBeAg has a different processing mechanism to that of the HBcAg, which remains in the cytoplasm and forms the viral capsid [46, 47]. Additionally, both these viral antigens are transcribed from the same ORF. The X and *Pol* genes code for HBx and polymerase proteins, respectively. The X protein has been shown to act as a transactivator [48] and is also thought to be involved in cell proliferation [49] and HBV replication in liver cells [49, 50]. The *surface* ORF comprises *pre-S1* and *pre-S2* genes. *pre-S1* codes for the large surface protein, while *pre-S2* codes for the middle and major surface proteins [51]. Collectively, these surface proteins are crucial in the generation of new viral envelopes which protect the nucleocapsid.

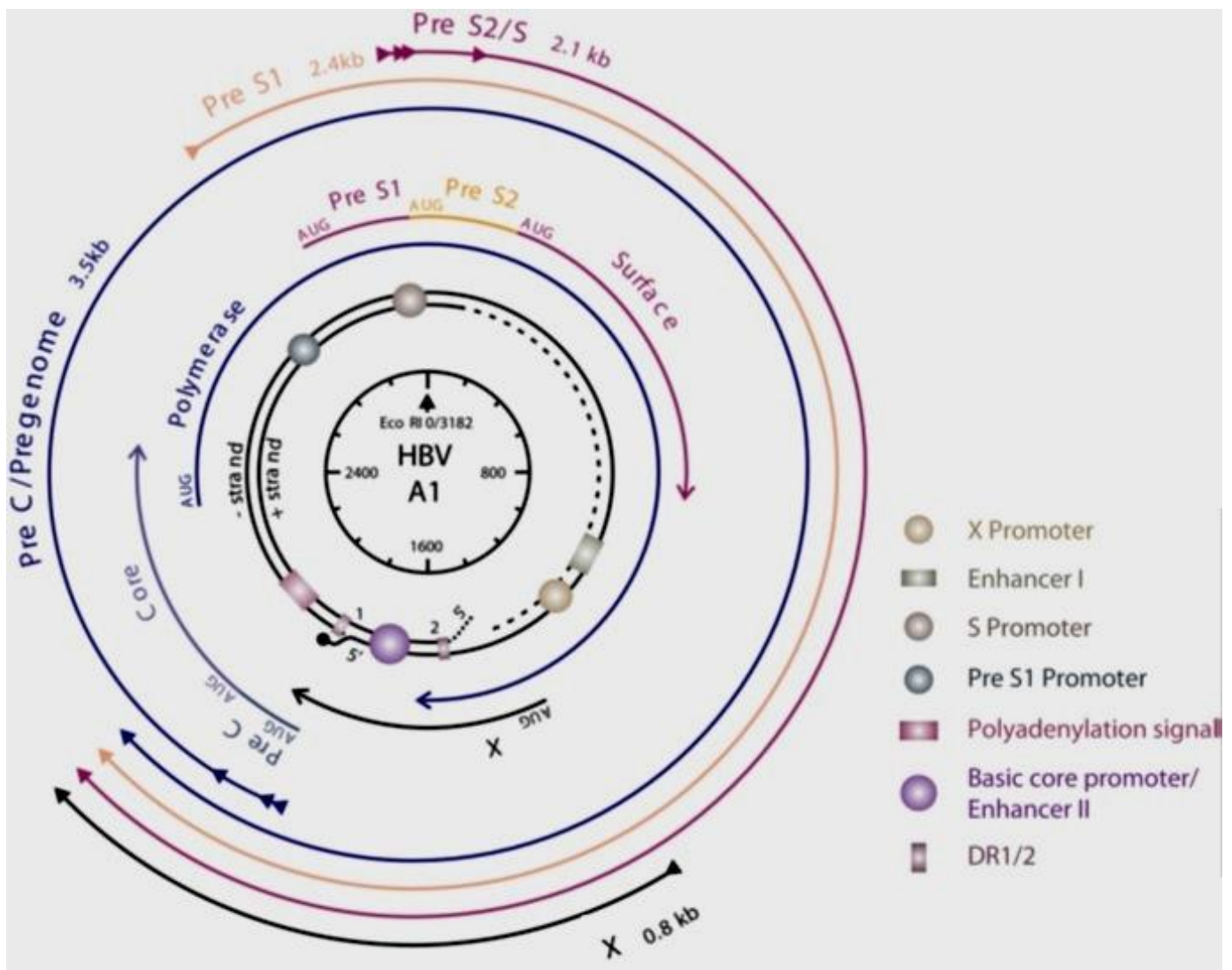


Figure 1.1. Genome organisation of HBV

HBV consists of a circular, partially double-stranded DNA genome. In infected hepatocytes, the rcDNA is produced following reverse transcription of pgRNA, shown in the middle of the circular genome map. The four viral RNAs are depicted by outermost arrows, and code for polymerase, core, HBx, HBcAg and surface proteins. The inner arrows represent ORFs; position of regulatory elements is depicted by rectangles, while circles indicate location of promoters within the viral genome. This diagram has been adapted from Moolla et al., 2002 [52].

Chapter 1

Although HBV mRNAs are transcribed from different ORFs, they share a single polyadenylation signal situated downstream of the BCP. New infections are as a result of transmission of viral particles that contain the rcDNA. Translation of viral mRNA occurs in the ribosomes to produce precore/core, core, S, Pol and X proteins (Fig. 1.2). The pgRNA is encapsidated into the nucleocapsid and the rcDNA is formed within the viral capsids. Subsequently, each capsid is surrounded by an envelope with large, middle and major surface proteins. The large surface protein has been shown to be essential for receptor binding and production of infectious HBV particles. As a result, liver-specificity of HBV is conferred by the large surface protein [53-56].

Viral entry into host cells is facilitated by attachment of glycosaminoglycan residues of the heparan sulfate proteoglycans to the pre-S region of HBV [57] (Fig. 1.2). The receptor responsible for HBV interaction remained elusive for a long period of time. Recent advancements led to the discovery of a receptor responsible for HBV infection [58, 59]. It has been demonstrated and confirmed that sodium taurocholate cotransporting polypeptide (NTCP) is responsible for viral entry into host hepatocytes [58, 59] by interacting with the pre-S1 surface protein of HBV [58]. The entry step is followed by internalisation of the capsid which may occur via clathrin-mediated endocytosis [60, 61]. In the cytoplasm, the mature capsid containing the rcDNA associates with nucleoporin 153 protein located in the nuclear membrane [62].

The association between the mature capsid and nucleoporin 153 promotes capsid dissociation and facilitates transport of the rcDNA to the nucleus. The pgRNA plays a

Chapter 1

critical role in the synthesis of the viral polymerase enzyme (Fig. 1.2). Viral reverse transcription is initiated by interaction between the polymerase and stem-loop epsilon (ϵ), a structural RNA sequence located near the 5' end of the pgRNA. Binding of viral polymerase to ϵ leads to pgRNA encapsidation [63, 64]. A 3 to 4 base DNA oligonucleotide is produced from the bulge of the epsilon sequence and is subsequently subjected to reverse transcription. A covalent bond links the polymerase to the 5' end of the DNA oligonucleotide. The oligonucleotide is then translocated to the 3' end of the pgRNA. Since a strong covalent bond connects the polymerase to the oligonucleotide, both molecules are translocated to the 3' end of the pgRNA. Polymerase facilitates binding of the oligonucleotide to a complementary sequence located at the 3'-proximal direct repeat1* (DR1*).

Thereafter, the oligonucleotide acts as a primer and reverse transcription of the DNA negative strand progresses [65, 66]. The polymerase degrades most of the pgRNA template by virtue of its RNaseH activity, leaving a short residual 5' capped oligonucleotide. The 5' end of the negative strand is then exchanged for the 3' end to enable circularisation and results in the formation of new rcDNA [65]. The nucleocapsid may be transported to the nucleus, thus, maintaining the cccDNA pool [67] (Fig. 1.2). Alternatively, nucleocapsids may be introduced into the secretory pathway and interact with surface proteins found in the endoplasmic reticulum to be released from the cells as new virions [67].

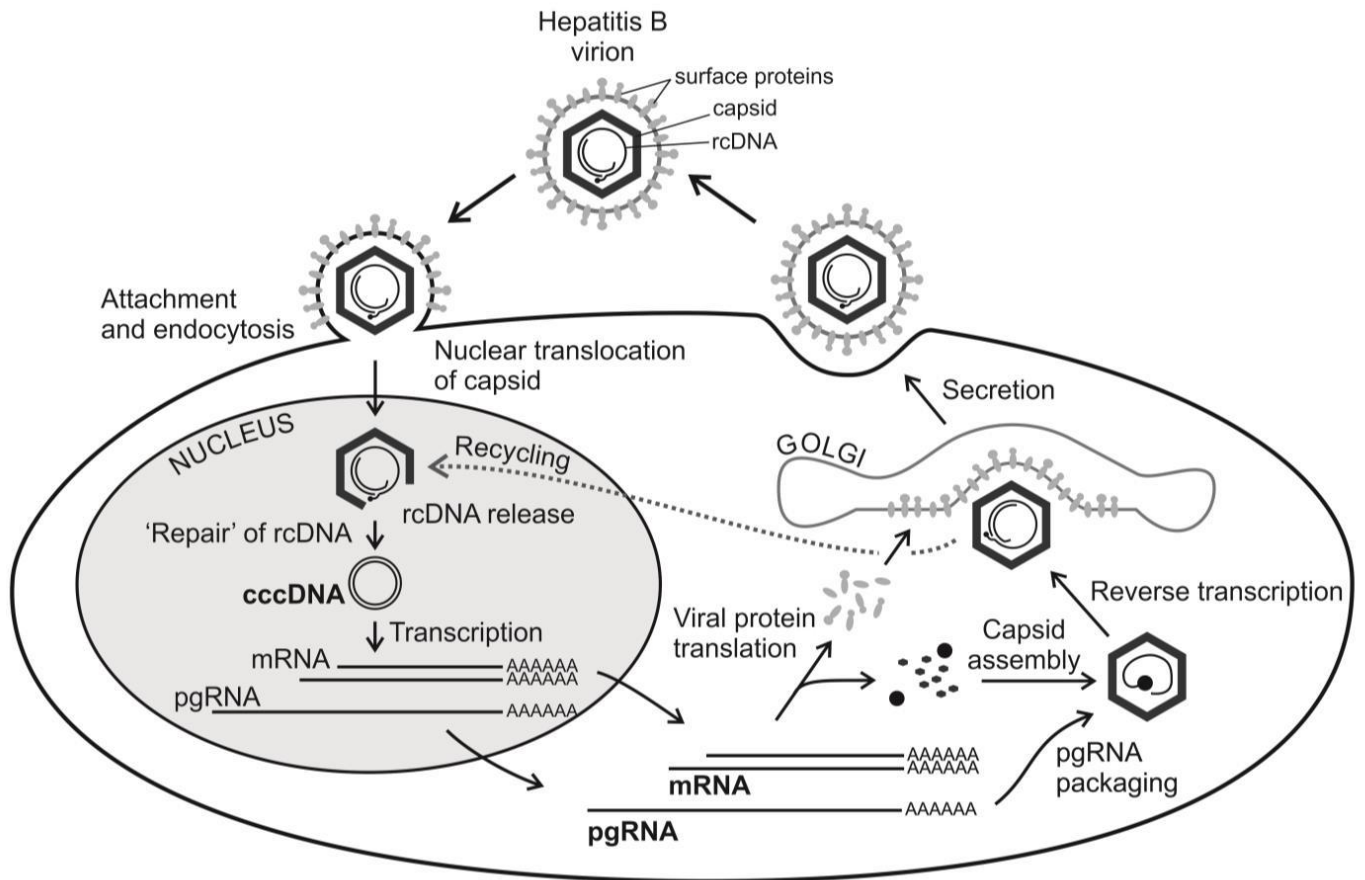


Figure 1.2. HBV replication cycle

The virions recognise and bind to the cell surface receptor. Following infection in target hepatocytes, the rcDNA is repaired to generate cccDNA which is important for viral replication and persistence. Synthesis of viral mRNA occurs in the ribosomes to produce precore/core, core, S, Pol and X proteins, followed by pgRNA encapsidation. The rcDNA is produced after reverse transcription of pgRNA and the resulting nucleocapsids are transported to the endoplasmic reticulum, enveloped and exported from the cell. Alternatively, nucleocapsids may be recycled into the nucleus and converted into cccDNA.

1.3. Current HBV prevention and treatment

A universal and effective HBV vaccine is available and provides protection in about 90-95% of vaccinated individuals [68]. Furthermore, the vaccine may be taken together with hepatitis B immune globulin (HBIG) to inhibit mother to child transmission during gestation and after birth [69]. To date, licensed HBV therapies include nucleotide and nucleoside analogues. These antiHBV chemotherapeutics block the reverse transcription step of viral replication [70] and include drugs such as lamivudine (Epivir), telbivudine (Tyzeka), adefovir (Hepsera), tenofovir (Viread) and entecavir (Baraclude) [71, 72]. Treatment with nucleotide/side chemotherapeutics has generally failed to eliminate HBsAg antigen secretion in infected individuals [73, 74].

Patients are advised to continue taking these analogues for life, as HBV replication may be re-established after stopping treatment [75]. The aim of this treatment regimen is to establish HBsAg seroconversion. Although seroconversion may lead to better prognosis, hepatocellular carcinoma and cirrhosis still pose a greater threat to chronically infected patients [76]. In general, the nucleotide/side drugs have few side effects and prolonged use of these regimens is necessary to sustain viral suppression.

Lamivudine is a reverse transcriptase inhibitor and results in decreased levels of rcDNA and cccDNA being produced [77-79]. Unfortunately, tyrosine-methionine-aspartate-aspartate (YMDD) escape mutants may arise as a result of long-term lamivudine monotherapy, thus, compromising the antiHBV activity of this drug [80].

Chapter 1

Adefovir has also been administered for HBV therapy, but displayed decreased efficacy relative to lamivudine. Moreover, nephrotoxicity has been observed after administering a high dosage of this antiviral agent [81]. Adefovir is capable of achieving effective HBV therapy in strains that are resistant to lamivudine [82, 83] and the number of escape mutants is also decreased [84]. In comparison to lamivudine, entecavir displays improved antiHBV activity [85, 86]. Furthermore, prolonged use of this drug improves liver histology [87, 88] and escape mutants are negligible [87, 89]. Recently approved nucleotide/side drugs for HBV therapy are telbivudine and tenofovir [90, 91]. These agents also display antiHIV activity [92] and may be conveniently used to treat HBV/HIV co-infections [93].

Relative to lamivudine [94, 95] and adefovir [96], telbivudine has superior antiviral efficacy. Unfortunately, administration of this drug is compromised by development of myalgia, drug-induced myopathy and emergence of escape mutants [97, 98]. Tenofovir is the most effective antiviral agent and the drug of choice for HBV monotherapy [99]. To date, escape mutants to tenofovir have not been identified; however, long-term mutational studies are required for detailed analysis. Currently, tenofovir and entecavir are the preferred regimens for chronic HBV therapy because of their superior antiviral efficacy and high barrier to viral resistance. Although these agents are capable of inhibiting HBV replication and improving liver histology, the major limitation is that they are unable to clear established cccDNA pools in chronically infected patients. Moreover, prolonged use of these drugs may lead to viral mutagenesis and HBV rebound is generally observed in patients that stop treatment.

Chapter 1

Furthermore, immunomodulators which act by activating the host immune system to combat infection have also been approved for treating chronic HBV infection. These include interferon alpha (IFN- α), interferon alpha-2a (IFN- α 2a), PEGylated IFN- α 2a, PEGylated IFN- α 2b and interferon beta (IFN- β). Previously, IFN- α and PEGylated IFN- α have been employed for short-term therapy, in which durable viral suppression was achieved in patients with chronic HBV infection [100-103]. However, side-effects were observed and antiHBV activity of immunomodulators depends mainly on the starting HBV viral load, genotype, host immune competence and the extent of liver damage. In a clinical setting, it has been demonstrated that IFN- α displays superior antiviral efficacy in individuals infected with HBV genotype A than genotype C, D, or E [104-106].

Efficacy of immunomodulators is generally unsatisfactory and not advisable for patients with HIV co-infection or cirrhosis [107]. Similarly, the levels of HBsAg seroconversion is also unsatisfactory in patients taking IFN therapeutics, and side effects such as autoimmune diseases and severe flu-like symptoms are common (reviewed in [108]). Although nucleotide/side analogues and immunomodulators can abrogate viral replication, they are unable to completely eradicate cccDNA, thus, allowing viral persistence. Consequently, there is still no effective cure for chronically infected individuals. Licensed therapeutic modalities are unable to convincingly clear chronic HBV infection and relapse is common after treatment withdrawal. Therefore, development of new and effective HBV therapy thus remains a priority.

1.4. RNA interference

RNA interference (RNAi) is a naturally occurring mechanism which regulates target gene expression in various eukaryotic organisms [109-113] (Fig. 1.3). This gene silencing mechanism is activated by primary microRNAs (pri-miRNAs) [114]. Cleavage of pri-miRNAs by the nuclear microprocessor complex comprising Drosha and DiGeorge syndrome critical region gene 8 (DGCR8) produces precursor miRNA (pre-miRNA) hairpins. Subsequently, exportin-5 transports the newly processed pre-miRNA molecules to the cytoplasm and additional processing of these hairpins by Dicer and transactivation response RNA binding protein (TRBP) leads to the formation of microRNAs (miRNAs). These miRNA duplexes are about 23 bp in length and their 3' ends contain 2 nucleotide overhangs. The two miRNA strands are incorporated into the RNA Induced Silencing Complex (RISC). This is followed by selection of one miRNA strand to effect target gene silencing [115] (Fig. 1.3).

The most frequently retained strand by the RISC is known as miRNA, while the less frequently retained strand is called miRNA*. The miRNA serves as the guide strand after incorporation into RISC, while the miRNA* assumes the role of a passenger strand. Similarly, selection of miRNA* by RISC allows it to be the leading strand, while the miRNA serves as a passenger strand. The leading strand is responsible for directing RISC to the target mRNA, while the passenger is removed and has no effect on subsequent RNAi stages. Incomplete base-pairing between target mRNA and guide strand results in translational suppression, while complete base-pairing results in degradation of target

mRNA. When artificial sequences resembling miRNA, pre-miRNA or pri-miRNA (i.e. exogenous RNAi activators) are introduced into a cell, the RNAi pathway is reprogrammed, leading to target gene silencing [116-119] (Fig. 1.3). RNAi-based approaches may be conveniently used to silence HBV replication. This is because HBV has several favourable features that are ideal for RNAi therapy and include:

- The overlapping nature of the ORFs contributes to HBV having a low mutation rate, as opposed to RNA viruses.
- Transcripts produced by viral genes overlap and possess similar 3' sequences that have a single transcription termination signal.
- The pgRNA is involved in the synthesis of rcDNA during reverse transcription and may be a convenient therapeutic target [120].

Consequently, a single RNAi effector molecule can target and silence many viral RNAs simultaneously. A number of HBV target sites have been silenced using expressed [118, 121-123] and synthetic RNAi activators [124-127]. These RNAi activators possess sequences that resemble naturally occurring molecules that participate in the RNAi pathway, thus, enabling them to be introduced into cells to effect target gene silencing.

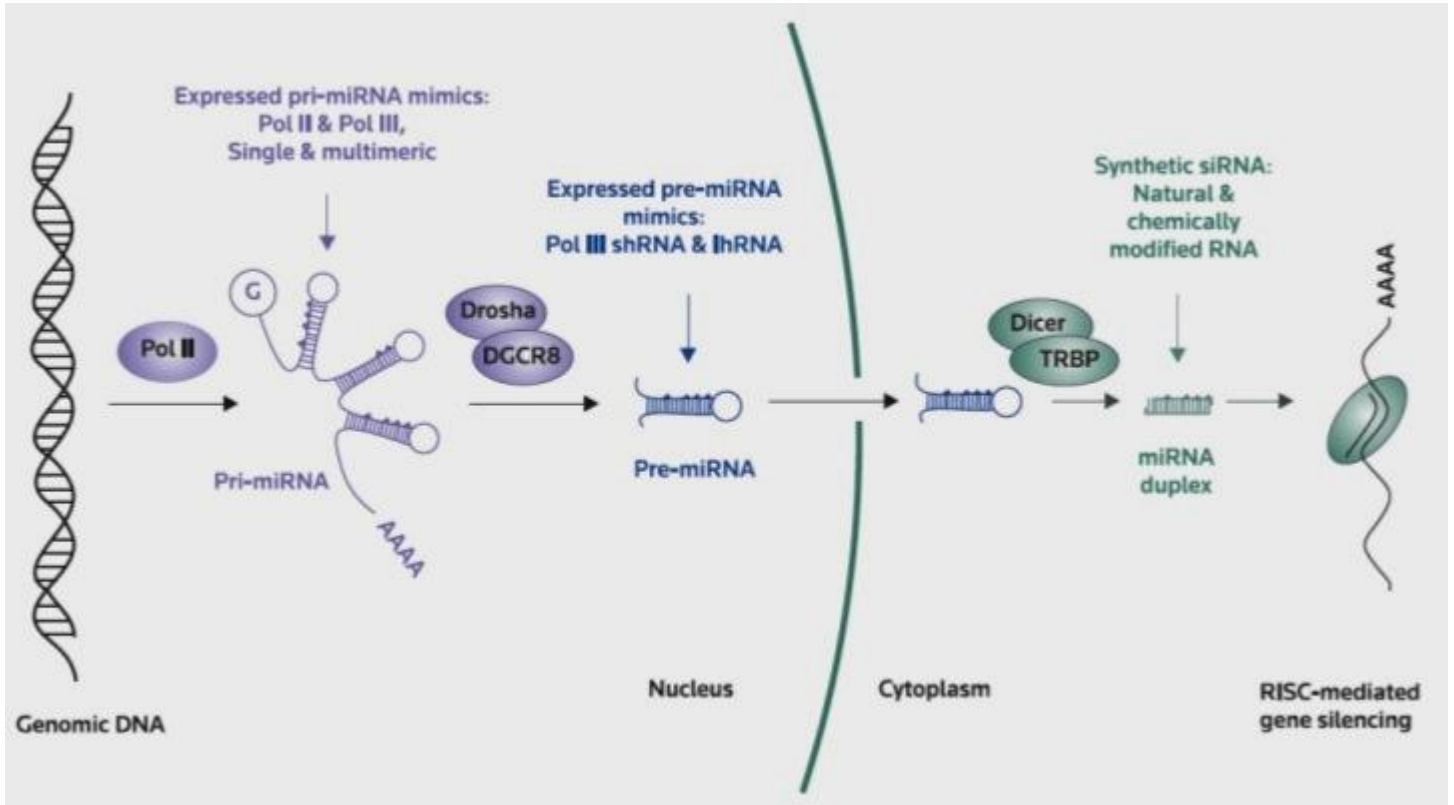


Figure 1.3. Schematic representation of the RNAi mechanism

Pri-miRNAs are processed by the Drosha/DGCR8 complex to form pre-miRNA molecules. Exportin-5 transports the newly processed pre-miRNA molecules to the cytoplasm and additional processing of these hairpins by Dicer and TRBP leads to the formation of miRNAs. The two miRNA strands are incorporated into RISC and the guide strand selected to effect target mRNA degradation or translational suppression. Introduction of exogenous activators of RNAi that resemble miRNA, pre-miRNA or pri-miRNA triggers the RNAi mechanism leading to target gene silencing. Diagrammatic illustration from Arbutnot, 2010 [128].

1.5. Expressed RNAi activators

Expressed RNAi activators are typically transcribed from RNA pol III to produce short hairpin RNA (shRNA) sequences. These sequences resemble pre-miRNA molecules, enabling them to participate in the RNAi pathway leading to target gene silencing. Most studies focusing on the utility of shRNA have mainly employed Pol III transcription regulatory elements, particularly U6 or H1 promoters [123, 129-131]. Advantages of employing these promoters include: (1) the ease of cloning and packaging into delivery systems, owing to their small size, and (2) effective construction of shRNAs may be achieved as the precise position of transcription and termination sites is known [132]. Limitations associated with the use of these promoters include: (1) lack of specificity as Pol III promoters are constitutively expressed in many cell types, (2) the promoters fail to offer spatial control required for the treatment of certain diseases [132], and (3) it is important to optimise the dosage of shRNAs expressed from U6 promoters, as over-expression may result in toxicity from saturation of the endogenous RNAi pathway [133]. As a result, various strategies have been investigated to counter these shortcomings [134-136]. Additionally, studies investigating the advantage of using inducible Pol III promoter systems have also been conducted with the aim of circumventing the undesirable effects associated with the use of Pol III promoters [134, 137-139].

Pol II promoters optimised to achieve moderate shRNA expression levels may also be employed to avoid toxicity associated with the use of powerful Pol III promoters [132, 140]. In contrast to Pol III promoters that are constitutively expressed across many cell

lines, Pol II promoters may be tissue specific [141]. The utility of Pol II promoters that express pri-miRNAs has also been investigated. This led to generation of effective pri-miRNAs being expressed from Pol II promoters. These therapeutic agents have subsequently been employed to target and suppress HBV replication [121, 142]. Since some pri-miRNAs are polycistronic, exogenous pri-miRNA mimics that are polycistronic have been evaluated [118]. Additionally, polycistronic expression has been achieved by a single Pol II [141] or Pol III promoter when interfering RNAs were designed to mimic miRNAs [131]. In some instances, multimerisation of these therapeutic agents allows simultaneous silencing of different HBV sites. This increases antiHBV efficacy and minimises the emergence of viral escape mutants [131, 132, 141, 142]. Importantly, treatment of chronic HBV infection necessitates prolonged half-life of the therapeutic agents to achieve a sustained antiHBV effect. Therefore, stable DNA templates encoding RNAi expression cassettes may be used to achieve durable antiHBV activity [143], a characteristic which is often lacking when using synthetic RNAi activators to achieve target gene knockdown.

1.6. Synthetic activators of RNAi and chemical modification of siRNAs

Synthetic RNAi activators have been explored for their ability to target and suppress replication of HBV in cell culture and *in vivo* [144-147]. Synthetic small interfering RNAs (siRNAs) are composed of RNA duplexes of approximately 21 bp (Fig. 1.4). Additionally,

these synthetic RNAi activators also possess 2-base 3' overhangs which improve RISC processing and target gene silencing. These features enable them to mimic miRNA duplexes and can then be applied to induce RNAi-based silencing following RISC processing [148]. Factors that contribute to siRNAs being ideal therapeutics for RNAi-based approaches include:

- The siRNA chemical synthesis process and quality control can be easily monitored.
- Dosage may be more easily regulated than with expressed RNAi activators.
- siRNAs may be delivered to mammalian cells using efficient non-viral vectors owing to their small size and cytoplasmic site of action.
- Favourable “drug-like properties” may be conferred to these RNAi effectors by incorporating chemical modifications [149, 150].

Despite these favourable properties, unfavourable qualities that impede therapeutic application of siRNA exist and include: (1) off-targeting effects [151], (2) innate immune stimulation [152, 153], (3) unsatisfactory biodistribution patterns, and (4) susceptibility of siRNAs to degradation by serum nucleases [154]. Improved stability of siRNAs against nuclease degradation results in increased half-life of these RNAi effectors in the circulation, which in turn, promotes sustained target gene silencing. Specificity implies that the administered siRNAs would result in decreased non-specific or off-target effects. Non-specific effects arise when siRNAs target and silence genes other than the gene of interest leading to unintended inactivation of other cellular mRNAs [151, 155, 156]. Immune stimulation may also manifest as a result of off-targeting of siRNAs and is generally

induced by Toll-like receptors (TLRs) e.g. TLR3, TLR7 and TLR8 [157]. These immune receptors function by identifying various RNA molecules and stimulate IFN response genes such as IFN- β , IFN- γ , interferon-induced protein with tetratricopeptide repeats 1 (IFIT1), oligoadenylate synthetase-1 (OAS-1), interleukin 6 (IL-6), IL-10, IL-12p70, monocyte chemoattractant protein-1 (MCP-1) and tumour necrosis factor (TNF). However, innate immune stimulation varies and mainly depends on the nature of the administered RNA and necessitates screening for activation of various IFN genes.

To circumvent the negative attributes associated with siRNA delivery, chemical modification of siRNAs has been employed. Indeed, incorporation of chemical groups into siRNAs generally renders them more potent, specific and stable, thus, improving the therapeutic utility of these RNAi effectors. Interestingly, siRNA specificity and activity have been demonstrated to be markedly enhanced particularly when the chemical groups are incorporated within the seed region (i.e. nucleotide 2 to 8 of the 5' region of the guide strand) (Fig. 1.4) [156, 158, 159]. It is thought that introducing chemical moieties within the siRNA seed region reduces off-target effects by minimising the interaction between RISC and partially complementary sequences [156].

The efficacy with which the seed region hybridises to cellular mRNAs determines target specificity [156] by reducing interaction with incomplete target sequences. Subsequently, this improves target specificity and decreases off-target effects. Off-target effects refer to silencing of genes other than the gene of interest. Therefore, in the application of antiHBV siRNAs, viral RNA is the on-target (i.e. desired target), while the host genes are off-

targets. Incorporation of chemical moieties, particularly at the 2' ribose position, changes the binding and thermodynamic properties of modified siRNAs [160-162]. Subsequently, this improves specificity of these RNAi effectors by minimising interaction between modified siRNAs and partial complementary targets without compromising the therapeutic efficacy of siRNAs [156]. It has been reported that some chemical modifications may decrease hybridisation between modified siRNAs and incomplete targets by reducing the free energy [156, 163] or thermostability of the seed region-mRNA complex [164]. Moreover, chemical modifications also introduce structural alterations to siRNAs. These conformational alterations may influence the efficiency of RISC processing whereby, weak hybridising targets (i.e. partial complementary targets) are removed from the guide strand before cleavage, while strong hybridising targets (i.e. complete complementary targets) are retained and efficiently processed by RISC [156]. Conformational changes and strong hybridisation of chemically modified siRNAs (as opposed to their unmodified counterparts), may also be responsible for improved target gene silencing by allowing efficient processing of modified therapeutic sequences by the RISC machinery [165]. In addition to conformational changes, RISC processing and siRNA efficacy may be markedly improved by introducing chemical groups that enhance recognition of 3' overhangs or alter the thermodynamic stability of siRNAs [166]. A diagram of the siRNA molecule is depicted in Fig. 1.4.

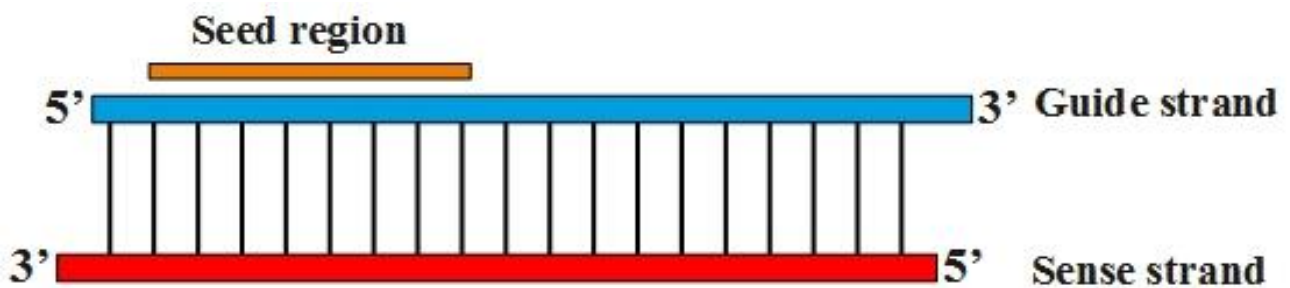


Figure 1.4. Graphical representation of the siRNA molecule

The double-stranded siRNA molecule is comprised of the guide (in blue) and sense (in red) strands. These synthetic RNAi activators are about 21 bp in length and also possess 2-base 3' overhangs which enhance RISC processing and target gene silencing. The 5' end of the RNA duplex consists of the phosphate group, while the hydroxyl moiety is present at the 3' end. The seed region (in orange) is critical for target recognition and incorporation of chemical groups into this region improves siRNA activity and specificity.

However, only moderate thermodynamic alterations of the guide seed region are tolerated, as extensive destabilisation may decrease interaction between modified siRNAs and target mRNA, leading to reduced siRNA activity [166].

Importantly, chemical groups should not distort the A-form helix of the guide strand-mRNA complex, as it prevents recognition by RISC and subsequently abolishes RNAi-mediated gene silencing [149]. Alterations of the A-form helix may disrupt protein binding, hydrogen bonding and decrease interactions between RISC and modified siRNAs, thus, preventing target gene silencing [149]. Various studies have been carried out to evaluate the advantage of using chemically modified as opposed to unmodified siRNAs. To date, most of these strategies have focused on incorporating chemical groups at the 2'-OH of ribose [166]. Addition of 2'-fluoro (2'-F), 2'-*O*-methyl (2'-*O*-Me) or 2'-methoxyethyl (2'-*O*-MOE) groups to siRNAs enhances silencing efficacy and resistance to nuclease degradation [167, 168]. Furthermore, addition of a chemical group at the 2'-OH site, particularly 2'-*O*-Me also prevents innate immune stimulation [169] by avoiding interaction with TLRs. It is also thought that chemically modified siRNAs may prevent immune stimulation by causing internalisation of receptor molecules or antagonising pathways associated with innate immune signalling [157]. Additionally, 2' modification with bulky chemical groups that do not alter the structure of the A-form helix [149] may prevent unwanted interaction between modified siRNAs and immune receptors, thereby, avoiding immune stimulation [170]. Other research groups also investigated the advantage of replacing ribose with sugars such as hexitol [164, 166, 171, 172]. Incorporation of chemical groups at different positions of the sense or guide strand may significantly

increase or decrease the silencing efficacy of siRNAs. This is true as addition of boranophosphate to the middle of the guide strand leads to poor activity, while incorporation of this chemical group to other positions results in improved silencing efficacy and resistance to nuclease degradation [173]. This illustrated that incorporation of chemical groups at key positions within the siRNA sense or guide strand is necessary to augment silencing efficacy.

Chemically modified siRNAs targeting conserved regions of HBV RNA have been employed to abrogate viral replication in cell culture and mice [158]. These modifications included 2'-F, (2'-O-Me), 2'-deoxy sugars and phosphorothioate linkages. Incorporation of these chemical groups resulted in enhanced stability of modified siRNAs in serum relative to the unmodified group [158]. Significant suppression of markers of HBV replication was achieved by modified siRNAs while their unmodified counterparts displayed unsatisfactory activity *in vitro*. Antiviral activity was also observed in mice following hydrodynamic co-injection of modified or unmodified siRNAs and HBV plasmid vector [158]. A marked decline in markers of HBV replication was observed in mice treated with antiHBV siRNAs relative to animals injected with control siRNA or saline. As in cell culture studies, pronounced HBV silencing was achieved with modified as opposed to unmodified siRNAs, thus demonstrating the utility of chemical modifications in effecting enhanced antiHBV activity in cell culture and mice. This observation highlighted the importance of chemical modifications with regard to improving siRNA stability and activity *in vitro* and *in vivo* [158].

In a separate study, the utility of employing lipoplexes containing altritol (ANA)-modified siRNAs was investigated [124]. These complexes were delivered to transgenic mice and targeted the conserved *HBx* ORF of HBV. Both unmodified and ANA-modified siRNAs were injected at a constant dose of 1 mg/kg mouse body weight and involved a maximum of four injections per week. The siRNAs were capable of silencing markers of HBV replication for 25 days without inducing hepatotoxicity [124]. Markers of innate immune stimulation were induced in mice treated with unmodified siRNA, but, this non-specific effect was abrogated in animals treated with modified siRNAs. Data from this study indicated that incorporation of the ANA chemical group into antiHBV siRNAs abrogates viral replication in transgenic mice without a substantial increase in hepatotoxicity and immune stimulation, and may potentially be utilised as effective antiHBV agents [124].

1.7. Delivery methods

1.7.1. Viral delivery methods

There are two types of delivery systems used to deliver RNAi effectors to target cells: viral and non-viral delivery systems. Viral systems are employed to deliver expressed RNAi activators, while non-viral vectors are usually used for the delivery of synthetic RNAi activators. Recombinant viruses such as Adenoviruses (Ads), Adeno-associated viruses (AAVs) and lentiviruses (LVs) achieve efficient transduction of liver cells, have broad tissue tropism and are capable of effecting long-term transgene expression in target hepatocytes. Consequently, viral systems have been widely used for basic research and

clinical studies [174-176]. However, drawbacks of utilising viral vectors to deliver therapeutic RNAi sequences include induction of the innate and adaptive immune response [177-180], cytotoxicity [181] and insertional mutagenesis [182].

1.7.2. Non-viral delivery methods

To circumvent the devastating manifestations associated with utilising viral vectors, several non-viral strategies have been invented and utilised for the delivery of therapeutic sequences to target cells. These include the use of cationic liposome-containing nucleic acids (lipoplexes) [124, 159, 183] and cationic polymer-containing nucleic acids (polyplexes) [184-186]. Both RNA and DNA molecules can be formulated with cationic liposomes or polymers to achieve efficient transgene delivery and target gene silencing in target tissues. The siRNA molecules are smaller in size compared to RNAi expression cassettes. Moreover, siRNAs have a cytoplasmic site of action, while DNA molecules need to be delivered to the nucleus. Collectively, these features enable siRNA administration and dose regulation easier to achieve relative to expressed RNAi activators. Furthermore, delivery of siRNAs to the cytoplasm encounters fewer challenges than administration of DNA to the nucleus. Favourable properties that advance the use of non-viral vectors include:

- Safe and regulated production process.
- Decreased immunogenicity and cytotoxicity.
- Integration into the host cell genome is greatly reduced.
- Versatility in accommodating small and large nucleic acids.

siRNA molecules may be formulated with liposomes to form siRNA lipoplexes, which can then be used to transport these therapeutic molecules to target cells *in vivo*. In such formulations, the siRNA molecules are linked to liposomal components by electrostatic interactions [187]. *In vivo* delivery of siRNA using liposomes is generally unsatisfactory, due to various shortcomings that need to be countered if efficient transgene delivery is to be realised. The drawbacks of this delivery system include unspecific tissue targeting, inefficient delivery of RNAi effectors, unsatisfactory circulation profile [188] and aggregation of liposomal components [189].

These limitations may be abolished by: (1) optimisation of siRNA and vector concentrations, (2) formulation of uniform small particle sizes of approximately 50-100 nm in diameter, (3) addition of molecules that have enhanced affinity for the cellular receptor and, (4) conjugation of liposomal components to polymers that mask the lipoplexes from the immune system. Incorporation of polyethylene glycol (PEG), for example enhances the half-life of lipoplexes *in vivo*. This is because PEG is capable of forming a water shell, leading to decreased adhesion of opsonin molecules that promote phagocytosis. Poor adhesion leads to masking of lipoplexes which subsequently prevents activation of liver immune cells and the mononuclear phagocyte system [188, 190, 191]. Addition of PEG into lipoplexes also improves the biodistribution and amount of siRNAs being delivered into target cells, relative to unPEGylated lipoplexes [188].

In addition to PEG, other essential liposomal components include 1,2-dioleoyl-sn-Glycero-3-Phosphoethanolamine (DOPE) which is commonly used as a helper fusion lipid and also

decreases toxicity of the lipoplex formulation [124, 192-197]. 3β -[N(N',N'-Dimethylaminoethane carbamoyl cholesterol)] (DC-Chol) is a cationic lipid [196-201] which binds to the negatively charged siRNA molecule. Carbohydrate molecules (e.g. galactose) have high affinity for the asialoglycoprotein receptor (ASGPr), which is found on the surface of liver cells and may be conveniently used to confer liver-specific delivery of siRNA lipoplexes [185, 186, 192-195, 202]. In most cases, hepatocytes are the most commonly targeted cells due to their accessibility by both viral and non-viral delivery systems. Delivery of therapeutic agents using the receptor targeting strategy is advantageous as it may increase specificity and the amount of effector molecules being administered into target cells. It has been demonstrated that association between the receptor and targeting molecule promotes clustering, which improves the binding affinity between the targeting molecule and receptor [203-205]. It has also been shown that recognition of galactose by ASGPr *in vivo* is dependent on the amount of galactose in the lipoplex formulation [206]. Additionally, pharmacokinetic investigations revealed that the number of galactose molecules on the surface proteins determines the binding efficacy of galactose to ASGPr [206]. For this reason, both natural and synthetic compounds derived from galactose have been produced with the aim of targeting the ASGPr on the surface of hepatocytes [185, 202, 207].

Following administration of siRNA lipoplexes, the complexes bind and gain access to the cells through clathrin-mediated endocytosis [208]. To ensure that the lipoplexes are released from the acidic endosomes before interacting with the lysosome, fusogenic lipids such as DOPE may be included in the lipoplex formulation. This prevents degradation of

the formulation as fusogenic lipids interact with the endosome, resulting in fusion between the endosome membrane and lipoplex membrane. This destabilises the endosome membrane [209] and allows siRNAs to be released into the cytoplasm, where they exert their therapeutic activity. In addition to fusogenic lipids, endosomolytic agents can also be used to prevent lysosomal degradation [209, 210]. This includes the use of haemagglutinin subunit 2 (HA2) and glutamic acid-alanine-leucine-alanine (GALA) [209]. Both peptides are pH-sensitive and undergo a conformational change under acidic conditions of the endosome [209]. This promotes fusion between the endosomolytic agent and the endosome membrane. Subsequently, this leads to destabilisation of the endosome membrane, thus, triggering the delivery of therapeutic agents into target tissues [209, 211, 212].

Various cationic liposomes have been employed to deliver siRNAs to target cells. Previously, stable nucleic acid lipid particle (SNALP) formulations were employed to facilitate delivery of 2'-OMe, 2'-F, phosphorothioate and 3', 5' inverted deoxy abasic modified siRNAs [159]. Following efficient antiviral activity in mammalian cells, these formulations were employed to inhibit viral replication *in vivo*. In this study, chemically modified SNALP-siRNAs displayed enhanced half-life in the plasma and liver compared to unformulated siRNA. Serum HBV DNA levels in mice were substantially reduced after administration of three daily injections at a dose of 3 mg/kg [159]. This antiHBV activity persisted for seven days and was dose-dependent. Additionally, a weekly administration of SNALP-siRNAs reduced serum HBV DNA levels for up to six weeks. Although there was in general no significant difference in antiHBV efficacy between modified and unmodified

siRNAs, administration of 3 mg/kg unmodified siRNA induced toxicity and innate immune stimulation in mice [159]. Conversely, toxicity and immune stimulation were abrogated after administering the same dose of modified siRNAs. Collectively, data gathered from this study demonstrated that the SNALP formulations are capable of delivering chemically modified antiHBV siRNAs to exert a sustained RNAi effect in target hepatocytes without a marked increase in toxicity or markers of innate immune stimulation [159].

Similarly to cationic liposomes, cationic polymers bind to effector molecules (e.g. siRNA or DNA) resulting in charge neutralisation, which facilitates delivery into target cells following endocytosis (reviewed in [213]). In contrast to lipoplexes that utilise clathrin-mediated endocytosis, polyplexes gain access into target cells by employing both the clathrin and caveolae-mediated endocytosis [208]. Lipoplexes require destabilisation of the endosome membrane to achieve endosomal release, while polyplexes utilise the “proton sponge” effect to accomplish endosomal escape. Indeed, cationic polymers such as polyethyleneimine (PEI) employ this mechanism to augment nucleic acid delivery. With this approach, the buffering capability of PEI inhibits nuclease enzymes in the lysosome and creates an osmolaric change of acidic vesicles. This causes the endosome to burst, thus, allowing the release of therapeutic agents into target cells [184, 214-216].

In a study conducted using a cationic polymer system, Dynamic PolyConjugates (DPCs) were employed to deliver 2'-OMe or 2'-F (2'-F) modified siRNAs to target hepatocytes

[186]. This formulation was composed of *N*-acetylgalactosamine that conferred liver-tropic delivery of particles. Co-injection of these vectors with 1-6 mg/kg anti coagulation factor VII (F7) siRNA significantly suppressed gene expression in HBV transient and transgenic mice as well as non-human primates, and the level of gene silencing was dose-dependent [186]. This impressive antiF7 activity was achieved without evidence of toxicity or an innate immune response in injected animals, even after four injections. Furthermore, a single injection of chemically modified siRNAs targeting conserved HBV regions effected simultaneous and prolonged silencing of viral DNA, RNA and proteins in injected mice, thus reinforcing the notion that DPCs have potential as therapeutic agents against chronic HBV infection [186].

Therapeutic properties of siRNAs may be enhanced by using chemical modifications and an efficient delivery system. Collectively, strategic incorporation of chemical groups at key positions within the guide or sense strand of siRNAs and development of a robust, competent and efficient non-viral delivery system are critical for improving specificity, stability and target gene silencing, while minimising unintended manifestations such as toxicity and innate immune stimulation in target cells. This will go a long way to promoting application of siRNA-mediated RNAi as therapy for chronic HBV infection in a clinical setting.

Chapter 1

Our current study was aimed at building on previous investigations that exploited chemically modified siRNA molecules and efficient non-viral delivery systems to achieve target gene silencing without a marked increase in toxicity and non-specific effects. Specifically, our study was aimed at assessing the utility of introducing novel 2'-*O*-guanidinopropyl (GP) moieties into the potent antiHBV siRNA (i.e. siRNA3) previously employed by Hean et al., 2010 [124]. Initially, single GP groups were incorporated into the guide strand and modified siRNAs were named based on the location of the GP moiety from the 5' end. The rationale for using a single siRNA, as opposed to multiple effector molecules include: (1) dose may be easily optimised with a single as opposed to multiple siRNA molecules, and (2) since all siRNAs targeted the *HBx* ORF of HBV, application of more than one RNAi effector molecule would potentially result in saturation of the natural RNAi system and non-specific effects such as innate immune stimulation.

Various chemical residues have already been employed to improve the therapeutic properties of siRNAs. However, this study was conducted because it introduces the novel GP-modification of antiHBV siRNAs. This modification is unique in that the amino moieties of the GP group and the carbon propyl linker may allow efficient charge neutralisation [217]. Additionally, charge neutralisation is also achieved by interaction between the cationic amine groups of GP residues and the anionic phosphate moieties of siRNAs. Therefore, this efficient charge neutralisation may improve therapeutic efficacy of modified siRNAs by facilitating delivery of therapeutic sequences into target hepatocytes.

These useful properties triggered the prospect of investigating RNAi-mediated gene silencing in cell culture and mice using GP-modified siRNAs.

Prior to conducting this study, 2'-*O*-aminoethyl modifications were utilised to enhance the utility of siRNAs [166]. This strategy was improved by subjecting the four ribonucleosides to alkylation using phalimidoethyltriflate [218]. However, the setbacks of this new approach included insufficient yields and challenges pertaining to the scaling up process. This led to the development of the novel GP modification as an alternative method of conferring useful therapeutic properties into siRNAs without compromising the yield of the chemical synthesis procedure [217]. To improve the yield, the crude 2'-*O*-aminopropyl served as the source of guanidino groups while *N,N'*-di-Boc-*N''*-triflyguanidine was used as a guanidinylation agent. This strategy significantly improved the production of all four GP nucleosides, namely adenosine (A), cytidine (C), guanosine (G) and uridine (U) [217]. Additionally, this modification provides several favourable characteristics that are not offered by previous 2'-OH modifications. The chemical synthesis procedure comprised cyanoethylation which involves addition of acrylonitrile to protected nucleosides. Subsequent Raney-Nickel reduction reaction produces propylamino molecules which are guanidinylated using triflyguanidine. This approach presents a novel strategy in which all four phosphoramidites are modified with the GP moiety, placed at the 2' position and incorporated into antiHBV siRNAs. Versatility of this chemical synthesis process is that it allows alterations at the 2'-*O*-aminopropyl position, while the amino moieties of the GP group and the carbon propyl linker may allow efficient charge neutralisation [217].

Although several non-viral delivery strategies have been devised for the administration of antiHBV siRNAs *in vivo*, only a limited number of delivery systems are capable of achieving efficient transgene delivery into target hepatocytes of various animal models. Collectively, our current study was focused on testing the use of novel GP-modified siRNAs in conjunction with an effective, competent, hepatotropic non-viral delivery system as an alternative strategy to combat chronic HBV infection.

1.8. Aims and objectives:

The aim of this study was to investigate the therapeutic advantage of utilising novel GP-modified siRNAs to counter HBV replication in cultured cells and mice. The siRNAs were designed to target the viral *HBx* ORF of genotype A (coordinates 1693 to 1711), as it is conserved and its sequence is common in all HBV transcripts. Efficient charge neutralisation between the amino groups of the GP residue and carbon propyl linker as well as the cationic amine groups of GP moieties and the anionic phosphate groups of siRNAs may facilitate delivery of therapeutic sequences into target hepatocytes.

The objective of this study was to assess the activity, specificity, stability, toxicity and to detect the siRNA-mediated cleavage product in cultured mammalian cells and mice following delivery of GP-modified siRNAs. Markers of viral replication were evaluated from cell culture and animal sera, and were indicative of the effect of siRNAs on HBV replication. Animal experimentations entailed preliminary assessment of antiHBV activity

Chapter 1

of modified siRNAs in a hydrodynamic injection (HDI) mouse model. Subsequent animal studies involved interrogation of antiHBV activity, specificity, toxicity and detection of the siRNA-mediated cleavage product in HBV transgenic mice following liposome-mediated delivery of GP-modified siRNAs.

Chapter 2: Materials and methods

Methods will be discussed in each result chapter.

CHAPTER 3

PUBLICATION 1

Recent advances in developing nucleic acid-based HBV therapy

Musa Marimani, Justin Hean, Kristie Bloom, Abdullah Ely, Patrick Arbuthnot

Future Microbiology **8** (11): 1489-1504 (2013)

This review article discusses milestones achieved in the field of gene therapy. Additionally, it details some of the challenges associated with the application of therapeutic RNAi sequences and gene editing technologies, reviews current developments and evaluates potential application of gene therapy in the treatment of chronic HBV infection.

Author's contribution:

Musa Marimani, Drs. Justin Hean and Kristie Bloom contributed to writing different sections of the review article. Specifically, Marimani compiled the following sections in the review article: “*Synthetic anti-HBV activators of RNAi, delivery of HBV-targeting RNAi activators and siRNA delivery*”. Prof. Arbuthnot and Dr. Ely supervised the project and also assisted with compiling the manuscript.

Recent advances in developing nucleic acid-based HBV therapy

Musa Marimani¹, Justin Hean¹, Kristie Bloom¹, Abdullah Ely¹ & Patrick Arbuthnot*¹

¹Antiviral Gene Therapy Research Unit, School of Pathology, Health Sciences, University of the Witwatersrand, Johannesburg, South Africa

*Author for correspondence: Tel.: +27 11 717 2365 ■ Fax: +27 11 717 2395 ■ patrick.arbuthnot@wits.ac.za

Chronic HBV infection remains an important public health problem and currently licensed therapies rarely prevent complications of viral persistence. Silencing HBV gene expression using gene therapy, particularly with exogenous activators of RNAi, holds promise for developing an HBV gene therapy. However, immune stimulation, off-targeting effects and inefficient delivery of RNAi activators remain problematic. Several new approaches have recently been employed to address these issues. Chemical modifications to anti-HBV synthetic siRNAs have been investigated and a variety of vectors are being developed for delivery of RNAi effectors. In this article, we review the potential utility of gene therapy for treating HBV infection.

HBV infects the liver to result in acute or chronic hepatitis [1,2]. It has been estimated that 350 million people suffer from chronic HBV infection, and these carriers are at increased risk for complicating cirrhosis and hepatocellular carcinoma. An effective preventative vaccine is available, but is of little use to individuals who are already infected with the virus. As a result, problems associated with HBV infection are likely to remain a significant public health problem for many years. Most infections in adults clear spontaneously; however, infection in children frequently leads to chronicity. Current therapies approved for HBV infection include nucleotide and nucleoside analogs, which act by inhibiting the reverse transcription step of viral replication [3,4]. Immunomodulators, such as IFN- α and polyethylene glycol (PEG) ylated IFN- α , are also licensed HBV therapies. The available therapeutics rarely eradicate HBV and re-establishment of replication often occurs after treatment withdrawal [5]. Consequently, development of new and more effective therapies is required to combat HBV infection.

HBV is a small, enveloped virus with a partially dsDNA genome of 3.2 kb (FIGURE 1) [6]. The viral genome is composed of relaxed circular DNA, which is formed after reverse transcription of a pregenomic RNA (pgRNA) intermediate. Conversion of relaxed circular DNA to covalently closed circular DNA (cccDNA) occurs in infected hepatocytes [7,8]. cccDNA is a very stable replication intermediate and serves as a template for transcription of pgRNA and mRNAs. Moreover, cccDNA persistence is responsible for chronicity of HBV infection and modest curative efficacy of current therapies [9,10]. During virion formation, HBV core particles are assembled in

the cytosol after pgRNA encapsidation [11]. The viral surface proteins are produced in the rough endoplasmic reticulum and transported to the Golgi. Budding and secretion of the capsids occurs via the Golgi to release HBV virions [12].

Discovery of the RNAi pathway [13] was an important development in the field of gene therapy and presented an opportunity for silencing of pathology-causing genes, such as those expressed by HBV. This pathway is triggered by primary miRNAs (pri-miRNAs), precursor miRNAs (pre-miRNAs), miRNAs and the mimics of these molecules (FIGURE 2) [14,15]. Naturally, endogenous pri-miRNAs are cleaved by the nuclear microprocessor complex, Drosha and DGCR8, to produce pre-miRNA hairpins. The pre-miRNAs are subsequently exported to the cytoplasm and further processed by the Dicer RNase III enzyme to form short duplex miRNAs of approximately 23 bp. The miRNA duplex is incorporated into the RNA induced silencing complex (RISC), after which one of the two RNA strands is selected as the mature miRNA and serves as an antisense guide to target mRNA. The passenger strand, named miRNA*, is degraded and plays no further part in RNAi. Complete base-pairing between the guide strand and its cognate mRNA leads to target cleavage by Ago 2, while partial base-pairing leads to translational suppression. The RNase H activity, PAZ and PIWI domains of Ago2 provide critical function to the slicing component of the RNAi machinery [16]. The mechanism of translational suppression mainly involves mRNA destabilization in processing bodies (P-bodies) [17] and, to a lesser extent, inhibition of ribosome function [18]. P-bodies are cytoplasmic foci containing mRNA

Keywords

■ delivery vectors ■ gene therapy ■ HBV ■ RNAi ■ siRNA

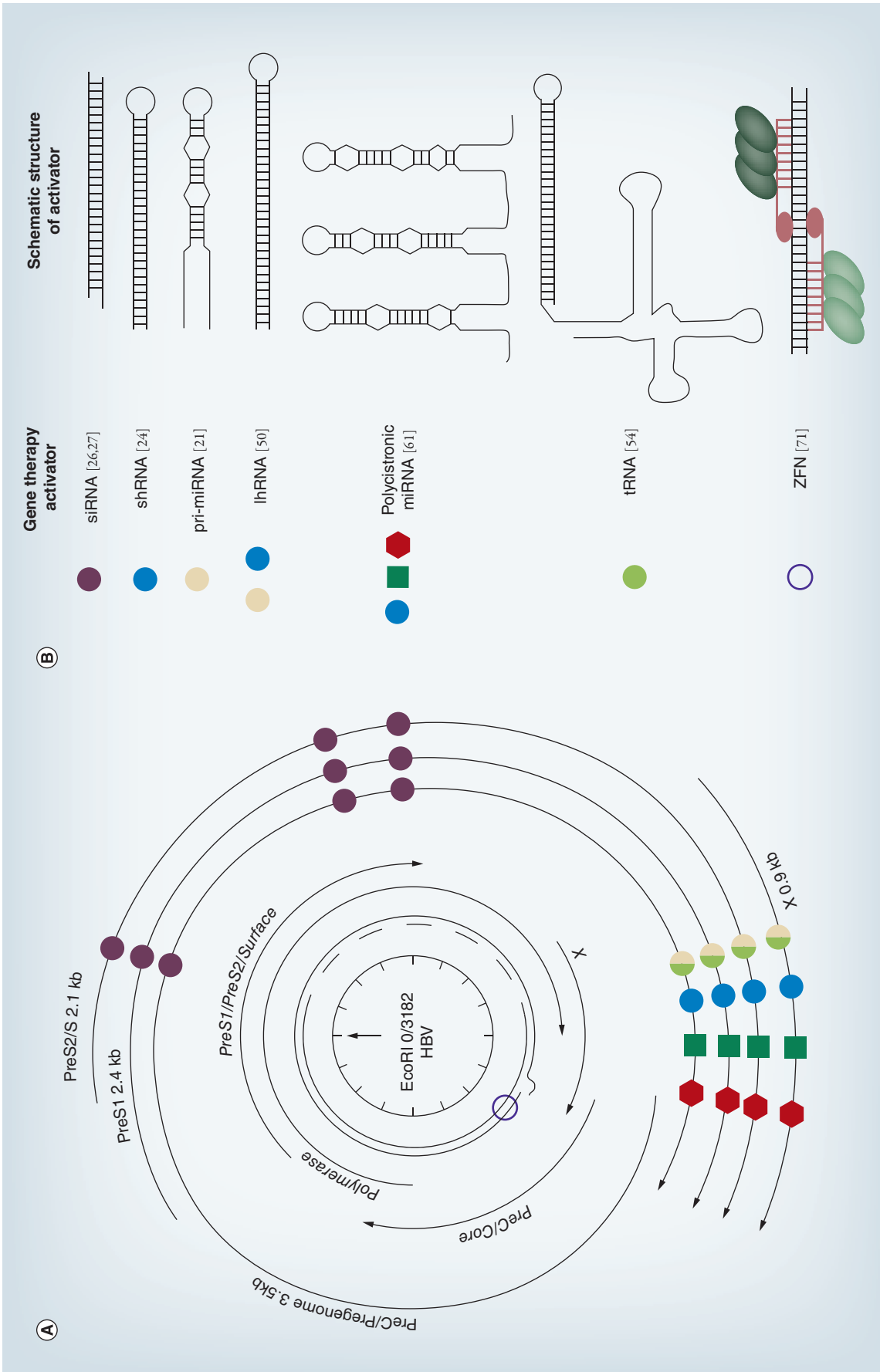


Figure 1. Organization of the HBV genome. (A) The partially double-stranded genome (center) contains several overlapping open reading frames, indicated by the immediate surrounding arrows. The four outer arrows indicate the four HBV transcripts, some of which contain multiple start codons. The overlapping nature of the genome enables silencing of several transcripts with one gene silencer. Representative target sites, which have been shown to be susceptible to gene therapy-based silencing, are indicated by the circles placed on the HBV transcripts. (B) Structures of the different types of RNAi: activators and ZFNs are shown with symbols corresponding to the target sites within the genome. lncRNA: Long-hairpin RNA; pri-miRNA: Primary miRNA; ZFN: Zinc finger nuclease.

targeted by miRNAs that are complexed to Ago1 and Ago2 from the RISC, and also include the scaffold protein GW182. Evidence indicates that complementarity between the seven nucleotides of the seed region of the guide strand, which comprise nucleotides 2–8 from the 5' end, and the target are all that is required to affect silencing and degradation in P-bodies [19].

The HBV genome is well suited to RNAi-based targeting. The pgRNA, which is greater than genome length, is an essential replication intermediate that may be disabled using RNAi-based methods [20–24]. There are four major overlapping open reading frames of the compact viral genome: *preC/core*, *polymerase*, *surface* and *X* (FIGURE 1). HBV transcripts also overlap with each other and have common 3' sequences that are defined by the single transcription termination signal. Single RNAi effector molecules may therefore have cognates in more than one of the viral RNAs. Supporting the idea that HBV is a suitable target for RNAi-based therapy, many sites of the viral genome have been successfully targeted by engineered synthetic and expressed RNAi activators [20,25]. Interestingly, the HBV ϵ packaging signal, which is a highly structured sequence with duplex stem and loop regions that are bound to viral and cellular proteins, was found to be a good RNAi target sequence [20]. Overall,

results suggest that no particular sequence of the HBV genome is particularly sensitive to silencing; rather it is the sequence-specific properties of the RNAi activators themselves that influence their effectiveness.

Synthetic anti-HBV activators of RNAi

Synthetic activators of RNAi have been used to silence HBV replication *in vitro* and *in vivo* [26–29]. siRNAs typically comprise dsRNAs of approximately 21 bp that have two nucleotide overhangs at their 3' ends. They therefore resemble mature miRNA duplexes and activate RNAi at the stage of guide strand incorporation into RISC [30]. As with all gene therapies, synthetic siRNAs have limitations in their application to treating HBV. Susceptibility to serum nuclease degradation [31], unfavorable bio-distribution, nonspecific immune stimulation [32,33] and silencing of host genes through partial hybridization to cellular mRNA, are some of the limiting factors. These undesirable effects may be attenuated by chemical modification of siRNAs, and this type of alteration has therefore been widely used to improve therapeutic properties of siRNAs. Initially, modifications to siRNAs included incorporation of 2'-*O*-methyl, 2'-fluoro or 2-methoxyethyl moieties, to increase durability of silencing by siRNAs and prolong

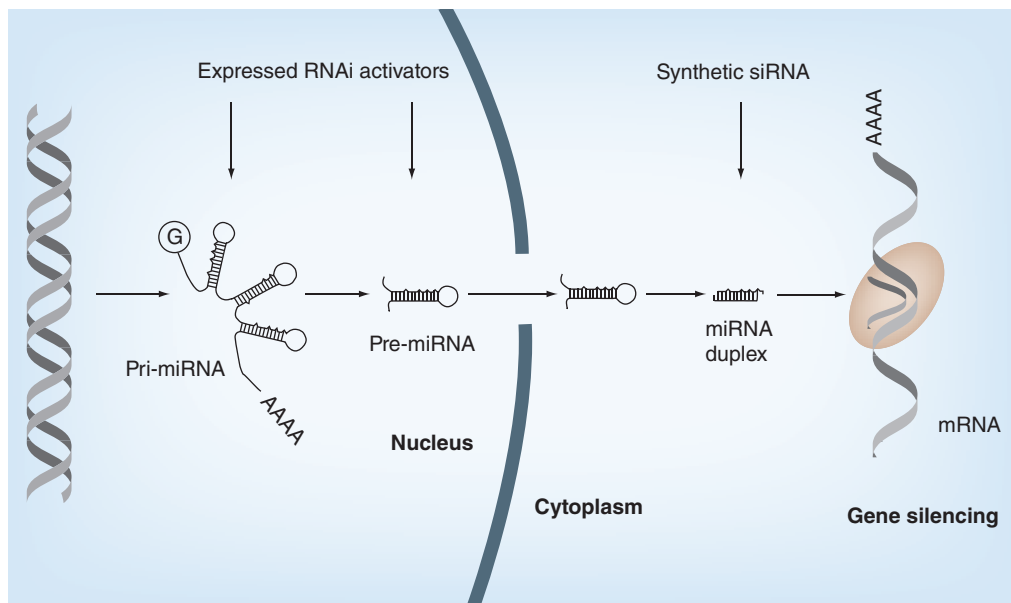


Figure 2. The RNAi pathway. Pri-miRNA sequences that are processed by the Drosha/DGCR8 microprocessor complex produce pre-miRNAs. Processing of pre-miRNAs yield miRNA duplexes. One of the strands from the miRNA duplex is selected within RNA induced silencing complex and guides the complex to target mRNA. Exogenous RNAi activators mimic pri-miRNA, pre-miRNA or mature miRNA and enter the pathway where indicated.

Pre-miRNA: Precursor miRNA; Pri-miRNA: Primary miRNA.

Reproduced with permission from [139] © 2010–2013 Prous Science, S.A.U. or its licensors. All rights reserved.

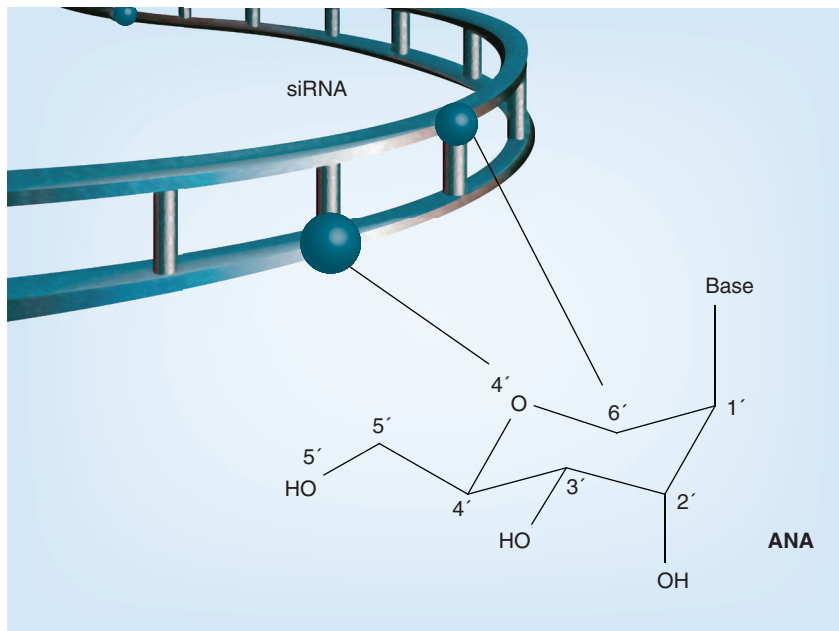


Figure 3. Structure of altritol nucleic acid containing two six-membered hexitol sugars incorporated into the sense and antisense strands of an anti-HBV siRNA. Structure of the six membered hexitol sugar is shown. ANA: Altritol nucleic acid.

their plasma stability [34,35]. Addition of moieties to the 2' and 4' positions of the ribose [36], changes to the natural phosphodiester linkages, and substitution of the ribose for sugars, such as hexitol, were subsequently used [37–40]. Interestingly, positioning of modifications at specific nucleotides within the sense or antisense strands of siRNAs influences their efficacy. For example, boranophosphonate-modified siRNAs show improved resistance to nucleases; however, incorporation of this modification at the center of the guide strand results in loss of silencing efficacy [41]. There are several chemical modifications to siRNAs that have resulted in improved therapeutic properties; however, only recent developments and those that are pertinent to advancing use of potentially therapeutic anti-HBV siRNAs will be discussed here.

One of the first studies to demonstrate enhanced anti-HBV activity of chemically modified siRNAs in a murine model was conducted by Morrissey *et al.* [42]. The siRNAs contained numerous modifications: inverted abasic residues at the 5' and 3' ends; phosphorothioate linkages; and substitution of 2' hydroxyl groups with fluoro, methyl or H groups. After administration as naked molecules, these siRNAs inhibited HBV replication *in vivo*; however, the high dose that was necessary to be effective was impractical for therapy. Stable nucleic acid lipid particle (SNALP) formulations, which assemble into uniform small size particles, were then used as a means for delivery.

SNALP-delivered siRNAs resulted in the suppression of markers of HBV replication over a 6-week period in mice subjected to hydrodynamic injection (HDI) with an HBV replication-competent plasmid. Attenuation of siRNA-mediated immunostimulation, affected by chemical modification, was also demonstrated in this study.

Other chemical modifications to anti-HBV siRNAs that have recently been investigated include altritol-containing nucleic acids, which are distinguished by containing six-membered sugar moieties (FIGURE 3) [43]. Helix stability and maintenance of RNA-like A-form structures are enhanced by the presence of the altritol moiety and may improve siRNA-mediated silencing [40]. Altritol nucleic acid (ANA) modifications were introduced at the 3' ends of the sense and antisense strands, and also at the 5' end of the sense strand of an anti-HBV siRNA, then complexed with liposomal vectors [43]. The ANA-modified siRNA-lipoplexes generally displayed increased anti-HBV efficacy when compared with their unmodified counterparts; however, they did cause minor hepatotoxicity. Analysis of immunostimulation using a cytometric bead array revealed that unmodified siRNA induced release of proinflammatory cytokines which was markedly attenuated in mice receiving the ANA-modified siRNA-lipoplexes.

To assess the efficacy of a different class of chemical modification, 2'-*O*-guanidinopropyl (GP) residues were incorporated into anti-HBV siRNAs (FIGURE 4) [44]. These alterations were included at each nucleotide position from two to 21 of the guide strand. In transfected liver-derived human Huh7 cells, GP-modified siRNAs were more effective than unmodified siRNAs and decreased gene expression by up to 95% [45]. Both unmodified and GP-modified siRNAs did not stimulate interferon-associated pathways or decrease cellular viability, but stability was improved by incorporation of the GP modification. GP-modified siRNAs also caused significant knockdown of markers of viral replication (HBsAg and circulating viral particle equivalents) *in vivo* using a murine HDI model.

Expressed RNAi activators against HBV infection

Treatment of chronic HBV infection by harnessing RNAi will require sustained presence of silencing molecules. Utilization of stable DNA templates encoding RNAi expression cassettes has the potential to enable prolonged inhibition of HBV replication [46]. Expression cassettes comprising DNA also have the advantage of

compatibility with highly efficient viral delivery vectors. Exogenously expressed RNAi intermediates vary, and may enter the RNAi pathway at different stages as mimics of pri-miRNAs, pre-miRNAs and miRNA-like structures (FIGURE 2). Typically anti-HBV RNAi expression cassettes contain a Pol II or Pol III promoter, a template encoding the RNAi activator sequence and a transcription termination sequence. Pol III transcription regulatory elements, usually U6 or H1 promoters, have been widely used for expression of shRNA that act as mimics of pre-miRNA. An advantage of these transcription regulatory elements is that they are capable of efficiently generating short transcripts with defined 5' and 3' ends [24]. Furthermore, they are active in a wide range of tissues, are small in size and contain most required regulatory elements upstream of the transcription initiation site [47].

To date, a variety of highly effective anti-HBV RNAi activators have been expressed from both Pol II and Pol III promoters. McCaffrey was the first to demonstrate the anti-HBV potential of expressed shRNAs in a murine model [48]. This observation was subsequently supported by other studies in which silencing in cultured cells and *in vivo* has been reported for Pol III-expressed shRNAs [24,49], long hairpin RNAs targeting the X open reading frame [50] and other HBV mRNA sequences [51–53]. As a substitute for the powerful U6 transcription regulator, H1 and tRNA^{Lys3} Pol III promoters have also been used successfully in anti-HBV expression cassettes [54]. In an alternative approach, Blazquez *et al.* demonstrated the advantage of utilizing both RNAi and U1 small nuclear RNA ribonucleoprotein-based inhibition as a therapeutic strategy against HBV [55,56]. Combinatorial approaches have also been used to improve HBV silencing, in which RNAi activators were used in conjunction with lamivudine, a licensed HBV drug [57]. In addition to the targeting of HBV genes, silencing of host dependency factors that are required for viral replication, such as heat shock cognate 70, may be used to limit risk of escape mutation occurring in the virus [58].

In 2006, Grimm *et al.* revealed that the high level of transcription of anti-HBV shRNAs from the U6 Pol III promoter resulted in toxicity *in vivo* from saturation of the endogenous RNAi pathway [59]. This important observation emphasized the need for controlled expression of RNAi activators, and led to investigating use of Pol II and weaker Pol III transcriptional elements to produce exogenous RNAi intermediates. Although inducible expression of Pol III promoters has been described

[60], Pol II regulators offer more versatility. Natural expression of pri-miRNAs from Pol II promoters has been harnessed to aid the design of artificial pri-miRNA Pol II expression sequences that target HBV genes [21], and multimerization of artificial pri-miRNAs to simulate natural pri-miRNAs allows for simultaneous targeting of several viral sites [61]. This approach improves efficacy and diminishes risk of viral escape. The exact number of simultaneously acting HBV-silencing RNAi activators required to prevent escape remains to be determined; however, it is likely that a trimeric cassette will be sufficient. Four silencing components of an artificial polycistronic pri-miRNA cassette, targeting the larger, more flexible HIV genome, were adequate to prevent emergence of viral escape [62,63]. A further advantage of using artificial pri-miRNAs over sh- or si-RNAs relates to the notion that exogenous sequences introduced at earlier steps of the RNAi pathway are processed more efficiently. It is thought that each stage of the pathway is functionally linked to the preceding event during miRNA biogenesis. Introducing exogenous pri-miRNAs into cells should therefore improve silencing, since their natural counterparts are produced at the initial stages of miRNA biogenesis.

Alternatives to RNAi-based HBV gene therapies

A recent alternative approach to inhibiting HBV replication using gene therapy entailed use of

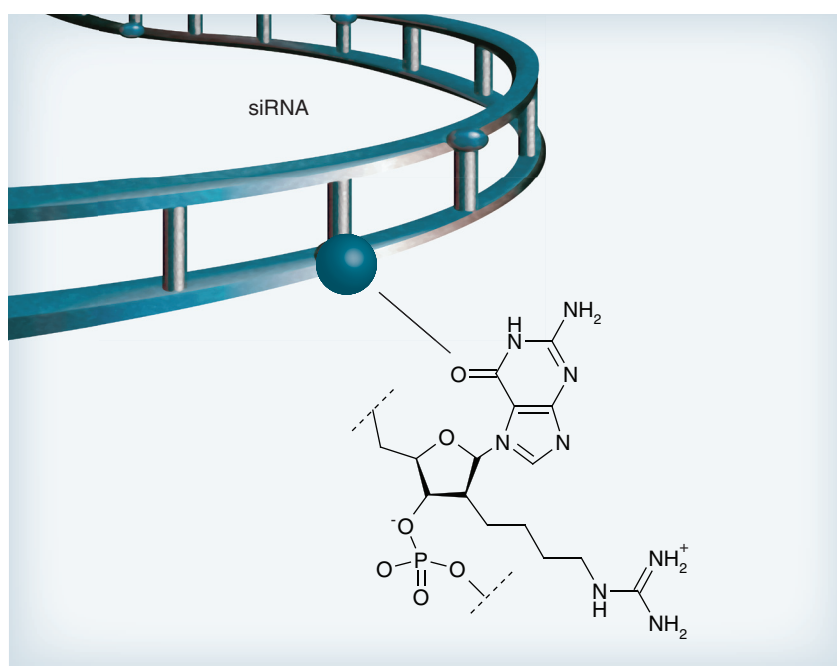


Figure 4. 2'-O-guanidinopropyl modifications at a single nucleotide of the guide strand of an anti-HBV siRNA.

an external guide sequence (EGS) to direct RNase P to cleave HBV RNA [64]. The EGS was designed to hybridize with HBV to form a secondary structure that mimics that of a tRNA precursor. RNase P naturally cleaves tRNA precursors and, using the EGS to create an artificial substrate, caused efficient degradation of HBV RNA. Good efficacy in cell culture and *in vivo*, using an attenuated *Salmonella* bacterial strain as vector, was demonstrated.

Failure to effectively treat chronic HBV infection has largely been ascribed to the persistence of the episomal cccDNA replication intermediate [65,66]. As cccDNA is epigenetic, it may serve as a dormant viral reservoir in the nucleus of hepatocytes. Although RNAi activators have shown promise as novel therapies, they inhibit viral replication post-transcriptionally. This mechanism of action is similar to that of licensed nucleoside and nucleotide analogs, which are incapable of eliminating cccDNA. Inability of RNAi activators to target the cccDNA directly is potentially a limitation, and reactivation of viral replication may occur after withdrawal of gene silencing sequences. Sequence-specific DNA-binding proteins, such as those derived from the zinc finger eukaryotic transcription factors, have been investigated as potential inhibitors of HBV gene expression [67]. Each zinc finger is capable of binding a specific nucleotide triplet and zinc finger proteins (ZFPs), comprising modules of fingers, may be designed to bind intended target DNA [68]. The ability of several ZFPs to inhibit gene expression from duck HBV (DHBV) cccDNA has been reported [67]. Arrays were designed to bind to either 9 or 18 bp target sequences within the enhancer region of DHBV and inhibit binding of transcription factors to viral regulatory elements. When tested *in vitro*, the ZFPs inhibited pgRNA expression by 32–42%. This resulted in a decrease in expression of core and surface proteins, with concomitant reduction in viral particle production.

Zinc finger arrays have also been successfully fused to nuclease domains to generate engineered DNA ‘molecular scissors’. Zinc finger nucleases (ZFNs), comprising ZFPs coupled to the nuclease domain of the FokI endonuclease, act as obligate dimers and are capable of introducing double-strand breaks at specific DNA target sequences [69,70]. Site-directed mutagenesis may result if the error prone, nonhomologous end joining pathway is activated to repair the double-stranded breaks. Cradick *et al.* investigated the ability of modularly assembled ZFNs

to cleave and disrupt HBV DNA targets [71]. ZFN pairs were designed to bind DNA of the *core* gene, particularly at the region encoding the overlapping common polyadenylation site. Each monomer ZFN component of the dimer comprised a three-finger array. A 6 bp spacer region was positioned between the left and right nucleases, and the dimer targeted an HBV sequence of 18 nucleotides. Using a replication-competent HBV target expression plasmid to test efficacy of the ZFNs *in vitro*, it was demonstrated that 36% of DNA targets were cleaved. In addition, activation of nonhomologous end joining resulted in mutations occurring in 6% of these cleaved sites. Out of the insertions and deletions identified, 81% produced frameshift mutations, which should cause disruption of translation of the core protein. This was the first study to explore designer nucleases as a potential anti-HBV gene therapy; however, the ability of these ZFNs to disable cccDNA has yet to be determined.

Other designer nucleases, the transcription activator-like effector nucleases (TALENs) [72,73] and the RNA-guided endonucleases (RGENs) [74,75], have recently been described. As with ZFNs, TALENs act as obligate dimers and comprise a transcription activator-like effector DNA-binding sequence fused to a FokI endonuclease domain. Sequence-specific DNA-binding domains are generated by concatamerization of transcription activator-like effector monomers, where each monomer confers individual nucleotide specificity through base recognition by distinct repeat variable diresidues. TALENs have advantages over ZFNs in that they are more specific to their intended cognates and are compatible with modular design. A major drawback of ZFN engineering is that the sequence context of the subunits often has a profound influence on target binding [76,77]. Unlike ZFNs, TALENs can easily be assembled by modular cloning techniques without the need for context-dependent selection [78]. In addition, TALENs have shown reduced cytotoxicity and off-target cleavage when compared with ZFNs [79]. While ZFNs and TALENs rely on protein-based DNA-binding domains, the RGENs use an RNA-guide of clustered regularly interspaced short palindromic repeats (CRISPRs) to recruit Cas9 (CRISPR-associated protein) which acts as an endonuclease. Although RGENs have recently been exploited for genome engineering [80–85], further investigation into cleavage activity and specificity is needed. TALENs and RGENs may therefore provide a promising

new approach to treating HBV and other viral infections [86].

Cell culture & animal models of HBV infection

To date, surrogate models of HBV infection have been used to establish the silencing efficacy of RNAi activators. These models imitate various stages of viral infection; however, none have the capacity to simulate all stages of the virus' lifecycle. Only recently has the HepaRG cell line been developed to achieve HBV infection of cells in culture [87]. As an alternative to infection of these cells, HBV has been introduced into cultured cells by transient or stable transfection of replication-competent plasmids. These plasmid-based systems have been widely used to assess the antiviral efficacy of the gene silencers against HBV. Recent developments have revealed a receptor that may be involved in natural HBV infection [88]. Sodium taurocholate cotransporting polypeptide has been associated with the uptake of HBV in hepatocytes. Ectopic expression of sodium taurocholate cotransporting polypeptide facilitated the infection of cells that are usually not permissive to HBV; furthermore, transfer of this gene to cells in culture and *in vivo* may enable improvement of current models of HBV infection [89].

Murine models are currently the most widely utilized to assess efficacy of RNAi activators *in vivo*. HDI is a convenient method of achieving HBV replication *in vivo*. The procedure entails the introduction of a replication-competent HBV plasmid into the liver, which then recapitulates viral gene expression, replication and release of virus and virus-like particles into the circulation [90,91]. Although this model does not result in a productive infection in mice, it is convenient to establish knockdown *in vivo*. In contrast to the transient expression of HBV plasmids in mice subjected to HDI, constitutive and stable virus replication occurs in HBV transgenic mice [92]. Therefore, these animals are suited to long-term studies on the efficacy of HBV gene silencers. However, HBV replication in transgenic mice does not mimic all the stages of natural HBV infection, such as viral entry and cccDNA formation. A third murine model is available, in which urokinase plasminogen activator severe combined immunodeficiency mice are xenografted with human hepatocytes [93]. Successful infection by HBV has been shown in these grafted animals. All stages of the HBV life cycle, including formation of the HBV cccDNA intermediate, are recapitulated in the animals.

Drawbacks of the urokinase plasminogen activator severe combined immunodeficiency xenograft model are that the immune response to HBV infection is compromised, and working with these animals is technically demanding. Consequently, their use for assessing efficacy of RNAi-based therapy has not been widely employed.

There are two naturally occurring *Hepadnavirus* infections that may be used as models to develop anti-HBV therapies. Woodchuck hepatitis virus [94] and DHBV [95]; both result in chronic hepatitis, and have been used to model human HBV pathogenesis. Woodchucks infected with woodchuck hepatitis virus have successfully been used to assess anti-HBV efficacy, of both antiviral drugs and immunostimulators, prior to clinical evaluation (reviewed in [96–98]). However, despite similarities in pathogenesis, differences in immune response and viral biology complicate the interpretation of efficacy of antiviral drugs tested in woodchucks.

Delivery of HBV-targeting RNAi activators

Although significant progress has been made in developing anti-HBV RNAi activators, *in vivo* delivery of potentially therapeutic sequences remains a major hurdle. To date, viral vectors for gene therapy have shown the most promise for delivery of expressed sequences and represent the most commonly used vector in clinical trials. By contrast, synthetic siRNAs have typically been incorporated into lipoplexes or conjugated to various molecules to achieve hepatocyte delivery after systemic administration.

siRNA delivery

Delivery of siRNAs to the liver is typically achieved through the use of various polymers, conjugates and lipoplexes as vectors. The synthetic nature of these carriers means that they are conveniently amenable to scalable synthesis, which is useful for clinical application. Obstacles that restrict efficient delivery of siRNAs to liver cells *in vivo* include susceptibility of the cargo to nuclease degradation, an innate immune response, sequestration by the reticuloendothelial system, inadequate tissue targeting, aggregation and instability of vectors. Some of these challenges may be addressed by optimizing vector formulations, employing different methods that enhance uptake of siRNAs by target cells, achieving siRNA protection from serum nuclease degradation and coupling of 'stealth' molecules to enable evasion of innate and adaptive immune responses [99].

A large variety of siRNA-containing lipid vector formulations have been designed for use *in vivo*, including liposomes, micelles, emulsions and SNALPs [100]. Assembly with siRNAs occurs through electrostatic interactions of lipids containing amines that bind negatively charged RNA and form lipid bilayer complexes [101]. Critical parameters that need to be controlled include optimization of the ratio of siRNA to lipid, a uniform small particle size, appropriate pharmacokinetics, tissue targeting, prevention of siRNA degradation and minimizing toxicity [100]. Selection of lipids for incorporation into the lipoplexes is also crucially important [102–104].

SNALPs are made up of cationic and fusogenic lipids, which facilitate delivery to target cells and endosomal release of the siRNA cargos. These vectors have been employed to deliver siRNAs in guinea pigs [105], nonhuman primates [106] and mice [42]. In a study aimed at developing RNAi therapy for HBV, Morrissey *et al.* used SNALPs covered with PEG to provide a neutral, hydrophilic environment and to enhance particle stability [42]. Anti-HBV siRNAs formulated with SNALPs were injected intravenously following HDI of mice. siRNA–SNALPs improved HBV silencing compared with unformulated siRNA, and this was thought to be as a result of prolonged half-life *in vivo*. Administration of siRNA–SNALPs also suppressed serum levels of HBV DNA for up to 6 weeks when using a weekly dosing regimen [42].

In another study, Hean *et al.* employed a cationic lipoplex comprising a helper fusion lipid dioleoylphosphatidyl ethanolamine, liver-targeting cholesterol galactoside component and ANA-modified anti-HBV siRNAs. HBV silencing was achieved in transgenic mice without triggering the innate immune response or inducing toxicity in injected mice [43]. Other studies reported anti-HBV efficacy of unmodified siRNAs in lipoplex formulations [107,108]. Complexes included a polyamine-conjugated cholesterol [108] or an aminoxy cholesterol lipid to enable postcoupling of ‘stealth’ PEG moieties [107]. The vectors achieved passive hepatotropism, and silencing of HBV replication in HBV transgenic mice was observed over a period of 4 weeks [107].

Many polymer-based siRNA vectors achieve gene delivery by encapsulating and condensing nucleic acids into small particles that are taken up into cells by endocytosis [109]. Polymers have been used to administer plasmid DNA; however, the *in vivo* efficiency of this type of gene delivery system is modest. Understandably, interest

has shifted to focusing on use of polymers to deliver smaller siRNAs to their more accessible cytoplasmic site of action. As with lipid-based vectors, a RNA-binding cationic group of polymer carriers is an important feature. These cationic polymers may be divided into synthetic (e.g., polyethylenimine and poly-L-lysine) and natural (e.g., chitosan and cationic polypeptides) groups.

In a recent study, dynamic polyconjugates were designed to deliver siRNAs to hepatocytes of HBV transgenic mice and nonhuman primates [110]. This dynamic polyconjugates complex was targeted to liver cells using *N*-acetylgalactosamine-conjugated melittin-like peptide (NAG-MLP) as a ligand. In transgenic mice and nonhuman primates, HBV silencing efficacy of siRNAs was assessed by determining the concentration of the product of an endogenous hepatic target gene, coagulation factor VII (F7), in the plasma. In mice, administration of 0.01 mg/kg cholesterol–siRNA reduced F7 expression by approximately 50%, while a higher dose of 0.1 mg/kg cholesterol–siRNA suppressed F7 expression by approximately 97% at 48 h after injection. Additionally, HBsAg secretion was suppressed by approximately 80% for 4 weeks after coinjecting a combination of cholesterol and anti-HBV siRNA, while the level of viral particle equivalents decreased by approximately 90% for 4 weeks following single administration. Importantly, serum activities of liver-derived ALT, AST and alkaline phosphatase were not increased, even when a high dose of NAG-MLP was administered [110]. In nonhuman primates (cynomolgus monkeys), expression of F7 in the plasma was reduced by approximately 30–60% after coinjection with 1 mg/kg NAG-MLP and 2 mg/kg cholesterol–siRNA, while coinjection with 3 mg/kg NAG-MLP and 2 mg/kg cholesterol–siRNA resulted in approximately 97–99% knockdown in F7 expression. Interestingly, F7 expression in the plasma decreased by approximately 80% for at least 4 weeks without evidence of toxicity. Collectively, data from this study demonstrated that codelivery of NAG-MLP with cholesterol–siRNA suppresses HBV replication and expression of an endogenous gene in murine and nonhuman primate models, respectively. These observations suggest that the approach could be exploited to advance RNAi-based HBV therapy.

In a study conducted by Kim *et al.*, apoA-I, a high-density lipoprotein, was utilized in the liposomal formulation for siRNA administration to hepatocytes of transgenic HBV mice [111]. apoA-I

was formulated on the lipid bilayer surface of the cationic lipid 1,2-dioleoyl-3-trimethylammonium-propane. Additionally, the cholesterol moiety was included to confer liver tropism. Data from this study revealed that administration of a single dose of apolipoprotein-siRNAs (≤ 2 mg/kg) resulted in decreased expression of viral protein in injected mice for up to 8 days [111].

In the only Phase I clinical trial reported to date, a formulation termed NUC B1000 was evaluated for its safety and anti-HBV activity in individuals with chronic HBV infection [112]. Four different HBV-targeting shRNAs, encoded in a plasmid and complexed to cholesterol spermidine nanoparticles, were administered to patients. Recipients displayed side effects, such as pharyngitis, chills, muscle pain and fever, after approximately 4–7 h post-NUC B1000 administration (5 mg of a single DNA dose); however, these effects were attenuated after treatment with antipyretics. Furthermore, induction in IFN- γ and IL-10 was observed in two recipients, while an induction in IL-8 was observed in a single participant after NUC B1000 administration. Decreased concentrations of HBsAg and HBV DNA were not reported in this study and suggest that dose increment may be required to suppress markers of viral replication.

Viral vectors for HBV gene therapy

The three main types of recombinant viral vectors that have been used for delivery of anti-HBV-expressed sequences are adenoviruses (Ads), adeno-associated viruses (AAVs) and lentiviruses (reviewed in [113]). To date, analysis of efficacy has progressed to a stage of testing in murine models and currently there are no gene therapy clinical trials that use viral vectors against HBV infection.

Globally, Ads have been used in the majority of clinical trials that rely on viral vector delivery (over 430 trials, constituting 23% of viral vector trials) [201]. Ads have several features that are useful for delivery of anti-HBV expression cassettes. They are:

- Naturally hepatotropic;
- Capable of transducing dividing and non-dividing cells;
- Amenable to high titer preparation;
- Capable of packaging large DNA inserts of up to 32 kb in length;
- Compatible with modification by polymers;
- Rarely integrated into host chromosomes [114–117].

A drawback of the therapeutic use of Ads is their powerful stimulation of innate and adaptive immune responses. This property may result in serious toxicity and attenuation of transgene delivery to target tissues. Countering immunostimulation by Ads may be achieved by conjugation to polymers such as PEG [118], in addition to the removal of virus protein-coding sequences from first generation, Ads to propagate second generation Ads and third generation Ads (gutless or helper dependent [HD] Ads) [119]. To date, five studies have been reported that demonstrate the utility of Ads for delivering anti-HBV sequences [53,120–123]. Early results demonstrated that first generation Ads are capable of efficient delivery of RNAi expression cassettes to the liver, to cause >90% knockdown of markers of HBV replication [53,120]. However, the effect was limited by the transient nature of suppression. Subsequently, it was shown that the PEG-ylation of first generation Ads carrying Pol III shRNA expression cassettes improved vector safety and efficacy [121]. HD Ads have delivered HBV-silencing sequences, and differences in HBV replication inhibition are largely ascribed to variable antiviral efficacy of the transduced RNAi expression cassette [122,123]. Nevertheless, the prolonged expression of transgenes that may be achieved with HD Ads is an important feature that is potentially useful for the treatment of chronic HBV infection.

In contrast to Ad vectors, AAVs have far smaller ssDNA genomes of 4.7 kb [124]. Recombinant AAVs are attractive vectors for RNAi therapy as they:

- Are not associated with pathology;
- Have low immunostimulatory properties;
- Have broad tissue tropism;
- Are capable of transducing dividing and non-dividing cell lines;
- Persist episomally with low risk of integration into the host genome [125,126].

AAVs, like other viral vectors, are amenable to the combination of viral serotypes to produce chimeras (pseudotypes) with desired tissue tropism and immunoevasive properties. This may entail the combination of one AAV genome (typically AAV2), with the capsid of another AAV serotype. Chen *et al.* produced a self-complementary double-stranded AAV2/8 pseudotyped vector for the hepatotropic delivery of anti-HBV RNAi-activating sequences *in vivo* [127]. Significant knockdown was achieved that peaked at 21 days after vector administration. The silencing effect then waned over 4 months, and was

thought to have resulted from an immune response to the vector [127,128]. The group then went on to show that changing the vector capsid pseudotype to that of AAV2/9 overcame the immune response and re-established HBV silencing [128]. AAVs are gaining in popularity and have shown promise for liver gene therapy to treat hemophilia B [129]. Although AAVs are used in only 5% of worldwide gene therapy trials [201], this proportion is likely to increase in the near future.

Recombinant retroviral vectors (lentiviruses and γ -retroviruses) were the first vectors to be used to transduce hepatocytes [130] and the first to be used in clinical trials [131]. Proviruses derived from these vectors integrate into the host genome to enable long-term transgene expression [132]. Although stable transgene expression is a significant benefit of transduction by lentiviral vectors, modest efficiency of hepatocyte transduction following systemic administration has limited their use for HBV therapy. As a result, lentiviral vectors have been favored for gene therapy of inherited diseases and HIV-1 infection [133]. An application for these vectors to RNAi-based treatment of HBV infection may, however, be found with *ex vivo* delivery. This would entail transduction of hepatocytes in culture, followed by their reinfusion to repopulate HBV-infected livers with hepatocytes that express anti-HBV expression cassettes. Constitutive production of the HBV-silencing sequences should make the hepatocytes refractory to HBV infection and provide a selective growth advantage. *Ex vivo* engraftment of hepatocytes has been achieved in nonhuman primates [134,135] and in the treatment of hyperbilirubinemic Gunn rats [136]. The remarkable progress that has recently been made with propagating hepatocyte-like cells from induced pluripotent stem cells [137] suggests that an *ex vivo* approach to RNAi-based HBV therapy may be feasible in the near future.

An interesting alternative approach, termed a 'Trojan horse', introduced RNAi activators targeting HBV that were expressed from a recombinant HBV vector [138]. Successful knockdown of HBV gene expression in cultured hepatocytes was observed. The vector may be afforded immunoprotection by the Dane particles in an infected patient's blood; however, the clinical utility of this approach remains to be established.

Conclusion

Since the landmark discovery of RNAi-based gene silencing in 1998 [13], several studies have

reported on the successful harnessing of the pathway to inhibit pathology-causing genes. Since RNAi functions in metazoan cells and viruses are dependent on parasitizing cells for their gene expression and replication, silencing of viral mRNA is well-suited to countering viral infection. Dependence of HBV proliferation on a pgRNA replication intermediate, as well as viral protein-coding transcripts, make it a good candidate for RNAi-based therapy. However, despite the impressive pace at which development of RNAi-based HBV therapy has progressed, obstacles need to be overcome before this method of treatment becomes a reality. As nucleic acids, RNAi activators do not have the properties of traditional small molecule drugs, and they require vectors for delivery to target hepatocytes. This poses challenges for optimizing pharmacokinetics, dose regulation, efficacy following repeat vector administrations and evasion of immune stimulation. HBV silencing observed *in vitro* often does not correlate with inhibition of viral replication *in vivo*. Moreover, most cell culture and animal models of HBV replication that have been tested do not simulate all the steps of HBV infection in humans, and this complicates successful extrapolation to clinical trials [112].

Studies to date have reported on various approaches to countering replication of HBV, and different parts of the viral genome have been effectively targeted. It appears that there is no particularly favorable target within the viral genome. Synthetic and expressed RNAi activators have both been used successfully and each of the groups have their advantages and disadvantages. Although unmodified synthetic siRNAs achieve silencing of HBV replication in cultured cells and *in vivo*, inclusion of chemical moieties is useful to enhance their efficacy. Nevertheless, since siRNAs are not renewable within cells, repeated administrations of siRNA-containing nonviral vector formulations will be a requirement for their anti-HBV therapeutic utility. Expressed anti-HBV RNAi activators may provide more durable silencing than their synthetic counterparts, which is useful to inhibit HBV replication over a long period. However, the requirement for viral vectors to deliver anti-HBV expression cassettes poses additional problems. Safety is a particular concern and this has been highlighted by past experiences of using adenoviral and retroviral vectors for treatment of inherited diseases. Difficulties with large scale preparation of recombinant viral vectors pose another obstacle to clinical application.

It is unclear whether RNAi-based drugs will be capable of eradicating the troublesome HBV cccDNA replication intermediate. Advancing use of engineered nucleases is therefore particularly

appealing. The specificity and efficiency of target sequence cleavage by TALENs may well find useful application to disabling HBV cccDNA. Investigating synergies between gene silencing

Executive summary

Harnessing RNAi for therapeutic gene silencing

- RNAi is a conserved gene silencing pathway that is present in metazoan cells.
- Synthetic or expressed exogenous intermediates of the RNAi pathway may be introduced into cells to achieve silencing of pathology-causing genes.

Inhibiting HBV replication with synthetic activators of RNAi

- Incorporation of chemical modifications into anti-HBV siRNAs improves their silencing efficacy, specificity, stability and limits off-target effects *in vivo*.
- Anti-HBV siRNAs containing a combination of different chemical modifications was one of the first demonstrations of the therapeutic potential of RNAi-based gene silencing.
- Recently it has been shown that altritol nucleic acid-modified siRNAs attenuate immunostimulation without compromising efficacy *in vivo*.
- Incorporation of a 2'-O-guanidinopropyl moiety within siRNAs results in improved activity, stability and specificity in cell culture and *in vivo*.

Expressed RNAi activators against HBV infection

- RNAi activators can be expressed from both Pol II and Pol III promoters.
- Pol II expression cassettes may provide the advantage of regulated, tissue-tropic expression.
- RNAi is unlikely to remove covalently closed circular DNA (cccDNA), the replication intermediate responsible for reactivation of HBV replication following treatment withdrawal.

Alternatives to RNAi-based gene therapies

- Latent cccDNA pools may cause reactivation of viral replication after cessation of therapy.
- Targeted mutation of cccDNA with transcription activator-like effector nucleases or zinc finger nucleases in combination with anti-HBV RNAi-based therapies may provide synergy for treating the chronic infection.

In vitro & in vivo models of HBV infection

- Only the HepaRG cell line can be infected with HBV.
- Murine hydrodynamic injection and transgenic models simulate HBV replication, but not infection of hepatocytes and formation of cccDNA.
- The urokinase plasminogen activator severe combined immunodeficiency humanized mouse model is able to maintain cccDNA, thereby providing the most accurate murine HBV infection disease model currently available.

siRNA delivery systems

- Both lipid- and polymer-based vectors allow efficient delivery of siRNAs to target tissues.
- The cationic group is a critical component in both these approaches.
- Most siRNA delivery studies have utilized cationic liposomes as they have:
 - High transfection efficiency;
 - Improved pharmacokinetic properties;
 - Low immunostimulation and toxicity;
 - Well-established protocols for formulation.

Viral vectors for gene therapy

- Adenoviruses (Ads) are widely used in clinical trials, but are associated with powerful immunostimulation.
- Ads are efficiently hepatotropic, and have been used successfully to deliver HBV gene silencers to HBV transgenic mice.
- The small adeno-associated virus genome size may accommodate RNAi cassettes.
- Adeno-associated viruses are also less immunogenic than Ads and display liver tropism.
- Lentiviral vectors are not suitable for HBV therapy *in vivo*, but have potential use for *ex vivo* treatment strategies.

Conclusion

- Use of chemically modified siRNAs, RNAi expression cassettes and cccDNA-disabling engineered nucleases have potential for developing more effective HBV therapies.
- Efficient and safe delivery vectors are required to achieve the sustained HBV gene silencing required to treat the virus infection.
- Recent improvements in delivery vector design and models of HBV infection should fast track *in vivo* studies of gene therapy-based anti-HBV efficacy.

and other HBV therapeutic approaches will be interesting. Combination of RNAi-based treatment with sequence-specific nucleases may well provide the means for effectively eliminating the virus.

Future perspective

The EMA approved the first human gene therapy for commercial use in 2012. If this treatment of lipoprotein lipase deficiency proves successful, it is likely to pave the way for an upsurge of gene therapies for a wide variety of diseases. An anti-HBV gene therapy for chronically infected patients would be important to a large demographic in sub-Saharan Africa and parts of Asia, and potentially could diminish serious morbidity and mortality associated with the infection. The significant advances in nucleic acid vectorology, together with improvements in efficacy of antiviral sequences, are providing momentum to the field. Moreover, the availability of animal models that simulate human persistent HBV infection more closely should facilitate progress

to evaluation in a clinical setting. Both interferon and nucleotide/side analogs are expected to remain the primary HBV therapies for the foreseeable future. However, clinical application of gene therapy for HBV will no doubt lead to changes in treatment regimens, and future protocols may include combinations of the different treatment modalities.

Financial & competing interests disclosure

Work in the authors' laboratory is generously supported by funding from the Ernst & Ethel Eriksen Trust, National Research Foundation of South Africa (GUNS 81768, 81692, 68339, 85981 and 77954), South African Medical Research Council, South African Poliomyelitis Research Foundation and from the German Research Foundation. The authors have no other relevant affiliations or financial involvement with any organization or entity with a financial interest in or financial conflict with the subject matter or materials discussed in the manuscript apart from those disclosed.

No writing assistance was utilized in the production of this manuscript.

References

Papers of special note have been highlighted as:

▪ of interest

▪▪ of considerable interest

- Arbutnot P, Kew M. Hepatitis B virus and hepatocellular carcinoma. *Int. J. Exp. Pathol.* 82(2), 77–100 (2001).
- El-Serag HB, Rudolph KL. Hepatocellular carcinoma: epidemiology and molecular carcinogenesis. *Gastroenterology* 132(7), 2557–2576 (2007).
- Hollinger FB, Lau DT. Hepatitis B: the pathway to recovery through treatment. *Gastroenterol. Clin. N. Am.* 35(2), 425–461 (2006).
- Dienstag JL. Hepatitis B virus infection. *N. Engl. J. Med.* 359(14), 1486–1500 (2008).
- Lee WM. Hepatitis B virus infection. *N. Engl. J. Med.* 337(24), 1733–1745 (1997).
- Lepere-Douard C, Trotard M, Le Seyec J, Gripon P. The first transmembrane domain of the hepatitis B virus large envelope protein is crucial for infectivity. *J. Virol.* 83(22), 11819–11829 (2009).
- Weiser B, Ganem D, Seeger C, Varmus HE. Closed circular viral DNA and asymmetrical heterogeneous forms in livers from animals infected with ground squirrel hepatitis virus. *J. Virol.* 48(1), 1–9 (1983).
- Sohn JA, Litwin S, Seeger C. Mechanism for cccDNA synthesis in hepadnaviruses. *PLoS ONE* 4(11), e8093 (2009).
- Seeger C, Summers J, Mason WS. Viral DNA synthesis. *Curr. Top. Microbiol. Immunol.* 168, 41–60 (1991).
- Tuttleman JS, Pourcel C, Summers J. Formation of the pool of covalently closed circular viral DNA in hepadnavirus-infected cells. *Cell* 47(3), 451–460 (1986).
- Birnbaum F, Nassal M. Hepatitis B virus nucleocapsid assembly: primary structure requirements in the core protein. *J. Virol.* 64(7), 3319–3330 (1990).
- Huovila AP, Eder AM, Fuller SD. Hepatitis B surface antigen assembles in a post-ER, pre-Golgi compartment. *J. Cell Biol.* 118(6), 1305–1320 (1992).
- Fire A, Xu S, Montgomery MK *et al.* Potent and specific genetic interference by double-stranded RNA in *Caenorhabditis elegans*. *Nature* 391(6669), 806–811 (1998).
- Provided the original description of gene silencing by dsRNA.**
- Ambros V. The functions of animal microRNAs. *Nature* 431(7006), 350–355 (2004).
- Reynolds A, Leake D, Boese Q *et al.* Rational siRNA design for RNA interference. *Nat. Biotechnol.* 22(3), 326–330 (2004).
- Song JJ, Smith SK, Hannon GJ, Joshua-Tor L. Crystal structure of Argonaute and its implications for RISC slicer activity. *Science* 305(5689), 1434–1437 (2004).
- Sen GL, Blau HM. Argonaute 2/RISC resides in sites of mammalian mRNA decay known as cytoplasmic bodies. *Nat. Cell Biol.* 7(6), 633–636 (2005).
- Guo H, Ingolia NT, Weissman JS, Bartel DP. Mammalian microRNAs predominantly act to decrease target mRNA levels. *Nature* 466(7308), 835–840 (2010).
- Lewis BP, Shih IH, Jones-Rhoades MW, Bartel DP, Burge CB. Prediction of mammalian microRNA targets. *Cell* 115(7), 787–798 (2003).
- Sun D, Rosler C, Kidd-Ljunggren K, Nassal M. Quantitative assessment of the antiviral potencies of 21 shRNA vectors targeting conserved, including structured, hepatitis B virus sites. *J. Hepatol.* 52(6), 817–826 (2010).
- Ely A, Naidoo T, Mufamadi S, Crowther C, Arbutnot P. Expressed anti-HBV primary microRNA shuttles inhibit viral replication efficiently *in vitro* and *in vivo*. *Mol. Ther. J. Am. Soc. Gene Ther.* 16(6), 1105–1112 (2008).
- Use of Pol II promoters for the expression of anti-HBV primary miRNA mimics was described here.**
- Giladi H, Ketzinel-Gilad M, Rivkin L *et al.* Small interfering RNA inhibits hepatitis B virus replication in mice. *Mol. Ther. J. Am. Soc. Gene Ther.* 8(5), 769–776 (2003).
- Shlomai A, Shaul Y. Inhibition of hepatitis B virus expression and replication by RNA interference. *Hepatology* 37(4), 764–770 (2003).

24. Carmona S, Ely A, Crowther C *et al.* Effective inhibition of HBV replication *in vivo* by anti-HBx short hairpin RNAs. *Mol. Ther. J. Am. Soc. Gene Ther.* 13(2), 411–421 (2006).
25. Keck K, Volper EM, Spengler RM *et al.* Rational design leads to more potent RNA interference against hepatitis B virus: factors effecting silencing efficiency. *Mol. Ther. J. Am. Soc. Gene Ther.* 17(3), 538–547 (2009).
26. Klein C, Bock CT, Wedemeyer H *et al.* Inhibition of hepatitis B virus replication *in vivo* by nucleoside analogues and siRNA. *Gastroenterology* 125(1), 9–18 (2003).
27. Konishi M, Wu CH, Wu GY. Inhibition of HBV replication by siRNA in a stable HBV-producing cell line. *Hepatology* 38(4), 842–850 (2003).
28. Qian ZK, Xuan BQ, Min TS *et al.* Cost-effective method of siRNA preparation and its application to inhibit hepatitis B virus replication in HepG2 cells. *World J. Gastroenterol.* 11(9), 1297–1302 (2005).
29. Hamasaki K, Nakao K, Matsumoto K *et al.* Short interfering RNA-directed inhibition of hepatitis B virus replication. *FEBS Lett.* 543(1–3), 51–54 (2003).
30. Elbashir SM, Harborth J, Lendeckel W *et al.* Duplexes of 21-nucleotide RNAs mediate RNA interference in cultured mammalian cells. *Nature* 411(6836), 494–498 (2001).
- **This fundamental article was the first to demonstrate that synthetic short duplex RNA could be used to activate gene silencing with exogenous sequences.**
31. Hoerter JA, Walter NG. Chemical modification resolves the asymmetry of siRNA strand degradation in human blood serum. *RNA* 13(11), 1887–1893 (2007).
32. Robbins M, Judge A, Ambegia E *et al.* Misinterpreting the therapeutic effects of small interfering RNA caused by immune stimulation. *Hum. Gene Ther.* 19(10), 991–999 (2008).
33. Han Q, Zhang C, Zhang J, Tian Z. Involvement of activation of PKR in HBx-siRNA-mediated innate immune effects on HBV inhibition. *PLoS ONE* 6(12), e27931 (2011).
34. Khvorova A, Reynolds A, Jayasena SD. Functional siRNAs and miRNAs exhibit strand bias. *Cell* 115(2), 209–216 (2003).
35. Schwarz DS, Hutvagner G, Du T *et al.* Asymmetry in the assembly of the RNAi enzyme complex. *Cell* 115(2), 199–208 (2003).
36. Engels JW, Odadzic D, Smicic R, Haas J. Chemical synthesis of 2'-O-alkylated siRNAs. *Methods Mol. Biol.* 623, 155–170 (2010).
37. Bramsen JB, Laursen MB, Nielsen AF *et al.* A large-scale chemical modification screen identifies design rules to generate siRNAs with high activity, high stability and low toxicity. *Nucleic Acids Res.* 37(9), 2867–2881 (2009).
- **This article, as well as [38], describes rules that can be applied to optimizing efficacy of chemically modified synthetic siRNAs.**
38. Bramsen JB, Pakula MM, Hansen TB *et al.* A screen of chemical modifications identifies position-specific modification by UNA to most potently reduce siRNA off-target effects. *Nucleic Acids Res.* 38(17), 5761–5773 (2010).
- **This article, as well as [37], describes rules that can be applied to optimizing efficacy of chemically modified synthetic siRNAs.**
39. Fisher M, Abramov M, Van Aerschot A *et al.* Biological effects of hexitol and alditrol-modified siRNAs targeting B-Raf. *Eur. J. Pharmacol.* 606(1–3), 38–44 (2009).
40. Fisher M, Abramov M, Van Aerschot A *et al.* Inhibition of MDR1 expression with alditrol-modified siRNAs. *Nucleic Acids Res.* 35(4), 1064–1074 (2007).
41. Hall AH, Wan J, Shaughnessy EE, Ramsay Shaw B, Alexander KA. RNA interference using boranophosphate siRNAs: structure-activity relationships. *Nucleic Acids Res.* 32(20), 5991–6000 (2004).
42. Morrissey DV, Lockridge JA, Shaw L *et al.* Potent and persistent *in vivo* anti-HBV activity of chemically modified siRNAs. *Nat. Biotechnol.* 23(8), 1002–1007 (2005).
- **One of the first comprehensive demonstrations that HBV may be inhibited *in vivo* using a RNAi-based gene silencing mechanism.**
43. Hean J, Crowther C, Ely A *et al.* Inhibition of hepatitis B virus replication *in vivo* using lipoplexes containing alditrol-modified antiviral siRNAs. *Artif. DNA PNA XNA* 1(1), 17–26 (2010).
44. Brzezinska J, D'Onofrio J, Buff MC *et al.* Synthesis of 2'-O-guanidinopropyl-modified nucleoside phosphoramidites and their incorporation into siRNAs targeting hepatitis B virus. *Bioorg. Med. Chem.* 20(4), 1594–1606 (2012).
45. Marimani M, Ely A, Bernhardt S *et al.* Inhibition of hepatitis B virus replication in cultured cells and *in vivo* using 2'-O-guanidinopropyl modified siRNAs. *Bioorg. Med. Chem.* doi:10.1016/j.bmc.2013.04.073 (2013) (Epub ahead of print).
46. Brunetti-Pierri N, Stapleton GE, Law M *et al.* Efficient, long-term hepatic gene transfer using clinically relevant HDAd doses by balloon occlusion catheter delivery in nonhuman primates. *Mol. Ther. J. Am. Soc. Gene Ther.* 17(2), 327–333 (2008).
47. Reddy R. Transcription of a U6 small nuclear RNA gene *in vitro*. Transcription of a mouse U6 small nuclear RNA gene *in vitro* by RNA polymerase III is dependent on transcription factor(s) different from transcription factors IIIA, IIIB, and IIIC. *J. Biol. Chem.* 263(31), 15980–15984 (1988).
48. McCaffrey AP. Inhibition of hepatitis B virus in mice by RNA interference. *Nat. Biotechnol.* 21(639–21644) (2003).
49. Kim YH, Lee JH, Paik NW, Rho HM. RNAi-based knockdown of HBx mRNA in HBx-transformed and HBV-producing human liver cells. *DNA Cell Biol.* 25(7), 412–417 (2006).
50. Weinberg MS, Ely A, Barichev S *et al.* Specific inhibition of HBV replication *in vitro* and *in vivo* with expressed long hairpin RNA. *Mol. Ther. J. Am. Soc. Gene Ther.* 15(3), 534–541 (2007).
51. Ren X, Luo G, Xie Z *et al.* Inhibition of multiple gene expression and virus replication of HBV by stable RNA interference in 2.2.15 cells. *J. Hepatol.* 44(4), 663–670 (2006).
52. Ren XR, Zhou LJ, Luo GB, Lin B, Xu A. Inhibition of hepatitis B virus replication in 2.2.15 cells by expressed shRNA. *J. Viral Hepat.* 12(3), 236–242 (2005).
53. Uprichard SL, Boyd B, Althage A, Chisari FV. Clearance of hepatitis B virus from the liver of transgenic mice by short hairpin RNAs. *Proc. Natl Acad. Sci. USA* 102(3), 773–778 (2005).
- **Efficacy in HBV transgenic mice of recombinant adenoviruses expressing anti-HBV sequences was demonstrated.**
54. Dyer V, Ely A, Bloom K, Weinberg M, Arbuthnot P. tRNA Lys3 promoter cassettes that efficiently express RNAi-activating antihepatitis B virus short hairpin RNAs. *Biochem. Biophys. Res. Commun.* 398(4), 640–646 (2010).
55. Blazquez L, Gonzalez-Rojas SJ, Abad A *et al.* Increased *in vivo* inhibition of gene expression by combining RNA interference and U1 inhibition. *Nucleic Acids Res.* 40(1), e8 (2012).
56. Blazquez L, Fortes P. U1 snRNP control of 3'-end processing and the therapeutic application of U1 inhibition combined with RNA interference. *Curr. Mol. Med.* 13(7), 1203–1216 (2013).
57. Chen Y, Du D, Wu J *et al.* Inhibition of hepatitis B virus replication by stably expressed shRNA. *Biochem. Biophys. Res. Commun.* 311(2), 398–404 (2003).
58. Bian Z, Xiao A, Cao M *et al.* Anti-HBV efficacy of combined siRNAs targeting viral

- gene and heat shock cognate 70. *Viol. J.* 9, 275 (2012).
59. Grimm D, Streetz KL, Jopling CL *et al.* Fatality in mice due to oversaturation of cellular microRNA/short hairpin RNA pathways. *Nature* 441(7092), 537–541 (2006).
- **The toxicity caused by overexpression of anti-HBV shRNAs, which results from saturation of the endogenous RNAi pathway, was shown in this study.**
60. Czauderna F, Santel A, Hinz M *et al.* Inducible shRNA expression for application in a prostate cancer mouse model. *Nucleic Acids Res.* 31(21), e127 (2003).
61. Ely A, Naidoo T, Arbutnot P. Efficient silencing of gene expression with modular trimeric Pol II expression cassettes comprising microRNA shuttles. *Nucleic Acids Res.* 37(13), e91 (2009).
- **Describes the use of polycistronic artificial primary miRNAs to target three different HBV sites simultaneously.**
62. ter Brake O, 't Hooft K, Liu YP, Centlivre M, von Eije KJ, Berkhout B. Lentiviral vector design for multiple shRNA expression and durable HIV-1 inhibition. *Mol. Ther. J. Am. Soc. Gene Ther.* 16(3), 557–564 (2008).
63. Berkhout B. Toward a durable anti-HIV gene therapy based on RNA interference. *Ann. N.Y. Acad. Sci.* 1175, 3–14 (2009).
64. Xia C, Chen YC, Gong H *et al.* Inhibition of hepatitis B virus gene expression and replication by ribonuclease. *Mol. Ther. J. Am. Soc. Gene Ther.* 21(5), 995–1003 (2013).
65. Caruntu FA, Molagic V. cccDNA persistence during natural evolution of chronic VHB infection. *Rom. J. Gastroenterol.* 14(4), 373–377 (2005).
66. Zoulim F. Antiviral therapy of chronic hepatitis B: can we clear the virus and prevent drug resistance? *Antivir. Chem. Chemother.* 15(6), 299–305 (2004).
67. Zimmerman KA, Fischer KP, Joyce MA, Tyrrell DL. Zinc finger proteins designed to specifically target duck hepatitis B virus covalently closed circular DNA inhibit viral transcription in tissue culture. *J. Virol.* 82(16), 8013–8021 (2008).
68. Klug A. The discovery of zinc fingers and their applications in gene regulation and genome manipulation. *Annu. Rev. Biochem.* 79, 213–231 (2010).
69. Kim YG, Cha J, Chandrasegaran S. Hybrid restriction enzymes: zinc finger fusions to Fok I cleavage domain. *Proc. Natl Acad. Sci. USA* 93(3), 1156–1160 (1996).
70. Cathomen T, Joung JK. Zinc-finger nucleases: the next generation emerges. *Mol. Ther. J. Am. Soc. Gene Ther.* 16(7), 1200–1207 (2008).
71. Cradick TJ, Keck K, Bradshaw S, Jamieson AC, McCaffrey AP. Zinc-finger nucleases as a novel therapeutic strategy for targeting hepatitis B virus DNAs. *Mol. Ther. J. Am. Soc. Gene Ther.* 18(5), 947–954 (2010).
- **Utility of covalently closed circular DNA-specific zinc finger nucleases for HBV therapy was described.**
72. Bogdanove AJ, Voytas DF. TAL effectors: customizable proteins for DNA targeting. *Science* 333(6051), 1843–1846 (2011).
73. Mussolino C, Cathomen T. TALE nucleases: tailored genome engineering made easy. *Curr. Opin. Biotechnol.* 23(5), 644–650 (2012).
74. Jinek M, Chylinski K, Fonfara I *et al.* A programmable dual-RNA-guided DNA endonuclease in adaptive bacterial immunity. *Science* 337(6096), 816–821 (2012).
75. Wiedenheft B, Sternberg SH, Doudna JA. RNA-guided genetic silencing systems in bacteria and archaea. *Nature* 482(7385), 331–338 (2012).
76. Ramirez CL, Foley JE, Wright DA *et al.* Unexpected failure rates for modular assembly of engineered zinc fingers. *Nat. Methods* 5(5), 374–375 (2008).
77. Sander JD, Dahlborg EJ, Goodwin MJ *et al.* Selection-free zinc-finger-nuclease engineering by context-dependent assembly (CoDA). *Nat. Methods* 8(1), 67–69 (2010).
78. Moscou MJ, Bogdanove AJ. A simple cipher governs DNA recognition by TAL effectors. *Science* 326(5959), 1501 (2009).
79. Mussolino C, Morbitzer R, Lutge F *et al.* A novel TALE nuclease scaffold enables high genome editing activity in combination with low toxicity. *Nucleic Acids Res.* 39(21), 9283–9293 (2011).
80. Cho SW, Kim S, Kim JM, Kim JS. Targeted genome engineering in human cells with the Cas9 RNA-guided endonuclease. *Nat. Biotechnol.* 31(3), 230–232 (2013).
81. Cong L, Ran FA, Cox D *et al.* Multiplex genome engineering using CRISPR/Cas systems. *Science* 339(6121), 819–823 (2013).
82. Hwang WY, Fu Y, Reyon D *et al.* Efficient genome editing in zebrafish using a CRISPR–Cas system. *Nat. Biotechnol.* 31(3), 227–229 (2013).
83. Jinek M, East A, Cheng A *et al.* RNA-programmed genome editing in human cells. *Elife* 2, e00471 (2013).
84. Mali P, Yang L, Esvelt KM *et al.* RNA-guided human genome engineering via Cas9. *Science* 339(6121), 823–826 (2013).
85. Qi LS, Larson MH, Gilbert LA *et al.* Repurposing CRISPR as an RNA-guided platform for sequence-specific control of gene expression. *Cell* 152(5), 1173–1183 (2013).
86. Schiffer JT, Aubert M, Weber ND *et al.* Targeted DNA mutagenesis for the cure of chronic viral infections. *J. Virol.* 86(17), 8920–8936 (2012).
87. Gripon P, Rumin S, Urban S *et al.* Infection of a human hepatoma cell line by hepatitis B virus. *Proc. Natl Acad. Sci. USA* 99(24), 15655–15660 (2002).
88. Yan H, Zhong G, Xu G *et al.* Sodium taurocholate cotransporting polypeptide is a functional receptor for human hepatitis B and D virus. *eLife* 1, e00049 (2012).
89. Zhong G, Yan H, Wang H *et al.* Sodium taurocholate cotransporting polypeptide mediates woolly monkey hepatitis B virus infection of Tupaia hepatocytes. *J. Virol.* 87(12), 7176–7184 (2013).
90. Liu F, Song YK, Liu D. Hydrodynamics-based transfection in animals by systemic administration of plasmid DNA. *Gene Ther.* 6(7), 1258–1266 (1999).
91. Yang PL, Althage A, Chung J, Chisari FV. Hydrodynamic injection of viral DNA: a mouse model of acute hepatitis B virus infection. *Proc. Natl Acad. Sci. USA* 99(21), 13825–13830 (2002).
92. Marion PL, Salazar FH, Liittschwager K *et al.* A transgenic mouse lineage useful for testing antivirals targeting hepatitis B virus. In: *Frontiers in Viral Hepatitis*. Schinazi RF, Sommadossi JP, Rice CM (Eds). Elsevier, Amsterdam, The Netherlands, 18, 197–210 (2003).
93. Meuleman P, Leroux-Roels G. The human liver-uPA-SCID mouse: a model for the evaluation of antiviral compounds against HBV and HCV. *Antiviral Res.* 80(3), 231–238 (2008).
94. Summers J, Smolec JM, Snyder R. A virus similar to human hepatitis B virus associated with hepatitis and hepatoma in woodchucks. *Proc. Natl Acad. Sci. USA* 75(9), 4533–4537 (1978).
95. Mason WS, Seal G, Summers J. Virus of Pekin ducks with structural and biological relatedness to human hepatitis B virus. *J. Virol.* 36(3), 829–836 (1980).
96. Korba BE, Cote P, Hornbuckle W, Tennant BC, Gerin JL. Treatment of chronic woodchuck hepatitis virus infection in the eastern woodchuck (*Marmota monax*) with nucleoside analogues is predictive of therapy for chronic hepatitis B virus infection in humans. *Hepatology* 31(5), 1165–1175 (2000).
97. Zoulim F, Berthillon P, Guerhier FL *et al.* Animal models for the study of HBV

- infection and the evaluation of new anti-HBV strategies. *J. Gastroenterol. Hepatol.* 17, S460–S463 (2002).
98. Roggendorf M, Yang D, Lu M. The woodchuck: a model for therapeutic vaccination against hepadnaviral infection. *Pathol. Biol.* 58(4), 308–314 (2010).
99. Tseng YC, Mozumdar S, Huang L. Lipid-based systemic delivery of siRNA. *Adv. Drug Deliv. Rev.* 61(9), 721–731 (2009).
100. Tiemann K, Rossi JJ. RNAi-based therapeutics – current status, challenges and prospects. *EMBO Mol. Med.* 1(3), 142–151 (2009).
101. Schroeder A, Levins CG, Cortez C, Langer R, Anderson DG. Lipid-based nanotherapeutics for siRNA delivery. *J. Intern. Med.* 267(1), 9–21 (2010).
102. Kim HS, Song IH, Kim JC *et al.* *In vitro* and *in vivo* gene-transferring characteristics of novel cationic lipids, DMKD (O,O'-dimyristyl-N-lysyl aspartate) and DMKE (O,O'-dimyristyl-N-lysyl glutamate). *J. Control. Release* 115(2), 234–241 (2006).
103. Obata Y, Suzuki D, Takeoka S. Evaluation of cationic assemblies constructed with amino acid based lipids for plasmid DNA delivery. *Bioconjug. Chem.* 19(5), 1055–1063 (2008).
104. Lv H, Zhang S, Wang B, Cui S, Yan J. Toxicity of cationic lipids and cationic polymers in gene delivery. *J. Control. Release: Official J. Control. Release Soc.* 114(1), 100–109 (2006).
105. Geisbert TW, Hensley LE, Kagan E *et al.* Postexposure protection of guinea pigs against a lethal ebola virus challenge is conferred by RNA interference. *J. Infect. Dis.* 193(12), 1650–1657 (2006).
106. Geisbert TW, Lee AC, Robbins M *et al.* Postexposure protection of non-human primates against a lethal Ebola virus challenge with RNA interference: a proof-of-concept study. *Lancet* 375(9729), 1896–1905 (2010).
107. Carmona S, Jorgensen MR, Kolli S *et al.* Controlling HBV replication *in vivo* by intravenous administration of triggered PEGylated siRNA-nanoparticles. *Mol. Pharm.* 6(3), 706–717 (2009).
108. Islam RU, Hean J, van Otterlo WA, de Koning CB, Arbuthnot P. Efficient nucleic acid transduction with lipoplexes containing novel piperazine- and polyamine-conjugated cholesterol derivatives. *Bioorg. Med. Chem. Lett.* 19(1), 100–103 (2009).
109. Gary DJ, Puri N, Won YY. Polymer-based siRNA delivery: perspectives on the fundamental and phenomenological distinctions from polymer-based DNA delivery. *J. Control. Release: Official J. Control. Release Soc.* 121(1–2), 64–73 (2007).
110. Wooddell CI, Rozema DB, Hossbach M *et al.* Hepatocyte-targeted RNAi therapeutics for the treatment of chronic hepatitis B virus infection. *Mol. Ther. J. Am. Soc. Gene Ther.* 21(5), 973–985 (2013).
- **Describes the efficacy of siRNA complexes for targeting gene silencing in nonhuman primates.**
111. Kim SI, Shin D, Choi TH *et al.* Systemic and specific delivery of small interfering RNAs to the liver mediated by apolipoprotein A-I. *Mol. Ther. J. Am. Soc. Gene Ther.* 15(6), 1145–1152 (2007).
112. Gish RG, Satishchandran C, Young M, Pachuk C. RNA interference and its potential applications to chronic HBV treatment: results of a Phase I safety and tolerability study. *Antiviral Ther.* 16(4), 547–554 (2011).
- **RNAi-based therapy of HBV was investigated in this Phase I trial.**
113. Ivacic D, Ely A, Arbuthnot P. Countering hepatitis B virus infection using RNAi: how far are we from the clinic? *Rev. Med. Virol.* 21(6), 383–396 (2011).
114. Ehrhardt A, Xu H, Kay MA. Episomal persistence of recombinant adenoviral vector genomes during the cell cycle *in vivo*. *J. Virol.* 77(13), 7689–7695 (2003).
115. Khare R, Chen CY, Weaver EA, Barry MA. Advances and future challenges in adenoviral vector pharmacology and targeting. *Curr. Gene Ther.* 11(4), 241–258 (2011).
116. Rauschhuber C, Noske N, Ehrhardt A. New insights into stability of recombinant adenovirus vector genomes in mammalian cells. *Eur. J. Cell Biol.* 91(1), 2–9 (2012).
117. Mowa MB, Crowther C, Arbuthnot P. Therapeutic potential of adenoviral vectors for delivery of expressed RNAi activators. *Expert Opin. Drug Deliv.* 7(12), 1373–1385 (2010).
118. Kreppel F, Kochanek S. Modification of adenovirus gene transfer vectors with synthetic polymers: a scientific review and technical guide. *Mol. Ther. J. Am. Soc. Gene Ther.* 16(1), 16–29 (2008).
119. Palmer DJ, Ng P. Methods for the production of helper-dependent adenoviral vectors. *Methods Mol. Biol.* 43, 333–353 (2008).
120. Carmona S, Ely A, Crowther C *et al.* Effective inhibition of HBV replication *in vivo* by anti-HBx short hairpin RNAs. *Mol. Ther.* 13(2), 411–421 (2006).
121. Crowther C, Ely A, Hornby J *et al.* Efficient inhibition of hepatitis B virus replication *in vivo*, using polyethylene glycol-modified adenovirus vectors. *Hum. Gene Ther.* 19(11), 1325–1331 (2008).
122. Mowa MB, Crowther C, Ely A, Arbuthnot P. Efficient silencing of hepatitis B virus by helper-dependent adenovirus vector-mediated delivery of artificial antiviral primary micro RNAs. *Micro RNA* 1, 19–25 (2012).
123. Rauschhuber C, Xu H, Salazar FH, Marion PL, Ehrhardt A. Exploring gene-deleted adenoviral vectors for delivery of short hairpin RNAs and reduction of hepatitis B virus infection in mice. *J. Gene Med.* 10(8), 878–889 (2008).
124. Srivastava A, Lusby EW, Berns KI. Nucleotide sequence and organization of the adeno-associated virus 2 genome. *J. Virol.* 45(2), 555–564 (1983).
125. Hauck B, Zhao W, High K, Xiao W. Intracellular viral processing, not single-stranded DNA accumulation, is crucial for recombinant adeno-associated virus transduction. *J. Virol.* 78(24), 13678–13686 (2004).
126. Schnepf BC, Jensen RL, Chen CL, Johnson PR, Clark KR. Characterization of adeno-associated virus genomes isolated from human tissues. *J. Virol.* 79(23), 14793–14803 (2005).
127. Chen CC, Ko TM, Ma HI *et al.* Long-term inhibition of hepatitis B virus in transgenic mice by double-stranded adeno-associated virus 8-delivered short hairpin RNA. *Gene Ther.* 14(1), 11–19 (2006).
128. Chen CC, Sun CP, Ma HI *et al.* Comparative study of anti-hepatitis B virus RNA interference by double-stranded adeno-associated virus serotypes 7, 8, and 9. *Mol. Ther. J. Am. Soc. Gene Ther.* 17(2), 352–359 (2009).
- **Demonstrates the efficacy of recombinant adeno-associated viruses for therapy of HBV.**
129. Nathwani AC, Tuddenham EG, Rangarajan S *et al.* Adenovirus-associated virus vector-mediated gene transfer in hemophilia B. *N. Engl. J. Med.* 365(25), 2357–2365 (2011).
130. Ferry N, Duplessis O, Houssin D, Danos O, Heard JM. Retroviral-mediated gene transfer into hepatocytes *in vivo*. *Proc. Natl Acad. Sci. USA* 88(19), 8377–8381 (1991).
131. Hacein-Bey-Abina S, Le Deist F, Carlier F *et al.* Sustained correction of X-linked severe combined immunodeficiency by *ex vivo* gene therapy. *N. Engl. J. Med.* 346(16), 1185–1193 (2002).
132. Verma IM, Weitzman MD. Gene therapy: twenty-first century medicine. *Annu. Rev. Biochem.* 74, 711–738 (2005).
133. Liu YP, Berkhout B. Lentiviral delivery of RNAi effectors against HIV-1. *Curr. Top. Med. Chem.* 9(12), 1130–1143 (2009).
134. Menzel O, Birraux J, Wildhaber BE *et al.* Biosafety in *ex vivo* gene therapy and

- conditional ablation of lentivirally transduced hepatocytes in nonhuman primates. *Mol. Ther. J. Am. Soc. Gene Ther.* 17(10), 1754–1760 (2009).
135. Birraux J, Menzel O, Wildhaber B *et al.* A step toward liver gene therapy: efficient correction of the genetic defect of hepatocytes isolated from a patient with Crigler-Najjar syndrome type 1 with lentiviral vectors. *Transplantation* 87(7), 1006–1012 (2009).
136. Nguyen TH, Birraux J, Wildhaber B *et al.* *Ex vivo* lentivirus transduction and immediate transplantation of uncultured hepatocytes for treating hyperbilirubinemic Gunn rat. *Transplantation* 82(6), 794–803 (2006).
137. Huang P, He Z, Ji S *et al.* Induction of functional hepatocyte-like cells from mouse fibroblasts by defined factors. *Nature* 475(7356), 386–389 (2011).
138. Shlomai A, Lubelsky Y, Har-Noy O, Shaul Y. The “Trojan horse” model-delivery of anti-HBV small interfering RNAs by a recombinant HBV vector. *Biochem. Biophys. Res. Commun.* 390(3), 619–623 (2009).
139. Arbuthnot P. Harnessing RNA interference for the treatment of viral infections. *Drug News Perspect.* 23(6), 341–350 (2010)

Website

201. Edelstein M. Gene therapy clinical trials worldwide (2012). www.abedia.com/wiley/vectors.php

CHAPTER 4

PUBLICATION 2

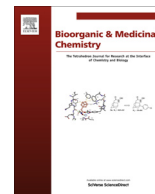
Inhibition of hepatitis B virus replication in cultured cells and *in vivo* using 2'-*O*-guanidinopropyl modified siRNAs

Musa D. Marimani, Abdullah Ely, Maximilian C.R. Buff, Stefan Bernhardt, Joachim W. Engels, Patrick Arbuthnot

Bioorganic and Medicinal Chemistry **21**: 6145-6155 (2013).

The article describes utility of GP-modified siRNAs by assessing their activity, stability, toxicity and specificity in cultured Human hepatoma 7 (Huh7) cells. The siRNAs harbouring the GP moiety at position 10, 17, 18 and 21 displayed improved antiHBV activity following co-transfection with pCH-9/3091 plasmid in Huh7 cells. This enhanced antiviral activity was achieved without inducing toxicity or innate immune stimulation, as assessed by MTT assay and RT-qPCR, respectively. Antiviral activity of modified siRNAs was also observed in HDI mice following administration of these therapeutic agents with an HBV plasmid vector. Evidence for improved antiHBV activity and target specificity suggests that incorporation of novel GP groups into siRNAs may be used as a strategy of advancing their therapeutic utility.

Author's contribution: Musa Marimani performed all biological experiments, analysed data and contributed to writing the manuscript. Prof. Arbuthnot and Dr. Ely supervised the project and also assisted with writing the paper. Our German collaborators: Prof. Engels, Dr. Buff and Mr. Bernhardt synthesised GP-modified siRNAs, performed high performance liquid chromatography (HPLC) and all experiments related to siRNA analysis, and also contributed in compiling the manuscript.



Inhibition of hepatitis B virus replication in cultured cells and in vivo using 2'-O-guanidinopropyl modified siRNAs



Musa D. Marimani^a, Abdullah Ely^a, Maximilian C. R. Buff^b, Stefan Bernhardt^b, Joachim W. Engels^{b,*}, Patrick Arbuthnot^{a,*}

^a Antiviral Gene Therapy Research Unit and African Network for Drugs and Diagnostics Innovation (ANDI) Centre of Excellence, School of Pathology, Health Sciences Faculty, University of the Witwatersrand, Private Bag 3, Wits, 2050 Johannesburg, South Africa

^b Goethe-University, Institute of Organic Chemistry & Chemical Biology, Max-von-Laue-Str. 7, 60438 Frankfurt am Main, Germany

ARTICLE INFO

Article history:

Available online 7 May 2013

Keywords:

HBV
RNAi
siRNAs
2'-O-Guanidinopropyl

ABSTRACT

Silencing hepatitis B virus (HBV) gene expression with exogenous activators of the RNA interference (RNAi) pathway has shown promise as a new mode of treating infection with the virus. However, optimizing efficacy, specificity, pharmacokinetics and stability of RNAi activators remains a priority before clinical application of this promising therapeutic approach is realised. Chemical modification of synthetic short interfering RNAs (siRNAs) provides the means to address these goals. This study aimed to assess the benefits of incorporating nucleotides with 2'-O-guanidinopropyl (GP) modifications into siRNAs that target HBV. Single GP residues were incorporated at nucleotide positions from 2 to 21 of the antisense strand of a previously characterised effective antiHBV siRNA. When tested in cultured cells, siRNAs with GP moieties at selected positions improved silencing efficacy. Stability of chemically modified siRNAs in 80% serum was moderately improved and better silencing effects were observed without evidence for toxicity or induction of an interferon response. Moreover, partially complementary target sequences were less susceptible to silencing by siRNAs with GP residues located in the seed region. Hydrodynamic co-injection of siRNAs with a replication-competent HBV plasmid resulted in highly effective knock down of markers of viral replication in mice. Evidence for improved efficacy, reduced off target effects and good silencing in vivo indicate that GP-modifications of siRNAs may be used to enhance their therapeutic utility.

© 2013 Elsevier Ltd. All rights reserved.

1. Introduction

Hepatitis B virus (HBV) infects the liver and may cause acute or chronic hepatitis. (reviewed in^{1,2}) Infection during early life, which may occur perinatally or as a result of horizontal spread in children, carries a high risk for chronicity. Globally it is now estimated that 350 million people are chronically infected with HBV. These individuals have an increased likelihood of developing complicating cirrhosis and hepatocellular carcinoma. Current drugs that have been approved for HBV treatment include the nucleotide and nucleoside analogues, which act by inhibiting the viral reverse transcriptase, as well as the immunomodulators, interferon alpha-2a and PEGylated interferon alpha-2a.³ Although these drugs are capable of suppressing viral replication to reduce liver damage, a limitation is that they rarely clear the infection. Development of

more effective drugs that are capable of eliminating HBV therefore remains an important priority.

Harnessing the RNA interference (RNAi) pathway has been shown to inhibit HBV gene expression effectively and is believed to have therapeutic potential. (reviewed in^{4,5}) RNAi is a natural gene silencing mechanism that occurs in cells of a variety of organisms including mammals, fungi and plants. (reviewed in^{6,7}) Naturally, expression of primary microRNAs (pri-miRNAs) initiates activation of this pathway. Cleavage of pri-miRNAs by the nuclear microprocessor complex, comprising Drosha and DGCR8, then results in formation of precursor miRNA (pre-miRNA) hairpins. After transport of these hairpins to the cytoplasm, they are processed by Dicer to form short duplex microRNAs (miRNAs) of about 23 base pairs. Incorporation of a miRNA into the RNA Induced Silencing Complex (RISC) is followed by selection of one of the two RNA strands to serve as a guide sequence for mRNA inactivation. Complete base-pairing between a guide and its cognate leads to mRNA degradation, while partial base-pairing leads to translational suppression. To silence HBV gene expression, the RNAi pathway can be reprogrammed with exogenous mimics that encode HBV-targeting guides. DNA cassettes that express antiHBV pri-miRNAs^{8,9}

* Corresponding authors. Tel.: +49 69 798 29150; fax: +49 69 798 29148 (J.W.E.); tel.: +27 11 717 2365; fax: +27 11 2395 (P.A.).

E-mail addresses: Joachim.Engels@chemie.uni-frankfurt.de (J.W. Engels), Patrick.Arbuthnot@wits.ac.za (P. Arbuthnot).

and pre-miRNAs,^{10,11} as well as synthetic miRNA analogues^{12–14} have been used successfully to inhibit replication of the virus.

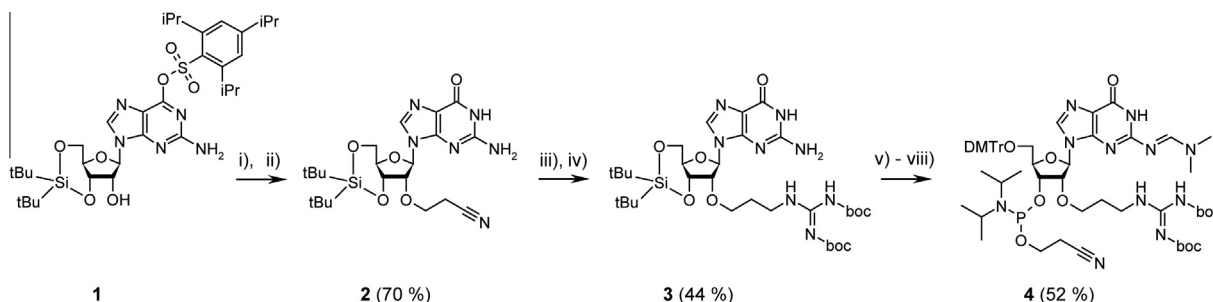
Synthetic small interfering RNAs (siRNAs) resemble miRNA duplexes and activate RNAi at the stage of guide strand incorporation into RISC. (reviewed in⁶) siRNAs are considerably smaller than pri-miRNA- or pre-miRNA-encoding DNA cassettes. As a result efficient delivery to target cells and better dose regulation are easier to achieve with siRNAs. However, susceptibility of siRNAs to serum nuclease degradation, problems with delivery and non-specific gene silencing remain problematic. Studies have shown that these difficulties may be mitigated by chemical modification of siRNA.^{15–19} Modifications have included addition of moieties to the 2' and 4' positions of the ribose,²⁰ changes to the natural phosphodiester linkages, and also substitution of naturally occurring ribose for other sugars such as hexitol.^{21,22} Importantly, introduction of chemical modifications into siRNAs may influence several steps leading from their administration to incorporation into RISC. Predicting efficacy is therefore difficult and empirical characterization of siRNA actions is necessary.

Synthetic siRNAs have successfully been used to target different regions of the HBV genome and results support the notion that RNAi-based gene silencers have therapeutic potential against the virus.⁵ In one study, a combination of chemical modifications to antiHBV siRNAs was used to inhibit HBV replication in a murine hydrodynamic injection model of HBV replication.¹² These effective antiHBV siRNAs were modified by addition of 2'-*O*-methyl (2'-*O*-Me) and 2'-fluoro (2'-F) moieties to the ribose, incorporation of phosphorothioate linkages and inverted deoxy abasic sites. Use of antiHBV siRNAs containing the hexitol six carbon sugar has also been used successfully in cultured cells and in vivo.¹⁴ In an earlier study, our groups have shown that incorporation of 2'-*O*-guanidinopropyl (GP) moieties at some positions of an antiHBV siRNAs improve stability and antiviral efficacy in cultured cells.²³ The positive charge of this modification also potentially neutralizes overall negative charge of the siRNAs to facilitate delivery to target cells. To characterize the utility of this siRNA chemical modification more fully, we have undertaken detailed analysis of GP-modifications that have been incorporated at different sites of a previously described effective antiHBV siRNA.¹⁴ Our data provide evidence for improved efficacy, reduced off target effects and good silencing in vivo by GP-modified siRNAs.

2. Results

2.1. Synthesis of 2'-*O*-guanidinopropyl-nucleosidephosphoramidites and their incorporation into antiHBV siRNAs

Procedures employed for the synthesis of 2'-*O*-guanidinopropyl-nucleosidephosphoramidites have previously been de-



Scheme 1. Improved method of synthesis of the 2'-*O*-guanidinopropyl-*N*²-dmf-guanosine phosphoramidite for oligoribonucleotide synthesis. (i) acrylonitrile, Cs₂CO₃, *tert*-butyl alcohol, rt; (ii) formic acid (70%), dioxane/water; (iii) Raney-Ni/H₂ (30 bar), NH₃, methanol, 30–60 min, rt; (iv) *N,N*-di-Boc-*N'*-triflylguanidine, Et₃N, CH₂Cl₂, 0 °C (30 min) to rt (30 min); (v) *N,N*-dimethylformamide dimethyl acetal, methanol, rt (12 h); (vi) Et₃N·3HF, THF, rt; (vii) 4,4'-dimethoxytrityl chloride, pyridine, rt; (viii) 2-cyanoethyl *N,N,N',N'*-tetraisopropyl phosphane, 4,5-dicyanoimidazole, CH₂Cl₂, rt.

scribed.²³ However, to circumvent the problem of a product mixture upon introduction of the isobutyryl group to the N²-position of guanosine, we developed a different protection strategy, which entailed incorporation of a dimethylformamidinium group (Scheme 1). The earlier synthesis procedure yielded a mixture of mono- and di-isobutyryl compounds. Although desired RNA oligonucleotides were formed after complete deprotection, yields and purity of the 2'-*O*-GP-guanosine phosphoramidite were considerably improved when using dimethylformamidinium protection. Standard phosphoramidite synthetic procedures with a prolonged coupling time of 30 min were employed to incorporate GP-containing nucleotides into the antisense guide strand of an effective antiHBV siRNA. This RNAi activator, siRNA3, targets the *HBx* open reading frame (ORF) of HBV genotype A from coordinates 1693 to 1711.¹⁴ Control siRNA3 without GP moieties is referred to in this study as being unmodified. It does however contain two dT residues at the 3' end of the sense strand to improve stability. Naming of the panel of twenty siRNA3 derivatives was according to the nucleotide position of the GP moiety. That is starting from the second nucleotide (GP2 siRNA3) and ending at the twenty first nucleotide (GP21 siRNA3) from the 5' end of the guide strand. Melting point studies of selected GP-modified antisense strands in combination with the unmodified sense strand resulted in very small destabilising effects considering the accuracy of the UV-method used (see Supplementary data).

2.2. Effective target silencing by GP-modified siRNAs following transfection of liver-derived cultured cells

Liver-derived Human hepatoma 7 (Huh7) cells were initially used to assess inhibition of markers of HBV replication. Target silencing was measured after co-transfection of each of the panel of siRNAs with either a dual luciferase reporter containing the HBV siRNA3 target (*psiCHECK-HBx*)²⁴ or a replication competent HBV target plasmid (pCH-9/3091)²⁵ (Fig. 1). Unmodified siRNA3 was included in all studies as a positive control, while the scrambled siRNA was used as a negative control.¹⁴

After co-transfecting Huh7 cells with the panel of siRNAs and the *psiCHECK-HBx* dual luciferase reporter plasmid, the ratio of *Renilla* to Firefly luciferase activity was measured (Fig. 1B). The HBV target sequence in this vector is located on the same transcript but downstream of the *Renilla luciferase* ORF. Since Firefly luciferase is separately and constitutively expressed on the same plasmid, the ratio of *Renilla* to Firefly luciferase activity was used conveniently as a normalized indicator of silencing efficacy. When compared to the scrambled siRNA control, GP-modified siRNAs decreased the ratio of *Renilla* to Firefly luciferase activity by up to 93% (GP10 siRNA3, GP17 siRNA3, GP 18 siRNA3 and GP21 siRNA3). GP-modified siRNAs with weakest activity inhibited *Renilla* luciferase activity with approximately similar efficacy to that of the unmodified siRNA3.

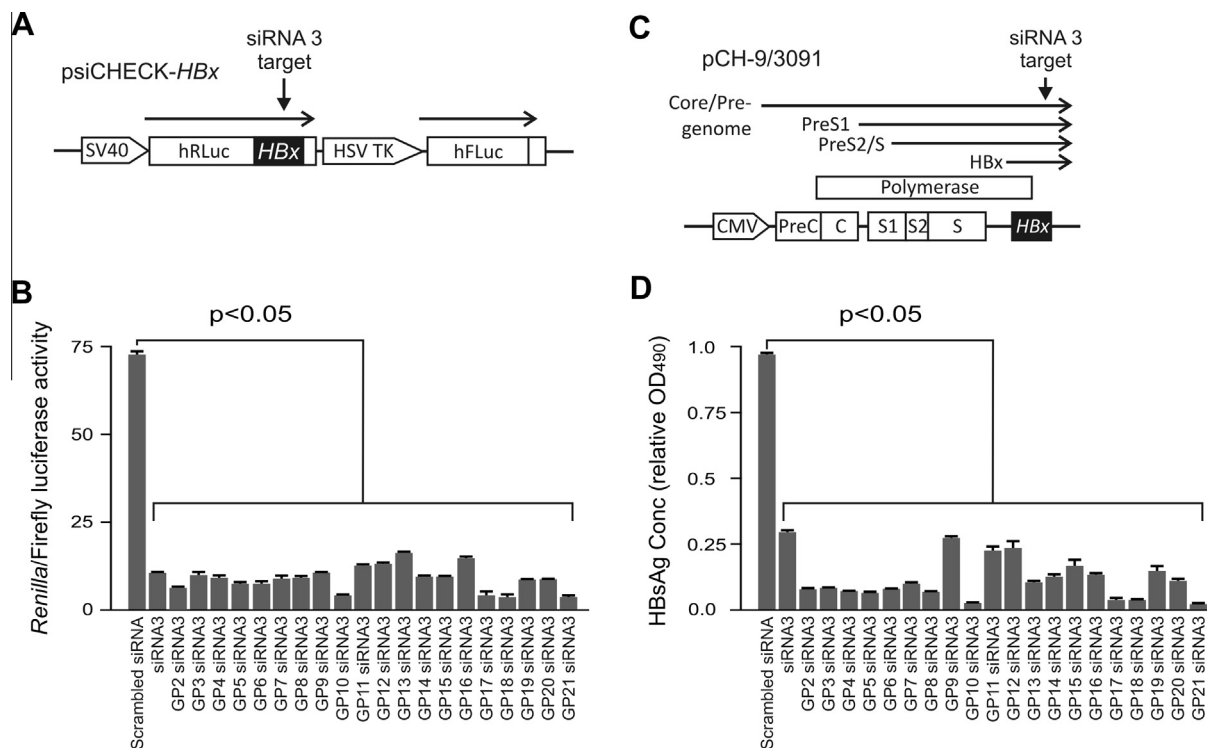


Figure 1. HBV target sequences and assessment of knockdown in transfected cultured cells. psiCHECK-HBx plasmid, with relevant sequences schematically illustrated in A, was used to co-transfect Huh7 cells. Dual-luciferase reporter gene assay was performed 48 h after transfection with the indicated unmodified or GP-modified siRNAs (B). Results are given as mean ratios of *Renilla* to Firefly luciferase activity. To assess effects on HBV replication in cultured cells, the pCH-9/3091 vector that contains replication competent HBV sequences (C) was used to transfect Huh7 cells. Surface antigen (HBsAg) concentrations in cell culture supernatants were measured by ELISA at 48 h after co-transfecting with pCH-9/3091 plasmid and indicated siRNAs (D). Values represent the means and standard deviation of three replicate transfections. Differences were considered statistically significant when analysis using the student *t*-test showed $p < 0.05$.

In a complementary experiment, transfection of Huh7 cells with siRNAs and the pCH-9/3091 replication competent plasmid, then measurement of HBV surface antigen (HBsAg) concentration in culture supernatants was used as an indicator of knockdown (Fig. 1D). Modified siRNAs effectively inhibited secretion of this marker of HBV replication. Compared to the scrambled siRNA control, inhibition of HBsAg secretion of about 90% was observed with GP2 siRNA3, GP3 siRNA3, GP4 siRNA3, GP5 siRNA3, GP6 siRNA3, GP7 siRNA3 and GP8 siRNA3, while about 95% inhibition was achieved with GP10 siRNA3, GP17 siRNA3, GP18 siRNA3 and GP21 siRNA3. Lowest target silencing was observed when cells were co-transfected with siRNAs containing modifications in the central region (GP9 siRNA3, GP11 siRNA and GP12 siRNA 3) of the guide strand and may be a result of a destabilizing effect at the site of Ago2 target cleavage. Interestingly, GP10 siRNA3 had good silencing efficiency. The reasons for this are not clear, but modification at position 10 may facilitate Ago2-mediated cleavage of the target. As with inhibition *Renilla* luciferase activity after psiCHECK-HBx transfection, the most effective GP-modified siRNAs inhibited HBsAg secretion significantly more effectively than did unmodified siRNA3. There was however some variation between the silencing efficacy of the siRNAs after transfecting with either pCH-9/3091 or psiCHECK-HBx vectors. This may be a result of differences in accessibility of the targets to the siRNAs within the different sequence contexts. Nevertheless, the data demonstrate that GP modifications confer improved silencing by the antiHBV siRNAs, and the efficacy is dependent on the positions of the modifications within the guide strand.

2.3. No evidence for activation of the interferon response or toxicity in cultured cells following transfection with GP-modified siRNAs

To assess whether GP-modified siRNAs stimulate an innate interferon (IFN) response, concentrations of mRNA transcribed from some IFN response genes were measured in HEK293 cells after transfection with each of the panel of siRNAs. Innate immunostimulation is attenuated in Huh7 liver-derived cells,²⁶ which is the reason for electing to assess the IFN response in the HEK293 line. Immunostimulatory effects of double stranded RNA are activated mainly by Toll-like receptor 3 (TLR3), TLR7 and TLR8.²⁷ These receptors recognise different forms of double stranded RNA and activate transcription of interferon response genes that encode a variety of proteins such as interferon-beta (IFN- β), Interferon-induced protein with tetratricopeptide repeats 1 (IFIT1) and Oligoadenylate synthetase-1 (OAS-1). Immunostimulatory effects vary depending on the nature of the synthetic double stranded RNA,²⁸ which makes it desirable to screen for induction of different IFN genes. Results from using reverse transcriptase quantitative PCR (RT-qPCR) to measure IFN- β , IFIT1 and OAS-1 mRNA are shown in Figure 2A. IFN- β , IFIT1 and OAS-1 mRNA concentrations measured after treatment of cells with poly(I:C), a positive control for IFN response induction, were normalized and used for comparison. IFN gene expression was significantly elevated in positive control cells that had been transfected with poly(I:C). However both unmodified and GP-modified siRNAs did not induce expression of IFN response genes, and their concentrations were similar to those detected in untransfected cells.

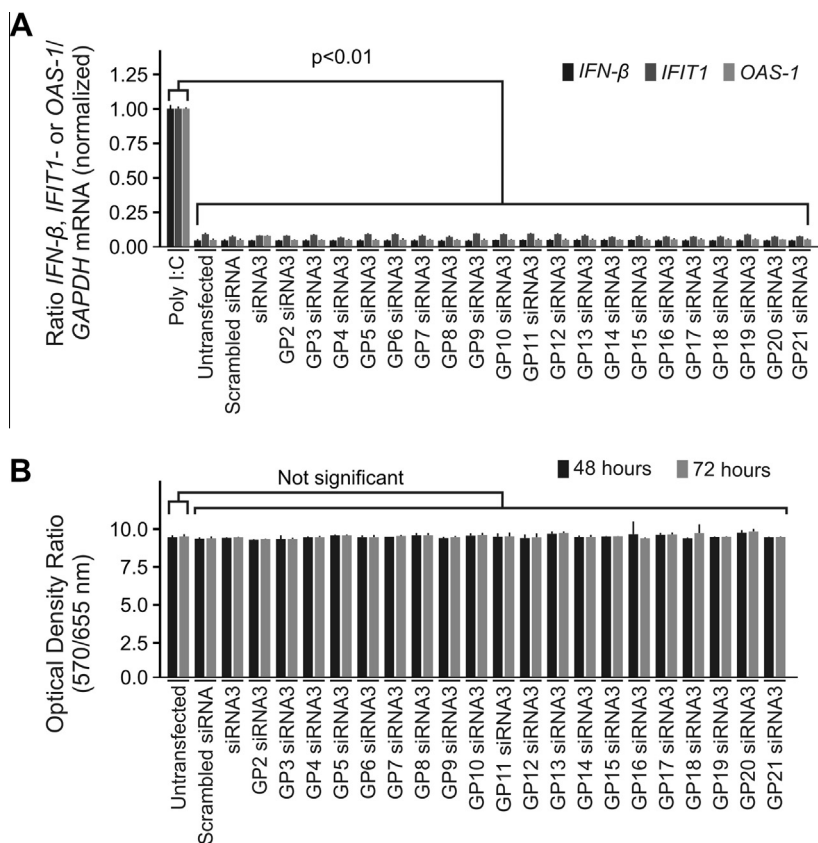


Figure 2. Assessment of stimulation of the innate IFN response and toxicity of siRNAs following transfection of cells. mRNA from *IFN-β*, *IFIT1*, *OAS-1* and *GAPDH* genes was reverse transcribed and amplified using qRT-PCR. Data, presented as a ratio of the concentrations of IFN response genes to the *GAPDH* housekeeping gene, was determined at 24 h after transfection (A). Cell viability was assessed using the MTT assay and determined at 48 and 72 h after transfection (B). Data analysis was carried out by calculating the ratio of optical density of transfected and untransfected cells at 570 and 650 nm. Values of data presented in A and B represent the means and standard deviation of 3 replicate transfections. Differences were considered statistically significant when analysis using the student *t*-test showed $p < 0.05$.

The sensitive MTT assay was conducted to investigate whether siRNAs caused toxicity to cultured cells (Fig. 2B). Compared to control cells the data showed that unmodified or GP-containing siRNAs did not cause significant toxicity in Huh7 cells at 48 and 72 h after transfection. Collectively, these observations indicate that GP-modified siRNAs did not cause toxicity or induction of an innate IFN immune response in cultured cells.

2.4. Influence of the position of the GP modification on silencing of complete and partial HBV targets

A panel of dual luciferase reporter plasmids was generated in which the HBV target sequences included variable numbers of nucleotides that were complementary to the siRNA3 guide strand. Different target sequences were inserted downstream of the *Renilla* luciferase ORF of psiCHECK and structures of the dual luciferase reporters are illustrated schematically in Figure 3A. The reporter plasmids with their targets were the following:

1. psiCHECK-siRNA3 complete target (psiCHECK-siRNA3 CT), complete base complementarity between target HBV and siRNA3 guide.
2. psiCHECK-siRNA3 incomplete target 1 (psiCHECK-siRNA3 IT1), three nucleotide mismatch at the 5' end of siRNA3 guide target site.
3. psiCHECK-siRNA3 incomplete target 2 (psiCHECK-siRNA3 IT2), five nucleotide mismatch at the 5' end of siRNA3 guide target site.

4. psiCHECK-siRNA3 seed only target (psiCHECK-siRNA3 SO), the HBV target sequence is complementary to the guide seed region, comprising nucleotides 1 to 8 from the 5' end of siRNA3.

Huh7 cells were co-transfected with various unmodified or GP-containing siRNAs, together with a reporter gene plasmid containing completely or partially complementary guide targets (Fig. 3B). As before, the siRNAs differed with respect to location of the GP modifications, and the ratio of *Renilla* to Firefly luciferase activity was used to assess knockdown efficacy of the modified siRNAs. Compared to a scrambled siRNA control, analysis showed that the *Renilla* luciferase activity was diminished by at least 85% when the reporter plasmid containing the complete target was co-transfected with the unmodified or GP-modified siRNA. These results are in accordance with the data shown in Figure 1, where knockdown efficiency was assessed against the complete HBV target. Silencing of the reporter gene that included SO and IT2 targets was attenuated when GP modifications were located at nucleotides 2 to 7. This suggests that the GP modifications within the seed-targeting region diminish the interaction of the siRNA guide with an incompletely matched cognate. Importantly, efficient knockdown of *Renilla* luciferase activity derived from psiCHECK-siRNA3 CT was achieved by siRNAs containing modifications within the seed-targeting region. GP13 siRNA3 also demonstrated diminished silencing of incomplete targets. The reason for this is unclear but may be a result of an effect of the GP13 modification on interaction of RISC components with target mRNA. Silencing of cellular targets caused by their complementarity to guide strands' seed sequences

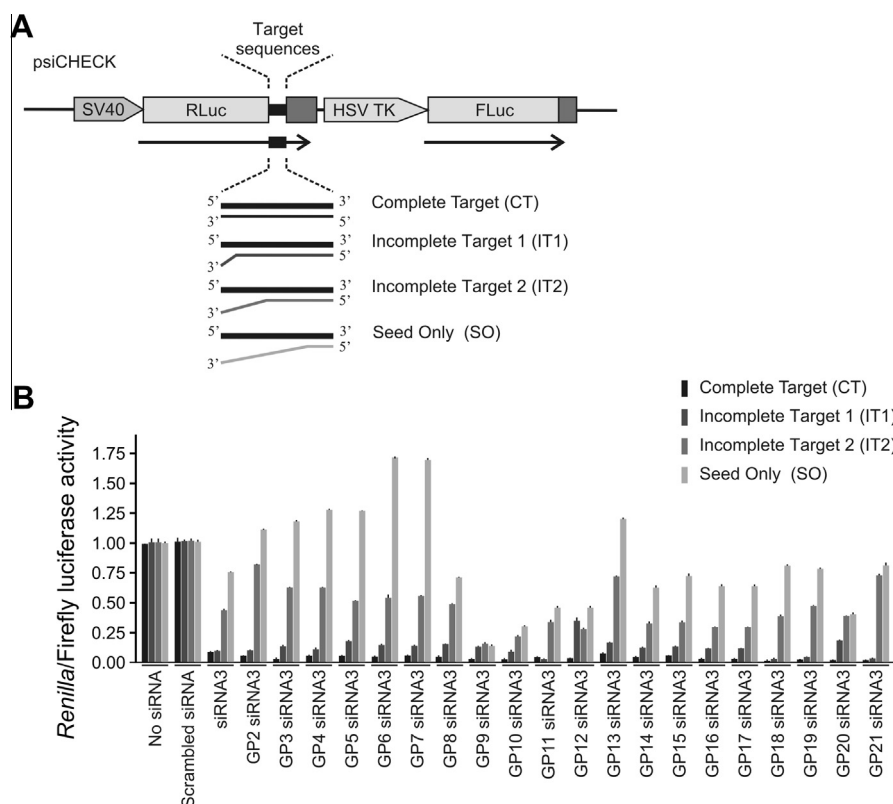


Figure 3. Silencing of complete and partial targets by GP-modified and control siRNAs. Four different target sequences of siRNA3 were cloned into psiCHECK 2.2 (A). psiCHECK-siRNA3 CT contained a sequence that was completely complementary to siRNA3. Partially complementary targets contained a three nucleotide mismatch at the 3' end (psiCHECK-siRNA3 IT1), a 5 nucleotide mismatch at the 3' end (psiCHECK-siRNA3 IT2) and the seed region alone (psiCHECK-siRNA3 SO). A dual-luciferase reporter gene-based assay was performed 48 h after co-transfection of each of the target plasmids with the panel of siRNAs (B). Data are presented as mean ratios of *Renilla* to Firefly luciferase activity and standard deviations are indicated by the error bars.

is widespread.^{34,35} This unintended effect is similar to the natural target regulation that is mediated by miRNAs interacting with their cellular targets. Resulting unintended inhibition of gene expression may cause toxicity and minimizing this effect is important for therapeutic use of siRNAs. Our findings suggest that siRNAs with GP modifications within the seed targeting region interact less efficiently with partially complementary targets to effect more specific silencing of intended complete targets.

2.5. Serum stability of GP-modified siRNAs

To assess whether GP modification affected siRNAs stability, control and GP-modified siRNAs were incubated in the presence of 80% foetal calf serum (FCS) for up to 48 h. As an indicator of degradation, siRNA bands detected after polyacrylamide gel electrophoresis and ethidium bromide staining were quantified using densitometry (Fig. 4). Employing this assay, control siRNA had a half-life of approximately 5 h. Importantly the control siRNA3 used in our study included two dT residues at the 3' end of the sense strand, which should confer protection against 3'–5' exonuclease activity. In general, GP-modified siRNAs were slightly more stable than the control siRNA3. As reported previously,²³ siRNAs with a GP moiety further from seed region (i.e., GP13 siRNA3 and GP19 siRNA3) displayed slightly increased stability.

2.6. Efficient silencing of HBV replication in vivo using GP-modified siRNAs

The murine hydrodynamic tail vein injection (HDI) method²⁹ was employed to determine the effects of control and GP-modified

siRNAs on HBV replication in vivo. The procedure initially involved co-transfection of siRNAs with pCH-9/3091 HBV replication competent plasmid,²⁵ and was followed by measurement of serum markers of HBV replication (Fig. 5). The siRNAs with GP modifications within the seed region at position 3, 4 or 5 were selected for in vivo studies. Selection was based on antiHBV efficacy in vitro (Fig. 1) and evidence for good target specificity (Fig. 3). As with studies on cultured cells, unmodified and scrambled siRNAs were used as positive and negative controls. AntiHBV effects of these siRNAs were assessed by measuring serum HBsAg concentrations (Fig. 5A) and qRT-PCR to determine circulating virus particle equivalents (VPEs) (Fig. 5B). The unmodified and GP-modified antiHBV siRNAs each effected knockdown of the viral antigen by 70–98%. This was observed when measurements were taken at days 3 and 5 after HDI. Of the siRNAs, GP4 siRNA3 and GP5siRNA3 were the most efficient. HBsAg concentration in the serum of mice injected with these siRNAs was approximately 2% of the controls. The numbers of circulating VPEs in the same mice were also measured using qPCR. The results corroborate observations made on HBsAg determinations in that unmodified and GP-modified siRNAs effected highly efficient knockdown of the number of circulating VPEs at both time points. At days 3 and 5, the numbers of VPEs were approximately 1.8×10^4 and 8×10^3 /mL of serum respectively in the negative control animals. The circulating VPEs in anti-HBV siRNA-treated animals were generally more than 100-fold lower and ranged from 0.5 to 2.5×10^3 /mL of serum. GP-modified and unmodified siRNAs had approximately equal efficacy in knocking down this marker of replication. Collectively, these data show that GP-modified siRNAs are highly efficient silencers of HBV gene expression in vivo. Moreover, based on the assessment of HBsAg

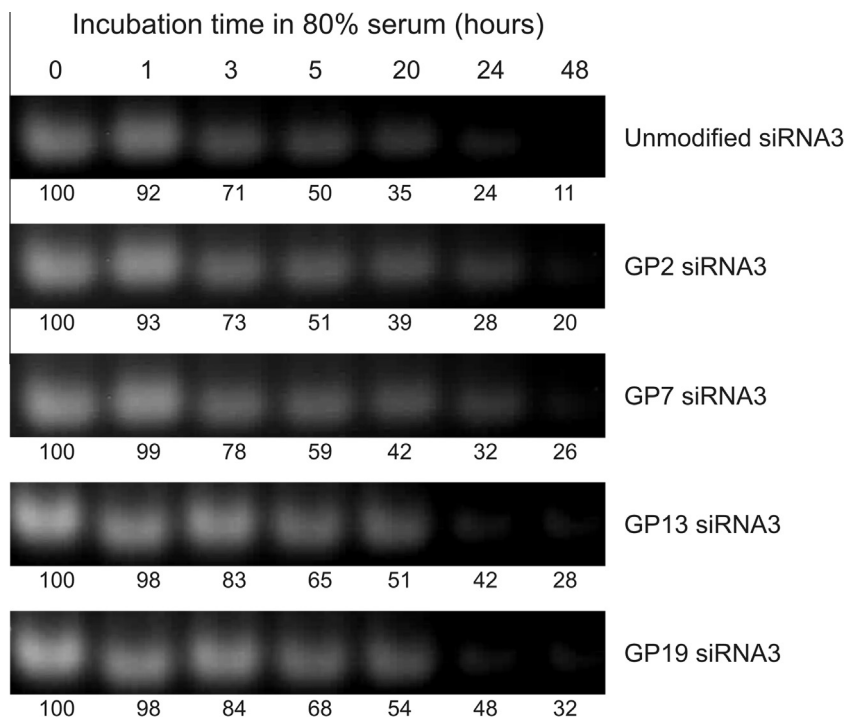


Figure 4. Stability of siRNAs in 80% FCS. Stability of unmodified siRNA, siRNAs containing GP-moieties within the seed region (GP2 siRNA3 and GP7 siRNA3) or siRNAs with GP-moieties outside seed region (GP13 siRNA3 and GP19 siRNA3) was determined after incubation in 80% FCS. Aliquots were collected during a time course from 0 to 48 h, subjected to polyacrylamide gel electrophoresis and bands corresponding to siRNA were quantified densitometrically. Values below each of the lanes represent the percentages of siRNAs, relative to the amount determined at time point of 0 h, calculated to be remaining at each time point.

secretion from treated mice, the efficiency of the modified siRNAs is better than that of the unmodified siRNA3.

3. Discussion

Use of chemical modifications to enhance properties of oligonucleotides that are intended for therapeutic silencing application has been widely investigated. (reviewed in³⁰) Early studies were aimed at improving efficacy of antisense sequences, and since discovery of the RNAi pathway, similar approaches have been extended to advance use of synthetic siRNAs. Although useful guidelines have been drafted, predicting the effects of particular chemical modifications on siRNA efficacy is difficult. Empirical assessment of alteration to natural siRNA structure is therefore critically important for their optimization for a particular application. Incorporation of modifications into siRNAs essentially aims to enhance their function by improving:

1. silencing efficacy,
2. specificity for a particular target mRNA,
3. avoidance of innate immunostimulation,
4. stability and
5. delivery to target tissue.

In this study, the potential utility of GP-modifications at the 2' position of ribose moieties within all four nucleotides at positions 2–21 of an siRNA that targets HBV has been analysed. Our findings indicate that this GP modification improves efficacy, specificity of guide interaction with its target and stability without causing toxicity or induction of an IFN response.

Good silencing efficacy of GP-modified siRNAs was demonstrated using dual luciferase and HBV replication models that were carried out on cells in culture. When assessed with the reporter gene assay, silencing efficacy of all GP-containing siRNAs was similar to that of unmodified siRNA. Although silencing of HBV

replication revealed an overall improved silencing efficiency of the GP-modified siRNAs, modifications positioned in the central region of the siRNA antisense strand had attenuated silencing efficiency. This observation is likely to be a result of the requirement for complete hybridization to occur at this region to enable target cleavage by Ago2 within RISC. Interestingly GP10 siRNA3, with GP modification at position 10, effected efficient silencing in cell culture. Ago2-mediated cleavage of target mRNA occurs at the site opposite this nucleotide.³¹ Facilitation of the cleavage reaction by a GP residue opposite the site of Ago2 action is an interesting possibility and will be the topic of future investigation. Good efficacy of the selected GP-modified siRNAs was corroborated by analysis carried out in vivo. This effective silencing in vivo is an important feature that indicates that GP modifications may have utility in a clinical context.

Successful advancement of therapeutic RNAi-based gene silencing is largely dependent on achieving minimal off target effects. In a clinical setting, these undesirable consequences may lead to toxicity. Non-specific interaction of guide strands with partially complementary cellular mRNA targets, and resultant inhibition of gene expression, is widespread and of particular concern.^{32–34} Modification with 2'-O-methyl residues at position 2 of the seed sequence has been reported to attenuate unintended silencing.³⁵ Our results support the notion that chemical modification of siRNA seed regions can be used to improve specificity. Moreover, we demonstrate that GP residues included at most of the seed region positions of antiHBV siRNA3 limit microRNA-like off-target silencing. These observations are also in line with the demonstration that non-bulky chemical modifications in the seed region are well tolerated.²² Importantly, overall silencing of the complete target by GP-modified siRNAs was not compromised.

In addition to off-target silencing of cellular mRNA, cellular toxicity and non-specific activation of the innate IFN response by siRNAs are also potentially problematic. Inclusion of chemical

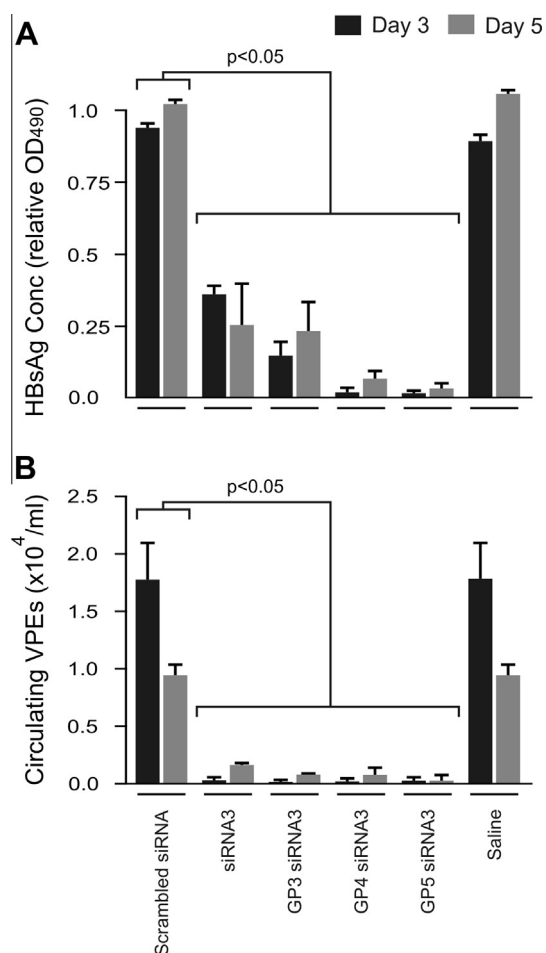


Figure 5. AntiHBV effects of siRNAs on markers of HBV replication in vivo. Mice were co-injected with 15 μ g HBV target plasmid pCH-9/3091 together with 1 nmol of GP-modified or unmodified control siRNAs. Serum concentrations of HBsAg (A) and circulating VPEs (B) were detected at days 3 and 5 after siRNA administration. Values represent the means and standard deviation of 5 replicate injections ($p < 0.05$).

modifications may be employed to overcome induction of the IFN response.^{19,30} Our data indicate that the unmodified siRNA3 does not induce the innate IFN response, and it is therefore difficult to assess whether the GP moieties ameliorate this innate immunostimulatory effect. Nevertheless, mRNA from IFN response genes were not increased following transfection of GP-containing siRNAs, which indicates that this chemical modification is not immunostimulatory per se. Moreover, since GP modifications at all of the positions from 2 to 21 showed a similar effect, the position of the moiety does not influence siRNA immunostimulation. The absence of toxicity, measurable using the sensitive MTT assay, also suggests that the chemical modification is also not directly toxic to cells.

Poor stability of naked siRNAs in serum may be a factor that diminishes efficacy of these silencing molecules. Enhancing duration of activity of siRNAs may be achieved through encapsulation within protecting nanoparticles or through chemical modification to confer resistance to nuclease degradation. The mechanism of degrading naked siRNA in serum is thought to result from activity of the 3'-5' exoribonuclease 1 (ERI1) enzyme,³⁶ and protection of naked siRNAs through modification at the 3' end improves stability of siRNAs.¹⁹ A commonly employed method of modifying 3' ends has been through incorporation of two dT residues at the 3' ends of siRNAs. In this study, dT residues were present at the 3' end of

the sense strand of the control siRNA3 as well as in each of the panel of siRNAs containing the GP modifications. Control siRNA3 had a half-life in 80% serum of approximately 5 h. This is longer than what is expected for completely unmodified siRNAs, and may result from the presence of the two dT residues at the 3' dinucleotide overhangs of the sense strand of siRNA3. A further, although modest, increase in the siRNAs half-life in 80% serum was achieved by incorporation of GP residues. This observation is in accordance with findings that we have previously reported,²³ and indicates that GP residues have a beneficial stabilizing effect on siRNAs.

Synthetic siRNAs with chemical modifications have previously been used successfully to silence replication of HBV.^{12,14} Morrissey et al. compared extensively modified with unmodified antiHBV siRNAs.¹² Improved potency, specificity and stability was observed with siRNAs that included (1) substitution of all 2'-OH residues on the RNA with 2'F, 2'O-Me or 2'H residues, (2) phosphorothioate linkages at selected sites and (3) terminal inverted ribose moieties. In mice that had been subjected to HDI with a HBV replication competent plasmid, administration of the modified siRNAs in stable nanoparticle lipid particle (SNALP) vectors resulted in efficient knockdown of viral replication. There have however been few studies to follow up on this report and the clinical utility of these extensively modified siRNAs has not been fully assessed.

siRNAs with therapeutic utility would be required to interact with several intra- and extracellular proteins during the events leading from their administration to contact of the guide strand with its target within RISC. Since many of these interactions are likely to be sensitive to chemical modifications, simplification of the chemical modifications may facilitate the drug development process. Our observation that siRNAs incorporating single GP moieties at selected sites improves their efficacy, specificity and stability without causing toxicity and innate immunostimulation is therefore promising. To advance use of GP-modified siRNAs for therapeutic use, current investigations are aimed at incorporating GP-modified siRNAs into non-viral vector formulations, assessing pharmacokinetic properties and optimizing efficacy against HBV in vivo.

4. Materials and methods

4.1. Chemical synthesis of GP-modified nucleosides

Synthesis of oligonucleoside precursors of the HBV-targeting siRNAs has previously been described.²³ However, to circumvent the problem of obtaining a product mixture upon introduction of the isobutryl group to the N2-position of guanosine, we established a different protection strategy, using the dimethylformamide group (Scheme 1).

4.1.1. Synthesis of the O⁶-(2,4,6-Triisopropylbenzenesulfonyl)-3',5'-O-di-*tert*-butylsilanediylguanosine (1)

O⁶-(2,4,6-Triisopropylbenzenesulfonyl)-3',5'-O-di-*tert*-butylsilanediylguanosine (1) was synthesised according to a previously described procedure.³⁷

4.1.2. 2'-O-(2-Cyanoethyl)-3',5'-O-di-*tert*-butylsilanediylguanosine (2)

Compound 1 (2.28 g, 3.3 mmol) was dissolved in *tert*-butanol (17 mL). Freshly distilled acrylonitrile (4.25 mL, 66 mmol) and cesium carbonate (1.16 g, 3.3 mmol) were added to the solution. After vigorous stirring at room temperature for 2–3 h, the mixture was filtered through celite. The solvent and excess reagents were removed in vacuo. The crude material was used for the next reaction without further purification. The residue was dissolved in 4 mL of a mixture of formic acid/dioxane/water (70:24:6, v/v/v). After stirring at room temperature for 1 h, water (150 mL) was

added to the mixture and the solution extracted with dichloromethane. The organic layer was dried over Na_2SO_4 and the solvent was evaporated. The residue was purified using silica gel column chromatography with dichloromethane/methanol (9:1, v/v) to give 1.1 g (70% over 2 steps) of **2** as a colourless foam. ^1H NMR (250 MHz, $\text{DMSO}-d_6$) δ [ppm] 10.71 (br s, 1H, NH), 7.89 (s, 1H, H8), 6.45 (br s, 2H, NH_2), 5.81 (s, 1H, $\text{H}1'$), 4.45–4.33 (m, 3H), 4.05–3.81 (m, 4H), 2.83–2.76 (m, 2H, $\text{O}-\text{CH}_2-\text{CH}_2-\text{CN}$), 1.06 (s, 9H, $\text{C}(\text{CH}_3)_3$), 1.01 (s, 9H, $\text{C}(\text{CH}_3)_3$); ^{13}C NMR (63 MHz, $\text{DMSO}-d_6$) δ [ppm] 156.51, 153.69, 150.50, 135.36, 118.71, 116.53, 87.25, 80.31, 76.35, 73.80, 66.64, 65.14, 27.12, 26.80, 22.07, 19.82, 18.29; MS (ESI) was calculated to be 477.2 for $\text{C}_{21}\text{H}_{33}\text{N}_6\text{O}_5\text{Si}$ ($\text{M}+\text{H}^+$), and found to be 477.5.

4.1.3. 2'-O-(2-Aminopropyl)-3',5'-O-di-tert-butylsilanediylguanosine (2a)

Compound **2** (500 mg, 1.06 mmol) was dissolved in dry methanol (5 mL). Raney nickel (ca. 0.5 mL of the methanol-washed sediment) and methanol (5 mL) saturated with ammonia were then added. The mixture was hydrogenated at 30 bar hydrogen-pressure for 1 h at room temperature. Thereafter the mixture was filtered through a glass filter and the catalyst was washed several times with methanol and a methanol/water mixture. The solvents were evaporated from the filtrate and the residue was used without further purification for the next reaction. MS (ESI) was calculated to be 481.3 for $\text{C}_{21}\text{H}_{37}\text{N}_6\text{O}_5\text{Si}$ ($\text{M}+\text{H}^+$), and found to be 481.8.

4.1.4. 2'-O-(N,N'-Di-tert-butoxycarbonylguanidinopropyl)-3',5'-O-di-tert-butylsilanediylguanosine (3)

N,N' -Di-boc- N'' -triflylguanidine (163 mg, 0.415 mmol) was dissolved in dichloromethane (2.1 mL) and triethylamine (54 μL) was then added. The solution was cooled in an ice bath and then 2'-O-(2-Aminopropyl)-3',5'-O-di-tert-butylsilanediylguanosine (**2a**) (200 mg, 0.42 mmol) was added. After 30 min the reaction mixture was removed from the ice bath then stirred for an additional 30 min at room temperature. The reaction solution was washed with saturated sodium bicarbonate solution and brine. After drying over Na_2SO_4 the solvent was evaporated. The residue was purified by column chromatography using dichloromethane/methanol (9:1, v/v) to give 270 mg (89%) of **3**. ^1H NMR (400 MHz, $\text{DMSO}-d_6$) δ [ppm] 11.49 (br s, 1H, NH), 10.66 (br s, 1H, NH), 8.56–8.53 (m, 1H, $\text{NH}-\text{CH}_2-$), 7.87 (s, 1H, H8), 6.39 (br s, 2H, NH_2), 5.86 (s, 1H, $\text{H}1'$), 4.42–4.38 (m, 1H, $\text{H}3'$), 4.30–4.27 (m, 2H, $\text{H}2'$, $\text{H}5'$), 4.06–3.93 (m, 3H, $\text{H}4'$, $\text{H}5'$, $\frac{1}{2} \times \text{O}-\text{CH}_2-\text{CH}_2-\text{CH}_2-\text{NH}-$), 3.72–3.67 (m, 1H, $\frac{1}{2} \times \text{O}-\text{CH}_2-\text{CH}_2-\text{CH}_2-\text{NH}-$), 3.51–3.30 (m, 2H, $\text{O}-\text{CH}_2-\text{CH}_2-\text{CH}_2-\text{NH}-$), 1.84–1.77 (m, 2H, $\text{O}-\text{CH}_2-\text{CH}_2-\text{CH}_2-\text{NH}-$), 1.46 (s, 9H, $-\text{CO}-\text{C}(\text{CH}_3)_3$), 1.39 (s, 9H, $-\text{CO}-\text{C}(\text{CH}_3)_3$), 1.06 (s, 9H, $-\text{Si}-\text{C}(\text{CH}_3)_3$), 0.97 (s, 9H, $-\text{Si}-\text{C}(\text{CH}_3)_3$); HRMS (MALDI) was calculated to be 723.3856 for $\text{C}_{32}\text{H}_{55}\text{N}_8\text{O}_9\text{Si}$ ($\text{M}+\text{H}^+$), and found to be 723.3880.

4.1.5. N²-Dimethylformamide-2'-O-(N,N'-di-tert-butoxycarbonylguanidinopropyl)-3',5'-O-di-tert-butylsilanediylguanosine (3a)

Compound **3** (1.12 g, 1.55 mmol) was dissolved in 25 mL dry methanol. N,N -Dimethylformamide dimethyl acetal (1.0 mL, 7.6 mmol) was added and the solution was stirred at room temperature overnight. After a reaction time of 12 h the solvents were removed in vacuo and the residue was purified by silica gel column chromatography using dichloromethane/methanol (19:1, v/v) to give 1.14 g (94%) of the dmf-protected derivative. ^1H NMR (400 MHz, $\text{DMSO}-d_6$) δ [ppm] 11.51 (s, 1H, N^1H), 11.40 (s, 1H, $\text{NH}-\text{boc}$), 8.54 (s, 1H, $-\text{N}=\text{CH}-\text{N}(\text{CH}_3)_2$), 8.47 (m, 1H, 2'-O- $\text{CH}_2-\text{CH}_2-\text{CH}_2-\text{NH}-$), 7.99 (s, 1H, H-8), 5.98 (s, 1H, $\text{H}1'$), 4.48–4.45 (m, 1H, $\text{H}5'$), 4.41–4.39 (m, 1H, $\text{H}2'$), 4.33–4.30 (m, 1H, $\text{H}5'$), 4.07–3.99 (m, 2H, $\text{H}3'$ and $\text{H}4'$), 3.98–3.77 (m, 2H, 2'-O- $\text{CH}_2-\text{CH}_2-\text{CH}_2-\text{NH}-$), 3.48–3.37 (m, 2H, 2'-O- $\text{CH}_2-\text{CH}_2-\text{CH}_2-\text{NH}-$), 3.14 (s, 3H,

$\text{N}-\text{CH}_3$), 3.04 (s, 3H, $\text{N}-\text{CH}_3$), 1.87–1.78 (m, 2H, 2'-O- $\text{CH}_2-\text{CH}_2-\text{CH}_2-\text{NH}-$), 1.47 (s, 9H, $-\text{CO}-\text{C}(\text{CH}_3)_3$), 1.37 (s, 9H, $-\text{CO}-\text{C}(\text{CH}_3)_3$), 1.06 (s, 9H, $-\text{Si}-\text{C}(\text{CH}_3)_3$), 1.00 ppm (s, 9H, $-\text{Si}-\text{C}(\text{CH}_3)_3$); ^{13}C NMR (75 MHz, $\text{DMSO}-d_6$) δ [ppm] 163.00, 157.60, 157.39, 157.35, 154.98, 151.95, 149.21, 136.96, 119.86, 88.07, 82.78, 80.59, 77.90, 76.48, 73.83, 69.64, 66.77, 44.41, 40.58, 34.54, 28.61, 27.86, 27.44, 27.08, 26.70, 22.06, 19.76; HRMS (MALDI) was calculated to be 800.4097 for $\text{C}_{35}\text{H}_{59}\text{N}_9\text{O}_9\text{SiNa}$ ($\text{M}+\text{Na}^+$), and found to be 800.4124.

4.1.6. N²-Dimethylformamide-2'-O-(N,N'-di-tert-butoxycarbonylguanidinopropyl)-guanosine (3b)

Compound **3a** (1.24 g, 1.59 mmol) was dissolved in dry tetrahydrofuran (17 mL). Triethylamine (470 μL , 3.18 mmol) and $\text{Et}_3\text{N}\cdot 3\text{HF}$ (943 μL , 5.79 mmol) were then added. After stirring at room temperature for 1 h the solvent was evaporated. The residue was purified using silica gel column chromatography with dichloromethane/methanol (9:1, v/v) to give 840 mg (83%) of compound **3b** as white foam. ^1H NMR (400 MHz, $\text{DMSO}-d_6$) δ [ppm] 11.50 (s, 1H, N^1H), 11.34 (s, 1H, $\text{NH}-\text{boc}$), 8.54 (s, 1H, $-\text{N}=\text{CH}-\text{N}(\text{CH}_3)_2$), 8.35 (m, 1H, 2'-O- $\text{CH}_2-\text{CH}_2-\text{CH}_2-\text{NH}-$), 8.10 (s, 1H, H8), 5.95–5.94 (m, 1H, $\text{H}1'$), 5.14–5.12 (m, 1H, 3'-OH), 5.08–5.05 (m, 1H, 5'-OH), 4.31–4.30 (m, 2H, $\text{H}2'$, $\text{H}3'$), 3.95–3.93 (m, 1H, $\text{H}4'$), 3.67–3.56 (m, 4H, $2 \times \text{H}5'$, $\text{O}-\text{CH}_2-\text{CH}_2-\text{CH}_2-\text{NH}-$), 3.36–3.33 (m, 2H, $\text{O}-\text{CH}_2-\text{CH}_2-\text{CH}_2-\text{NH}-$), 3.16 (s, 3H, $\text{N}-\text{CH}_3$), 3.04 (s, 3H, $\text{N}-\text{CH}_3$), 1.77–1.74 (m, 2H, $\text{O}-\text{CH}_2-\text{CH}_2-\text{CH}_2-\text{NH}-$), 1.47 (s, 9H, $-\text{CO}-\text{C}(\text{CH}_3)_3$), 1.37 (s, 9H, $-\text{CO}-\text{C}(\text{CH}_3)_3$); ^{13}C NMR (75 MHz, $\text{DMSO}-d_6$) δ [ppm] 162.98, 157.84, 157.44, 157.24, 155.10, 151.89, 149.61, 136.41, 119.77, 85.26, 85.23, 82.75, 81.36, 78.00, 68.51, 67.87, 60.81, 40.54, 37.86, 34.53, 28.65, 27.85, 27.50; HRMS (MALDI) was calculated to be 660.3076 for $\text{C}_{27}\text{H}_{43}\text{N}_9\text{O}_9\text{Na}$ ($\text{M}+\text{Na}^+$), and found to be 660.3087.

4.1.7. N²-Dimethylformamide-2'-O-(N,N'-di-tert-butoxycarbonylguanidinopropyl)-5'-O-(4,4'-dimethoxytrityl)-guanosine (3c)

Compound **3b** (840 mg, 1.32 mmol) was dissolved in dry pyridine (30 mL). 4,4'-Dimethoxytrityl chloride (670 mg, 1.98 mmol) was added and the solution was stirred for 3 h at room temperature. After the reaction was complete according to TLC, the reaction was quenched with methanol and the solvents were evaporated. The residue was purified by silica gel column chromatography using dichloromethane/methanol (100:0 to 95:5, v/v; the column was packed with dichloromethane containing 0.5% triethylamine) to give 1.08 g (87%) of the tritylated compound **3c**. ^1H NMR (400 MHz, $\text{DMSO}-d_6$) δ [ppm] 11.51 (s, 1H, N^1H), 11.38 (s, 1H, $\text{NH}-\text{boc}$), 8.50 (s, 1H, $-\text{N}=\text{CH}-\text{N}(\text{CH}_3)_2$), 8.40 (m, 1H, 2'-O- $\text{CH}_2-\text{CH}_2-\text{CH}_2-\text{NH}-$), 7.94 (s, 1H, H8), 7.38–7.20 (m, 9H, DMTr), 6.86–6.82 (m, 4H, DMTr), 6.01–6.00 (m, 1H, $\text{H}1'$), 5.16–5.13 (m, 1H, 3'-OH), 4.35–4.30 (m, 2H, $\text{H}2'$, $\text{H}3'$), 4.08–4.05 (m, 1H, $\text{H}4'$), 3.73 (s, 6H, $2 \times \text{O}-\text{CH}_3$), 3.71–3.61 (m, 2H, 2'-O- $\text{CH}_2-\text{CH}_2-\text{CH}_2-\text{NH}-$), 3.40–3.35 (m, 2H, 2'-O- $\text{CH}_2-\text{CH}_2-\text{CH}_2-\text{NH}-$), 3.28–3.16 (m, 2H, $2 \times \text{H}5'$), 3.09 (s, 3H, $\text{N}-\text{CH}_3$), 3.02 (s, 3H, $\text{N}-\text{CH}_3$), 1.80–1.74 (m, 2H, 2'-O- $\text{CH}_2-\text{CH}_2-\text{CH}_2-\text{NH}-$), 1.44 (s, 9H, $-\text{CO}-\text{C}(\text{CH}_3)_3$), 1.34 (s, 9H, $-\text{CO}-\text{C}(\text{CH}_3)_3$); ^{13}C NMR (100 MHz, $\text{DMSO}-d_6$) δ [ppm] 162.96, 157.97, 157.95, 157.72, 157.48, 157.20, 155.10, 151.89, 149.59, 144.71, 136.15, 135.43, 135.30, 129.59, 129.57, 127.67, 127.57, 126.55, 119.83, 113.02, 85.53, 85.37, 82.72, 82.69, 81.04, 77.96, 69.02, 68.22, 63.55, 54.90, 40.54, 37.99, 34.54, 28.66, 27.82, 27.49; HRMS (MALDI) was calculated to be 962.4383 for $\text{C}_{48}\text{H}_{61}\text{N}_9\text{O}_{11}\text{Na}$ ($\text{M}+\text{Na}^+$), and found to be 962.4408.

4.1.8. N²-Dimethylformamide-2'-O-(N,N'-di-tert-butoxycarbonylguanidinopropyl)-5'-O-(4,4'-dimethoxytrityl)-guanosine 3'-(cyanoethyl)-N,N'-diisopropylphosphoramidite (4)

Compound **3c** (1.08 g, 1.15 mmol) was dissolved in dichloromethane (25 mL), then 2-cyanoethyl- N,N,N' -tetraisopropylami-

nophosphane (590 μ L, 1.76 mmol) and 4,5-dicyanoimidazole (199 mg, 1.69 mmol) were added. After 4 h TLC showed complete consumption of the starting material. The reaction solution was then washed twice with saturated sodium bicarbonate solution and once with brine. After drying over Na_2SO_4 the solvent was evaporated and the residue was purified using silica gel column chromatography with dichloromethane/acetone/methanol (4:0:1 to 3:0:2 to 2:1:2 to 2:2:1, v/v), the column was packed with eluent containing 0.5% triethylamine). The residue was dissolved in a small amount (5 mL) of dichloromethane. This solution was dripped into a flask with hexane (500 mL) to form a white precipitate. Two thirds of the solvent was evaporated and the residual solvent was decanted carefully. The precipitate was redissolved in benzene and lyophilised to give 1.01 g (77%) of the phosphoramidite (**4**). According to ^{31}P NMR spectrum the product was still containing a small amount of the hydrolysed phosphitylation reagent but this did not interfere with the oligonucleotide synthesis. ^1H NMR (400 MHz, $\text{DMSO}-d_6$) δ [ppm] 11.50–11.48 (m, 1H, NH), 11.39 (s, 1H, NH), 8.44–8.42 (m, 1H, $-\text{N}=\text{CH}-\text{N}(\text{CH}_3)_2$), 8.39–8.34 (m, 1H, $2'-\text{O}-\text{CH}_2-\text{CH}_2-\text{CH}_2-\text{NH}-$), 7.96 (s, 1H, H8), 7.37–7.19 (m, 9H, DMTr), 6.85–6.78 (m, 4H, DMTr), 6.07–6.05 (m, 1H, H1'), 4.64–4.58 (m, 1H, H3'), 4.48–4.44 (m, 1H, H2'), 4.26–4.19 (m, 1H, H4'), 3.80–3.23 (m, 10H), 3.73–3.70 (m, 6H, $2 \times \text{OCH}_3$), 3.07 (s, 3H, $\text{N}-\text{CH}_3$), 3.02 (s, 3H, $\text{N}-\text{CH}_3$), 2.77–2.74 (m, 1H, $-\text{P}-\text{O}-\text{CH}_2-\text{CH}_2-\text{CN}$), 2.55–2.52 (m, 1H, $-\text{P}-\text{O}-\text{CH}_2-\text{CH}_2-\text{CN}$), 1.80–1.72 (m, 2H, $2'-\text{O}-\text{CH}_2-\text{CH}_2-\text{CH}_2-\text{NH}-$), 1.44–1.34 (m, 18H, $2 \times -\text{CO}-\text{C}(\text{CH}_3)_3$), 1.20–0.93 (m, 12H, $-\text{N}((\text{CH}(\text{CH}_3)_2)_2)$); ^{31}P NMR (121 MHz, $\text{DMSO}-d_6$) δ [ppm] 149.21, 148.93.

4.2. AntiHBV siRNAs

The GP moieties were incorporated into the antisense strand of a previously characterised antiHBV siRNA sequence, siRNA3, which targets HBV genotype A from coordinates 1693 to 1711.¹⁴ Oligonucleotides comprising unmodified and GP-modified antiHBV siRNAs were synthesised on an Expedite 8909 synthesiser using phosphoramidite chemistry.²³ 5-Ethylthio-1*H*-tetrazole (0.35 M in acetonitrile) was used as activator. Commercially obtained unmodified 2'-TBDMS-phosphoramidites were benzoyl-(A), isobutyryl-(G) or acetyl-(C) protected. With a coupling time of 30 min the coupling efficiency of the modified phosphoramidites was as good as for the unmodified phosphoramidites. (Trityl-protocol diagrams of the oligonucleotide syntheses wherein the new phosphoramidite (**4**) was used, are depicted in the [Supplementary data](#).) After completion of synthesis, 30 min of deprotection in 3% trichloroacetic acid in dichloromethane was carried out to ensure complete cleavage of the boc groups. The RNA oligomers were cleaved from the controlled-pore-glass (CPG) support by incubation at 40 °C for 24 h using an ethanol:ammonia (32% in H_2O) solution (1:3). The 2'-TBDMS groups were deprotected by incubation for 90 min at 65 °C with a triethylamine, *N*-methylpyrrolidinone and Et_3N -3HF mixture. RNA oligomers were precipitated with BuOH at -80 °C for 60 min followed by centrifugation at 0 °C and were purified by anion exchange HPLC using a *Dionex* DNAPac PA-100 column. The oligonucleotides were desalted in a subsequent reverse phase HPLC step. Identity was confirmed by mass spectroscopy on a *Bruker* micrOTOF-Q II and the data are deposited in the supplement. The purity of the oligos is about 90%. An exemplary chromatogram of GP10 siRNA3 synthesised with the new phosphoramidite (**4**) can be found in the [Supplementary data](#). The intended guide, 5'-UUG AAG UAU GCC UCA AGG UCG-3', was modified at each of positions 2–21 from the 5' end. Thermodynamic stability of these modified strands in combination with the unmodified sense strand were measured by temperature dependent UV spectroscopy and reported as ΔTm , see supplement. The sense strand oligonucleotide, with sequence 5'-ACC UUG AGG CAU ACU UCA AdTdT-3', had two

dT residues at the 3' end. siRNA with scrambled unmodified sequences comprised antisense, 5'-UUAU UGG GUG UGC GGU CAC GGT-3', and sense, 5'-CGU GAC CGC ACA CCC AAU ATT-3', strands was used as a control.

4.3. Target vectors

pCH-9/3091 is an HBV replication competent plasmid containing a greater than genome length HBV sequence.²⁵ The pCI-eGFP reporter plasmid, used in some cases to verify equivalent transfection efficiencies, produces enhanced green fluorescent protein from the CMV immediate early promoter/enhancer.³⁸ The psiCHECK-HBx vector contains the HBx target sequence downstream of the Renilla luciferase ORF and a separate constitutively active Firefly luciferase cassette.³⁹ The complete, incomplete and seed only targets of siRNA3 were generated by removing HBx from psiCHECK, then substituting this sequence with various annealed oligonucleotides in the backbone. This backbone was prepared by digesting psiCHECK-HBx with *Xho*I and *Not*I followed by purification of the 6.2 kb fragment. To generate the panel of siRNA3 target insert sequences, pairs of forward and reverse oligonucleotides (Integrated DNA Technologies, Iowa, USA) were heated to 95 °C for 5 min, then cooled to room temperature. Sequences of the oligonucleotides were the following: complete target forward (CT F): 5'-TCG AGC GAC CTT GAG GCA TAC TTC AAG TCG ACC AGC TGG C-3', complete target reverse (CT R): 5'-GGC CGC CAG CTG GTC GAC TTG AAG TAT GCC TCA AGG TCG C-3', incomplete target 1 forward (IT1 F): 5'-TCG AGC GAC ACC GAG GCA TAC TTC AAG TCG ACC AGC TGG C-3', incomplete target 1 reverse (IT1 R): 5'-GGC CGC CAG CTG GTC GAC TTG AAG TAT GCC TCG GTG TCG C-3', incomplete target 2 forward (IT2 F): 5'-TCG AGA TCA ACC GAG GCA TAC TTC AAG TCG ACC AGC TGG C-3', incomplete target 2 reverse (IT2 R): 5'-GGC CGC CAG CTG GTC GAC TTG AAG TAT GCC TCG GTT GAT C-3', seed only target forward (SO F): 5'-TCG AGA TCA ACC ACT AAC TAC TTC AAG TCG ACC AGC TGG C-3', and seed only target reverse (SO R): 5'-GGC CGC CAG CTG GTC GAC TTG AAG TAG TTA GTG GTT GAT C-3'. The annealed oligonucleotides, which had sticky ends complementary to those generated by *Not*I and *Xho*I restriction digestion, were then ligated to the psiCHECK backbone fragment according to standard procedures and the sequences of positive clones were verified (Inqaba Biotech Industries, South Africa). Resulting dual luciferase target plasmids were psiCHECK-siRNA3 Complete Target (psiCHECK-siRNA3 CT), psiCHECK-siRNA3 Incomplete Target 1 (psiCHECK-siRNA3 IT1), psiCHECK-siRNA3 Incomplete Target 2 (psiCHECK-siRNA3 IT2), and psiCHECK-siRNA3 Seed Only Target (psiCHECK-siRNA3 SO).

4.4. Transfections and HBV knockdown assessment in vitro by ELISA and dual-luciferase assays

The Huh7 line was maintained in DMEM (Lonza, Basel, Switzerland) supplemented with 10% FCS (Gibco BRL, UK). One day before transfection, cells were seeded in 24-well plates at a confluency of 40%. To assess target knockdown, Lipofectamine 2000 (Invitrogen, CA, USA) was employed to transfect cells with 100 ng of either pCH-9/3091 or psiCHECK-HBx, 100 ng pCI-eGFP and 32.5 ng siRNA (10 nM final concentration). The ratio of Lipofectamine to target plasmids was 1:1 (mL:mg), while that of Lipofectamine to siRNAs was 1:3 (mL:mg). Unmodified and scrambled siRNAs were included as positive and negative controls, respectively. Forty eight hours after transfection, growth medium was collected and HBsAg concentration was measured by ELISA using the MONOLISA HBsAg ULTRA kit (Bio-Rad, CA, USA). Cells transfected with psiCHECK-HBx were lysed and assessed for luciferase activity using the Dual-Luciferase Reporter Assay System (Promega, WI, USA). The average

ratio of *Renilla* luciferase to Firefly luciferase activity was calculated from a minimum of three replicates.

4.5. Assessing induction of the interferon response by antiHBV siRNAs

The HEK293 line was maintained in DMEM supplemented with 10% FCS, penicillin (50 IU/mL) and streptomycin (50 µg/mL) (Gibco BRL, UK). On the day prior to transfection, wells of 2 cm diameter were each seeded with 250 000 HEK293 cells. Transfection was carried out with 800 ng of unmodified or GP-containing siRNAs using Lipofectamine (Invitrogen, CA, USA) according to the manufacturer's instructions. As a positive control for induction of the IFN response, cells were also transfected with 800 ng poly (I:C) (Sigma, MI, USA). Two days after transfection, RNA was extracted with Tri Reagent (Sigma, MI, USA) according to the manufacturer's instructions.

To assess induction of the IFN response genes, IFN-β and GAPDH cDNA preparation and qPCR amplification were performed according to the procedures described by Song et al.⁴⁰ with minor modifications. All qPCRs were carried out using the Roche Lightcycler V.2. Controls included water blanks and RNA extracts that were not subjected to reverse transcription. Taq ready mix with SYBR green (Sigma, MO, USA) was used to amplify and detect DNA during the reaction. Thermal cycling parameters consisted of a hotstart for 30 sec at 95 °C, followed by 50 cycles of 58 °C for 10 sec, 72 °C for 7 sec and then 95 °C for 5 sec. Specificity of the PCR products was verified by melting curve analysis and agarose gel electrophoresis. The primer combinations used to amplify IFN-β, OAS-1, IFIT1 and GAPDH mRNA were IFN-β forward: 5'-TCC AAA TTG CTC TCC TGT TGT GCT-3', IFN-β reverse: 5'-CCA CAG GAG CTT CTG ACA CTG AAA A-3', OAS-1 forward: 5'-CGA GGG AGC ATG AAA ACA CAT TT-3', OAS-1 reverse: 5'-GCA GAG TTG CTG GTA GTT TAT GAC - 3', IFIT1 forward: 5'-CCC TGA AGC TTC AGG ATG AAG G - 3', IFIT1 reverse: 5'-AGA AGT GGG TGT TTC CTG CAA G-3', GAPDH forward 5'-AGG GGT CAT TGA TGG CAA CAA TAT CCA-3', GAPDH reverse 5'-TTT ACC AGA GTT AAA AGC AGC CCT GGT G-3'.

4.6. Influence of GP modifications of siRNAs on cell viability using the MTT assay

The MTT [3-(4,5-Dimethylthiazol-2-yl)-2,5-diphenyltetrazolium bromide] reagent was purchased from Sigma (St. Louis, MO, USA). Huh7 cells were seeded in 96-well plates at a confluency of 40% a day before transfection and untransfected cells were used as controls. To assess toxicity, Lipofectamine 2000 (Invitrogen, CA, USA) was employed to transfect cells with 25 ng pCH-9/3091, 25 ng pCI-eGFP and 8.125 ngsiRNA (2.5 nM final concentration). Transfection ratios of Lipofectamine to plasmids and siRNAs were 1:1 and 1:3 (mL:mg), respectively. Twenty microliters of MTT solution (5 mg/mL dissolved in 1 × Dulbecco's Phosphate Buffered Saline) was added into each well, gently mixed for 5 min and incubated (37 °C, 5% CO₂) for 4 h. Culture medium from each well was gently removed by aspiration and formazan (blue product of MTT metabolism) was resuspended in 200 µl DMSO with constant mixing for 5 min. Data analysis, carried out in triplicate at time points of 48 and 72 h after transfection, was performed by calculating the ratio of optical density at 570 nm and 650 nm.

4.7. Influence of the position of GP modifications on silencing of complete and partial HBV targets using the dual luciferase reporter assay

To measure knockdown efficiency of 2'-O-guanidinopropyl-modified siRNAs that were completely or partially complementary to targets, Huh7 cells were co-transfected with 100 ng of either

psiCHECK-siRNA3 CT, psiCHECK-siRNA3 IT1, psiCHECK-siRNA3 IT2 or psiCHECK-siRNA3 SO, 100 ng pCI-eGFP and 32.5 ng siRNA (10 nM final concentration). Ratios of Lipofectamine to plasmids and siRNAs were 1:1 and 1:3 (mL:mg), respectively. Detection of *Renilla* and Firefly luciferase activity was conducted 48 h after transfection according to the procedures described above.

4.8. Assessment of siRNA stability in FCS

siRNAs were added to 80% FCS at a final concentration of 10 nM, then incubated at 37 °C for 0, 1, 3, 5, 20, 24 and 48 h. Aliquots of 10 µl were loaded on a 15% denaturing polyacrylamide gel, subjected to electrophoresis, visualised under UV transillumination and RNA bands were quantified by densitometry (Syngene G-Box, SYNGENE, UK).

4.9. AntiHBV effects of GP-modified and unmodified siRNAs in vivo

The siRNAs with sense strand GP modifications in position 3, 4 or 5 were selected for studies in vivo. The murine hydrodynamic tail vein injection model of HBV replication²⁹ was employed to assess antiHBV effects of siRNAs in mice. Experiments on animals were conducted in accordance with protocols approved by the University of the Witwatersrand Animal Ethics Screening Committee. A saline solution comprising 10% of the mouse's body weight was injected via the tail vein over 10 seconds. The saline solution included a combination of 15 µg of HBV target plasmid (pCH-9/3091), 15 µg of pCI-eGFP plasmid and 1 nmol of GP-modified or unmodified siRNAs. At days 3 and 5 after injection, blood samples were collected. HBsAg and circulating VPEs were measured according to previously described methods.^{8,9}

4.10. Statistical analysis

Data are expressed as the mean ± standard error of the mean. Statistical variation was considered significant when $P < 0.05$ and was calculated using nonparametric student t-tests with the GraphPad Prism software package (GraphPad Software, Inc., CA, USA).

Acknowledgements

We gratefully acknowledge financial assistance from the Ernst & Ethel Eriksen Trust, National Research Foundation of South Africa (NRF), Medical Research Council, the Poliomyelitis Research Foundation (PRF) and from the German Research Foundation (DFG). We also thankfully acknowledge the helpful assistance of Corvin Steidinger, Christian Schuch and Timo Weinrich in the synthesis of the GP modified monomers.

Supplementary data

Supplementary data associated with this article can be found, in the online version, at <http://dx.doi.org/10.1016/j.bmc.2013.04.073>.

References and notes

- Arbuthnot, P.; Kew, M. *Int. J. Exp. Pathol.* **2001**, *82*, 77.
- Hollinger, F. B.; Lau, D. T. *Gastroenterol. Clin. North Am.* **2006**, *35*, 425.
- Ayoub, W. S.; Keeffe, E. B. *Aliment. Pharmacol. Ther.* **2011**, *34*, 1145.
- Arbuthnot, P.; Longshaw, V.; Naidoo, T.; Weinberg, M. S. *J. Viral Hepat.* **2007**, *14*, 447.
- Ivacik, D.; Ely, A.; Arbuthnot, P. *Rev. Med. Virol.* **2011**, *21*, 383.
- Kim, D.; Rossi, J. *Biotechniques* **2008**, *44*, 613.
- Kim, V. N.; Han, J.; Siomi, M. C. *Nat. Rev. Mol. Cell Biol.* **2009**, *10*, 126.
- Ely, A.; Naidoo, T.; Arbuthnot, P. *Nucleic Acids Res.* **2009**, *37*, e91.

9. Ely, A.; Naidoo, T.; Mufamadi, S.; Crowther, C.; Arbuthnot, P. *Mol. Ther.* **2008**, *16*, 1105.
10. Carmona, S.; Ely, A.; Crowther, C.; Moolla, N.; Salazar, F. H.; Marion, P. L.; Ferry, N.; Weinberg, M. S.; Arbuthnot, P. *Mol. Ther.* **2006**, *13*, 411.
11. McCaffrey, A. P.; Nakai, H.; Pandey, K.; Huang, Z.; Salazar, F. H.; Xu, H.; Wieland, S. F.; Marion, P. L.; Kay, M. A. *Nat. Biotechnol.* **2003**, *21*, 639.
12. Morrissey, D. V.; Lockridge, J. A.; Shaw, L.; Blanchard, K.; Jensen, K.; Breen, W.; Hartsough, K.; Machemer, L.; Radka, S.; Jadhav, V.; Vaish, N.; Zinnen, S.; Vargeese, C.; Bowman, K.; Shaffer, C. S.; Jeffs, L. B.; Judge, A.; MacLachlan, I.; Polisky, B. *Nat. Biotechnol.* **2005**, *23*, 1002.
13. Giladi, H.; Ketzinel-Gilad, M.; Rivkin, L.; Felig, Y.; Nussbaum, O.; Galun, E. *Mol. Ther.* **2003**, *8*, 769.
14. Hean, J.; Crowther, C.; Ely, A.; Ul Islam, R.; Barichievy, S.; Bloom, K.; Weinberg, M. S.; Van Otterlo, W. A.; De Koning, C. B.; Salazar, F.; Marion, P.; Roesch, E. B.; Lemaitre, M.; Herdewijn, P.; Arbuthnot, P. *Artif DNA PNA XNA* **2010**, *1*, 17.
15. Morrissey, D. V.; Blanchard, K.; Shaw, L.; Jensen, K.; Lockridge, J. A.; Dickinson, B.; McSwiggen, J. A.; Vargeese, C.; Bowman, K.; Shaffer, C. S.; Polisky, B. A.; Zinnen, S. *Hepatology* **2005**, *41*, 1349.
16. Elbashir, S. M.; Harborth, J.; Lendeckel, W.; Yalcin, A.; Weber, K.; Tuschl, T. *Nature* **2001**, *411*, 494.
17. Hornung, V.; Guenther-Biller, M.; Bourquin, C.; Ablasser, A.; Schlee, M.; Uematsu, S.; Noronha, A.; Manoharan, M.; Akira, S.; de Fougerolles, A.; Endres, S.; Hartmann, G. *Nat. Med.* **2005**, *11*, 263.
18. Judge, A. D.; Sood, V.; Shaw, J. R.; Fang, D.; McClintock, K.; MacLachlan, I. *Nat. Biotechnol.* **2005**, *23*, 457.
19. Behlke, M. A. *Oligonucleotides* **2008**, *18*, 305.
20. Engels, J. W.; Odadzic, D.; Smicius, R.; Haas, J. *Methods Mol. Biol.* **2010**, *623*, 155.
21. Bramsen, J. B.; Laursen, M. B.; Nielsen, A. F.; Hansen, T. B.; Bus, C.; Langkjaer, N.; Babu, B. R.; Hojland, T.; Abramov, M.; Van Aerschot, A.; Odadzic, D.; Smicius, R.; Haas, J.; Andree, C.; Barman, J.; Wenska, M.; Srivastava, P.; Zhou, C.; Honcharenko, D.; Hess, S.; Muller, E.; Bobkov, G. V.; Mikhailov, S. N.; Fava, E.; Meyer, T. F.; Chattopadhyaya, J.; Zerial, M.; Engels, J. W.; Herdewijn, P.; Wengel, J.; Kjems, J. *Nucleic Acids Res.* **2009**, *37*, 2867.
22. Bramsen, J. B.; Pakula, M. M.; Hansen, T. B.; Bus, C.; Langkjaer, N.; Odadzic, D.; Smicius, R.; Wengel, S. L.; Chattopadhyaya, J.; Engels, J. W.; Herdewijn, P.; Wengel, J.; Kjems, J. *Nucleic Acids Res.* **2010**, *38*, 5761.
23. Brzezinska, J.; D'Onofrio, J.; Buff, M. C.; Hean, J.; Ely, A.; Marimani, M.; Arbuthnot, P.; Engels, J. W. *Bioorg. Med. Chem.* **2012**, *20*, 1594.
24. Weinberg, M. S.; Ely, A.; Barichievy, S.; Crowther, C.; Mufamadi, S.; Carmona, S.; Arbuthnot, P. *Mol. Ther.* **2007**, *15*, 534.
25. Nassal, M. J. *J. Virol.* **1992**, *66*, 4107.
26. Li, K.; Chen, Z.; Kato, N.; Gale, M., Jr.; Lemon, S. M. *J. Biol. Chem.* **2005**, *280*, 16739.
27. Robbins, M.; Judge, A.; Liang, L.; McClintock, K.; Yaworski, E.; MacLachlan, I. *Mol. Ther.* **2007**, *15*, 1663.
28. Pei, Y.; Tuschl, T. *Nat. Methods* **2006**, *3*, 670.
29. Yang, P. L.; Althage, A.; Chung, J.; Chisari, F. V. *Proc. Natl. Acad. Sci. U.S.A.* **2002**, *99*, 13825.
30. Rettig, G. R.; Behlke, M. A. *Mol. Ther.* **2012**, *20*, 483.
31. Liu, J.; Carmell, M. A.; Rivas, F. V.; Marsden, C. G.; Thomson, J. M.; Song, J. J.; Hammond, S. M.; Joshua-Tor, L.; Hannon, G. J. *Science* **2004**, *305*, 1437.
32. Aagaard, L.; Rossi, J. J. *Adv. Drug Deliv. Rev.* **2007**, *59*, 75.
33. Soifer, H. S.; Rossi, J. J.; Saetrom, P. *Mol. Ther.* **2007**, *15*, 2070.
34. Jackson, A. L.; Burchard, J.; Schelter, J.; Chau, B. N.; Cleary, M.; Lim, L.; Linsley, P. S. *RNA* **2006**, *12*, 1179.
35. Jackson, A. L.; Burchard, J.; Leake, D.; Reynolds, A.; Schelter, J.; Guo, J.; Johnson, J. M.; Lim, L.; Karpilow, J.; Nichols, K.; Marshall, W.; Khvorova, A.; Linsley, P. S. *RNA* **2006**, *12*, 1197.
36. Eder, P. S.; DeVine, R. J.; Dagle, J. M.; Walder, J. A. *Antisense Res. Dev.* **1991**, *1*, 141.
37. Mukobata, T.; Ochi, Y.; Ito, Y.; Wada, S.; Urata, H. *Bioorg. Med. Chem. Lett.* **2010**, *20*, 129.
38. Passman, M.; Weinberg, M.; Kew, M.; Arbuthnot, P. *Biochem. Biophys. Res. Commun.* **2000**, *268*, 728.
39. Weinberg, M.; Passman, M.; Kew, M.; Arbuthnot, P. *J. Hepatol.* **2000**, *33*, 142.
40. Song, E.; Lee, S. K.; Dykxhoorn, D. M.; Novina, C.; Zhang, D.; Crawford, K.; Cerny, J.; Sharp, P. A.; Lieberman, J.; Manjunath, N.; Shankar, P. J. *J. Virol.* **2003**, *77*, 7174.

Inhibition of hepatitis B virus replication in cultured cells and *in vivo* using 2'-O-guanidinopropyl modified siRNAs

Supplementary Information

Musa D. Marimani^a, Abdullah Ely^a, Maximilian C.R. Buff^b, Stefan Bernhardt^b, Joachim W. Engels^{b*} and Patrick Arbuthnot^{a*}

^a*Antiviral Gene Therapy Research Unit and African Network for Drugs and Diagnostics Innovation (ANDI) Centre of Excellence, School of Pathology, Health Sciences Faculty, University of the Witwatersrand, Private Bag 3, Wits 2050, Johannesburg, South Africa.*

^b*Goethe-University, Institute of Organic Chemistry & Chemical Biology, Max-von-Laue-Str. 7, 60438 Frankfurt am Main, Germany.*

*Corresponding authors:

J.W.Engels: Tel.: +49 69 798 29150; fax: +49 69 798 29148,

E-mail address: Joachim.Engels@chemie.uni-frankfurt.de

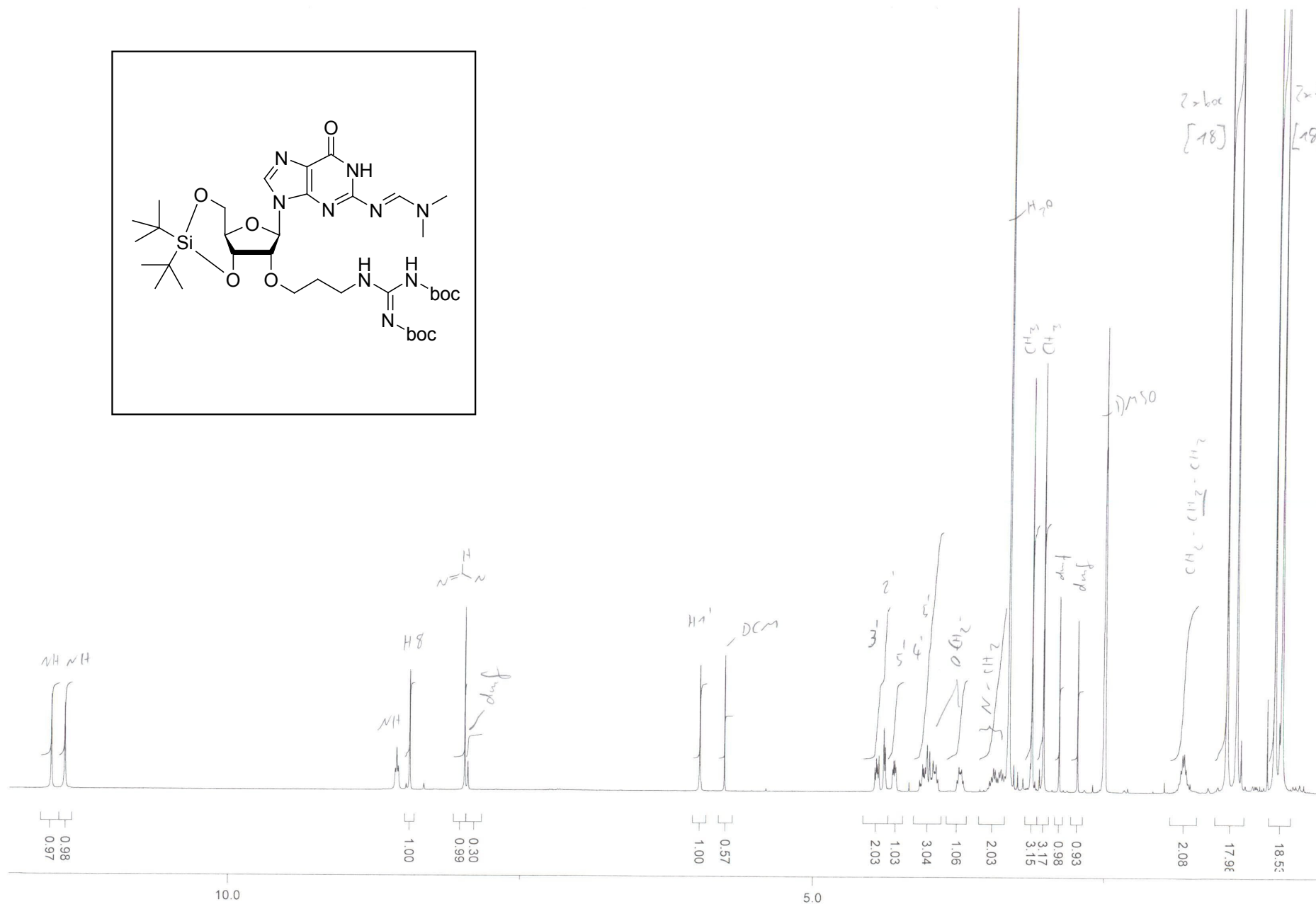
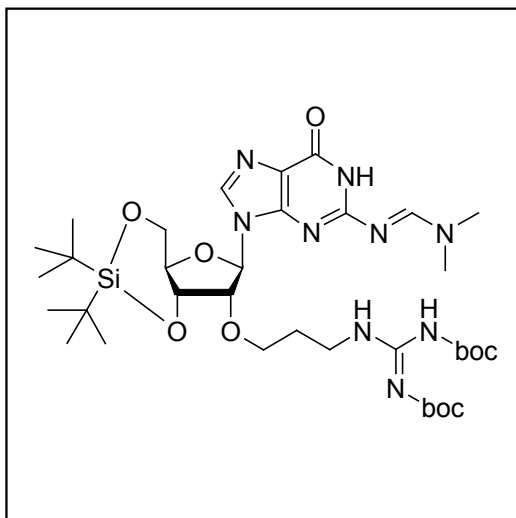
and

P.Arbuthnot: Tel.: +27 11 717 2365; fax: +27 11 2395,

E-mail address: Patrick.Arbuthnot@wits.ac.za

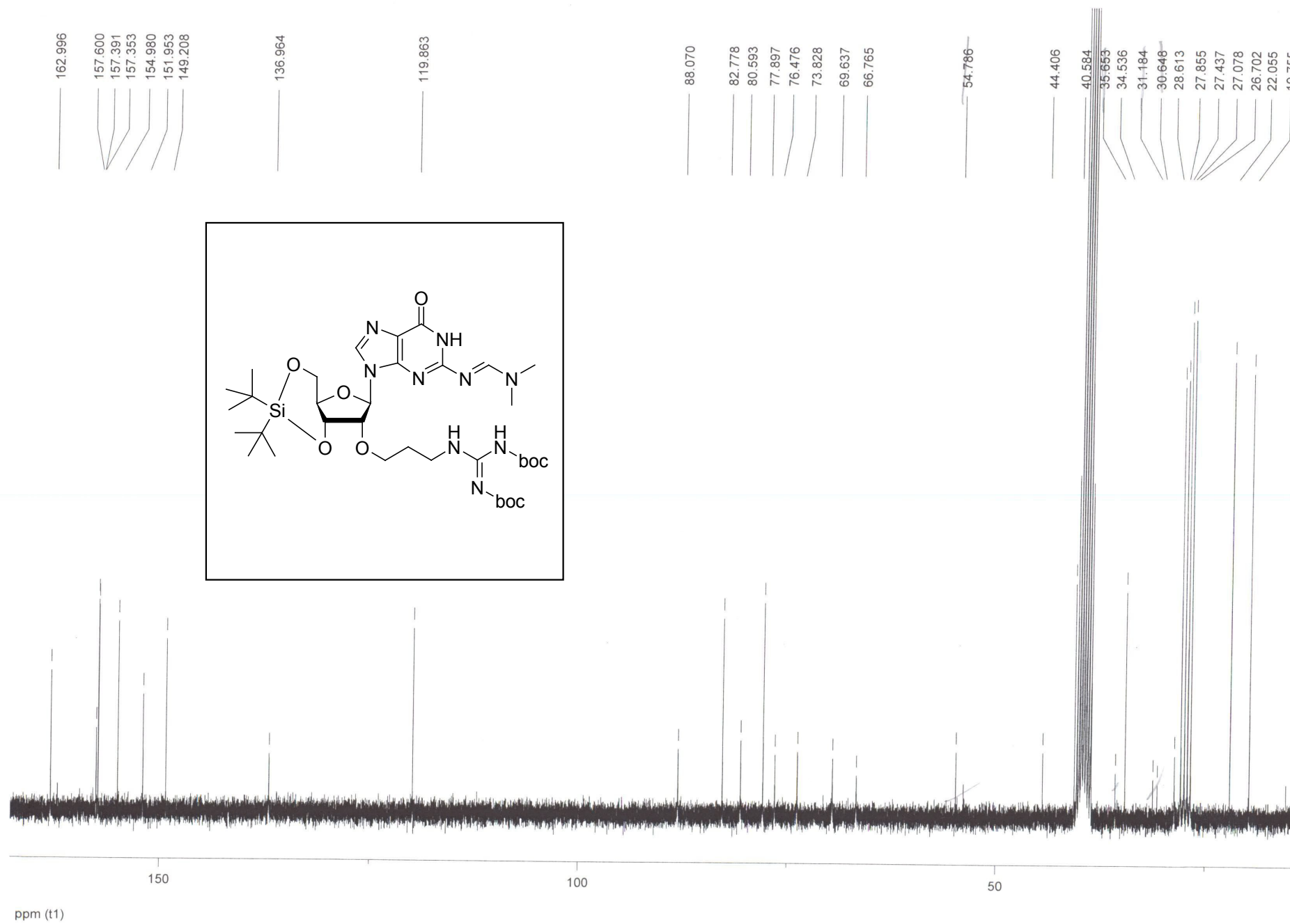
¹H NMR of N2-Dimethylformamidine-2'-O-(N,N'-di-tert-butoxycarbonylguanidinopropyl)-3',5'-O-di-tert-butylsilanediylguanosine (3a)	S3
¹³C NMR of N2-Dimethylformamidine-2'-O-(N,N'-di-tert-butoxycarbonylguanidinopropyl)-3',5'-O-di-tert-butylsilanediylguanosine (3a)	S4
¹H NMR of N2-Dimethylformamidine-2'-O-(N,N'-di-tert-butoxycarbonylguanidinopropyl)-guanosine (3b)	S5
¹³C NMR of N2-Dimethylformamidine-2'-O-(N,N'-di-tert-butoxycarbonylguanidino-propyl)-guanosine (3b)	S6
¹H NMR of N2-Dimethylformamidine-2'-O-(N,N'-di-tert-butoxycarbonylguanidinopropyl)-5'-O-(4,4'-dimethoxytrityl)-guanosine (3c)	S7
¹³C NMR of N2-Dimethylformamidine-2'-O-(N,N'-di-tert-butoxycarbonylguanidinopropyl)-5'-O-(4,4'-dimethoxytrityl)-guanosine (3c)	S8
¹H NMR of N2-Dimethylformamidine-2'-O-(N,N'-di-tert-butoxycarbonylguanidinopropyl)-5'-O-(4,4'-dimethoxytrityl)-guanosine 3'-(cyanoethyl)-N,N-diisopropylphosphoramidite (4)	S9
³¹P NMR of N2-Dimethylformamidine-2'-O-(N,N'-di-tert-butoxycarbonylguanidinopropyl)-5'-O-(4,4'-dimethoxytrityl)-guanosine 3'-(cyanoethyl)-N,N-diisopropylphosphoramidite (4)	S10
Trityl protocol diagrams of oligo-syntheses with the new amidite (4)	S11
Exemplary RP-HPLC-Chromatogramm of GP10 siRNA3	S12
MS data of the synthesised oligos	S13
Δ Tm values of modified oligos	S14

¹H NMR (400 MHz) in DMSO-d₆

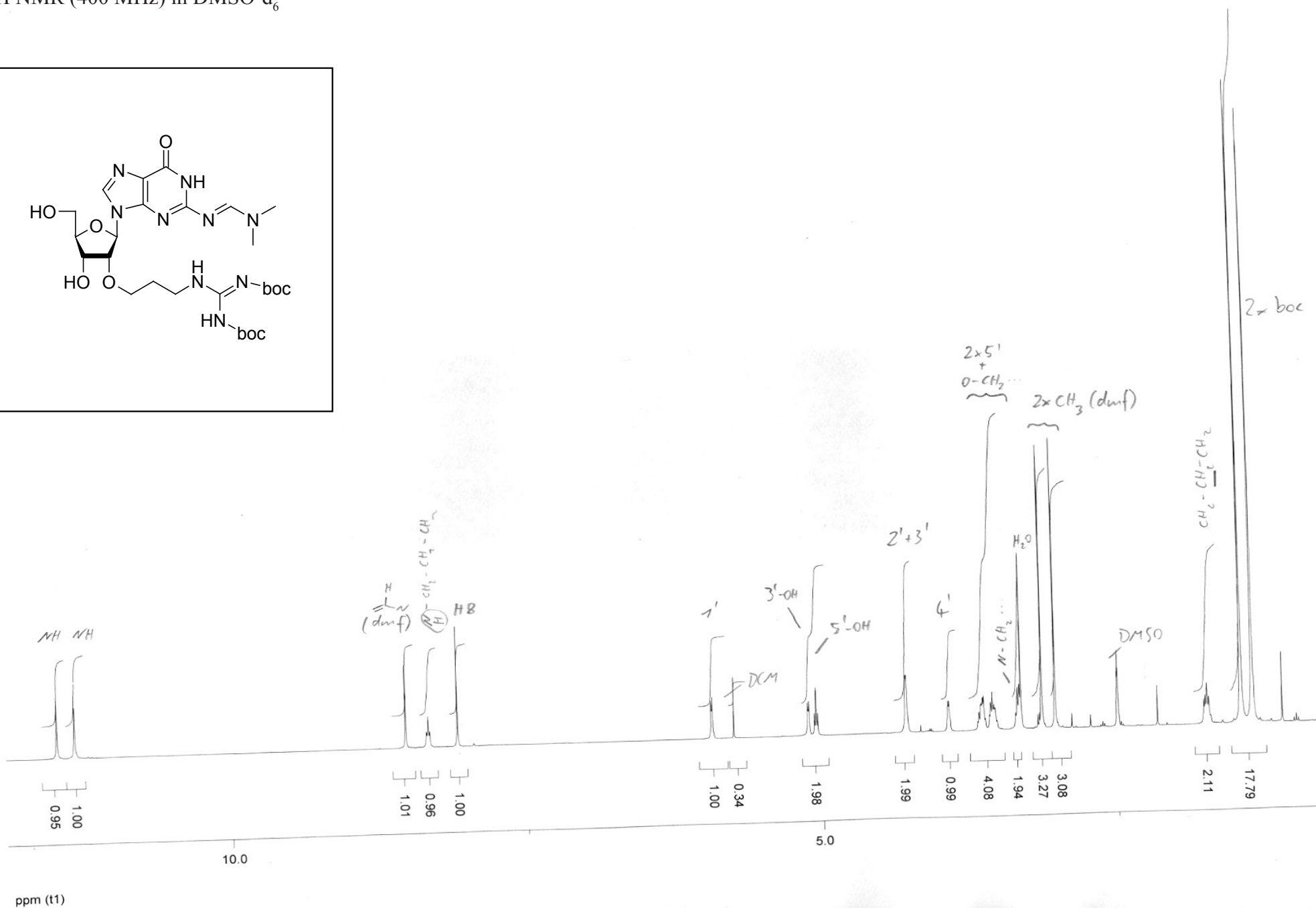
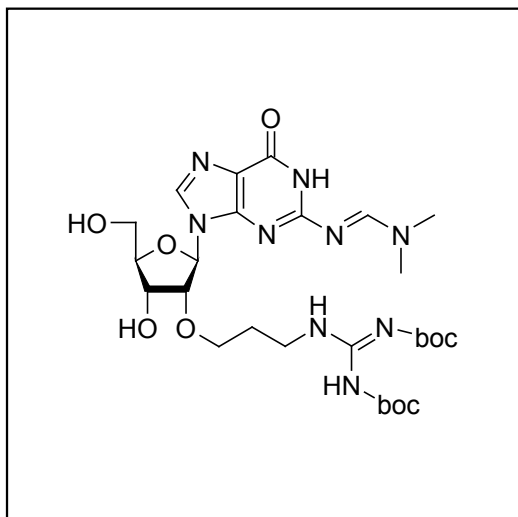


ppm (t1)

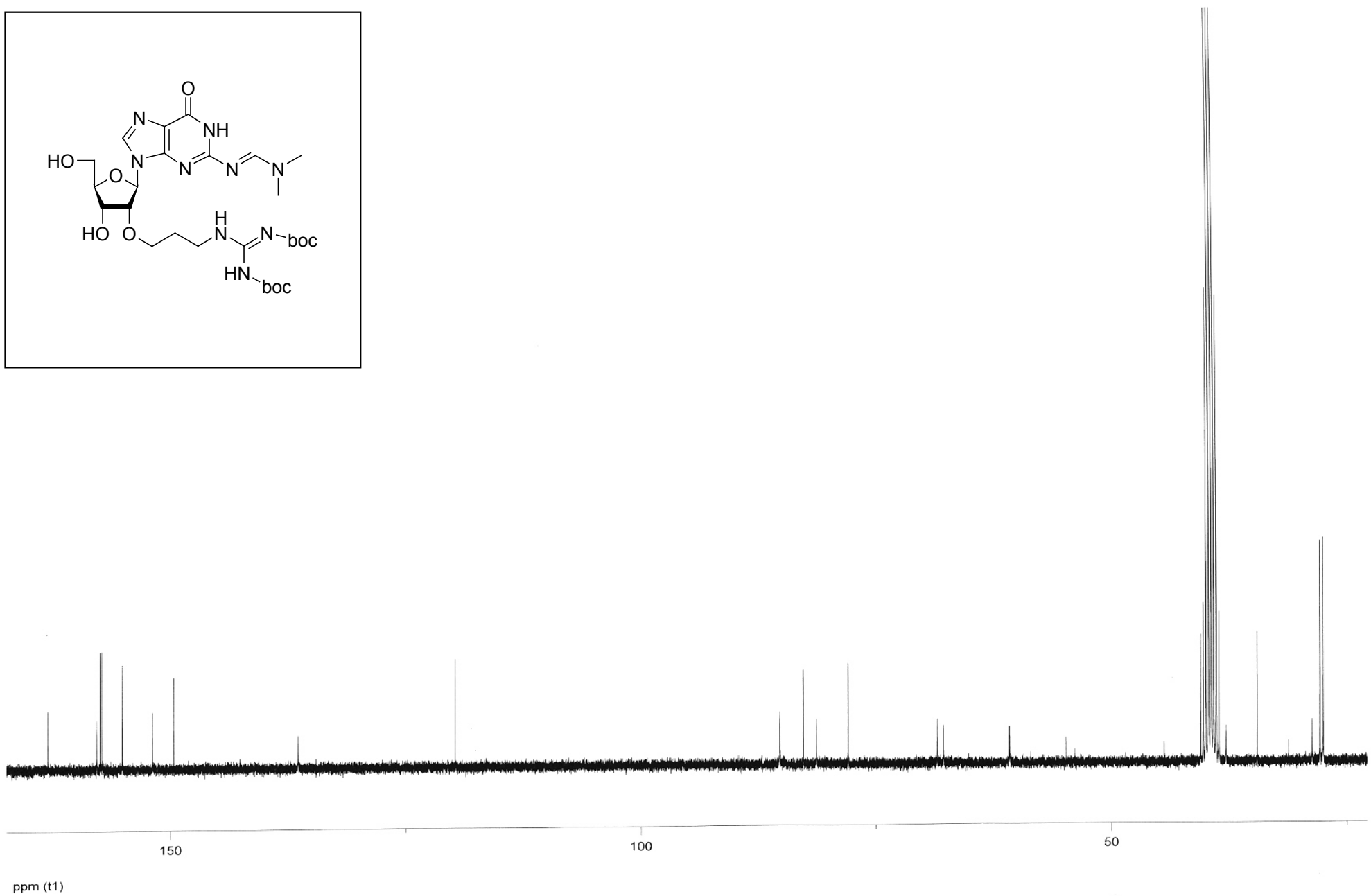
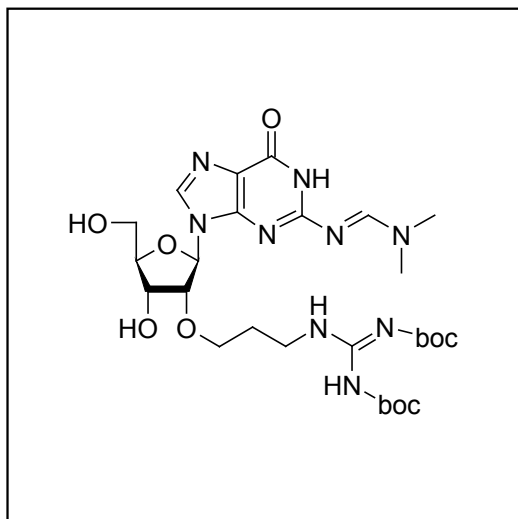
^{13}C NMR (75 MHz) in DMSO-d_6



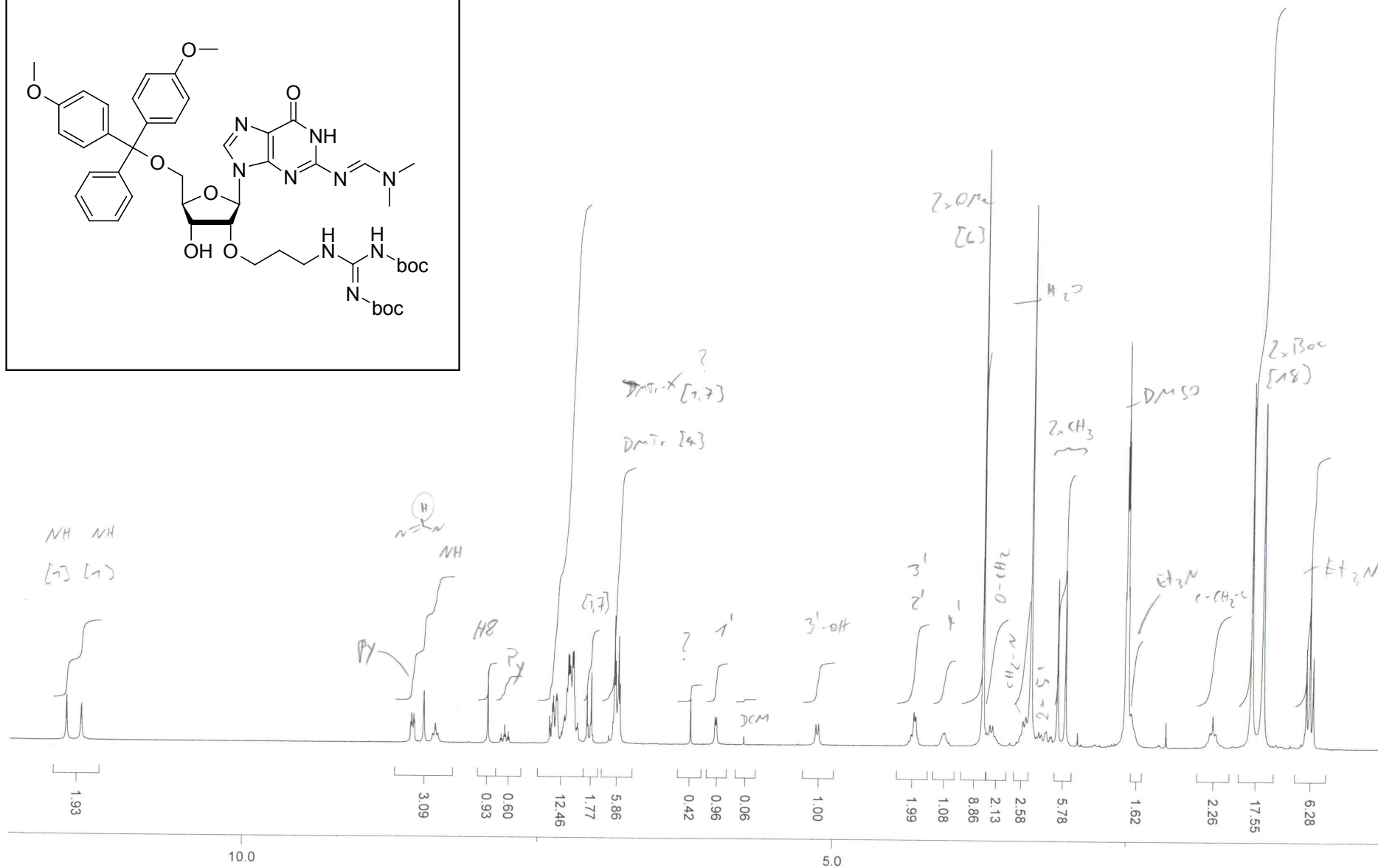
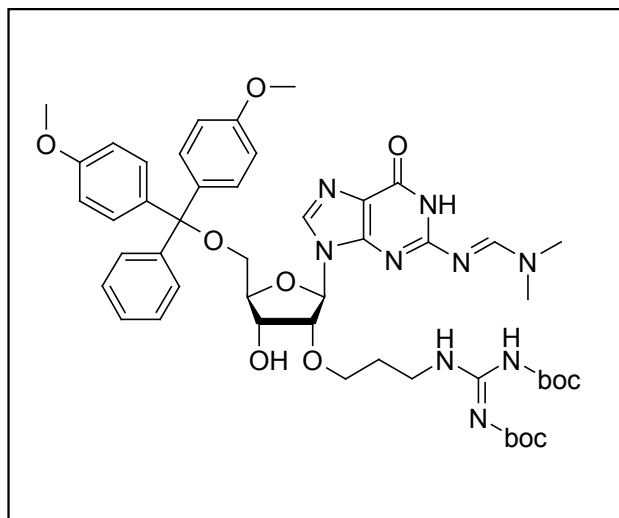
^1H NMR (400 MHz) in DMSO-d_6



^{13}C NMR (75 MHz) in DMSO-d_6

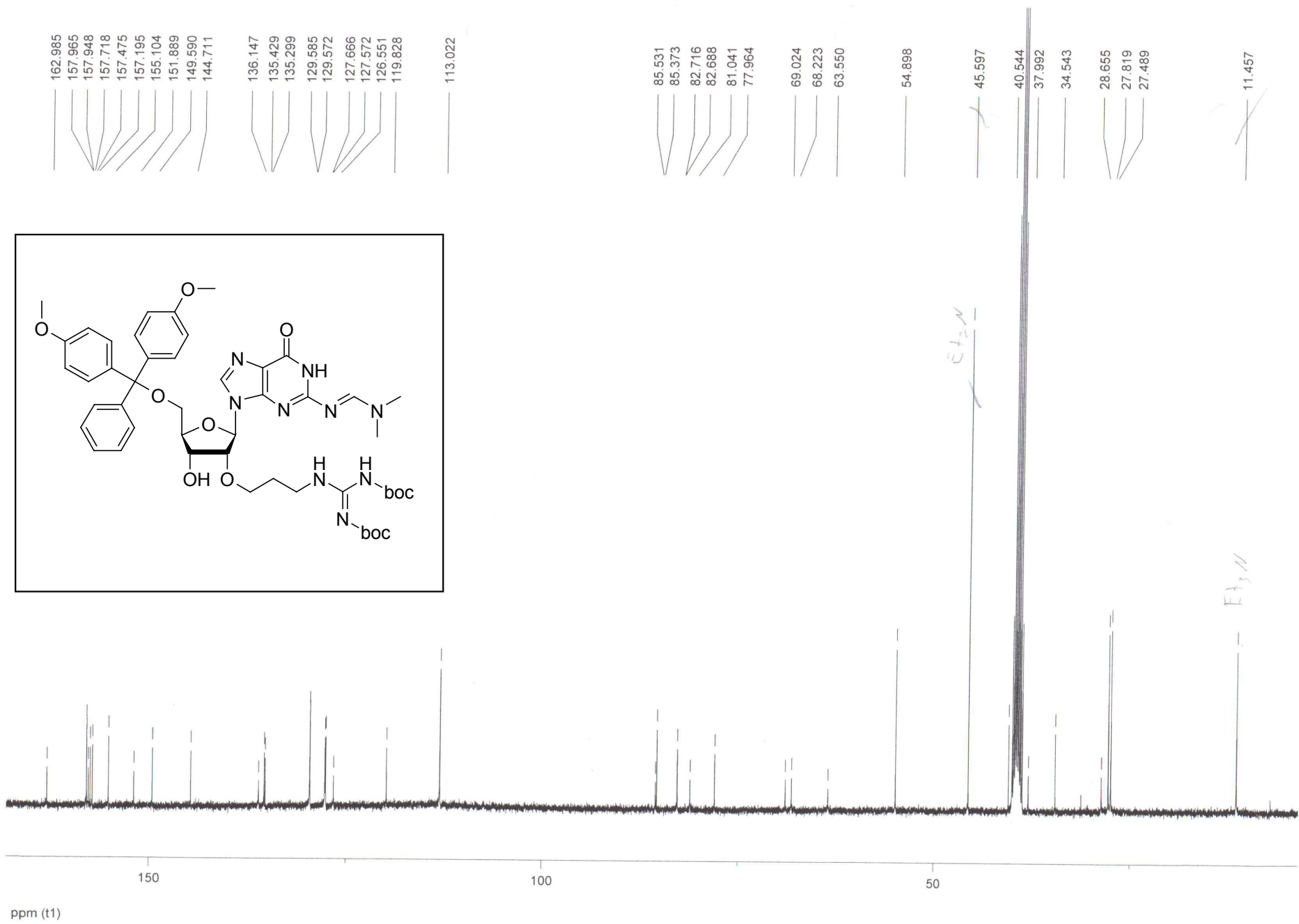


¹H NMR (400 MHz) in DMSO-d₆

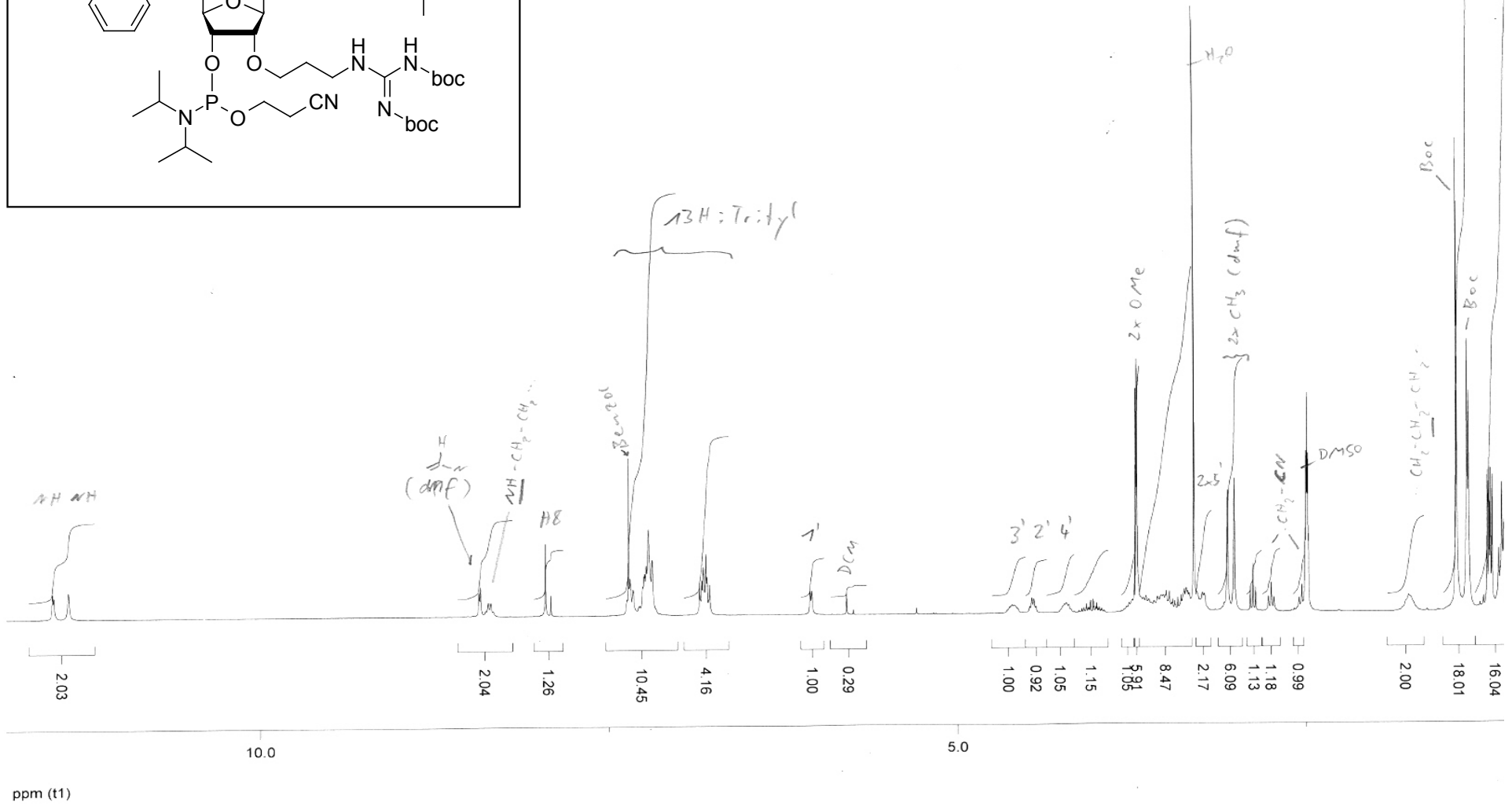
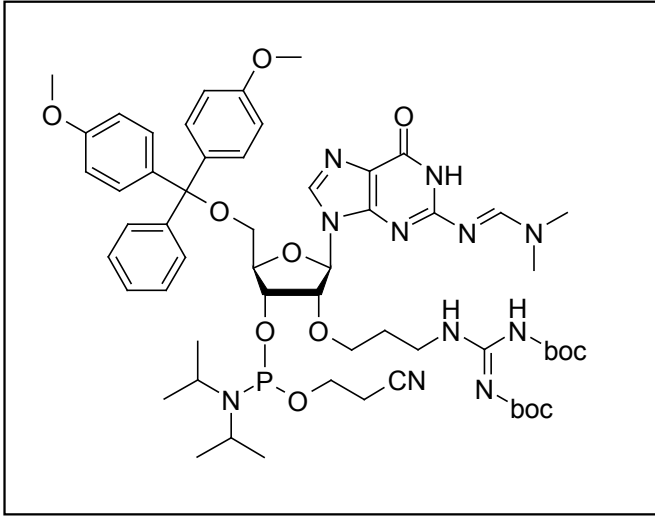


ppm (t1)

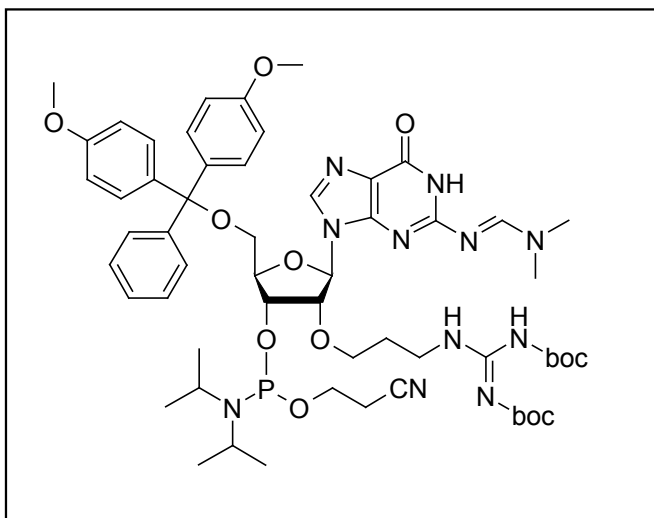
^{13}C NMR (100 MHz) in DMSO-d_6



¹H NMR (400 MHz) in DMSO-d₆

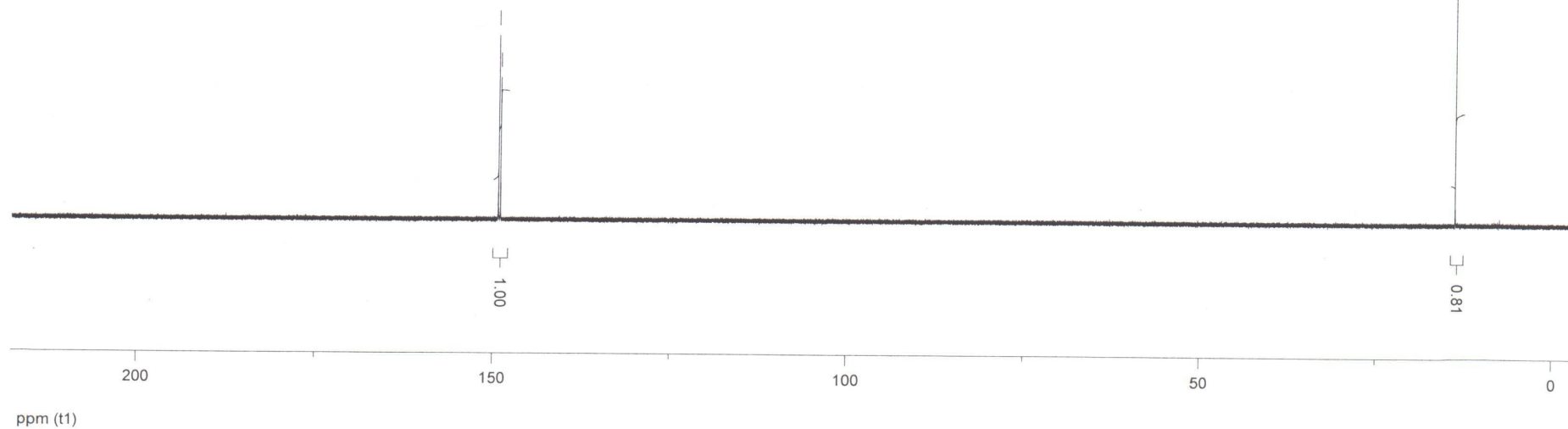
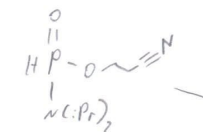


^{31}P NMR (121 MHz) in DMSO-d_6

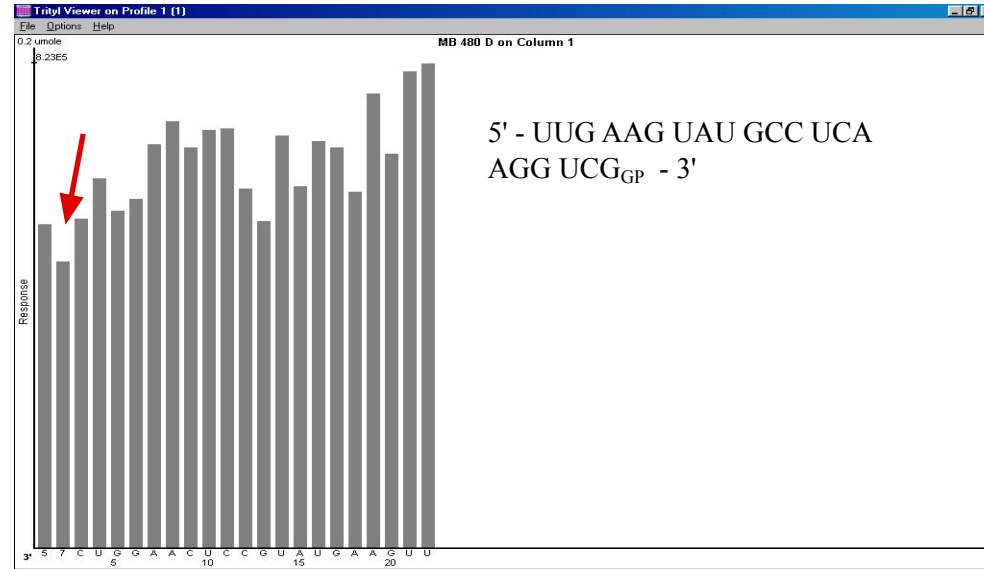
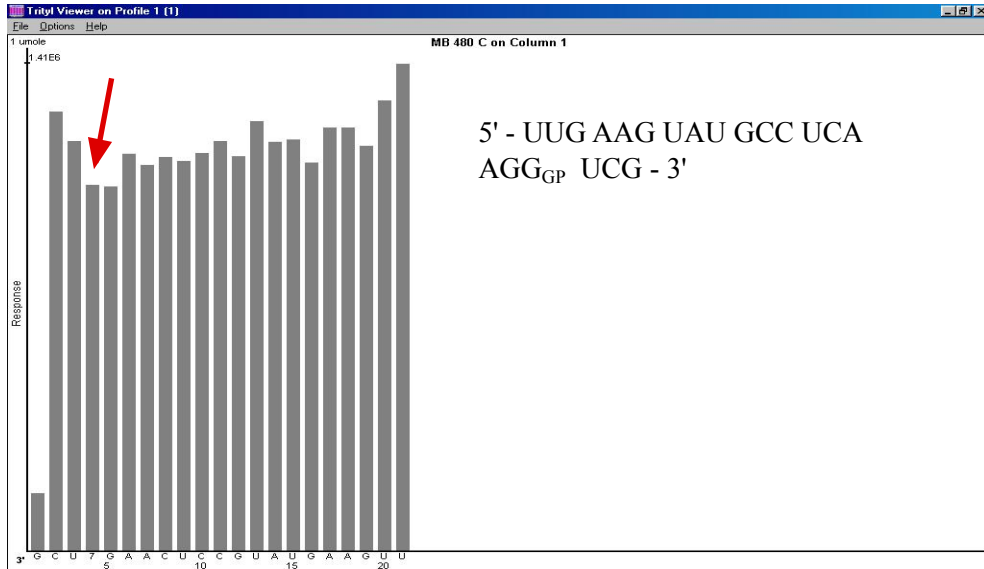
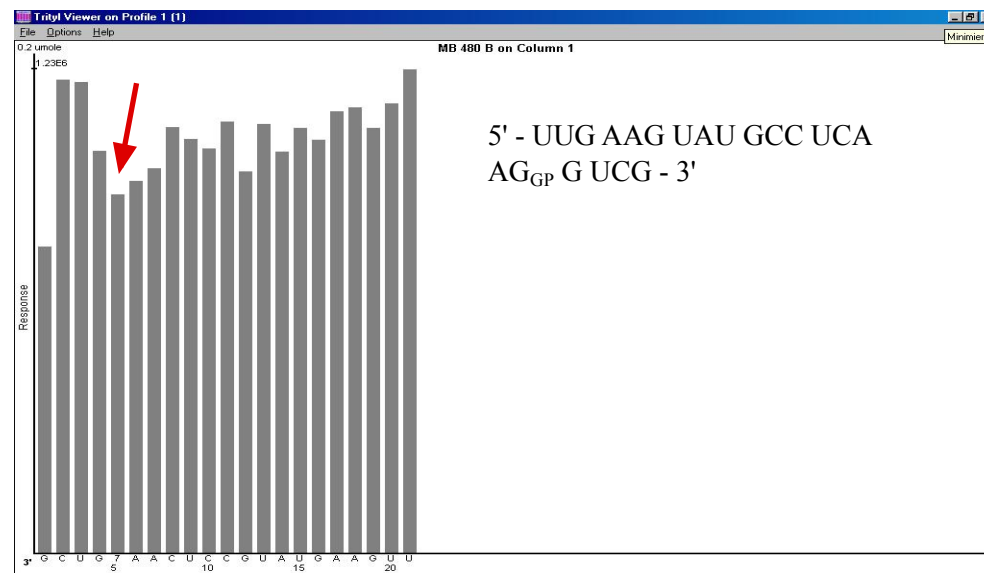
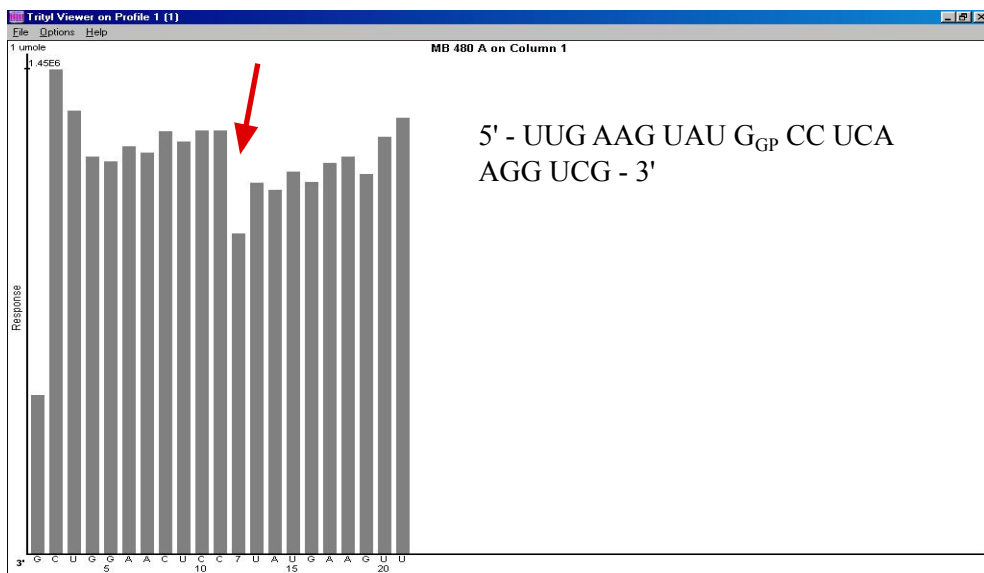


149.208
148.925

13.870

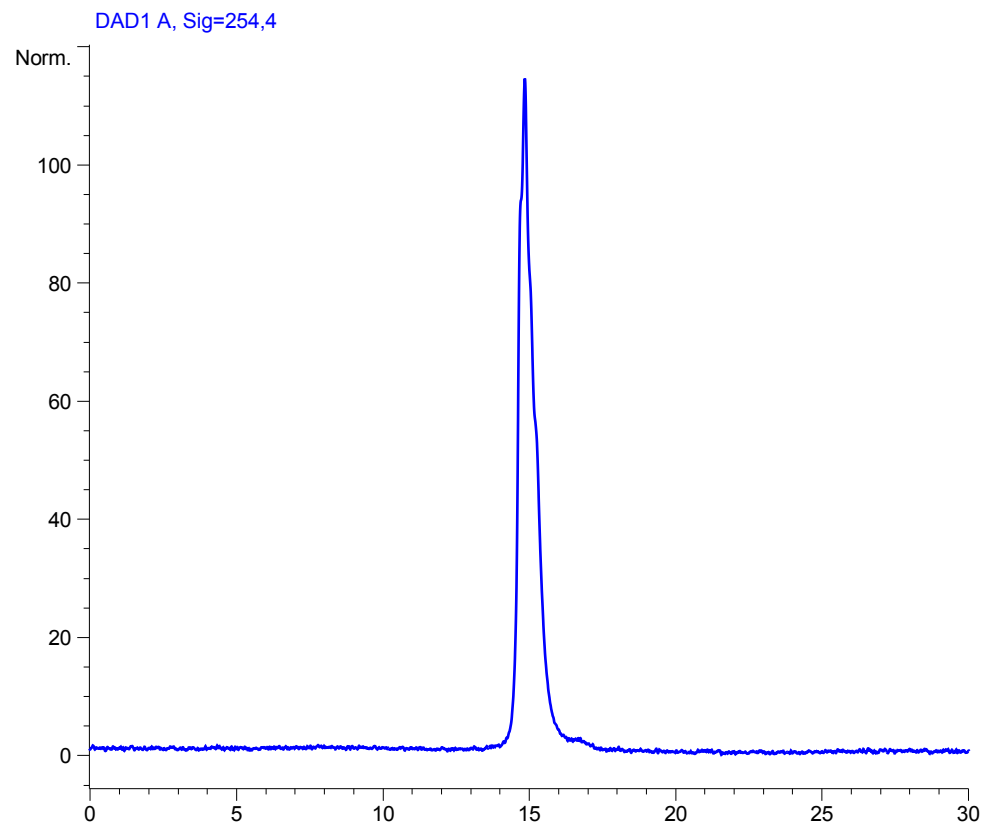


Trityl protocols of the syntheses of modified oligonucleotides



The red arrow marks the GP-modified nucleotide. Slightly reduced coupling efficiency in the synthesis corresponding to the trityl protocol in the upper left might be a result of insufficient purging of the supply line of the synthesiser with the modified amidite solution.

Analytical RP-Chromatogram of the sequence: 5' - UUG AAG UAU G_{GP} CC UCA AGG UCG - 3'



Exemplary reverse phase chromatogram of the purified RNA (GP10 siRNA3, 400 pmol) using a Nucleosil 100-5 C18 column (4.6 x 250 mm, *CS Chromatography*) (acetonitrile, 0.1 M triethylammonium acetate solution pH = 7; prerun: 2 min 5 % acetonitril; gradient: 5 % to 35 % acetonitrile in 30 minutes, flow: 1 mL/min, detector: 254 nm).

MS data of the synthesised oligos measured on a *Bruker* microTOF QII

Name	Sequence	M_{calc.}	M_{exp.}
GP2 siRNA3	5- UU _{GP} G AAG UAU GCC UCA AGG UCG -3'	6809.0	6809.1
GP3 siRNA3	5- UUG _{GP} AAG UAU GCC UCA AGG UCG -3'	6809.0	6809.5
GP4 siRNA3	5- UUG A _{GP} AG UAU GCC UCA AGG UCG -3'	6809.0	6809.4
GP5 siRNA3	5- UUG AA _{GP} G UAU GCC UCA AGG UCG -3'	6809.0	6809.4
GP6 siRNA3	5- UUG AAG _{GP} UAU GCC UCA AGG UCG -3'	6809.0	6809.4
GP7 siRNA3	5- UUG AAG U _{GP} AU GCC UCA AGG UCG -3'	6809.0	6809.1
GP8 siRNA3	5- UUG AAG UA _{GP} U GCC UCA AGG UCG -3'	6809.0	6809.4
GP9 siRNA3	5- UUG AAG UAU _{GP} GCC UCA AGG UCG -3'	6809.0	6809.1
GP10 siRNA3	5- UUG AAG UAU G _{GP} CC UCA AGG UCG -3'	6809.0	6809.5
GP11 siRNA3	5- UUG AAG UAU GC _{GP} C UCA AGG UCG -3'	6809.0	6809.4
GP12 siRNA3	5- UUG AAG UAU GCC _{GP} UCA AGG UCG -3'	6809.0	6809.4
GP13 siRNA3	5- UUG AAG UAU GCC U _{GP} CA AGG UCG -3'	6809.0	6809.1
GP14 siRNA3	5- UUG AAG UAU GCC UC _{GP} A AGG UCG -3'	6809.0	6809.4
GP15 siRNA3	5- UUG AAG UAU GCC UCA _{GP} AGG UCG -3'	6809.0	6809.3
GP16 siRNA3	5- UUG AAG UAU GCC UCA A _{GP} GG UCG -3'	6809.0	6809.4
GP17 siRNA3	5- UUG AAG UAU GCC UCA AG _{GP} G UCG -3'	6809.0	6809.5
GP18 siRNA3	5- UUG AAG UAU GCC UCA AGG _{GP} UCG -3'	6809.0	6809.5
GP19 siRNA3	5- UUG AAG UAU GCC UCA AGG U _{GP} CG -3'	6809.0	6809.4
GP20 siRNA3	5- UUG AAG UAU GCC UCA AGG UC _{GP} G -3'	6809.0	6809.4
GP21 siRNA3	5- UUG AAG UAU GCC UCA AGG UCG _{GP} -3'	6809.0	6809.5

ΔT_m values of modified oligos

Name	Sequence	ΔT_m (°C)
GP4 siRNA3	5- UUG A _{GP} AG UAU GCC UCA AGG UCG -3'	- 1.9
GP5 siRNA3	5- UUG AA _{GP} G UAU GCC UCA AGG UCG -3'	- 1.1
GP8 siRNA3	5- UUG AAG UA _{GP} U GCC UCA AGG UCG -3'	- 0.9
GP9 siRNA3	5- UUG AAG UAU _{GP} GCC UCA AGG UCG -3'	- 0.9
GP11 siRNA3	5- UUG AAG UAU GC _{GP} C UCA AGG UCG -3'	- 1.6
GP12 siRNA3	5- UUG AAG UAU GCC _{GP} UCA AGG UCG -3'	- 0.6
GP14 siRNA3	5- UUG AAG UAU GCC UC _{GP} A AGG UCG -3'	- 0.8
GP16 siRNA3	5- UUG AAG UAU GCC UCA A _{GP} GG UCG -3'	- 0.1
GP19 siRNA3	5- UUG AAG UAU GCC UCA AGG U _{GP} CG -3'	- 0.4
GP20 siRNA3	5- UUG AAG UAU GCC UCA AGG UC _{GP} G -3'	0.3
GP21 siRNA3	5- UUG AAG UAU GCC UCA AGG UCG _{GP} -3'	- 1.3

Melting point studies were accomplished on a *JASCO V650 Spectrophotometer*. A 1.15 μM solution of the duplex of the unmodified sense strand (5' - ACC UUG AGG CAU ACU UCA AdTdT - 3') and the appropriate modified antisense strand was prepared in PBS (phosphate buffered saline, pH = 7.4). The absorption was measured at 260 nm and the temperature was cycled from 90 °C to 50 °C and back to 90 °C. The experiment was done in triplicate for each siRNA combination.

SUPPLEMENTARY METHODS:

4.1. Transfections and antiHBV activity of GP-modified siRNAs *in vitro* by ELISA and Dual-luciferase assays

Huh7 cells were used to investigate antiviral activity of GP-modified siRNAs. Cells were maintained in Dulbecco's Modified Eagle Medium (DMEM, Lonza, Basel, Switzerland) comprised of Penicillin (50 IU/ml, Gibco[®], Life Technologies, CA, USA), Streptomycin (50 µg/ml, Gibco[®], Life Technologies, CA, USA) and 10% foetal calf serum (FCS, Gibco[®], Life Technologies, CA, USA). Cells were maintained in 24-well plates at 40% confluence, a day prior to transfection. For transfections, Lipofectamine[®] 2000 (Life Technologies, CA, USA) was employed to deliver 100 ng of either psiCHECK-*HBx* or pCH-9/3091 target plasmid, 100 ng pCI-eGFP and 10 nM siRNA (32.5 ng) and incubated at 37°C and 5% CO₂. The ratio of Lipofectamine[®] 2000 to siRNAs was 3:1 (ml:mg), while that of Lipofectamine[®] 2000 to plasmid vectors was 1:1 (ml:mg). The scrambled or non-targeting siRNA and unmodified siRNA3 were employed as negative and positive controls, respectively.

Two days post-transfection, culture medium was harvested from cells treated with pCH-9/3091 and HBsAg concentration was assessed by Enzyme-Linked Immunosorbent Assay (ELISA) using the MONOLISA[™] HBs Ag ULTRA kit (Bio-Rad, CA, USA). Briefly, 100 µl of harvested supernatant was added to each well of the ELISA plate. Additionally, 100 µl of the ELISA negative control (R3, in quadruplicate) and ELISA positive control (R4) were included as additional experimental controls. Fifty microlitres of the conjugate solution (R6 + R7) was dispensed into each well. The ELISA plate was covered with an adhesive film and incubated at 37°C for one and a half hours. Thereafter, the adhesive film was removed; wells emptied by aspiration and washed a minimum of 5 times using a Microplate Washer (Bio-

Chapter 4

Rad, CA, USA). One hundred microlitres of freshly prepared enzyme development solution (R8 + R9) was dispensed into each well and incubated at room temperature in the dark for 35 minutes. Subsequently, 100 μ l of stopping solution (R10) was added into all wells, gently mixed and incubated at room temperature for 4 minutes. Optical density was measured at 450/620-700 nm using a plate reader (Bio-Rad, CA, USA) within 30 minutes of stopping the reaction.

In a parallel experiment, luciferase activity was assessed from cells transfected with psiCHECK-*HBx* using the Dual-Luciferase[®] Reporter Assay System (Promega, WI, USA), unless otherwise stated. Growth medium was removed from transfected cells by aspiration. Cell lysis was achieved by dispensing 100 μ l of 1 \times passive lysis buffer into each well of the 24-well plate containing transfected cells and incubated with shaking at room temperature for 15 minutes. Ten microlitres of each lysate was transferred into a Costar[®] 96-well assay plate (Corning Inc, NY, USA). In this assay, the activities of firefly (*Photinus pyralis*) and sea pansy (*Renilla reniformis*) luciferase were measured consecutively from a single sample using a luminometer (VERITAS Microplate Luminometer, TURNER BioSystems, MA, USA) equipped with reagent auto-injectors. The activity of firefly luciferase was measured first after adding 1 \times Luciferase Assay Reagent II (LAR II) to produce a luminescent signal. After quantification, 1 \times Stop & Glo[®] Reagent was added into the same sample, quenched firefly luciferase reaction and initiated *Renilla* luciferase activity. The psiCHECK-*HBx* plasmid comprises an independent active Firefly luciferase cassette, while the *HBx* region is located downstream of the *Renilla luciferase* ORF. The ratio of *Renilla* to Firefly luciferase activity was utilised to indicate relativised silencing efficacy.

4.2. Assessment of innate immune stimulation of antiHBV siRNAs *in vitro*

Human Embryonic Kidney 293 (HEK293) cells were employed to investigate immunostimulatory effects of antiHBV siRNAs *in vitro*, since innate immune stimulation is attenuated in Huh7 cells. The HEK293 cells were maintained in DMEM comprised of Penicillin (50 IU/ml), Streptomycin (50 µg/ml) and 10% FCS. Cells were maintained in 24-well plates at 20% confluence, a day prior to transfection. Transfections were performed with 100 ng of pCH-9/3091, 100 ng pCI-eGFP and 800 ng siRNA using Lipofectamine[®] 2000 and incubated at 37°C and 5% CO₂. As a positive control for immune stimulation, cultured cells were treated with 100 ng pCH-9/3091, 100 ng pCI-eGFP and 800 ng polyinosinic:polycytidylic acid, Poly(I:C) (Sigma, MI, USA). The ratio of Lipofectamine[®] 2000 to siRNAs was 3:1 (ml:mg), while that of Lipofectamine[®] 2000 to plasmid vectors and Poly(I:C) was 1:1 (ml:mg).

Forty eight hours post-transfection, total RNA was extracted using Tri Reagent[®] (Sigma, MI, USA). Growth medium was removed from all wells by aspiration and 250 µl of Tri Reagent[®] was added to each well and gently mixed. The mixtures were transferred to 1.7 ml microcentrifuge tubes and incubated at room temperature for 5 minutes. Fifty microlitres of chloroform was added into each sample, gently mixed by inverting tubes and centrifuged at 12 000 × g at 4°C for 20 minutes. Subsequently, 100 µl of the upper aqueous phase was transferred to new 1.7 ml microcentrifuge tubes; an equal volume of isopropanol was added and mixed by inverting tubes. Samples were incubated at -70°C for 2 hours and centrifuged at 12 000 × g at 4°C for 20 minutes. The resulting supernatants were discarded, pellets washed with 200 µl 70% ethanol and centrifuged at 12 000 × g at 4°C for 5 minutes. The supernatants were discarded, pellets resuspended in 50 µl nuclease-free water (Thermo

Chapter 4

Scientific, MA, USA) and stored at -70°C until use. One microgram of total RNA was reverse transcribed using the QuantiTect[®] Reverse Transcription Kit (Qiagen, GmbH, Germany), according to manufacturer's instructions. First, genomic DNA contamination was removed with gDNA Wipeout Buffer in a final volume of 14 μl . cDNA synthesis (reverse transcription) was carried out using 14 μl of RNA, 4 μl of Quantiscript RT Buffer (5 \times), 1 μl of Quantiscript[®] Reverse Transcriptase and 1 μl of RT Primer Mix. The reaction mixture was incubated at 42°C for 30 minutes.

To assess induction of IFN genes, *IFN- β* , *IFIT1*, *OAS-1* and *Glyceraldehyde 3-phosphate dehydrogenase (GAPDH)* reverse transcription quantitative polymerase chain reaction (RT-qPCR) was performed. The RT-qPCR reaction mixtures (Sensimix[™] Capillary Kit, BIOLINE, MA, USA) were prepared using 10 pmol of each human primer pair (Integrated DNA Technologies, IA, USA) and 2 μl of cDNA template. The primer sequences employed for amplifications were: *IFN- β* forward: 5'-TCC AAA TTG CTC TCC TGT TGT GCT-3', *IFN- β* reverse: 5'-CCA CAG GAG CTT CTG ACA CTG AAA A-3', *IFIT1* forward: 5'-CCC TGA AGC TTC AGG ATG AAG G-3', *IFIT1* reverse: 5'-AGA AGT GGG TGT TTC CTG CAA G-3', *OAS-1* forward: 5'-CGA GGG AGC ATG AAA ACA CAT TT-3', *OAS-1* reverse: 5'-GCA GAG TTG CTG GTA GTT TAT GAC-3', *GAPDH* forward 5'-AGG GGT CAT TGA TGG CAA CAA TAT CCA-3' and *GAPDH* reverse: 5'-TTT ACC AGA GTT AAA AGC AGC CCT GGT G-3'.

All amplification reactions were performed using the Roche Lightcycler V.2 (Roche Diagnostics, Germany) and controls included RNA samples that were not treated with reverse transcriptase as well as water blanks. Cycling conditions comprised: hotstart for 30 seconds at

95°C, followed by 50 cycles of denaturation at 95°C for 5 seconds, annealing at 58°C for 10 seconds and extension at 72°C for 7 seconds. Additionally, specificity of the amplicons was confirmed by melting curve analysis. Crossing-point analysis was used to calculate relative mRNA concentrations. Data analysis was performed at 48 hours post-transfection and was calculated as the ratio to the *GAPDH* reference gene mRNA concentrations.

4.3. AntiHBV effects of unmodified and GP-modified siRNAs in a hydrodynamic mouse model

The siRNAs containing GP moieties in position 3, 4 and 5 were employed for preliminary animal investigations. Experiments on animals were conducted in accordance with protocols approved by the University of the Witwatersrand Animal Ethics Screening Committee (Appendix 7.1). The murine HDI model was used to investigate therapeutic efficacy of siRNAs *in vivo* and the experimental mice (NMRI strain) weighed between 20-22 g. Subsequently, mice were injected via the tail vein using a saline solution corresponding to 10% of the animal's body weight. This solution was comprised of 1 nmol siRNA, 15 µg pCI-eGFP plasmid and 15 µg HBV replication plasmid (pCH-9/3091). At days 3 and 5 after injection, blood samples were collected from behind the eyes of injected animals using a retro orbital puncture and animals were humanely sacrificed after completion of the experiment.

Blood samples were incubated at 4°C for 2 hours, centrifuged at $8\,000 \times g$ at 4°C for 10 minutes and serum samples collected from the upper phase. Subsequently, serum samples were used to measure HBsAg by ELISA and circulating viral particle equivalents (VPEs) by quantitative polymerase chain reaction (qPCR). A 1:50 serum dilution in saline was

performed and 100 µl of each sample was used to perform ELISA, as described in **Supplementary Methods Section 4.1**. A 1:5 dilution of serum samples in saline was prepared and used for DNA extraction using the MagNA Pure LC Total Nucleic Acid Isolation Kit according to manufacturer's instructions (Roche Diagnostics, Germany). Subsequently, qPCR was conducted by amplifying five microlitres of DNA with 10 pmol each of mouse HBV surface primers (Integrated DNA Technologies, IA, USA), forward 5'-TGCACCTGTATTCCCATC-3' and reverse 5'-CTGAAAGCCAAACAGTGG-3'. All amplification reactions were performed using the Roche Lightcycler V.2. Cycling conditions comprised: hotstart for 30 seconds at 95°C, followed by 50 cycles of denaturation at 95°C for 5 seconds, annealing at 57°C for 10 seconds and extension at 72°C for 7 seconds. Additionally, HBV standard samples were included in the qPCR and run concurrently with experimental samples and melting curve analysis was used to confirm specificity of the amplification reaction.

CHAPTER 5

PUBLICATION 3

Inhibition of replication of hepatitis B virus in transgenic mice following administration of hepatotropic lipoplexes containing guanidinopropyl-modified siRNAs

Musa D. Marimani, Abdullah Ely, Maximillian C.R Buff, Stefan Bernhardt, Joachim W. Engels, Daniel Scherman, Virginie Escriou, Patrick Arbuthnot

Journal of Controlled Release **209**: 198-206 (2015).

The paper illustrates the advantage of utilising liver-specific lipoplexes containing GP-modified siRNAs. In HBV transgenic mice, GP-modified siRNAs displayed sustained antiHBV activity by suppressing markers of viral replication for up to 14 days, while the unmodified siRNA was only active for up to 7 days. Our data indicate that application of novel GP-modified siRNAs in conjunction with a competent delivery system improves therapeutic utility of these RNAi effectors by enhancing antiHBV activity and specificity, while minimising toxicity and innate immune response.

Author's contribution: Musa Marimani performed all biological experiments, analysed data and contributed to writing the manuscript. Prof. Arbuthnot and Dr. Ely supervised the project and also assisted with compiling the paper. Our German collaborators: Prof. Engels, Dr. Buff and Mr. Bernhardt synthesised GP-modified siRNAs, performed HPLC, Mass Spectrometry (MS) and all experiments related to siRNA analysis, and also contributed to writing the manuscript. Our French collaborators: Prof. Scherman and Dr. Escriou synthesised liver-tropic liposomes, performed characterisation thereof, and also contributed in compiling the manuscript.



Inhibition of replication of hepatitis B virus in transgenic mice following administration of hepatotropic lipoplexes containing guanidinopropyl-modified siRNAs



Musa D. Marimani^a, Abdullah Ely^a, Maximilian C.R. Buff^c, Stefan Bernhardt^c, Joachim W. Engels^c, Daniel Scherman^b, Virginie Escriou^b, Patrick Arbuthnot^{a,*}

^a Wits/SA MRC Antiviral Gene Therapy Research Unit, School of Pathology, Health Sciences Faculty, University of the Witwatersrand, Johannesburg, Private Bag 3, Wits 2050, South Africa

^b UTCBS, CNRS UMR8258, INSERM U1022, Université Paris Descartes, Chimie ParisTech, 75006 Paris, France

^c Goethe-University, Institute of Organic Chemistry & Chemical Biology, Max-von-Laue-Str. 7, 60438 Frankfurt am Main, Germany

ARTICLE INFO

Article history:

Received 4 March 2015

Received in revised form 24 April 2015

Accepted 27 April 2015

Available online 30 April 2015

Keywords:

HBV

siRNA

Lipoplex

Guanidinopropyl modification

Polyglutamate

RNAi

ABSTRACT

Chronic infection with hepatitis B virus (HBV) occurs commonly and complications that arise from persistence of the virus are associated with high mortality. Available licensed drugs have modest curative efficacy and advancing new therapeutic strategies to eliminate the virus is therefore a priority. HBV is susceptible to inactivation by exogenous gene silencers that harness RNA interference (RNAi) and the approach has therapeutic potential. To advance RNAi-based treatment for HBV infection, use in vivo of hepatotropic lipoplexes containing siRNAs with guanidinopropyl (GP) modifications is reported here. Lipoplexes contained polyglutamate, which has previously been shown to facilitate formulation and improve efficiency of the non-viral vectors. GP moieties were included in a previously described anti-HBV siRNA that effectively targeted the conserved viral X sequence. Particles had physical properties that were suitable for use in vivo: average diameter was approximately 50–200 nm and surface charge (zeta potential) was +65 mV. Efficient hepatotropic delivery of labeled siRNA was observed following systemic intravenous injection of the particles into HBV transgenic mice. Good inhibition of markers of viral replication was observed without evidence of toxicity. Efficacy of the GP-modified siRNAs was significantly more durable and formulations made up with chemically modified siRNAs were less immunostimulatory. An RNAi-mediated mechanism was confirmed by demonstrating that HBV mRNA cleavage occurred in vivo at the intended target site. Collectively these data indicate that GP-modified siRNAs formulated in anionic polymer-containing lipoplexes are effective silencers of HBV replication in vivo and have therapeutic potential.

© 2015 Elsevier B.V. All rights reserved.

1. Introduction

Infection with hepatitis B virus (HBV) remains a health problem of considerable importance. It is estimated that 350 million people are chronically infected with the virus, and at high risk for the life-threatening complications of cirrhosis and liver cancer [1,2]. Although there is an effective vaccine to prevent transmission of HBV, immunization is not administered to many populations where the infection is endemic. Currently licensed treatments for HBV infection include nucleoside and nucleotide analogs, which function as inhibitors of the viral reverse transcriptase. Immunomodulatory interferon-alpha (IFN- α), modified with polyethylene glycol (PEG) or in its native form, is also available for treatment of the infection. Unfortunately the licensed drugs have modest curative efficacy against HBV [3] and to minimize risks for complications from the infection, improvements in treatment is a priority.

The genome of HBV has a compact arrangement with restricted sequence plasticity. As a result, the virus has limited ability to generate escape mutants and use of nucleic acids that have an inhibitory effect by hybridization to viral targets is potentially a useful therapeutic strategy. Replication of HBV has been shown to be susceptible to silencing by exogenous activators of the RNA interference (RNAi) pathway (reviewed in [4]), and harnessing this gene silencing mechanism has potential for therapeutic application. Specific silencing of intended targets may be induced by introducing various artificial mimics of the RNAi pathway into hepatocytes. Inhibition is dependent on the interaction of a guide strand derived from RNAi activators with intended mRNA targets. Both expressed and synthetic RNAi activators have been employed successfully against HBV and each class of gene silencers has advantages. Expressed RNAi activators may cause lasting inhibition of viral replication and are amenable to incorporation into recombinant viral vectors. Although efficient, dose regulation is difficult to achieve and delivery of RNAi activators with recombinant viruses may be complicated by induction of an immune response to the vectors. Moreover, preparation

* Corresponding author.

E-mail address: Patrick.Arbuthnot@wits.ac.za (P. Arbuthnot).

of recombinant viral vectors is costly and not easily scalable for wide-spread clinical use.

Synthetic activators of RNAi typically comprise duplexes of RNA, which resemble the products of Dicer. Short interfering RNAs (siRNAs) may be prone to degradation, off target effects and immunostimulation. To minimize these effects and improve silencing potency, a variety of chemical modifications has been employed (reviewed in [5,6]). These include alterations to the 2'-OH group of the ribose moiety, changes to the phosphodiester backbone and substitutions of ribose for alternative sugars. Modifications to the 2' OH group include incorporation of 2'-O-methyl (2'OMe), 2'-fluoro (2'-F), locked nucleic acids (LNAs), acyclic unlocked nucleic acids (UNAs), 2'-O-methoxyethyl (2'MOE), and deoxy residues. Recently we demonstrated that incorporating guanidinopropyl (GP) groups into the ribose components of HBV-targeting siRNAs improves their efficacy [7]. These moieties achieve some charge neutralization of siRNAs, which is useful to facilitate delivery of nucleic acid-based gene silencers. Importantly the modifications also improve stability and specificity of target knockdown by attenuating off target interaction of the seed with mRNA sequences.

siRNAs have a cytoplasmic site of action, which is convenient for delivery to target tissues. Various non-viral vector formulations have been developed for therapeutic use of synthetic siRNAs. Stable nucleic acid lipid particles (SNALPs) delivered gene silencers efficiently *in vivo* to inhibit HBV replication in murine models of the viral infection [8]. Other lipoplex formulations have included polyamine-conjugated cholesterol [9] or aminoxycholesterol lipid to facilitate post coupling of 'stealth' polyethylene glycol moieties [10]. Recently, synthetic anti-HBV siRNAs have been delivered *in vivo* using Dynamic PolyConjugates (DPCs) [11,12]. Promising results indicating effective inhibition of HBV replication have led to development of the technology to stage II of clinical trial (<http://www.arrowheadresearch.com/programs-overview>). Although these advances are encouraging, optimization of conveniently assembled non-viral vectors and identifying the most suitable chemically modified gene silencers for incorporation into the formulations continues to be important. Previously we have shown that improvement in the efficiency of the non-viral vectors is brought about by addition of polyglutamate [13,14]. Here we report on delivery of GP-modified siRNAs using these novel polyanion-containing hepatotropic lipoplexes. Evaluation in a model that stringently simulates the human condition of chronic HBV infection demonstrated that efficient and safe silencing of viral replication is achieved.

2. Materials and methods

2.1. Preparation and characterization of siRNA-containing lipoplexes

Cationic liposomes were formed by combining equimolar amounts of cationic lipid 2-[3-[Bis-(3-amino-propyl)-amino]-propylamino]-N-ditetradecylcarbamoyl methyl-acetamide (DMAPAP) [15] and 1,2-dioleoyl-sn-glycero-3-phosphoethanolamine (DOPE) (Avanti Polar Lipids, AL, USA). Procedures for preparation of the liposomes have previously been described [16]. siRNA-containing lipoplexes were formed by combining equal masses of siRNA and polyglutamate (Poly-L-glutamic acid sodium salt, Sigma-Aldrich, MO, USA), which were made up in 150 mM NaCl. This solution was then added to the cationic liposome suspension, also made up in 150 mM NaCl, then rapidly mixed by vortexing. Typically, 15 µg siRNA (1.13 nmol) and 15 µg polyglutamate (3 to 10 nmol) were diluted in 100 µl saline and mixed with 100 µl saline containing 20 µl of a 20 mM suspension of DMAPAP/DOPE (400 nmol each). Lipoplexes were allowed to form by incubating at room temperature for 30 min before use. The charge ratio was calculated as the molar ratio of positive charges from DMAPAP to negative charges of siRNA and polyglutamate. Each molecule of DMAPAP has 3 positive charges. siRNAs and polyglutamate have 3.03 and 6.58 nmoles of negative charge per µg respectively.

Size and zeta (ζ) potential measurements were performed using a Malvern Zetasizer (Nano series) Nano ZS (Malvern, UK). Liposomes or lipoplexes were prepared in 100 µl of NaCl (150 mM). Final lipid concentrations were 0.4 mM for the liposomes and 0.334 µM for the siRNA-containing lipoplexes. For ζ potential measurements, liposomes (lipid 0.04 mM) and lipoplexes (siRNA 33.4 nM) were prepared in 15 mM NaCl.

A drop of the lipoplex suspension (siRNA concentration 400 nM) was initially applied to a Formvar and carbon-coated copper grid of 200 mesh (Agar Scientific, UK), which had been pre-treated with 0.1% bacitracin. The sample was allowed to adsorb for 2 min, blotted with filter paper, stained with 4% aqueous uranyl acetate then viewed using a JEM 100S transmission electron microscope.

2.2. Synthesis of siRNAs containing GP moieties

The GP-modified siRNAs were synthesized as previously described [17]. One, two, three or four GP moieties were incorporated at different positions of the antisense strand of a previously characterized anti-HBV siRNA, called siRNA3 (antisense, 5'UUGAAGUAUGCCUCAAGGUCG3') [18]. The sense strand (5'ACCUUGAGGCAUACUCAAAdTdT3') did not possess any GP modification, but instead contained two deoxyribonucleotides (dTdT) at the 3' end. The siRNA3 derivatives were named according to the position of the nucleotide, determined from the 5' end of the guide strand, that contained the GP moiety [7,17]. The control scrambled siRNA comprised the following complementary strands: antisense, 5'GCGAAGUGACCAGCGAAUACdT3' and sense, 5'UAUUCG CUGGUCACUUCGUdTdT3'.

2.3. Plasmids and transfection

pCH-9/3091 is a viral replication competent plasmid that has a greater than genome length HBV sequence [19]. The complete and partial targets of siRNA3 were produced by inserting appropriate oligonucleotide sequences into psiCHECK as has previously been described [7]. The liver-derived human hepatoma (Huh7) cells were cultured in DMEM (Lonza, Basel, Switzerland) containing 10% FCS (Life Technologies, CA, USA). Transfection, measurement of reporter activity and HBsAg concentrations in culture supernatants were performed as has been described [7,20,21].

2.4. Assessment of biodistribution of labeled siRNAs following intravenous administration of lipoplexes to HBV transgenic mice

Animal studies were performed according to protocols approved by the University of the Witwatersrand Animal Ethics screening Committee. To enable assessment of biodistribution, the sense strand of the siRNAs was labeled with Alexa Fluor 750 at the 3' end (Inqaba Biotech Industries, South Africa). Lipoplexes were injected into the tail veins of HBV transgenic mice at a dose of 1 µg of siRNA per g of the mouse's body weight. Control mice were injected with an equivalent dose of uncomplexed GP3 siRNA3 or saline. At 10 min after injection, mice were killed and the kidneys, liver, lungs and spleen were taken for imaging *ex vivo*. Fluorescence in harvested organs, determined using a filter set at 745 nm, was measured using the IVIS Kinetic Bioluminescence imager (PerkinElmer, MA, USA). Subsequently, tissues were processed following overnight incubations at 4 °C in 20% paraformaldehyde then in 30% sucrose. Sections (~5 µm) were stained with 4',6-diamidino-2-phenylindole (DAPI, Life Technologies, CA, USA) prior to viewing with a confocal microscope (Zeiss, LSM 780, Oberkochen, Germany).

2.5. Anti-HBV effects *in vivo* of siRNA-containing lipoplexes

The HBV transgenic mice contain replication-competent viral sequences [22]. Blood samples were collected at days 0 (baseline), 3, 5, 7, 14, 18 and 21 after injections of the lipoplexes or control samples.

Serum concentrations of HBV surface antigen (HBsAg) were quantified using the Monolisa™ HBs Ag ULTRA assay kit (Bio-Rad, CA, USA) as described previously [23]. Circulating viral particle equivalents (VPEs) were assayed by quantitating viral DNA in serum samples using real-time qPCR carried out using the Roche Lightcycler v.2. or the Bio-Rad CFX96 Touch™ Real-Time PCR Detection System (Bio-Rad, CA, USA), as has been described [20,24]. Alanine transaminase (ALT) activity was measured in serum samples using the accredited facilities of the South African National Health Laboratory Service (NHLS, Johannesburg, South Africa). Extraction of RNA from the liver samples was carried out using Tri Reagent®, and was performed according to procedures recommended by the supplier (Life Technologies, CA, USA). Total RNA was reverse transcribed with the QuantiTect® Reverse Transcription Kit (Qiagen GmbH, Germany) according to the manufacturer's instructions. To amplify murine *GAPDH*, HBV surface and core mRNA, the following primer sets were used: mGAPDH F (5'AGGGGTCATTGATGGCAACAATATCCA3') and mGAPDH R (5'TTTACCAGAGTTAAAAGCAGCCCTGGTG3'), HBV Surface F (5'TGCACCTGTATCCATC3') and HBV Surface R (5'CTGAAAGCCAAACAGTGG3'), HBV Core F (5'ACCACCAAATGCCCTAT3') and HBV Core R (5'TTCTGCGACGGCGA3'). PCR analysis was performed using the SsoFast™ EvaGreen® Supermix (Bio-Rad, CA, USA) with standard conditions for thermocycling. To identify RNAi-mediated cleavage of HBV mRNA, total hepatic RNA was subjected to analysis using the 5' RACE procedure as has been described [25].

2.6. Evaluation of innate immune stimulation in vivo by siRNA-containing lipoplexes

To investigate innate immune stimulation in mice, the animals received intravenous injections of the lipoplex formulations, poly (1:1)

or liposome alone. The doses of the siRNAs were consistently 1 µg per g of a mouse's body weight. Six hours after injection, blood samples were collected and livers harvested. Interleukin 6 (IL-6), interleukin 10 (IL-10), Monocyte Chemoattractant Protein-1 (MCP-1), interferon gamma (IFN-γ), Tumor Necrosis Factor alpha (TNF-α) and interleukin 12p70 (IL-12p70) protein were measured in serum samples using the Cytometric Bead Array (CBA) Mouse Inflammation Kit (BD Biosciences, CA, USA) with minor previously described modifications [26–28]. Liver samples were subjected to RNA extraction using Tri Reagent®, the RNA reverse transcribed using the QuantiTect® Reverse Transcription Kit (Qiagen GmbH, Germany) and resulting cDNA used to quantify *IFN-β* and *OAS-1* mRNA levels by RT-qPCR using procedures that have previously been described [21,29].

2.7. Statistical analysis

Data are represented as the mean ± standard error of the mean (± SEM). Two-tailed Student's t tests were performed using GraphPad Prism version 4.00 (GraphPad software, CA, USA). P values of <0.05 were regarded as statistically significant.

3. Results

3.1. Non-viral lipoplexes for delivery of GP-modified siRNAs

To achieve hepatotropic delivery of GP-modified siRNAs, cationic lipid-based formulations were employed (Fig. 1A). Polyglutamate, an anionic polymer, was included in the complexes to limit toxicity and enhance efficacy of the siRNA-containing vectors [14]. Polyethylene glycol (PEG) was however omitted from the formulations as this polymer

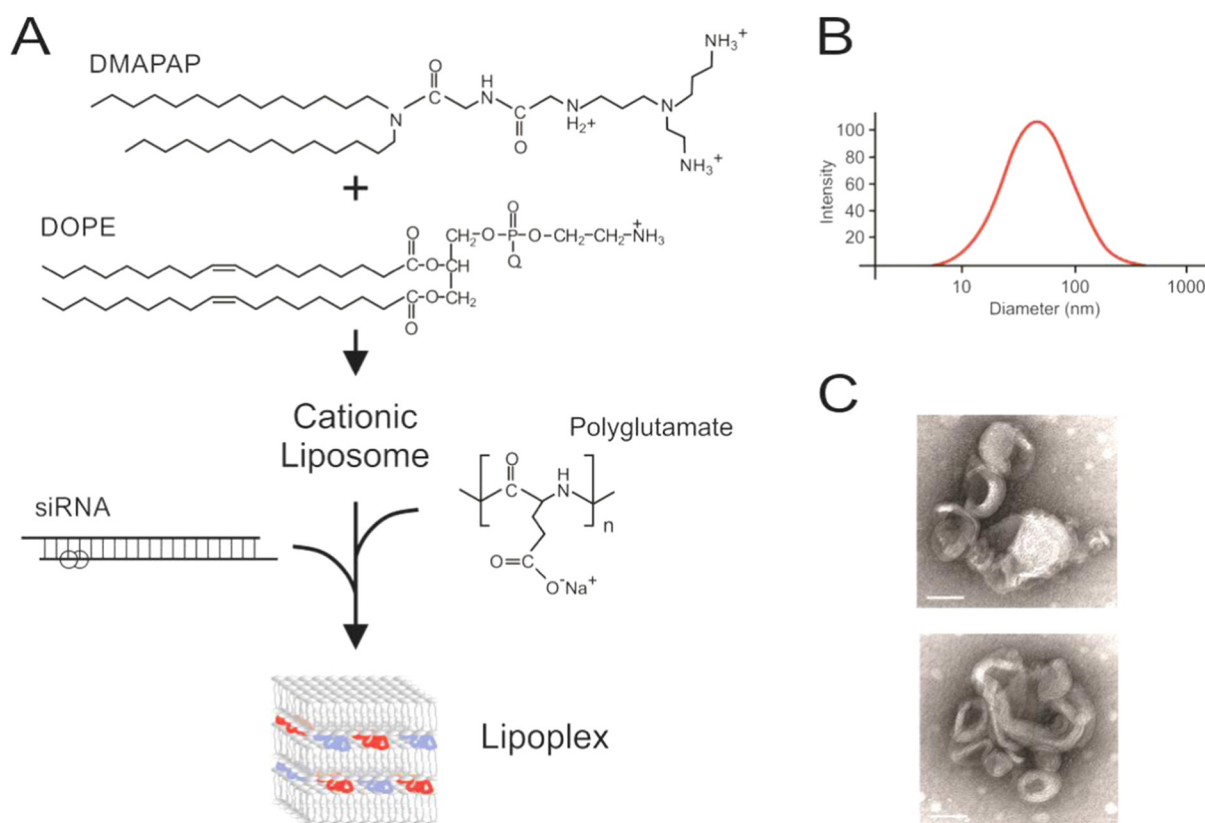


Fig. 1. Formulation of siRNA-containing lipoplexes. A. The non-viral vectors comprised a cationic lipid (2-[3-Bis-(3-amino-propyl)-amino]-propylamino)-N-ditetradecylcarbamoyl methylacetamide, DMAPAP) and neutral lipid (1,2-dioleoyl-sn-glycero-3-phospho-ethanolamine, DOPE), which were combined to form the cationic liposome. Polyglutamate and the siRNA molecules were combined with the liposomes to form lipoplexes. Formulations were generated after pre-association of siRNA with polyglutamate (1.5 kDa) (1/1, w/w) at a N/P charge ratio 6. B. Representative particle size distribution of the GP siRNA-containing lipoplexes. C. Transmission electron microscopy revealed a typical multilamellar arrangement suggesting that siRNAs were entrapped within the organized lipoplexes. Scale bar indicates 50 nm.

appeared to compromise silencing efficacy of siRNAs within the lipoplexes [14]. A charge ratio (N/P) of 6 was used to complex the cationic lipids with siRNAs, and has been shown to be optimal for hepatotropic delivery in vivo with these vectors. Lipoplexes had a uniform diameter that ranged from 50 to 200 nm for the GP-siRNA3-containing lipoplexes (Fig. 1B) and was similar to the size of 45 to 180 nm for the lipoplexes containing unmodified siRNA3. The ζ potential was slightly more positive for the GP3-siRNA3-containing lipoplexes (65 ± 1 mV) when compared to that of the particles containing unmodified siRNA (57 ± 1 mV). The polydispersity index of the particle sizes, which ranged between 0.5 and 1.1, was not influenced by inclusion of polyglutamate. Transmission electron microscopy of the particles revealed multilamellar structures (Fig. 1C), which are typical of cationic lipid-based siRNA particles. These features of the lipoplexes were considered suitable for their assessment as vectors for delivery of HBV-targeting chemically modified siRNAs.

3.2. Guanidinopropyl-modified HBV-targeting siRNAs

siRNAs that were delivered with hepatotropic non-viral vectors were derived from a previously described HBV-targeting RNAi activator called siRNA3 [18]. The intended guide strand of this gene silencer is complementary to sequences in the viral X open reading frame (ORF) (Fig. 2A). X is well conserved in genotypes of HBV and is present in all

of the viral transcripts, which makes it a good target to counter replication of the virus. The structure of the synthetic siRNA was typical and included a 19 bp duplex with additional overhangs of two nucleotides at either 3' end. To improve stability and antiviral efficacy, GP moieties were incorporated at positions 3 or 4 from the 5' end of the antisense strand of the siRNA (Fig. 2B) siRNAs [7]. Evaluation in transfected cultured cells demonstrated that inclusion of additional GP modifications did not improve specificity and efficacy of the siRNAs (Supp. Figs. 1 & 2).

3.3. Biodistribution of labeled siRNAs following administration of lipoplex formulations

To assess biodistribution of the siRNAs in mice, the gene silencers were labeled at their 3' ends with Alexa Fluor 750. Lipoplexes containing these labeled siRNAs were administered intravenously to mice. Mice were killed 10 min after the injections and fluorescence was detected in the kidneys, liver, lungs and spleen (Fig. 3). After intravenous injection, most of the naked labeled GP3 siRNA3 accumulated in the kidneys and lungs but fluorescence in the liver and spleen was barely detectable (Fig. 3A&D). When complexed to the liposomes delivery to the liver was favored and diminished fluorescence was detectable in the kidneys, lungs and spleen (Fig. 3B&D). Microscopy confirmed hepatotropic delivery of the labeled siRNAs, and most cells were labeled with the fluorescent siRNAs. Small amounts of the labeled siRNAs were detectable in the kidneys, spleen and lungs. Fluorescence was not detectable macro- and microscopically in the control animal that received saline (Fig. 3C). Based on the good efficiency of hepatotropic delivery of siRNAs with the lipoplex vectors, these formulations were tested for efficacy against HBV replication in HBV transgenic mice [30].

3.4. Antiviral effects of GP-modified siRNAs following systemic administration of lipoplexes to HBV transgenic mice

The HBV transgenic mice contain an integrated replication-competent greater-than-genome-length viral sequence (Fig. 2A) [22]. Transcription and translation of the transgenic DNA results in HBV replication in hepatocytes in these animals. Although infection of murine hepatocytes does not occur, long term replication of HBV in the transgenic animals approximates chronic HBV infection of humans [22,31]. A limitation of the transgenic model is that covalently closed circular DNA (cccDNA) of HBV is not formed in murine hepatocytes [32]. Production of the viral replication intermediate does occur following HBV infection of severe combined immunodeficient (SCID) mice that have been xenografted with human hepatocytes [33]. Although this property is advantageous, procedures required to generate the chimeric animals are challenging. Also, the immunocompromised state of xenografted SCID mice eliminates the role of host immune responses during a therapeutic response. Based on convenience of HBV transgenic mice, status of the immune system and stringent simulation of viral replication in chronically infected individuals, we elected to use this murine model to assess efficacy of lipoplexes containing GP-modified siRNAs.

Following injection of the formulations, HBsAg and circulating VPEs were measured as indicators of viral replication (Fig. 4). Administration of formulated scrambled siRNAs or saline caused no significant effect on the markers of viral replication during the three week period of follow up. Formulations containing the unmodified siRNA3 caused knockdown of HBsAg concentrations by about 86% at days 3 and 5, and diminished to 70% at day 7 after injection (Fig. 4A). The effect on circulating VPEs was similar, and significant inhibition was observed during the week after the mice received the antiviral formulations (Fig. 4B). GP-modified siRNAs caused similar early suppression of HBsAg concentrations and circulating VPEs. However, GP-containing siRNAs achieved more durable HBsAg silencing than their unmodified counterpart. With formulations containing GP3 siRNA3 and GP4 siRNA3,

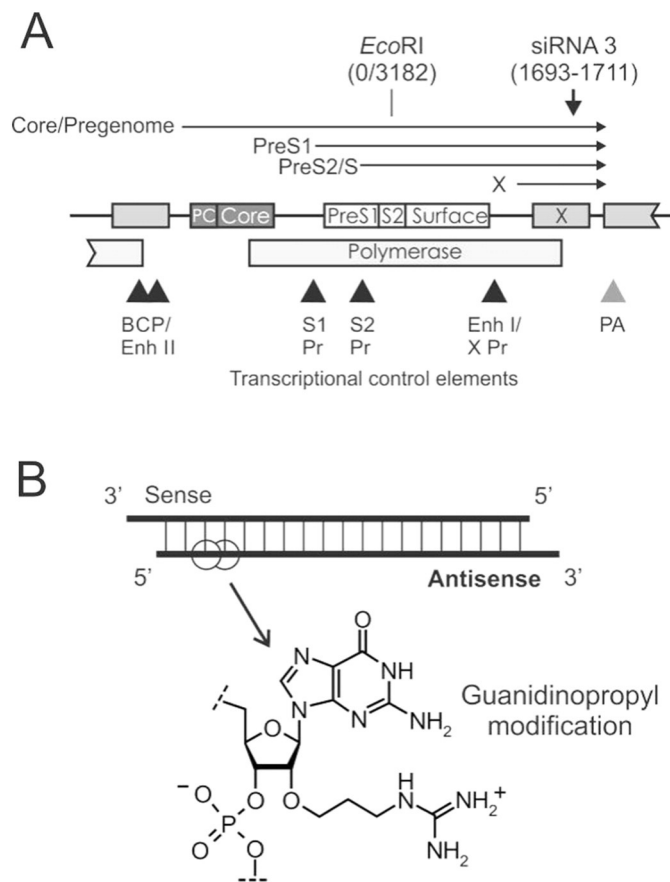


Fig. 2. Schematic illustration of HBV targets and guanidinopropyl (GP)-modified siRNAs. A. Linear depiction of greater-than-genome length HBV DNA that is integrated into the genome of HBV transgenic mice. Coordinates of the viral genome are calculated relative to the position of the single *EcoRI* site. The site targeted by siRNA3 (nucleotides 1693 to 1711) is depicted as a vertical arrow. The four groups of viral transcripts are indicated as horizontal arrows. *Precore* (PC), *core*, *preS1*, *preS2* (S2), *surface*, *polymerase* and *X* viral open reading frames (ORFs) are indicated as the labeled rectangles. Transcriptional regulatory elements are indicated by the arrowheads below the ORF-encoding viral DNA. B. siRNAs comprising duplexes of RNA with dinucleotide overhangs at the 3' ends had GP residues incorporated at positions 3 or 4 from the 5' end of the antisense strand.

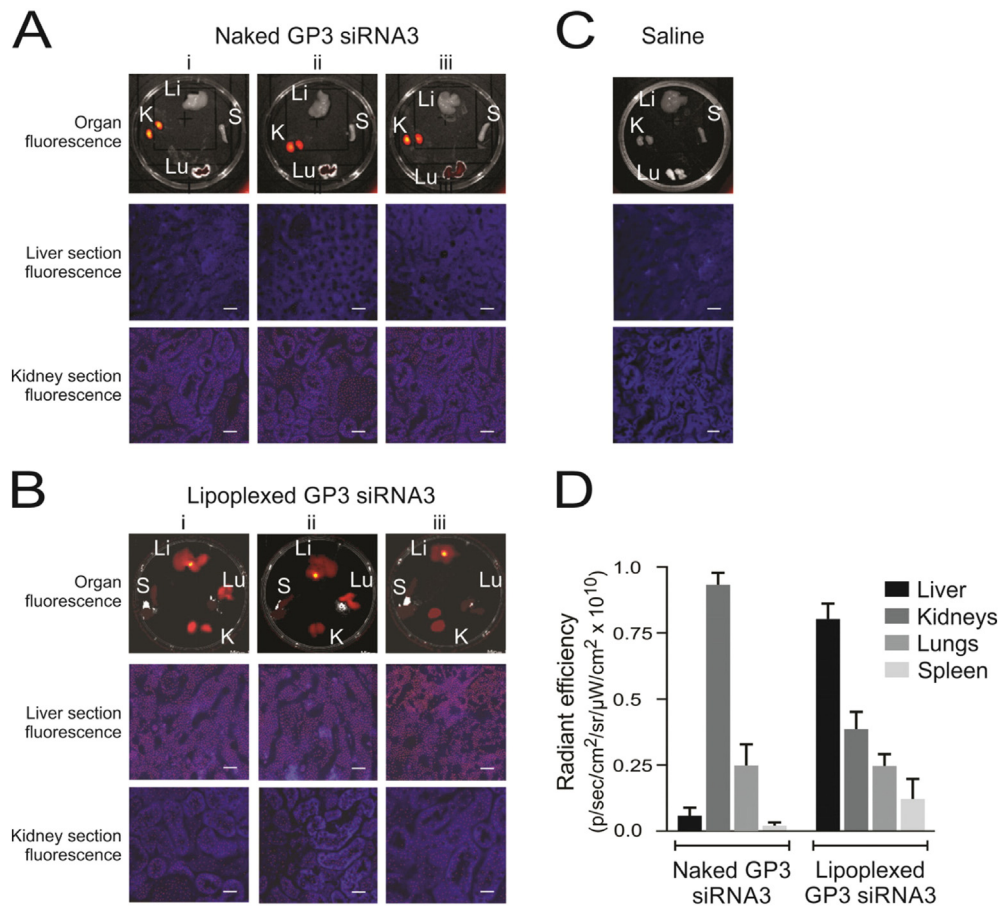


Fig. 3. Biodistribution of siRNAs in HBV transgenic mice. Representative fluorescence images obtained from samples harvested 10 min after injection of lipoplexes containing Alexa Fluor 750-labeled siRNAs. Three mice (i–iii) received intravenous injection of the uncomplexed naked labeled siRNA (A) and three mice (i–iii) received labeled siRNA within polyglutamate-containing lipoplexes (B). One mouse, which received a saline injection, served as the negative control (C). Fluorescence detectable in livers (Li), lungs (Lu), kidneys (Ki) and spleen (S) are shown in the top row of images. Microscopy of frozen sections from liver and kidney samples are also shown below. The scale bar indicates 50 μm. Quantitation of fluorescence, radiant efficiency, was measured in the organs of mice given naked GP3-siRNA3 or lipoplexed GP3-siRNA3 (D). Data are represented as the mean radiant efficiency (\pm SEM) for each organ from the three animals.

concentrations of both HBsAg and circulating VPEs were significantly diminished up to and including day 14 after administration of the lipoplexes. Compared to the baseline values at this time point, the concentrations of HBsAg were reduced by approximately 70% and circulating VPEs were diminished by 75–80%. Concentrations of the markers returned to baseline values at day 21 after receiving lipoplexes containing GP3 siRNA3 and GP4 siRNA3.

Transgenic mice receiving saline and GP3 siRNA3 were killed at day 18, while experiments with those treated with scrambled siRNA, unmodified siRNA3 and GP4 siRNA3 were terminated on day 21 after animals were injected. Viral RNA concentrations in harvested mouse livers were determined using quantitative amplification of viral *surface* and *core* sequences (Supp. Fig. 3). Compared to the mice that received saline, intrahepatic concentrations of viral *surface* and *core* RNA in mice treated with GP3 siRNA3 were reduced by about 40% at the termination of the experiments. Similarly when compared to mice treated with scrambled siRNA, unmodified siRNA3 diminished intrahepatic viral RNA concentrations by 20–25%. However, the silencing efficacy was higher in mice treated with GP4 siRNA3. In these animals intracellular concentrations of viral RNA sequences were significantly suppressed by about 42%. Collectively these data indicate that delivery of GP-modified siRNAs efficiently inhibits markers of HBV replication in transgenic mice. Moreover, since HBV gene expression predominates in hepatocytes of the animals [22,31], inhibition of markers of viral replication is further support of the hepatotropism of the formulations.

3.5. Verification of siRNA-mediated cleavage of HBV mRNA in vivo

Previously we showed that GP3 siRNA3 and GP4 siRNA3 caused similar predicted HBV target cleavage in transfected liver-derived cells [25]. This indicates that target cleavage is not influenced by positioning of the GP residue at the third or fourth nucleotide from the 5' end of the guide. The 5' RACE technique was again employed here to verify an RNAi-mediated intrahepatic effect of the GP-modified siRNAs. The expected amplification product of 217 bp was detected after analysis of RNA extracts from mice that were treated with formulations containing unmodified siRNA3 and GP3 siRNA3 (Fig. 5A). Conversely, no products of PCR were detected in animals that had received the scrambled siRNA. DNA sequencing confirmed the presence of the ligated RNA oligonucleotide and predicted cleaved mRNA products (Fig. 5B). HBV mRNA cleavage occurred at position 10 from the 5' end of the antisense strand, which is in accordance with the canonical RNAi-mediated target cleavage by Ago2 [34,35].

3.6. Assessment of toxic and immunostimulatory effects following administration of siRNA-containing lipoplexes to HBV transgenic mice

To investigate effects of the formulations on release of pro-inflammatory cytokines, a CBA was carried out (Fig. 6). Concentrations of IL-6, IL-10, MCP-1, IFN- γ , TNF- α and IL-12p70 were measured in

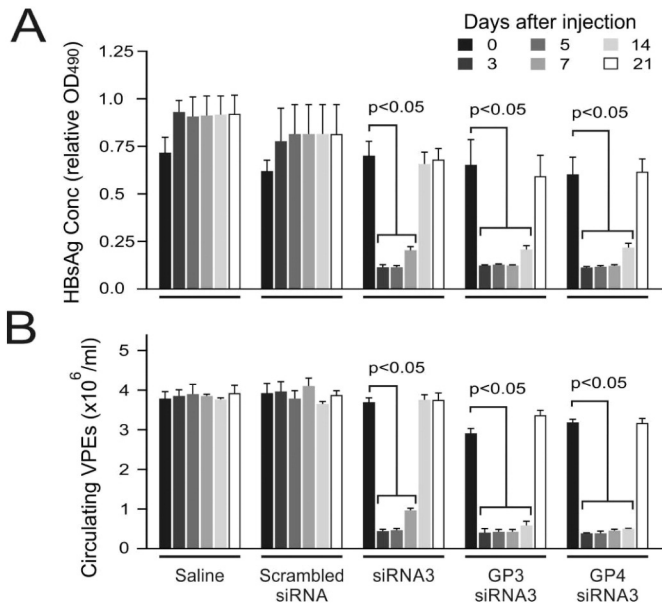


Fig. 4. Anti-HBV effects of siRNAs on serum markers of HBV replication in transgenic mice. The HBV transgenic mice were injected with siRNA-containing lipoplexes. Guanidinopropyl (GP) residues were positioned at the third (GP3 siRNA3) or fourth (GP4 siRNA3) nucleotides from the 5' end of the antisense strand of the siRNAs. Unmodified anti-HBV siRNA (siRNA3) or scrambled siRNA were also administered after complexing to the liposome and polyglutamate components. Control animals received intravenous saline or injection of a formulated scrambled siRNA duplex. Serum concentrations of HBsAg (A) and circulating viral particle equivalents (VPEs) (B) were detected from day 3 to 21 after injection. Values represent the means (\pm SEM) of replicate injections of four mice per group. Statistically significant differences between the samples, determined using the Student's two tailed paired *t* test, are indicated.

the serum of mice 6 h after they had received the lipoplexes. In the animals that received poly (I:C), a positive control for stimulation of the innate immune response, serum concentrations of IL-6, MCP-1, IFN- γ and TNF- α were significantly elevated. Secretion of pro-inflammatory cytokines was not induced after injection of liposomes that did not contain nucleic acids. However, systemic injection of mice with unmodified siRNA3 resulted in significantly elevated concentrations of IL-6, MCP-1, IFN- γ and TNF- α at 6 h after the administration. Conversely formulations containing GP-modified siRNAs caused only a modest induction of MCP-1, and other markers of inflammation were not elevated.

Measurement of alanine aminotransferase (ALT) activity in serum samples of mice revealed that this marker of hepatotoxicity was not elevated in mice that received the lipoplex formulations (Supp. Fig. 4). Moreover, measurements for each of the groups were not statistically significantly different to those obtained from the control mice that received a saline injection. To assess induction of the innate interferon response following systemic injection of the siRNA-containing lipoplexes, mRNA derived from *IFN- β* and *OAS-1* genes was quantified relative to the amount of *GAPDH* mRNA (Supp. Fig. 5). mRNA concentrations of the IFN response genes were similar in liver cells of mice that had received the liposomes alone and the siRNA-containing lipoplexes. These values were significantly lower than those obtained from samples extracted from mice that had received poly (I:C). The data thus indicate that the liposomal component of the non-viral vectors was not immunostimulatory and modification of siRNAs with GP residues attenuated an innate immune response.

4. Discussion

Studies have demonstrated that activators of the RNAi pathway effectively inhibit replication of HBV (reviewed in [4]). Since HBV has a compact genome, ability of the virus to evade inhibitory effects of

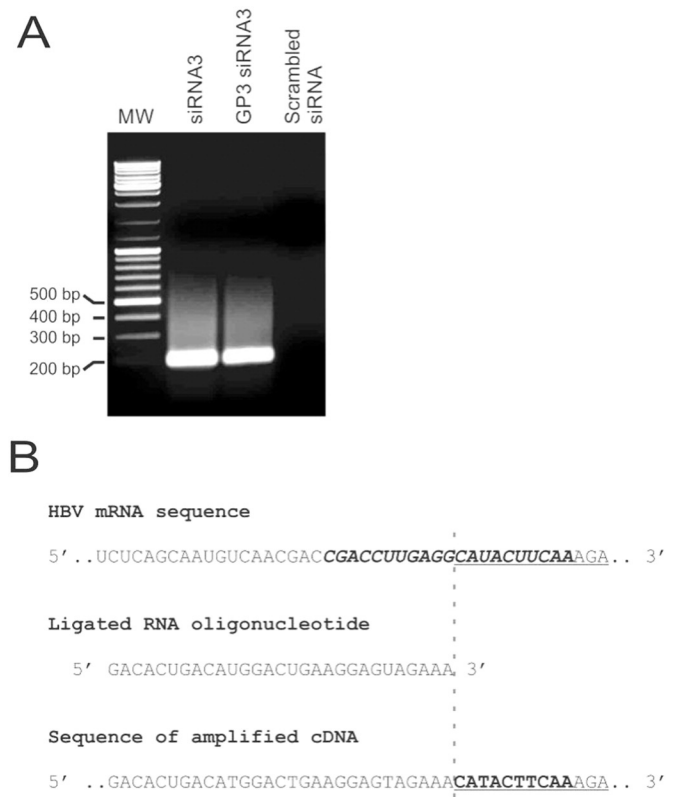


Fig. 5. Detection of siRNA-mediated cleavage of HBV mRNA in vivo. A. A linker oligonucleotide was ligated to hepatic RNA and then subjected to RT PCR (5' RACE). Products obtained from samples of animals that were treated with lipoplexes containing either unmodified siRNA3 or GP3 siRNA3 were subjected to agarose gel electrophoresis. B. Similar sequences of ligated amplified products were obtained from samples of mice that were treated with siRNA3 or GP3 siRNA3 (bottom). For comparison, sequences of the HBV target (top) and ligated oligonucleotide (middle) are shown.

hybridizing nucleic acids is constrained. Given the dependence of the virus on pregenomic RNA, an essential replication intermediate, cleavage of target viral RNA by an RNAi-mediated mechanism is well suited to therapeutic application. In this study, we used GP-modified siRNAs to target the conserved X region of the viral pregenome that was common to all of the HBV transcripts. Liposome-based non-viral vectors were employed to deliver GP-modified siRNAs. Formulations that are made up entirely of synthetic constituents, such as have been described here, have distinct advantages. Modular components are amenable to large scale synthesis required for clinical application and chemical modification enables alteration of biological properties to suit particular applications. Nevertheless, lipoplexes should have several important features before they may be considered efficient vehicles for hepatotropic delivery of anti-HBV siRNAs. Complexes need to be stable, enhance the half-life of siRNAs in the circulation, be positively charged and ensure targeted delivery to the liver [9,36,37]. The size and charge of lipoplexes are also critical for efficient hepatotropic delivery. The fenestration of hepatic sinusoidal endothelial cells have diameters that range in size between 150 and 175 nm [38]. To cross this barrier and gain access to hepatocytes, siRNA-containing lipoplexes should therefore ideally have a diameter of less than 100 nm.

The anionic polymer- and GP siRNA-containing lipoplexes used here had diameters ranging from 50–200 nm and ζ potentials of approximately +65 mV. These properties are expected to enhance stability and facilitate siRNA delivery to hepatocytes [39–41]. Intended hepatotropic transport of the lipoplexes was confirmed by demonstrating localization of labeled siRNAs in hepatocytes of HBV transgenic mice. Efficient silencing was shown in this stringent model of HBV

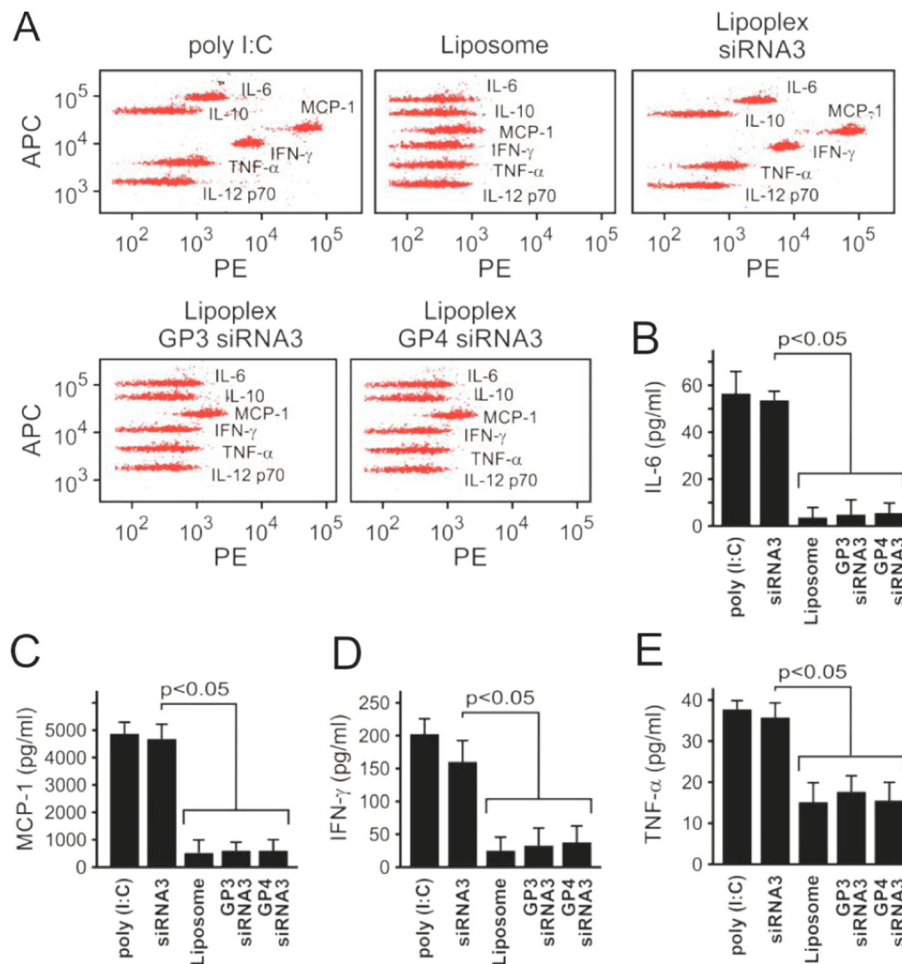


Fig. 6. Assessment of cytokine induction in HBV transgenic mice following intravenous administration of lipoplexes containing siRNAs. A. Representative data from the assay using the cytometric bead array to quantify interleukin 6 (IL-6), interleukin 10 (IL-10), monocyte chemoattractant protein-1 (MCP-1), interferon gamma (IFN- γ), tumor necrosis factor alpha (TNF- α) and interleukin 12p70 (IL-12p70) concentrations. Measurements were made 6 h after injection of the indicated lipoplexes. Administration of equivalent amounts of liposome or poly (I:C) were used as controls. Mean concentrations of IL-6 (B), MCP-1 (C), IFN- γ (D) and TNF- α (E) obtained at 6 h following administration of lipoplexes, liposome and poly (I:C) are shown. Means (\pm SEM) were calculated from replicate injections of four mice per group. Statistically significant differences between the samples, determined using the student's two tailed paired t test, are indicated.

replication, which is further support of hepatotropism of the lipoplexes. Inhibitory effects of the formulations containing GP-modified siRNAs were more sustained than their unmodified counterparts. Verification of the expected cleavage of HBV mRNA targets, demonstrated using 5' RACE, confirmed an RNAi-mediated effect. The lipoplexes did not induce an innate immune response and the GP modification of the siRNAs attenuated release of pro-inflammatory cytokines.

Reduced immunostimulation is important to diminish toxicity, improve duration of silencing and enable repeated administration of the formulations. Previous work from members of our group demonstrated that inclusion of polyglutamate in the lipoplexes improved safety by reducing release of pro-inflammatory cytokines following administration *in vivo* [13]. The complexes used in this study thus included two immunostimulating components: polyglutamate as part of the vector and GP residues of the siRNA. Comparison to our earlier studies using anti-HBV siRNAs in transgenic murine models of HBV replication shows that the formulations used here have enhanced silencing efficacy and good safety [10,42]. The minimal immunostimulation by the lipoplexes containing GP-modified siRNAs suggests that repeat administration of the formulations would be effective with minimal toxicity. The mechanism by which the GP moiety attenuates immunostimulation is incompletely understood. Previous studies using chemically modified siRNAs have established that changes to the 2'OH of the ribose limit

stimulation of Toll-like receptors (TLRs) and other sensors of duplex RNA such as OAS-1 (reviewed in [5]). Activation of downstream interferon response genes is limited and immunostimulation is therefore reduced. It seems likely that GP-modified siRNAs would operate by a similar mechanism. As the liposomal component of the lipoplexes is also minimally immunostimulatory (Fig. 6), the combination with GP-modified siRNAs imparts features that may have utility for therapeutic application.

A useful strategy for silencing HBV gene expression has been demonstrated here, which compares favorably to approaches to countering HBV replication with siRNAs that have previously been reported [8,10,11,18]. Demonstration of immune-attenuated effects, hepatotropism of the lipoplexes, good durability of silencing, convenient methods for synthesis and formulating the particles are advantageous. These fabrication procedures are amenable to large scale preparation which will be required for therapeutic application to treatment of chronic HBV infection. Persistence of HBV in infected individuals remains an important global health problem [1,2]. Whether the viral replication intermediate comprising cccDNA can be eliminated after sustained gene silencing remains to be established. Nevertheless, the lipoplex formulations described here have useful features that may be exploited alone or in combination with newly developed gene editing strategies [24] to cure chronic HBV infection.

5. Conclusions

GP-modified siRNAs, formulated in novel hepatotropic lipoplexes containing anionic polymers, achieved efficient inhibition of HBV replication in HBV transgenic mice. Moreover, GP-modified siRNAs displayed improved anti-HBV efficacy *in vivo* when compared to their unmodified counterpart. Toxicity or induction of an innate immune response was not observed after injection of lipoplexes containing the GP-modified siRNAs. However, release of pro-inflammatory cytokines occurred in mice that received the unmodified siRNAs. Analysis using 5' RACE confirmed that the RNAi pathway was activated to effect cleavage of HBV mRNA *in vivo*. These data indicate that delivery of GP-modified siRNAs within polymer-containing lipoplexes may be useful for therapeutic application.

Acknowledgments

Financial assistance that was received from the South African National Research Foundation (NRF, GUNs 81768, 81692, 68339, 85981 & 77954), Medical Research Council, Poliomyelitis Research Foundation (PRF), the Health and Welfare Sector Education and Training Authority (HWSETA), Ernst & Ethel Eriksen Trust and the NRF/German Research Foundation (DFG) Research Cooperation Programme (Grant Unique ID Number 70707) is gratefully acknowledged. We are also appreciative to Patti Kay and Pamela Sharp for their assistance with flow cytometry and confocal microscopy, respectively. We are grateful to R. Lai-Kuen for technical assistance with TEM at the CRP2 Imaging Platform.

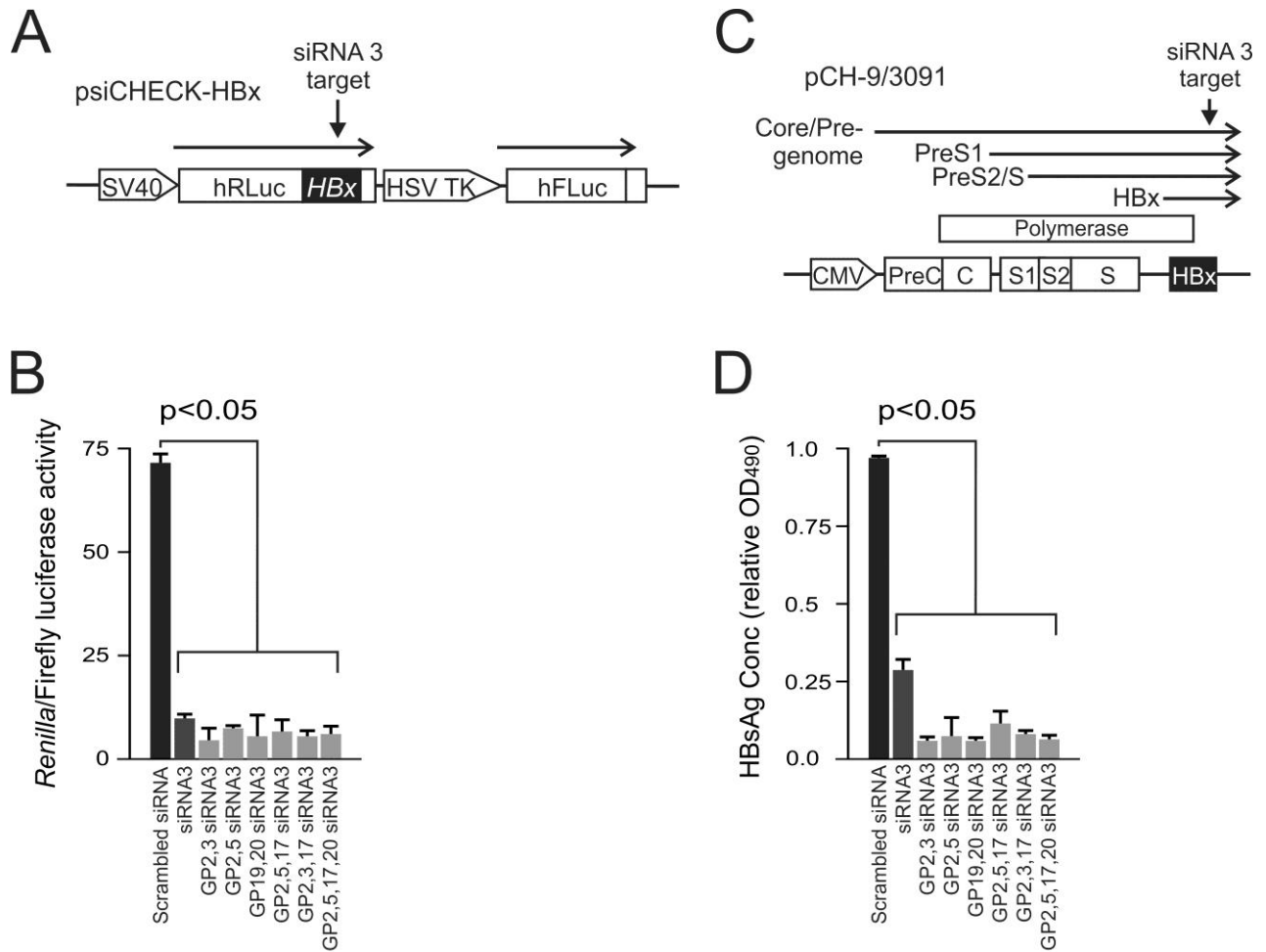
Appendix A. Supplementary data

Supplementary data to this article can be found online at <http://dx.doi.org/10.1016/j.jconrel.2015.04.042>.

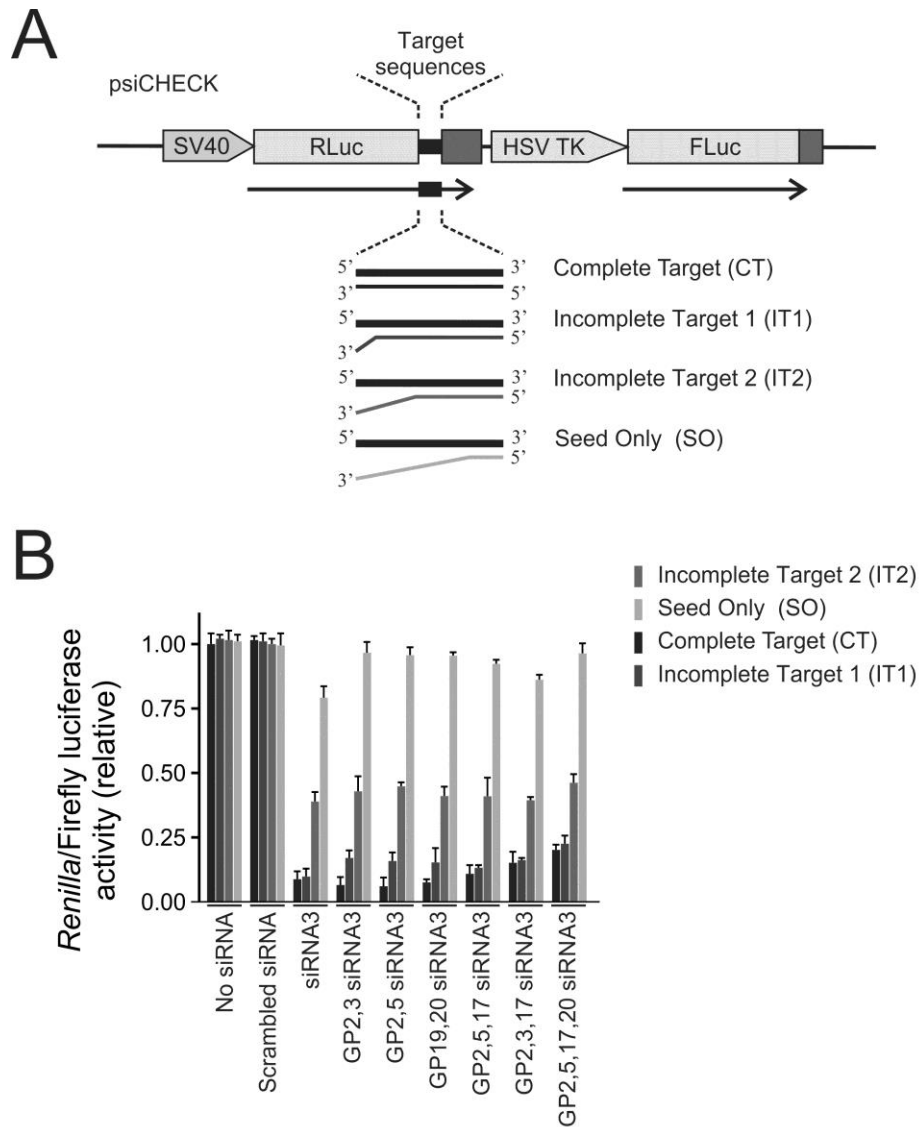
References

- P. Arbutnot, M. Kew, Hepatitis B virus and hepatocellular carcinoma, *Int. J. Exp. Pathol.* 82 (2001) 77–100.
- R.P. Beasley, L.Y. Hwang, Hepatocellular carcinoma and hepatitis B virus, *Semin. Liver Dis.* 4 (1984) 113–121.
- W.S. Ayoub, E.B. Keeffe, Review article: current antiviral therapy of chronic hepatitis B, *Aliment. Pharmacol. Ther.* 34 (2011) 1145–1158.
- D. Ivacic, A. Ely, P. Arbutnot, Countering hepatitis B virus infection using RNAi: how far are we from the clinic? *Rev. Med. Virol.* 21 (2011) 383–396.
- M.A. Behlke, Chemical modification of siRNAs for *in vivo* use, *Oligonucleotides* 18 (2008) 305–319.
- J.W. Engels, Gene silencing by chemically modified siRNAs, *New Biotechnol.* 30 (2013) 302–307.
- M.D. Marimani, A. Ely, M.C. Buff, S. Bernhardt, J.W. Engels, P. Arbutnot, Inhibition of hepatitis B virus replication in cultured cells and *in vivo* using 2'-O-guanidinopropyl modified siRNAs, *Bioorg. Med. Chem.* 21 (2013) 6145–6155.
- D.V. Morrissey, J.A. Lockridge, L. Shaw, K. Blanchard, K. Jensen, W. Breen, K. Hartsough, L. Machemer, S. Radka, V. Jadhav, N. Vaish, S. Zinnen, C. Vargeese, K. Bowman, C.S. Shaffer, L.B. Jeffs, A. Judge, I. MacLachlan, B. Polisky, Potent and persistent *in vivo* anti-HBV activity of chemically modified siRNAs, *Nat. Biotechnol.* 23 (2005) 1002–1007.
- R.U. Islam, J. Hean, W.A. van Otterlo, C.B. de Koning, P. Arbutnot, Efficient nucleic acid transduction with lipoplexes containing novel piperazine- and polyamine-conjugated cholesterol derivatives, *Bioorg. Med. Chem. Lett.* 19 (2009) 100–103.
- S. Carmona, M.R. Jorgensen, S. Kolli, C. Crowther, F.H. Salazar, P.B. Marion, M. Fujino, Y. Natori, M. Thanou, P. Arbutnot, A.D. Miller, Controlling HBV replication *in vivo* by intravenous administration of triggered PEGylated siRNA-nanoparticles, *Mol. Pharm.* 6 (2009) 706–717.
- C.I. Wooddell, D.B. Rozema, M. Hossbach, M. John, H.L. Hamilton, Q. Chu, J.O. Hegge, J.J. Klein, D.H. Wakefield, C.E. Oropeza, J. Deckert, I. Roehl, K. Jahn-Hofmann, P. Hadwiger, H.P. Vornlocher, A. MacLachlan, D.L. Lewis, Hepatocyte-targeted RNAi therapeutics for the treatment of chronic hepatitis B virus infection, *Mol. Ther.* 21 (2013) 973–985.
- S.C. Wong, J.J. Klein, H.L. Hamilton, Q. Chu, C.L. Frey, V.S. Trubetskoy, J. Hegge, D. Wakefield, D.B. Rozema, D.L. Lewis, Co-injection of a targeted, reversibly masked endosomolytic polymer dramatically improves the efficacy of cholesterol-conjugated small interfering RNAs *in vivo*, *Nucleic Acid Ther.* 22 (2012) 380–390.
- A. Schlegel, P. Bigey, H. Dhotel, D. Scherman, V. Escricou, Reduced *in vitro* and *in vivo* toxicity of siRNA-lipoplexes with addition of polyglutamate, *J. Control. Release* 165 (2013) 1–8.
- A. Schlegel, C. Largeau, P. Bigey, M. Bessodes, K. Lebozec, D. Scherman, V. Escricou, Anionic polymers for decreased toxicity and enhanced *in vivo* delivery of siRNA complexed with cationic liposomes, *J. Control. Release* 152 (2011) 393–401.
- G. Byk, D. Scherman, B. Schwartz, C. Dubertret, Lipopolyamines as transfection agents and pharmaceutical uses thereof, in: US Patent No. 6171612, 2001.
- H. Rhinn, C. Largeau, P. Bigey, R.L. Kuen, M. Richard, D. Scherman, V. Escricou, How to make siRNA lipoplexes efficient? Add a DNA cargo, *Biochim. Biophys. Acta* 1790 (2009) 219–230.
- J. Brzezinska, J. D'Onofrio, M.C. Buff, J. Hean, A. Ely, M. Marimani, P. Arbutnot, J.W. Engels, Synthesis of 2'-O-guanidinopropyl-modified nucleoside phosphoramidites and their incorporation into siRNAs targeting hepatitis B virus, *Bioorg. Med. Chem.* 20 (2012) 1594–1606.
- J. Hean, C. Crowther, A. Ely, R. Ul Islam, S. Barichiev, K. Bloom, M.S. Weinberg, W.A. van Otterlo, C.B. de Koning, F. Salazar, P. Marion, E.B. Roesch, M. Lemaitre, P. Herdewijn, P. Arbutnot, Inhibition of hepatitis B virus replication *in vivo* using lipoplexes containing alitol-modified antiviral siRNAs, *Artif. DNA PNA XNA* 1 (2010) 17–26.
- M. Nassal, The arginine-rich domain of the hepatitis B virus core protein is required for pregenome encapsidation and productive viral positive-strand DNA synthesis but not for virus assembly, *J. Virol.* 66 (1992) 4107–4116.
- S. Carmona, A. Ely, C. Crowther, N. Moolla, F.H. Salazar, P.L. Marion, N. Ferry, M.S. Weinberg, P. Arbutnot, Effective inhibition of HBV replication *in vivo* by anti-HBx short hairpin RNAs, *Mol. Ther.* 13 (2006) 411–421.
- M.S. Weinberg, A. Ely, S. Barichiev, C. Crowther, S. Mufamadi, S. Carmona, P. Arbutnot, Specific inhibition of HBV replication *in vitro* and *in vivo* with expressed long hairpin RNA, *Mol. Ther.* 15 (2007) 534–541.
- P.L. Marion, F.H. Salazar, K. Liittschwager, B.B. Bordier, C. Seeger, M.A. Winters, A.D. Cooper, J.M. Cullen, Chapter 18 — a transgenic mouse lineage useful for testing antivirals targeting hepatitis B virus, in: F.S. Raymond, S. Jean-Pierre, J.-P.S., Charles M. Rice, A2, Raymond F. Schinazi, M.R. Charles (Eds.), *Frontiers in Viral Hepatitis*, Elsevier, Amsterdam 2003, pp. 197–210.
- A. Ely, T. Naidoo, S. Mufamadi, C. Crowther, P. Arbutnot, Expressed anti-HBV primary microRNA shuttles inhibit viral replication efficiently *in vitro* and *in vivo*, *Mol. Ther.* 16 (2008) 1105–1112.
- K. Bloom, A. Ely, C. Mussolino, T. Cathomen, P. Arbutnot, Inactivation of hepatitis B virus replication in cultured cells and *in vivo* with engineered transcription activator-like effector nucleases, *Mol. Ther.* 21 (2013) 1889–1897.
- M.C. Buff, S. Bernhardt, M.D. Marimani, A. Ely, J.W. Engels, P. Arbutnot, Use of guanidinopropyl-modified siRNAs to silence gene expression, *Methods Mol. Biol.* 1218 (2015) 217–249.
- C. Crowther, A. Ely, J. Hornby, S. Mufamadi, F. Salazar, P. Marion, P. Arbutnot, Efficient inhibition of hepatitis B virus replication *in vivo*, using polyethylene glycol-modified adenovirus vectors, *Hum. Gene Ther.* 19 (2008) 1325–1331.
- C. Crowther, M.B. Mowa, A. Ely, P.B. Arbutnot, Inhibition of HBV replication *in vivo* using helper-dependent adenovirus vectors to deliver antiviral RNA interference expression cassettes, *Antivir. Ther.* 19 (2014) 363–373.
- M.B. Mowa, C. Crowther, A. Ely, P. Arbutnot, Inhibition of hepatitis B virus replication by helper dependent adenoviral vectors expressing artificial anti-HBV pri-miRs from a liver-specific promoter, *Biomed Res. Int.* 2014 (2014) 718743.
- E. Song, P. Zhu, S.K. Lee, D. Chowdhury, S. Kussman, D.M. Dykxhoorn, Y. Feng, D. Palliser, D.B. Weiner, P. Shankar, W.A. Marasco, J. Lieberman, Antibody mediated *in vivo* delivery of small interfering RNAs via cell-surface receptors, *Nat. Biotechnol.* 23 (2005) 709–717.
- P.L. Marion, F.H. Salazar, K. Liittschwager, B.B. Bordier, C. Seegers, M.A. Winters, A.D. Cooper, J.M. Cullen, A transgenic mouse lineage useful for testing antivirals targeting hepatitis B virus, in: R.F. Schinazi, J.-P. Sommadossi, C.M. Rice (Eds.), *Frontiers in Viral Hepatitis*, Elsevier Science, Amsterdam 2003, pp. 197–202.
- L.G. Guidotti, B. Matzke, H. Schaller, F.V. Chisari, High-level hepatitis B virus replication in transgenic mice, *J. Virol.* 69 (1995) 6158–6169.
- A.K. Raney, C.M. Eggers, E.F. Kline, L.G. Guidotti, M. Pontoglio, M. Yaniv, A. McLachlan, Nuclear covalently closed circular viral genomic DNA in the liver of hepatocyte nuclear factor 1 alpha-null hepatitis B virus transgenic mice, *J. Virol.* 75 (2001) 2900–2911.
- P. Meuleman, L. Libbrecht, R. De Vos, B. de Hemptinne, K. Gevaert, J. Vandekerckhove, T. Roskams, G. Leroux-Roels, Morphological and biochemical characterization of a human liver in a uPA-SCID mouse chimera, *Hepatology* 41 (2005) 847–856.
- S.M. Elbashir, J. Martinez, A. Patkaniowska, W. Lendeckel, T. Tuschl, Functional anatomy of siRNAs for mediating efficient RNAi in *Drosophila melanogaster* embryo lysate, *EMBO J.* 20 (2001) 6877–6888.
- J. Martinez, A. Patkaniowska, H. Urlaub, R. Luhrmann, T. Tuschl, Single-stranded antisense siRNAs guide target RNA cleavage in RNAi, *Cell* 110 (2002) 563–574.
- A.L. Cardoso, S. Simoes, L.P. de Almeida, J. Pelisek, C. Culumsee, E. Wagner, M.C. Pedrosa de Lima, siRNA delivery by a transferrin-associated lipid-based vector: a non-viral strategy to mediate gene silencing, *J. Gene Med.* 9 (2007) 170–183.
- A. Santel, M. Aleku, O. Keil, J. Endruschat, V. Esche, G. Fisch, S. Dames, K. Löffler, M. Fechtner, W. Arnold, K. Giese, A. Klippel, J. Kaufmann, A novel siRNA-lipoplex technology for RNA interference in the mouse vascular endothelium, *Gene Ther.* 13 (2006) 1222–1234.
- E. Wisse, R.B. De Zanger, K. Charels, P. Van Der Smissen, R.S. McCuskey, The liver sieve: considerations concerning the structure and function of endothelial fenestrae, the sinusoidal wall and the space of Disse, *Hepatology* 5 (1985) 683–692.

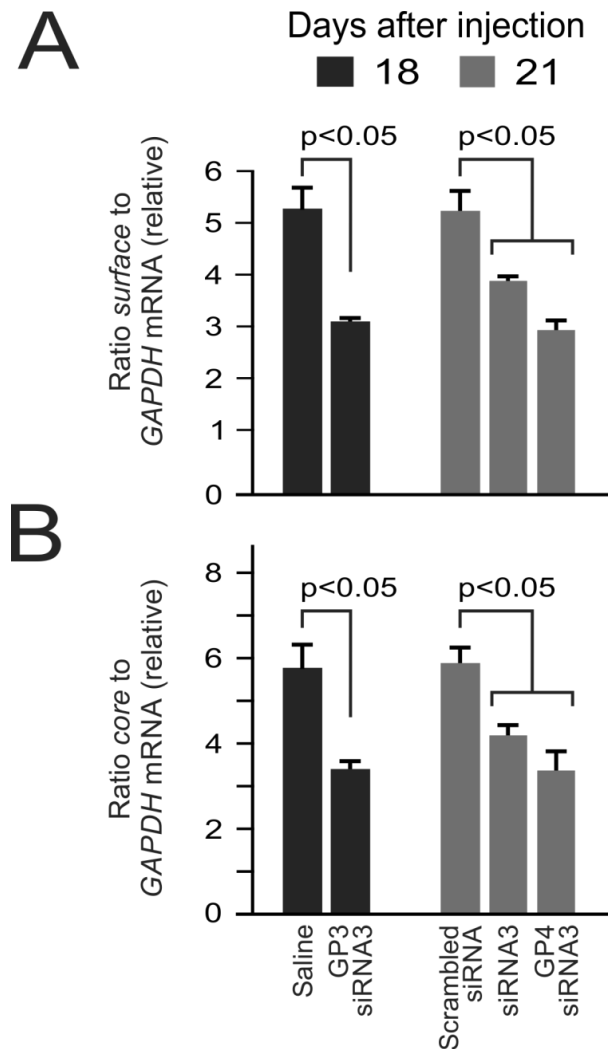
- [39] R.J. Hunter, B.R. Midmore, H. Zhang, Zeta potential of highly charged thin double-layer systems, *J. Colloid Interface Sci.* 237 (2001) 147–149.
- [40] H.J. Kim, A. Ishii, K. Miyata, Y. Lee, S. Wu, M. Oba, N. Nishiyama, K. Kataoka, Introduction of stearyl moieties into a biocompatible cationic polyaspartamide derivative, PAsp(DET), with endosomal escaping function for enhanced siRNA-mediated gene knockdown, *J. Control. Release* 145 (2010) 141–148.
- [41] W.J. Song, J.Z. Du, T.M. Sun, P.Z. Zhang, J. Wang, Gold nanoparticles capped with polyethyleneimine for enhanced siRNA delivery, *Small* 6 (2010) 239–246.
- [42] M. Mevel, N. Kamaly, S. Carmona, M.H. Oliver, M.R. Jorgensen, C. Crowther, F.H. Salazar, P.L. Marion, M. Fujino, Y. Natori, M. Thanou, P. Arbuthnot, J.J. Yaouanc, P.A. Jaffres, A.D. Miller, DODAG; a versatile new cationic lipid that mediates efficient delivery of pDNA and siRNA, *J. Control. Release* 143 (2010) 222–232.



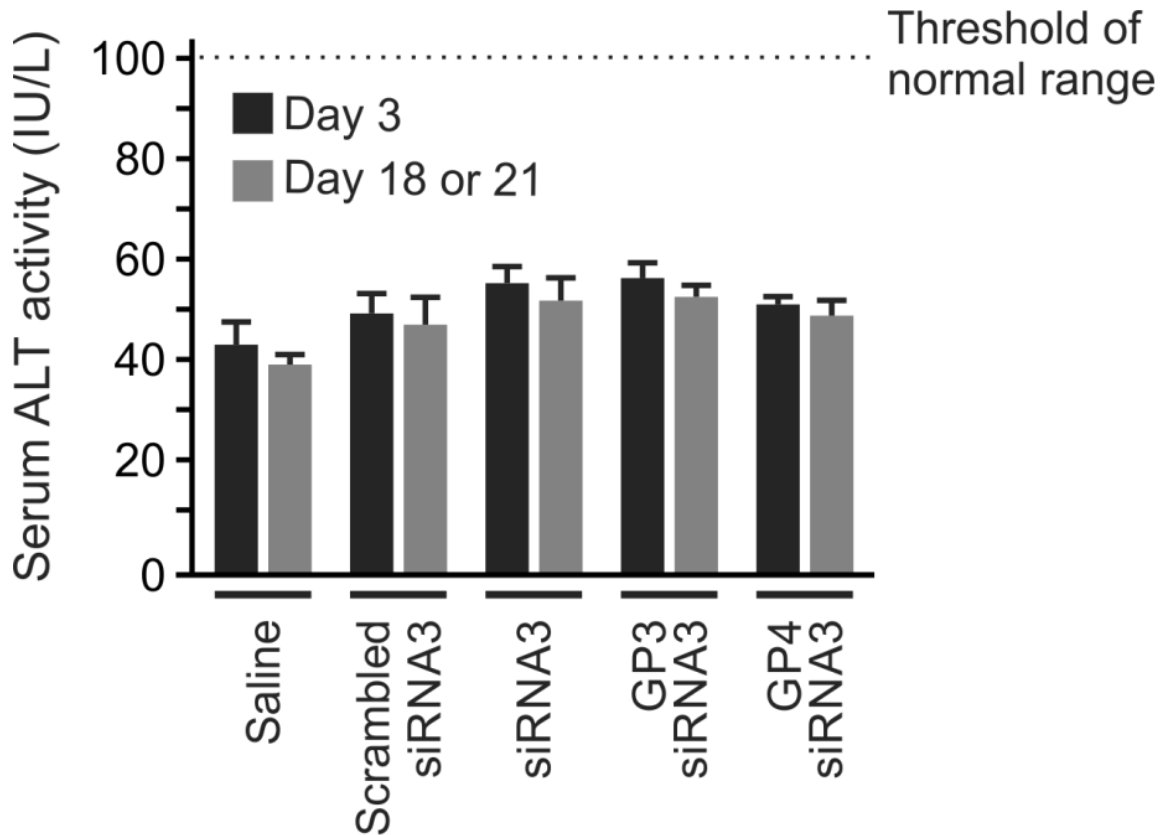
Supplementary Figure 1. Silencing of HBV target sequences by siRNAs containing multiple GP residues. psiCHECK-HBx plasmid, which contains the HBx target downstream of the Renilla luciferase reporter, is schematically illustrated in **A**. Dual-luciferase reporter gene assay was performed 48 hours after transfection of Huh7 cells with the indicated unmodified or GP-modified siRNAs (**B**). Results are given as mean ratios of Renilla to Firefly luciferase activity. To assess effects on HBV replication, the viral replication-competent plasmid, pCH-9/3091 was used to transfect Huh7 cells (**C**). Surface antigen (HBsAg) concentrations in cell culture supernatants were measured using ELISA that was carried out 48 hours after co-transfecting with the indicated siRNAs (**D**). Values represent the means and standard error of the mean of three replicate transfections. Differences were considered statistically significant when analysis using the Student's t test showed $p < 0.05$.



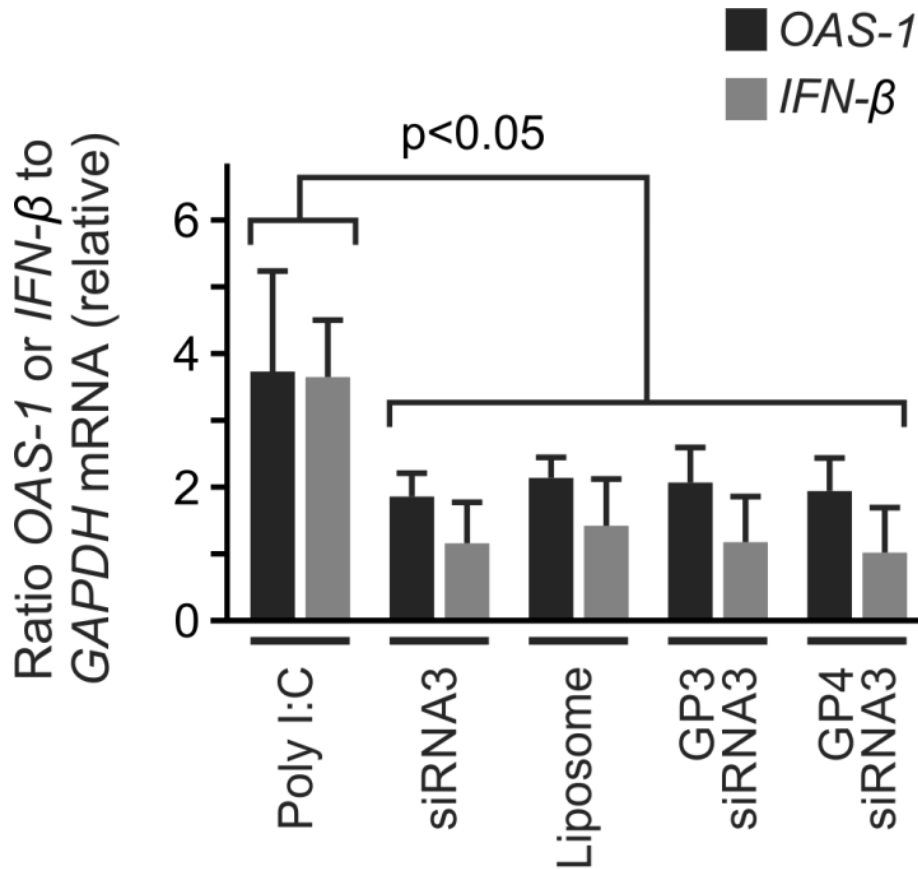
Supplementary Figure 2. Silencing of complete and partial targets by siRNAs containing multiple GP moieties. Four different sequences of siRNA3 were cloned into the dual-luciferase reporter plasmid, psiCHECK 2.2 (A). psiCHECK-siRNA3 CT contained a completely complementary target to siRNA3. Partially complementary targets contained a 3 nucleotide mismatch at the 3' end (psiCHECK-siRNA3 IT1), a 5 nucleotide mismatch at the 3' end (psiCHECK-siRNA3 IT2) and the seed region alone (psiCHECK-siRNA3 SO). A dual-luciferase reporter gene-based assay was performed 48 hours after co-transfecting Huh7 cells with each of the target plasmids with the panel of siRNAs (B). Data are presented as mean ratios of *Renilla* to Firefly luciferase activity (\pm SEM) from three replicate transfection experiments.



Supplementary Figure 3. Effect of siRNAs on intrahepatic concentrations of viral RNA encoding *surface* and *core* open reading frames. HBV transgenic mice were injected with lipoplexes containing siRNAs that were unmodified or contained guanidinopropyl (GP) residues. Mouse livers were harvested at day 18 or 21 post-administration. Viral mRNAs, relative to *GAPDH* mRNA, were quantified using RT-qPCR with primers specific for *surface* (**A**) and *core* (**B**) viral sequences. Values represent the means (\pm SEM) from replicate injections of four animals. Statistically significant differences between the samples, determined using the Student's two tailed paired t test, are indicated.



Supplementary Figure 4. Assessment of hepatotoxicity following intravenous administration of lipoplexes. HBV transgenic mice were injected with saline or formulations containing the indicated siRNAs. Blood samples were collected at day 3 and day 18 or 21 after administration. The threshold of the accepted normal range, < 100 IU/L, is indicated. Means (\pm SEM) were calculated from replicate injections of four different mice.



Supplementary Figure 5. Assessment of stimulation of the innate IFN response in HBV transgenic mice following intravenous administration of the siRNA-containing lipoplexes. Hepatic mRNA was prepared 6 hours subsequent to intravenous injection of mice with poly (I:C), liposome or lipoplexes containing unmodified (siRNA3) or guanidinopropyl (GP) siRNAs (GP3 siRNA3 and GP4 siRNA3). After reverse transcription, the samples were subjected to quantitative PCR to measure concentrations of mRNA from *OAS-1*, *IFN-β* and *GAPDH* genes. Data are presented as a ratio of the concentrations of mRNA from the IFN response genes relative to concentration of the *GAPDH* mRNA. Values represent the means and standard error of the means following injection of four different animals. Statistically significant differences between the samples, determined using the student's two tailed paired t test, are indicated.

SUPPLEMENTARY METHODS:

5.1. Characterisation and biodistribution of PG adjuvant-siRNA lipoplexes in HBV transgenic mice

The HBV transgenic mouse model was employed as it has the HBV sequence stably integrated into its genome and is capable of producing viral DNA, RNA and protein levels that mimic those of chronically infected individuals. These mice were generated by using the viral DNA sequence derived from HBV 1.3 [219]. This redundant DNA construct is located slightly upstream of HBV Enhancer I, and covers the whole HBV genome and ends downstream of the viral polyadenylation site. In these mice, viral mRNA expression is significantly higher in centrilobular liver cells relative to any other region in the hepatic lobule. Replication of viral DNA mainly occurs within the nucleocapsid particles that are formed in the cytoplasm of centrilobular liver cells. As a result, this mouse model is convenient for assessing the effect of antiHBV therapeutics on chronic HBV infection by examining markers of viral replication, pathogenesis and immune response [219].

The polyglutamate (PG) adjuvant liposomes were complexed with unmodified or GP-modified siRNAs to form PG adjuvant-siRNA lipoplexes. To enable tracking of the delivered siRNAs in injected mice, a modified sense strand with an Alexa Flour 750 label at its 3' end (Inqaba Biotech Industries, South Africa) was used. The lipoplexes were prepared by mixing 15 µg of GP3 siRNA3 and 15 µg of PG adjuvant in 100 µl saline into a single tube (**tube 1**). The second tube (**tube 2**) contained 15 µl of liposome dissolved in 100 µl saline. The contents of **tube 1** were transferred to **tube 2** and vigorously vortexed for at least 1 minute. The mixture was incubated at room temperature for at least 30 minutes. The PG adjuvant-siRNA lipoplexes were subjected to particle sizing and zeta potential was measured using the ZetaPALS Zeta Potential Analyzer (Brookhaven, NY, USA) using Dynamic Light Scattering

(DLS). Zeta potential was measured to determine the surface charge of the lipoplexes by Hückel analysis, after they were dissolved in 1 ml saline solution (pH 7.0). Three replicate measurements of particle sizing and zeta potential were performed (Appendix 7.2). The HBV transgenic mice were weighed and their body weight ranged between 20-22 g. Lipoplex samples were again briefly vortexed for 15 seconds before filling the injection syringe. Thereafter, 200 µl of PG adjuvant-GP3 siRNA3 lipoplex was injected into HBV transgenic mice via the tail vein and the total dose was 1 mg/kg (Table 5.1). Control mice were injected with 200 µl naked GP3 siRNA3 or saline. The injection scheme was as follows:

Table 5.1: Experimental groups used for assessing biodistribution of siRNAs in HBV transgenic mice

Experimental groups	Number of animals
Group 1: 1 mg/kg naked GP3 siRNA3, single dose	n=3
Group 2: 1 mg/kg PG adjuvant-GP3 siRNA3 lipoplex, single dose	n=3
Group 3: Saline, single injection	n=1

At 10 minutes post-injection, mice were sacrificed and the kidneys, liver, lungs and spleen were harvested for *ex vivo* imaging. Biodistribution of siRNAs in injected mice was assessed by measuring Alexa Flour 750 fluorescence at 745 nm in harvested organs using the IVIS Kinetic Bioluminescence imager (PerkinElmer, MA, USA). Subsequently, tissues were fixed in 20% paraformaldehyde at 4°C overnight, followed by suspension in 30% sucrose solution and kept at 4°C overnight. Thin sections (~5 µm) of harvested tissues were cut using an ultramicrotome (Thermo Scientific, MA, USA) and stained with 4',6-diamidino-2-

phenylindole (DAPI, Invitrogen™, Life Technologies, CA, USA) for 15 minutes. Sections were gently soaked in saline and placed on glass slides. Confocal microscopy (Zeiss, LSM 780, Oberkochen, Germany) detecting both DAPI staining and Alexa Fluor 750 fluorescence was performed to verify biodistribution and cellular localisation of siRNAs in injected mice at 40 × and 63 × magnifications.

5.2. AntiHBV effects and toxicity of PG adjuvant-siRNA lipoplexes in HBV transgenic mice

A separate group of HBV transgenic mice was employed to investigate antiHBV efficacy and toxicity of PG adjuvant-siRNA lipoplexes in injected animals using the injection scheme illustrated in Table 5.2.

Table 5.2: Experimental groups used for assessing activity and toxicity of siRNAs in transgenic mice

Experimental groups	Number of animals
Group 1: Saline, single injection	n=4
Group 2: 1 mg/kg PG adjuvant-scrambled siRNA lipoplex, single dose	n=4
Group 3: 1 mg/kg PG adjuvant-siRNA3 lipoplex, single dose	n=4
Group 4: 1 mg/kg PG adjuvant-GP3 siRNA3 lipoplex, single dose	n=4
Group 5: 1 mg/kg PG adjuvant-GP4 siRNA3 lipoplex, single dose	n=4

Chapter 5

At day 0 (baseline), 3, 5, 7, 14 and 18 or 21 post-administration blood samples were collected from injected mice and incubated at 4°C for 2 hours. Samples were centrifuged at $8\,000 \times g$ at 4°C for 10 minutes and serum collected from the upper phase. Subsequently, serum samples were used to measure HBsAg by ELISA and circulating VPEs by qPCR using mouse HBV surface primers, as described in **Supplementary Methods Section 4.3**.

Serum samples were also used to perform the ALT toxicity test at day 3, 18 and 21 using the accredited diagnostic protocols of the South African National Health Laboratory Service (NHLS, Johannesburg, South Africa). The HBV transgenic mice injected with saline and PG adjuvant-GP3 siRNA3 lipoplex were sacrificed at day 18 post-injection, while those treated with scrambled siRNA, PG adjuvant-siRNA3 and PG adjuvant-GP4 siRNA3 were sacrificed at day 21 post-administration. Mouse livers were collected and subjected to DNA extraction using the QIAamp DNA Mini Kit (Qiagen, GmbH, Germany) with minor modifications. Briefly, harvested mouse livers were weighed, saline added (1 ml saline for every gram of liver) and the organs homogenised. Fifty microlitres of the homogenates were transferred to 1.5 ml microcentrifuge tubes. One hundred microlitres of Buffer ATL was dispensed into each tube, followed by addition of 20 μ l Proteinase K. Samples were mixed by vortexing and incubated at 56°C in a shaking water bath until the tissue was completely lysed.

Samples were centrifuged at $13\,000 \times g$ for 1 minute to collect drops from the inside of the lid. Two hundred microlitres of Buffer AL was dispensed into each tube, mixed by pulse-vortexing for 15 seconds followed by incubation at 70°C for 10 minutes. Samples were briefly centrifuged at $13\,000 \times g$ for 1 minute to collect drops from the inside of the lid. To each sample, 200 μ l of 100% ethanol was dispensed and mixed by pulse-vortexing for 15 seconds. After mixing, samples were briefly centrifuged at $13\,000 \times g$ for 1 minute to collect

drops from the inside of the lid. The resulting mixture was carefully applied to the QIAamp Spin Column (in a 2 ml collection tube) without wetting the rim. Samples were centrifuged at $8\,000 \times g$ for 1 minute. The QIAamp Spin Column was placed in a clean 2 ml collection tube and the tube containing the flow-through was discarded. Thereafter, 500 μ l Buffer AW1 was added to the QIAamp Spin Column without wetting the rim and centrifuged at $8\,000 \times g$ for 1 minute. The QIAamp Spin Column was placed in a clean 2 ml collection tube and the tube containing the flow-through was discarded. Five hundred microlitres of Buffer AW2 was applied to the QIAamp Spin Column without wetting the rim, followed by centrifugation at $13\,000 \times g$ for 3 minutes. The QIAamp Spin Column was placed in a new 2 ml collection tube and centrifuged at $13\,000 \times g$ for 1 minute to collect residual buffer. The QIAamp Spin Column was placed in a clean 1.5 ml microcentrifuge tube and the collection tube containing the flow-through was discarded. Two hundred microlitres of Buffer AE was added to the QIAamp Spin Column, incubated at room temperature for 1 minute and centrifuged at $8\,000 \times g$ for 1 minute. Subsequently, the eluate was reapplied to the QIAamp Spin Column, incubated at room temperature for 1 minute and centrifuged at $8\,000 \times g$ for 1 minute. DNA samples were subjected to qPCR using mouse HBV surface primers as described in **Supplementary Methods Section 4.3**.

Additionally, from the same liver samples, RNA extraction was performed using Tri Reagent[®]. Harvested mouse livers were weighed, Tri Reagent[®] added (1 ml Tri Reagent[®] for every gram of liver) and organs homogenised. Fifty microlitres of the homogenates were transferred into 1.7 ml microcentrifuge tubes. Ten microlitres of chloroform was added to each sample, gently mixed by inverting tubes and incubated for 3 minutes. Samples were centrifuged at $12\,000 \times g$ at 4°C for 20 minutes. Subsequently, the upper aqueous phase was transferred to new 1.7 ml microcentrifuge tubes; an equal volume of isopropanol was added

and mixed by inverting tubes. Samples were incubated at -70°C for 2 hours and centrifuged at $12\,000 \times g$ at 4°C for 20 minutes. The supernatants were discarded, pellets washed with $200\ \mu\text{l}$ 70% ethanol and centrifuged at $12\,000 \times g$ at 4°C for 5 minutes. The supernatants were discarded, pellets resuspended in $50\ \mu\text{l}$ nuclease-free water and stored at -70°C until use. One microgram of total RNA was subjected to Genomic DNA Elimination and reverse transcription as described in **Supplementary Methods Section 4.2**. The resulting cDNA was subjected to RT-qPCR using $10\ \text{pmol}$ of either mouse HBV *core* (Integrated DNA Technologies, IA, USA), BCP1: 5'-ACC ACC AAA TGC CCC TAT-3' and BCP2: 5'-TTC TGC GAG GCG GCG A-3' or *surface* primers, as described in **Supplementary Methods Section 4.3**.

5.3. Innate immune stimulation of PG adjuvant-siRNA lipoplexes in HBV transgenic mice

A separate group of HBV transgenic mice was employed to investigate innate immune stimulation following administration of PG adjuvant-lipoplexes. These mice were injected via the tail vein with Poly(I:C), PG adjuvant liposome, unmodified siRNA3, GP3 siRNA3 or GP4 siRNA3 (Table 5.3). At 6 hours post-injection, blood samples were collected and livers obtained after mice were sacrificed. Serum samples were obtained from animal blood as described in **Supplementary Methods Section 4.3** to assess the release of proinflammatory cytokines using the CBA mouse inflammation kit (BD Biosciences, CA, USA), with minor modifications. Specifically, this assay was employed to measure IL-6, IL-10, MCP-1, IFN- γ , TNF and IL-12p70 protein levels after administration of PG adjuvant lipoplexes.

Table 5.3: Experimental groups used for assessing immunostimulatory effects of siRNAs in transgenic mice

Experimental groups	Number of animals
Group 1: 2 ml saline and 100 µg Poly(I:C) (HDI), single dose	n=4
Group 2: 15 µg PG adjuvant liposome, single dose	n=4
Group 3: 1 mg/kg PG adjuvant-siRNA3 lipoplex, single dose	n=4
Group 4: 1 mg/kg PG adjuvant-GP3 siRNA3 lipoplex, single dose	n=4
Group 5: 1 mg/kg PG adjuvant-GP4 siRNA3 lipoplex, single dose	n=4

Briefly, serum samples were diluted 2-fold in saline. The “Top Standard” solution (5000 pg/ml) was prepared by dissolving the Mouse Inflammation Standard in 2 ml assay diluent and incubated at room temperature for 15 minutes. The 12 × 75 mm Falcon™ Round-Bottom Polystyrene tubes (BD Biosciences, CA, USA) were labelled and arranged in the following order: 1:2 (2500 pg/ml), 1:4 (1250 pg/ml), 1:8 (625 pg/ml), 1:16 (312 pg/ml), 1:32 (156 pg/ml), 1:64 (80 pg/ml), 1:128 (40 pg/ml) and 1: 256 (20 pg/ml). Additionally, one tube containing the assay diluent was used as a negative control (0 pg/ml).

Three hundred microlitres of assay diluent was dispensed into each labelled tube. A serial dilution was performed by transferring 300 µl from the “Top Standard” to the 1:2 dilution tube and gently mixed. Subsequently, 300 µl from the 1:2 dilution tube was transferred to the 1:4 dilution tube and so on up to the 1:256 dilution tube. Six Capture Bead suspensions (specific for each cytokine to be analysed) were mixed by vortexing for 15 seconds and 10 µl of each Bead was added into a single tube “mixed Capture Beads”. Fifty microlitres of the

“mixed Capture Beads” were transferred to each assay tube followed by addition of 50 μ l Phycoerythrin (PE) detection reagent. All samples were incubated in the dark at room temperature for 2 hours, washed with 1 ml wash buffer and centrifuged at $200 \times g$ for 5 minutes. The wash buffer was gently removed and the beads resuspended in fresh 300 μ l wash buffer solution. Samples were placed in the flow cytometry instrument (BD, LSRFortessaTM) and the BD CBA Software (BD Biosciences, CA, USA) was used to assess the levels of inflammatory cytokines in injected mice. Mouse livers were subjected to RNA extraction using Tri Reagent[®] as described in **Supplementary Methods Section 5.2**. The extracted RNA was used to investigate immunostimulatory effects of PG adjuvant-siRNA lipoplexes in mouse livers following administration in transgenic mice. RNA was subjected to Genomic DNA Elimination and reverse transcription using the QuantiTect[®] Reverse Transcription Kit, and RT-qPCR using mouse *IFN- β* , *OAS-1* and *GAPDH* primers as described in **Supplementary Methods Section 4.2**.

5.4. Detection of siRNA-mediated mRNA cleavage *in vivo* by 5' RACE

5.4.1. Ligation of RNA to GeneRacerTM RNA Oligo

All reagents used to perform 5' Rapid Amplification of cDNA ends (5' RACE) were from Life Technologies (GeneRacerTM Kit, Life Technologies, CA, USA), unless otherwise stated. Specifically, the RNA ligase-mediated amplification of cDNA ends (RLM-RACE) technique was applied to detect the mRNA cleavage product in injected mice following siRNA administration. Total RNA extracted from mouse livers (**Supplementary Methods Section 5.2**) was also ligated to the GeneRacerTM RNA Oligo without prior dephosphorylation or removal of the mRNA cap structure. The ligation reactions were performed by adding 7 μ l of RNA (100 ng/ μ l) to the tubes with the pre-aliquoted, lyophilised GeneRacerTM RNA Oligo

Chapter 5

(0.25 µg) and briefly centrifuged at $12\,000 \times g$ at 4°C for 1 minute. The reaction mixtures were transferred to 1.7 ml microcentrifuge tubes and incubated at 65°C for 5 minutes. Samples were placed on ice for 2 minutes and centrifuged at $12\,000 \times g$ at 4°C for 1 minute. To each tube, 1 µl of ligase Buffer (10 ×), 1 µl ATP (10 mM), 1 µl RNaseOut™ (40 U/ µl) and 1 µl of T4 RNA ligase (5 U/µl) were added and incubated at 37°C for 1 hour. After incubation, the ligated RNA was precipitated using the phenol-chloroform protocol. Briefly, ninety microlitres of Diethylpyrocarbonate-treated water (DEPC water) and 100 µl of phenol-chloroform were added to the RNA transcripts and mixed by vigorously vortexing for 30 seconds. The mixtures were centrifuged at $13\,000 \times g$ for 5 minutes.

One hundred microlitres of the top aqueous phase from each sample was transferred to a new 1.7 ml microcentrifuge tube. Two microlitres of mussel glycogen (10 mg/ml) and 10 µl of sodium acetate (3M, pH 5.2) were dispensed into each tube and gently mixed. This was followed by addition of 220 µl 95% ethanol, briefly mixed by inverting tubes and incubated at -20°C overnight. Following incubation, samples were centrifuged at $13\,000 \times g$ at 4°C for 20 minutes and the resulting supernatants discarded. Five hundred microlitres of 70% ethanol was dispensed into each tube, mixed by gently inverting tubes and centrifuged at $13\,000 \times g$ at 4°C for 2 minutes. The ethanol was gently removed and the pellets were air-dried at room temperature for 2 minutes. Subsequently, the RNA transcripts were resuspended in 10 µl DEPC water and stored at -70°C until use.

5.4.2. Reverse transcription of ligated RNA

To the tubes containing 10 µl of ligated RNA, the following reagents were added to initiate cDNA synthesis: 1 µl of the gene-specific RT primer (10 pmol) (5'-AGGGTCGATGTCCATGCCCC-3'; Integrated DNA Technologies, IA, USA), 1 µl dNTP

mix (10 mM each) and 1 μ l of nuclease-free water. The reaction mixtures were briefly centrifuged at $12\,000 \times g$ at 4°C for 20 seconds and incubated at 65°C for 5 minutes. Samples were placed on ice for 2 minutes and centrifuged at $12\,000 \times g$ at 4°C for 20 seconds. This was followed by addition of 4 μ l First Strand Buffer (5 \times), 1 μ l DTT (0.1 M), 1 μ l SuperScriptTM III RT (200 U/ μ l) and 1 μ l RNaseOutTM (40 U/ μ l). Samples were centrifuged at $12\,000 \times g$ at 4°C for 20 seconds and incubated at 55°C for 1 hour. Reverse transcriptase was inactivated at 70°C for 15 minutes, samples placed on ice for 2 minutes and centrifuged at $12\,000 \times g$ at 4°C for 20 seconds. One microlitre of RNaseH (2 U) was added to the samples followed by incubation at 37°C for 20 minutes. Samples were recentrifuged at $12\,000 \times g$ at 4°C for 20 seconds. Subsequently, 10 μ l cDNA aliquots were prepared and stored at -20°C to prevent degradation from frequent freeze-thaw cycles.

5.4.3. Amplification of cDNA by 5' RACE-PCR, cloning and DNA sequencing

cDNA was amplified by 5' RACE-PCR using 2 \times Phusion Master Mix (Thermo Scientific, MA, USA), 10 pmol each of the forward GeneRacerTM 5' primer (5'-CGACTGGAGCACGAGGACACTGA-3', Life Technologies, CA, USA), reverse gene-specific PCR primer (5'-CAAGAGATGATTAGGCAGAGGTG-3', Integrated DNA Technologies, IA, USA) and 1.25 μ l cDNA template (100 ng/ μ l). All PCR amplification reactions were performed in a thermocycler (T100TM Thermal Cycler, Bio-Rad, CA, USA) using the following cycling conditions: one cycle of 98°C for 30 seconds (initial denaturation), 27 cycles of denaturation at 98°C for 10 seconds, annealing at 63°C for 30 seconds and extension at 72°C for 30 seconds. The final extension step was performed at 72°C for 10 minutes. Amplified PCR products were subjected to electrophoresis on a 2% agarose gel at 100 volts for 45 minutes and visualised under UV transillumination (G:Box, Syngene, Cambridge, UK) (Appendix 7.4.1) [220].

Chapter 5

The PCR products were purified using the MinElute Gel Extraction kit (Qiagen, GmbH, Germany). Briefly, the section of the gel containing the DNA of interest was excised using a clean sharp blade and transferred to 1.7 ml microcentrifuge tubes. The gel slices were weighed and 3 volumes of QG buffer were added. Gel slices were melted by incubating the tubes at 50°C for 10 minutes. A gel volume of isopropanol was added into each tube, mixed and applied to the spin columns. Samples were centrifuged for 1 minute at room temperature and the flow-through was discarded. Five hundred microlitres of QG buffer was applied to each column and centrifuged at $10\,000 \times g$ for 1 minute. The flow-through was discarded and the columns washed with 750 μ l of PE buffer. Samples were centrifuged at $10\,000 \times g$ for 1 minute and the flow-through was discarded. The columns were placed in clean 1.7 ml tubes and 20 μ l of Buffer EB was added to the column matrix. Samples were incubated at room temperature for 2 minutes and the DNA was eluted by centrifugation at $10\,000 \times g$ for 1 minute.

The purified PCR products were ligated to the pTZ57R/T plasmid using the InsTAclone PCR cloning kit (Thermo Scientific, MA, USA). Ligation was performed using T4 DNA ligase (5 U), pTZ57R/T plasmid (0.17 pmol ends) and 3 μ l purified PCR product (200 ng/ μ l). Samples were incubated at 14°C overnight. One hundred microlitres of chemically competent bacteria (*E. coli* DH5 α) was transformed with 10 μ l of ligation reaction and spread on ampicillin-containing Luria Bertani agar plates coated with 40 μ l 5-bromo-4-chloro-3-indolyl- β -D-galactopyranoside (X-gal, 20 mg/ml, Sigma, MI, USA) and 8 μ l of Isopropyl β -D-1-thiogalactopyranoside (IPTG, 100 mM, Sigma, MI, USA). Plates were inverted and incubated at 37°C overnight. Subsequently, ten individual white colonies were picked using sterile

Chapter 5

procedures. Each colony was inoculated into 10 ml of ampicillin-containing Luria Bertani broth and incubated at 37°C overnight with shaking.

Standard plasmid mini preparations were performed using the alkaline lysis method. Briefly, cultures were centrifuged at $2\,500 \times g$ for 15 minutes at 4°C and the supernatants were discarded. Three hundred microlitres Buffer P1 (10 mM EDTA, 50 mM Tris, pH 8.0 and 100 µg/ml RNase A) was added to the pellets and transferred to sterile 2 ml microcentrifuge tubes. To each tube, 300 µl Buffer P2 (200 mM sodium hydroxide and 1% SDS) was dispensed, mixed and incubated at room temperature for 5 minutes. Three hundred microlitres of Buffer P3 (3 M potassium acetate, pH 5.5) was added into the samples and mixed by inverting the tubes. Samples were centrifuged at $13\,000 \times g$ for 10 minutes at 4°C, and approximately 800 µl of the resulting supernatant was transferred to a new 2 ml microcentrifuge tube. An equal volume of isopropanol was added, mixed by inverting tubes and incubated at -20°C for 2 hours. After incubation, samples were centrifuged at $13\,000 \times g$ at 4°C for 30 minutes. The resulting supernatants were discarded, pellets resuspended in 100 µl of water and stored at -20°C until use.

Positive clones were identified by digesting plasmid DNA (1 µg) with *Apa*LI (10 U, Thermo Scientific, MA, USA). Samples were incubated at 37°C for 1 hour and subjected to electrophoresis on a 2% agarose gel at 100 volts for 45 minutes and visualised under UV transillumination. Presence of two DNA fragments of approximately 1859 bp and 1246 bp indicated successful cloning of the PCR products into pTZ57R/T. Positive clones were verified by automated DNA sequencing (Inqaba Biotech Industries, South Africa) using the M13 reverse primer 5'-CAGGAAACAGCTATGAC-3' (Inqaba Biotech Industries, South Africa). The expected 5' RACE product was identified by the presence of sequences derived

Chapter 5

from both the ligated GeneRacerTM RNA oligonucleotide and predicted mRNA cleavage product (Appendix 7.4.2) [220].

Chapter 6: General discussion and conclusion

The goal of this study was to assess the advantage of using novel GP-modified siRNAs over unmodified siRNA3 to inhibit HBV replication in cultured Huh7 cells and mice. Data presented in this work provide novelty to the field of gene therapy as it demonstrates that incorporation of the GP moiety improves the specificity and silencing efficacy of the siRNAs, thus, enhancing their antiHBV effects in cultured mammalian cells [217, 221] (Chapter 4), HDI mouse model [221] (Chapter 4) and transgenic mice [220] (Chapter 5) relative to unmodified siRNA3. Moreover, these antiviral effects were enhanced without a marked induction of non-specific effects such as innate immune stimulation and cytotoxicity [220, 221] (Chapter 4 and 5). Furthermore, this was consistent with previous studies which reported an increase in suppression of markers of HBV replication *in vivo* following liposome-mediated delivery of chemically modified siRNAs, without a marked induction of the innate immune response as opposed to the unmodified siRNAs [124, 159, 170].

The pCH-9/3091 plasmid used for transient transfections in cell culture belongs to HBV genotype D. Genotype A differs from genotype D within the siRNA3 target site by one nucleotide, this discrepancy is unlikely to affect silencing efficiency. This is mainly because in the RNAi mechanism, incomplete base-pairing between target mRNA and guide strand results in translational suppression, while complete base-pairing results in degradation of target mRNA. Translational suppression results in decreased levels of proteins being manufactured which subsequently leads to reduced levels of mRNA being produced. Therefore, this would still allow the siRNAs to activate RNAi-mediated gene silencing, regardless of the single nucleotide mismatch.

It is not well-elucidated how incorporation of a GP moiety improves therapeutic properties of antiHBV siRNAs such as specificity and silencing efficacy. However, it has been demonstrated that incorporation of chemical groups into siRNAs, particularly in the seed region, decreases off-target effects by minimising the interaction between RISC and incomplete target sequences [156]. Modification of 2' ribose has been shown to change the binding and thermodynamic properties of modified siRNAs [160-162]. This leads to improved specificity of modified siRNAs by reducing interaction with partial complementary targets without diminishing efficacy of these RNAi effectors [156]. It has also been postulated that modified siRNAs may prevent immune stimulation by triggering internalisation of receptor molecules or by antagonising pathways associated with innate immune signalling [157].

Furthermore, modification of the 2' position with bulky chemical groups without altering the A-form helix of the guide strand-mRNA complex [149, 222] may also prevent interaction between modified siRNAs and immune receptors, thereby, avoiding immune stimulation [170]. The GP moiety constitutes a bulky chemical modification and was placed at the 2' position without distorting the structure of the A-form helix. Therefore, these features may enhance specificity of GP-modified siRNAs, particularly those with seed modifications, by: (a) avoiding interactions with TLRs, (b) inhibiting pathways associated with innate immune stimulation or (c) altering thermodynamic properties of modified siRNAs. Consequently, these properties may have contributed to GP-modified siRNAs, as opposed to unmodified siRNA3, being able to discriminate between complete and incomplete targets by regulating the strength of seed region hybridisation to various target constructs, leading to improved specificity [221] (Chapter 4) and modest immune stimulation [220] (Chapter 5).

Chapter 6

The mechanism with which the GP modification improves therapeutic activity is yet to be unravelled. It has previously been reported that chemical residues introduce structural alterations to siRNAs that may influence the efficiency of RISC processing [156]. The ability of GP-modified siRNAs to hybridise strongly to complete as opposed to incomplete targets coupled with conformational changes introduced by the GP moiety may be responsible for the superior therapeutic efficacy of modified siRNAs over the unmodified siRNA3 [217, 220, 221] (Chapter 4 and 5). These attributes may increase interaction between GP-modified siRNAs and RISC components, leading to enhanced retention of the guide strand followed by improved target gene silencing.

In addition to suppressing HBsAg expression and the number of circulating VPEs, both sets of antiHBV siRNAs also markedly reduced viral *surface* and *core* levels in transgenic mice [220] (Chapter 5). The HBsAg and VPEs levels were significantly suppressed in mice treated with unmodified siRNA for up to day 7 post-administration, while the GP-modified siRNAs displayed prolonged antiHBV activity that persisted for up to 14 days post-injection. However, at day 18 and 21 post-administration, the HBsAg and VPEs levels in mice treated with antiHBV siRNAs returned to baseline levels [220] (Chapter 5). In contrast, quantification of intrahepatic RNA levels from mouse livers revealed significant suppression of these markers of HBV replication in mice treated with unmodified and GP-modified siRNAs at day 18 and 21 post-administration [220] (Chapter 5). This discrepancy may be due to the fact that both ELISA and qPCR were used to measure HBsAg and VPEs levels, respectively from mice sera. In our study, sera were obtained from blood samples collected from behind the eyes of injected animals using a retro orbital puncture. Although serum samples are routinely used in diagnostic tests to evaluate various biomarkers, they do not provide accurate results compared to assessment from the site of interest (e.g. mouse liver).

Chapter 6

Therefore, subsequent qPCR amplifications relied on quantification of intrahepatic RNA levels directly from mouse livers. This approach is more sensitive and accurate than evaluation from mice sera, as it relied on assessment of markers of HBV replication directly from infected mouse livers.

The RNAi mechanism of action was confirmed after detecting the siRNA-mediated mRNA cleavage product *in vitro* (Appendix 7.3.1 and 7.3.2) [223] and *in vivo* (Appendix 7.4.1 and 7.4.2) [220] (Chapter 5) using the sensitive 5' RACE technique. This conclusively demonstrated that silencing of markers of HBV replication in cultured cells and injected animals was due to an RNAi effect. Importantly, the position or number of GP moieties incorporated into the siRNA guide strand did not change the site of cleavage, which consistently occurred at position 11 *in vitro* (Appendix 7.3.2) [223] and 10 *in vivo* (Appendix 7.4.2) [220] (Chapter 5). The discrepancy in the position of target mRNA cleavage *in vitro* and *in vivo* can be accounted for, as previous studies demonstrated that following Argonaute loading into RISC, the RISC machinery uses the siRNA guide strand to recognise RNA comprising complementary sequences. This leads to direct cleavage of target mRNA occurring in nucleotides 10-11 from the 5' end of the siRNA guide strand [224, 225]. It is also possible that physiological differences in cultured mammalian cells and injected animal cells may have contributed to the 5' RACE discrepancy, with regard to the site of target mRNA cleavage occurring at position 10 or 11. Collectively, our data highlighted the importance of using GP-modified siRNAs coupled with a competent hepatotropic non-viral delivery system to achieve efficient and safe RNAi-based therapy against chronic HBV infection. Findings emanating from this study may be used as a platform for future studies that may focus on the effect of a second or third administration of GP-modified siRNA

Chapter 6

lipoplexes into HBV transgenic mice, and their implications on silencing efficacy, sustainability, hepatotoxicity and immune stimulation.

To advance this strategy to a clinical setting, several outstanding factors not covered by our study need to be satisfied. For example, the HBV transgenic mouse model [219] employed in our study is suitable for studying antiHBV activity of GP-modified siRNAs as it is capable of secreting high levels of viral DNA, RNA and proteins which closely resembles that of chronically infected individuals. Furthermore, these mice also possess a functional immune system which is well-suited for investigating non-specific effects following administration of modified siRNAs. However, the limitation is that this model does not contain human hepatocytes and is incapable of producing cccDNA. Moreover, the HBsAg levels vary greatly between mice, thus, necessitating screening of HBsAg concentrations before investigating antiHBV efficacy *in vivo*.

To date, the urokinase plasminogen activator-severe combined immunodeficiency (uPA-SCID) mouse is the only animal model capable of establishing human HBV infection [226]. These mice consist of engrafted human hepatocytes, thus, making the uPA-SCID system ideal for studying human HBV infection. The engrafted human cells populate the liver, resulting in the formation of chimaeric livers comprised of mouse and human hepatocytes. Extensive colonisation of mouse livers by human hepatocytes renders them susceptible to human HBV infection. Furthermore, these human hepatocytes produce cccDNA during infection, thus, allowing active viral replication to be established. Therefore, these features advance the use of uPA-SCID mice as a relevant model for investigating antiHBV activity of GP-modified siRNAs. However, the limitation is that these mice are immunocompromised, thus, making this model unsuitable for conducting rigorous analysis of therapeutic efficacy or

investigating immunostimulatory effects of GP-modified siRNAs. Depending on the antiviral activity of modified siRNAs in the uPA-SCID model, subsequent efficacy studies may be conducted in woodchucks, non-human primates and human subjects. Importantly, efficacy studies in these systems may require dose regulation, as an effective dose of 1 mg/kg in transgenic mice may not necessarily translate to the same amount of efficacy and durability in other animal models.

For clinical application, the use of modified siRNAs and licensed antiHBV drugs (i.e. combination therapy) may provide a robust approach of eradicating chronic HBV infection. Additionally, application of gene therapy in conjunction with gene editing technologies may also be an effective strategy of accomplishing clinical success. Various HBV sites have been successfully targeted and disrupted using gene editing strategies such as zinc finger nucleases (ZFNs) [227], transcription activator-like effector nucleases (TALENs) [228, 229] and clustered regularly interspaced short palindromic repeat (CRISPR)/CRISPR-associated protein 9 (Cas9) [230-232]. Impressively, these systems have also been employed to target, cleave and disrupt the cccDNA of HBV which is essential for viral replication and persistence [228, 229, 231].

Cleavage of target DNA using gene editing strategies induces the formation of double-stranded breaks in the target sequence. This is followed by DNA repair which allows subsequent binding and cleavage of viral DNA to occur. Homology directed repair (HDR) and non-homologous end joining (NHEJ) are responsible for DNA repair [227, 233-236]. The HDR mechanism uses homologous DNA sequences to achieve accurate repair of cleaved target DNA, while the NHEJ process is error prone and results in deletions and insertions being introduced at the cleavage site. Therefore, application of gene editing technologies may

weaken the virus following multiple cleavage events, leading to mutation of target cccDNA sequence [237]. The inability of the cccDNA pool to be re-established within the host cells may halt viral replication and persistence, thus allowing symptom alleviation and eradication of chronic HBV infection.

In conclusion, GP-modified siRNAs generally displayed improved antiHBV activity relative to unmodified siRNA3 in cultured mammalian cells and mice. Incorporation of a GP-moiety within the seed region improves specificity of siRNAs (compared to unmodified siRNA3) by abolishing unwanted off-target effects, but this strategy does not seem to significantly improve stability of these RNAi effectors against serum nuclease degradation. Neither modified nor unmodified siRNAs significantly induce the innate IFN pathway or toxicity in cell culture and HBV transgenic mice. Conversely, the unmodified siRNA3 triggers the release of proinflammatory cytokines in transgenic mice. However, this immunostimulatory effect is generally attenuated in mice treated with siRNAs harbouring the GP-moiety, in which modest MCP-1 activation was observed. Silencing of markers of HBV replication *in vitro* and *in vivo* resulted from an RNAi effect exerted by both sets of siRNAs as confirmed by 5' RACE analysis. Data from this particular investigation indicate that application of novel GP-modified siRNAs and an efficient liver-tropic non-viral delivery system improves therapeutic properties of these RNAi activators by achieving sustained antiHBV efficacy, while minimising toxicity and innate immune stimulation in cultured cells and transgenic mice, thus, augmenting the prospect of siRNA therapy against chronic HBV infection.

Chapter 7: Appendix

7.1. Animal Ethics Clearance Certificate



STRICTLY CONFIDENTIAL

ANIMAL ETHICS SCREENING COMMITTEE (AESC)

CLEARANCE CERTIFICATE NO. 2013/39/04

APPLICANT: Mr M Marimani

SCHOOL: Medical School
DEPARTMENT: Molecular Medicine & Haematology
LOCATION: Faculty of Health Sciences

PROJECT TITLE: Inhibition of hepatitis B virus (HBV) replication in transgenic mice using 2-O guanidinopropyl(GP) modified siRNAs

Number and Species

110 Mice

Approval was given for to the use of animals for the project described above at an AESC meeting held on 20/08/2013. This approval remains valid until 19/08/2015.

The use of these animals is subject to AESC guidelines for the use and care of animals, is limited to the procedures described in the application form and is subject to any additional conditions listed below:

None.

Signed:  Date: 20/8/2013
(Chairperson, AESC)

I am satisfied that the persons listed in this application are competent to perform the procedures therein, in terms of Section 23 (1) (c) of the Veterinary and Para-Veterinary Professions Act (19 of 1982)

Signed:  Date: 20/08/2013
(Registered Veterinarian)

cc: Supervisor: Prof P Arbuthnot
Director: CAS

Appendix 7.2: Particle sizing and zeta potential of siRNA-lipoplexes:

7.2.1. Particle sizing of siRNA3-lipoplexes:

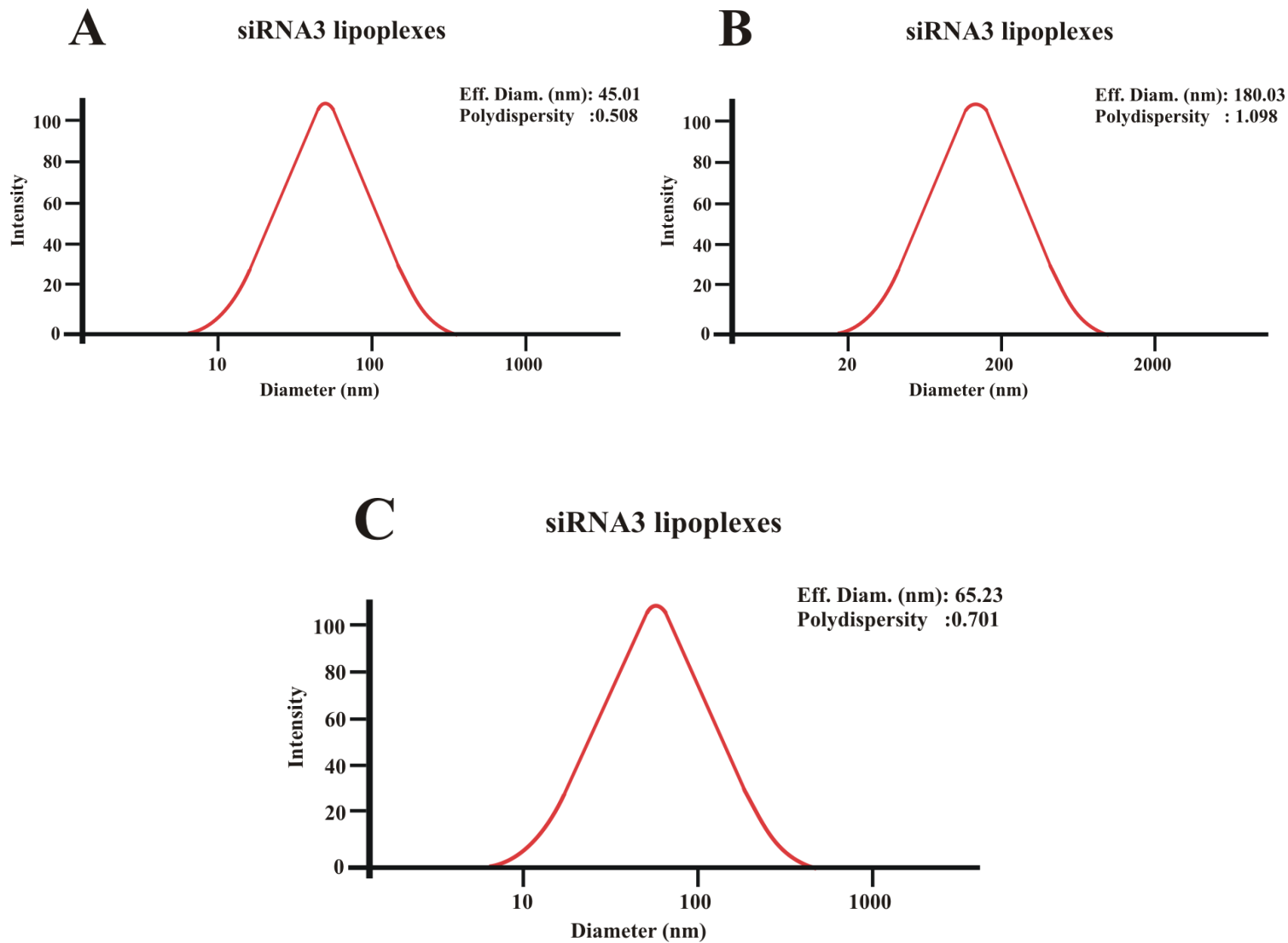
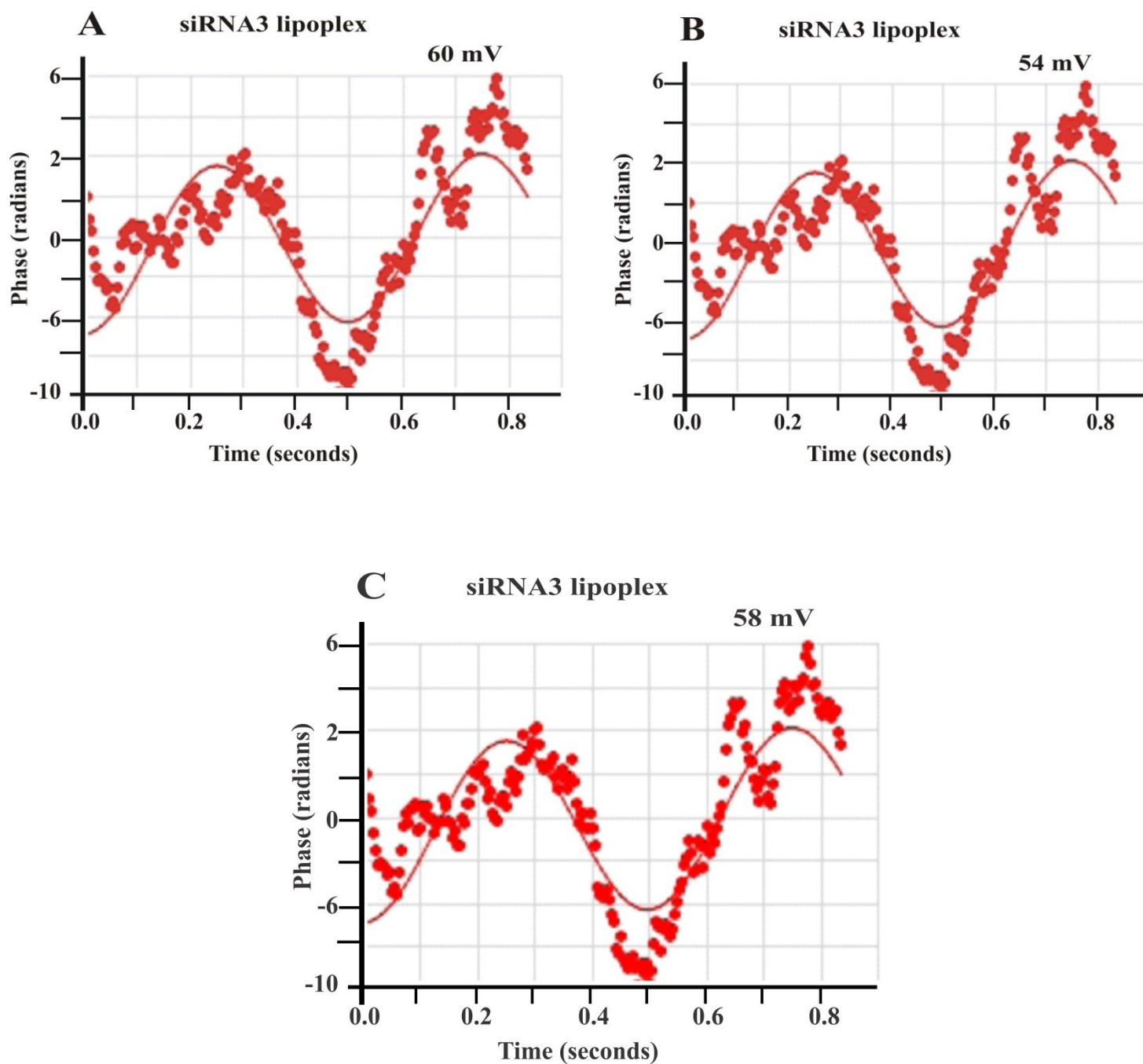


Figure 7.2.1. Particle sizing of PG adjuvant-siRNA3 lipoplexes

The negatively charged siRNAs were complexed to positively charged PG adjuvant liposomes to form siRNA3 lipoplexes and analysed by DLS. Particle size of unmodified siRNA3 lipoplexes ranged from 45-180 nm in diameter with a polydispersity index of 0.508-1.098.

7.2.2. Zeta potential of siRNA3-lipoplexes:**Figure 7.2.2. Zeta potential of PG adjuvant-siRNA3 lipoplexes**

The negatively charged siRNA3 molecules were complexed to cationic PG adjuvant liposomes to form siRNA3 lipoplexes. The surface charge of unmodified siRNA3 lipoplexes was determined by Hückel analysis and ranged between +54 to +60 mV.

7.2.3. Particle sizing of GP3 siRNA3-lipoplexes:

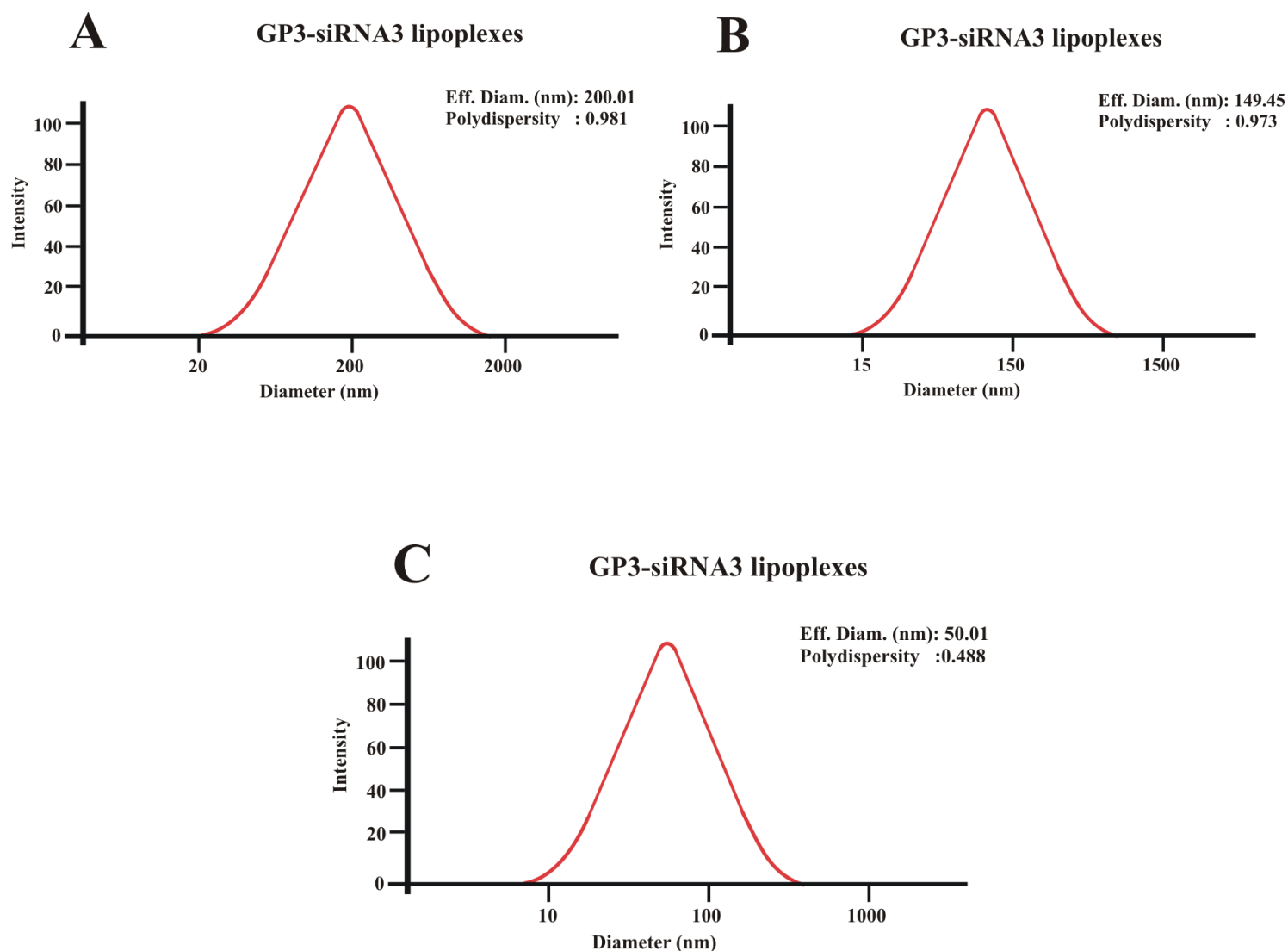
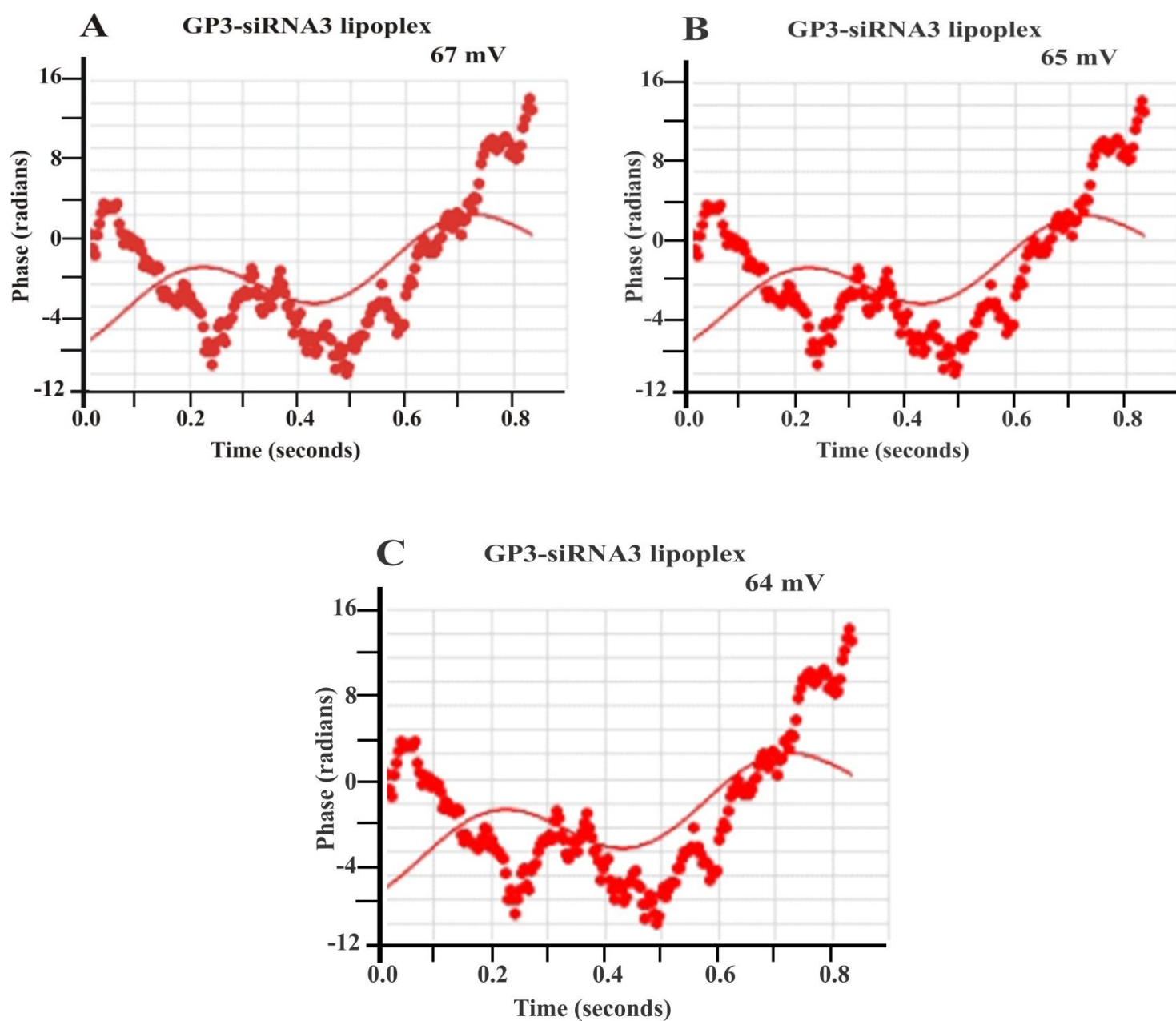


Figure 7.2.3. Particle sizing of PG adjuvant-GP3 siRNA3 lipoplexes

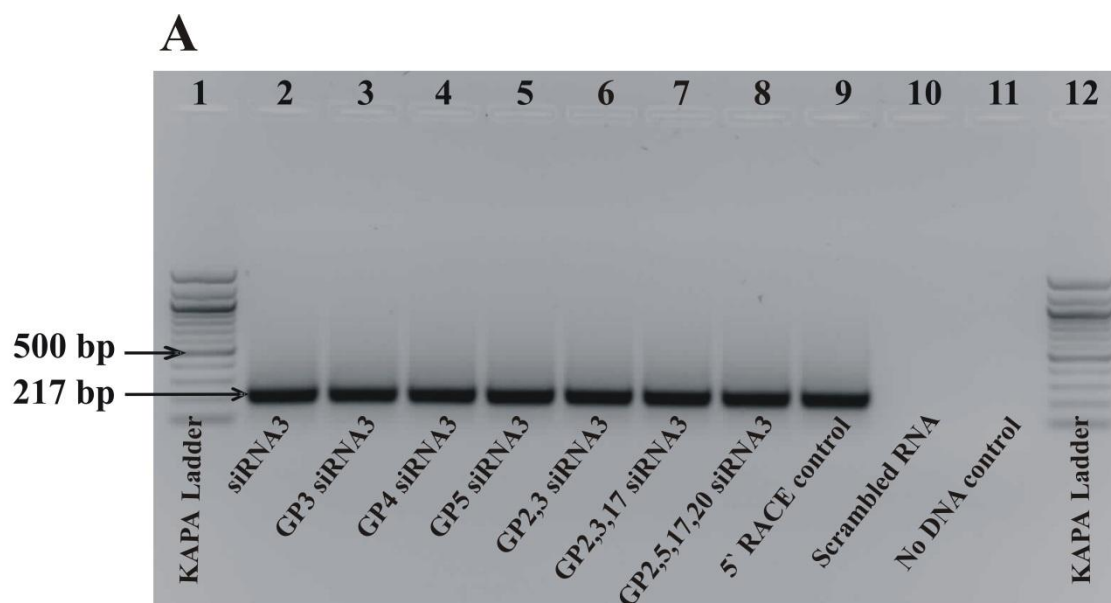
The negatively charged GP3 siRNAs were complexed to positively charged PG adjuvant liposomes to form GP3 siRNA3 lipoplexes and analysed by DLS. Particle size of GP3 siRNA3 lipoplexes ranged between 50-200 nm in diameter with a polydispersity index of 0.488-0.981.

7.2.4. Zeta potential of GP3 siRNA3-lipoplexes:**Figure 7.2.4. Zeta potential of PG adjuvant-GP3 siRNA lipoplexes**

The negatively charged GP3 siRNA3 molecules were complexed to cationic PG adjuvant liposomes to form GP3 siRNA3 lipoplexes. The surface charge of modified siRNA3 lipoplexes was determined by Hückel analysis and ranged between +64 to +67 mV.

7.3. Detection of siRNA-mediated mRNA cleavage product in cultured cells by 5' RACE

7.3.1. Detection of cleavage product by 5' RACE-PCR and DNA sequencing:



B

Sequence of GeneRacer™ RNA oligo

1. 5'-...**GACACUGACAUGGACUGAAGGAGUAGAAA**-3'

Target mRNA sequence

2. 5'-CGACCUUGAG**GCAUACUUC**A-3'

Positive 5' RACE PCR product

3. 5'-...**GCACTGACATGGACTGAAGGAGTAGAAA****GCACTACTTCAA**-3'

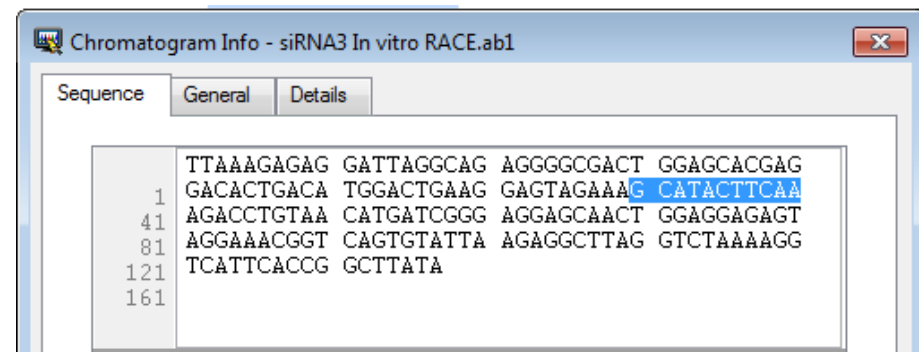
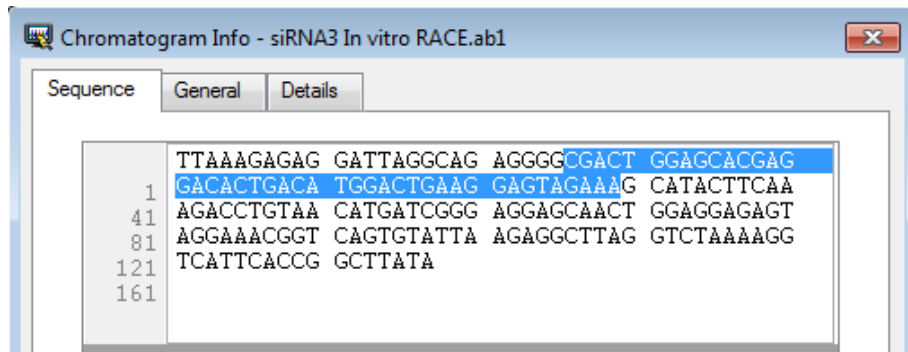
Figure 7.3.1. Detection of siRNA-mediated mRNA cleavage product *in vitro*

Agarose gel electrophoresis of amplified PCR products after reverse transcription of mRNA comprising the GeneRacer™ RNA oligo ligated to the 5' end of the target RNA (A). Sequences of the ligated GeneRacer™ RNA oligo (in red), mRNA cleavage product (in blue) and a positive 5' RACE product composed of sequences derived from the RNA oligo and mRNA cleavage product (B).

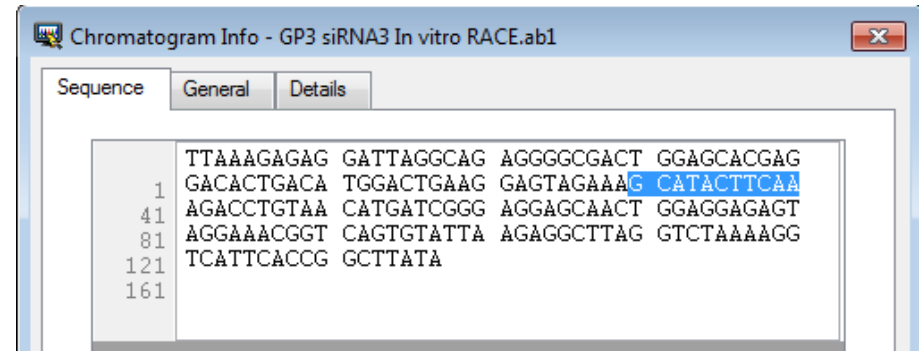
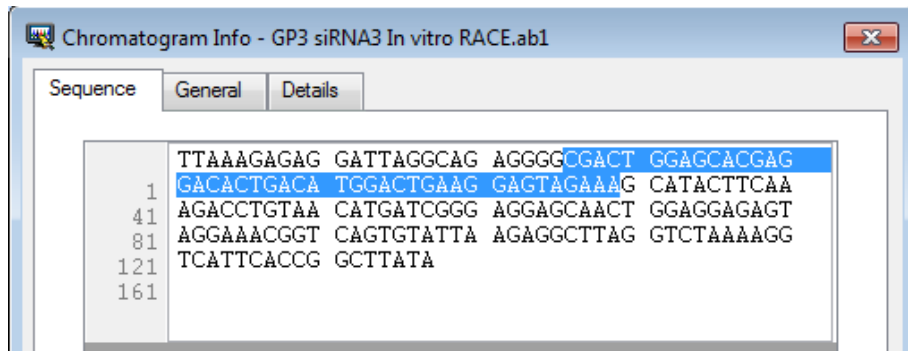
7.3.2. Representative sequencing data of siRNA samples used for the 5' RACE experiment *in vitro*:

Sequences of ligated RNA oligo (left panel) and amplified cleavage product *in vitro* (right panel):

siRNA3



GP3 siRNA3



GP4 siRNA3

Chromatogram Info - GP4 siRNA3 In vitro RACE.ab1

Sequence General Details

1	TTAAAGAGAG	GATTAGGCAG	AGGGGCGACT	GGAGCACGAG
41	GACACTGACA	TGGACTGAAG	GAGTAGAAA	G CATACTTCAA
81	AGACCTGTAA	CATGATCGGG	AGGAGCAACT	GGAGGAGAGT
121	AGGAAAACGGT	CAGTGTATTA	AGAGGCTTAG	GTCTAAAAGG
161	TCATTCACCG	GCTTATA		

Chromatogram Info - GP4 siRNA3 In vitro RACE.ab1

Sequence General Details

1	TTAAAGAGAG	GATTAGGCAG	AGGGGCGACT	GGAGCACGAG
41	GACACTGACA	TGGACTGAAG	GAGTAGAAA	G CATACTTCAA
81	AGACCTGTAA	CATGATCGGG	AGGAGCAACT	GGAGGAGAGT
121	AGGAAAACGGT	CAGTGTATTA	AGAGGCTTAG	GTCTAAAAGG
161	TCATTCACCG	GCTTATA		

GP5 siRNA3

Chromatogram Info - GP5 siRNA3 In vitro RACE.ab1

Sequence General Details

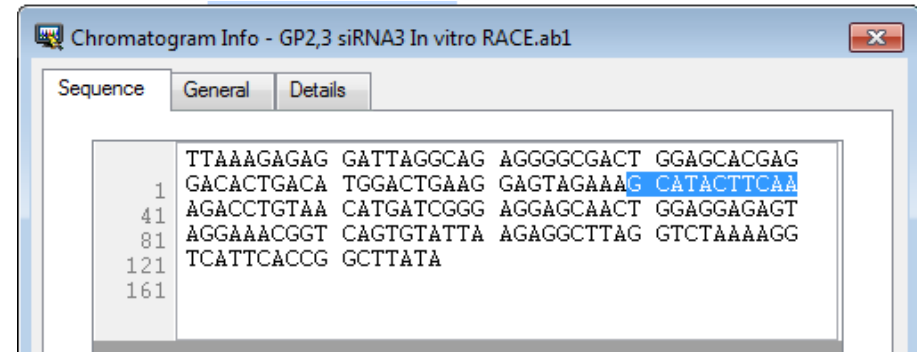
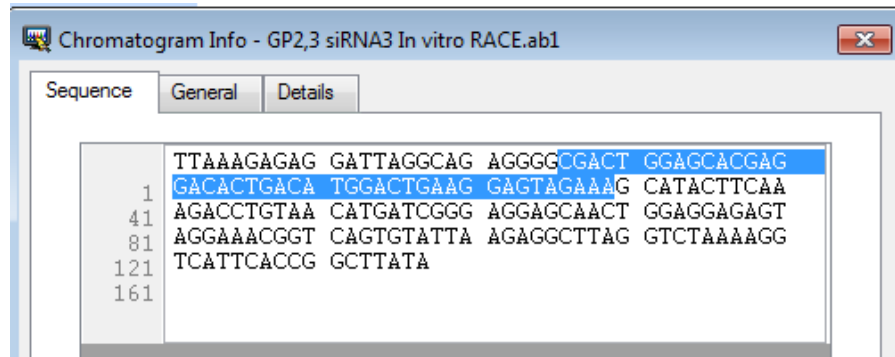
1	TTAAAGAGAG	GATTAGGCAG	AGGGGCGACT	GGAGCACGAG
41	GACACTGACA	TGGACTGAAG	GAGTAGAAA	G CATACTTCAA
81	AGACCTGTAA	CATGATCGGG	AGGAGCAACT	GGAGGAGAGT
121	AGGAAAACGGT	CAGTGTATTA	AGAGGCTTAG	GTCTAAAAGG
161	TCATTCACCG	GCTTATA		

Chromatogram Info - GP5 siRNA3 In vitro RACE.ab1

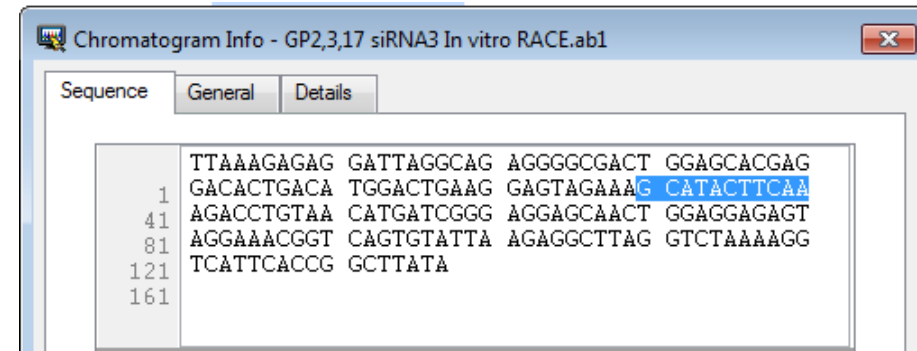
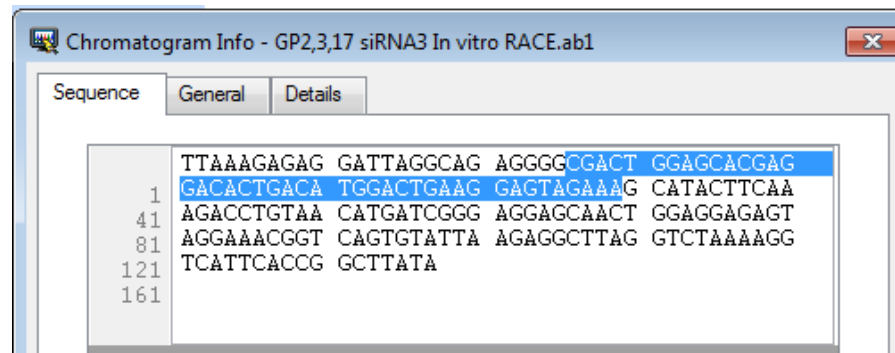
Sequence General Details

1	TTAAAGAGAG	GATTAGGCAG	AGGGGCGACT	GGAGCACGAG
41	GACACTGACA	TGGACTGAAG	GAGTAGAAA	G CATACTTCAA
81	AGACCTGTAA	CATGATCGGG	AGGAGCAACT	GGAGGAGAGT
121	AGGAAAACGGT	CAGTGTATTA	AGAGGCTTAG	GTCTAAAAGG
161	TCATTCACCG	GCTTATA		

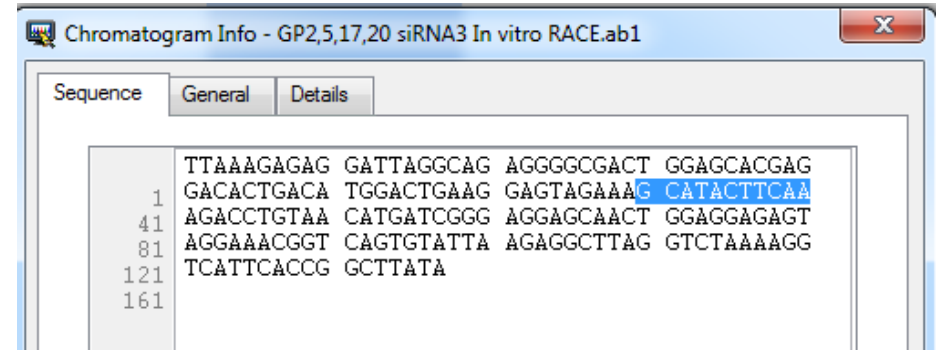
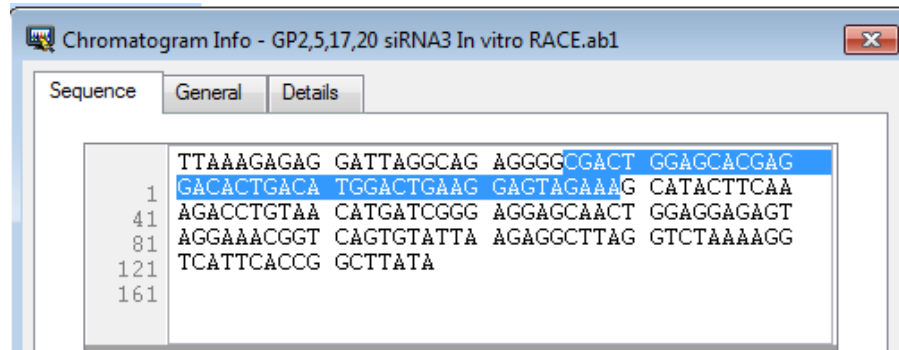
GP2.3 siRNA3



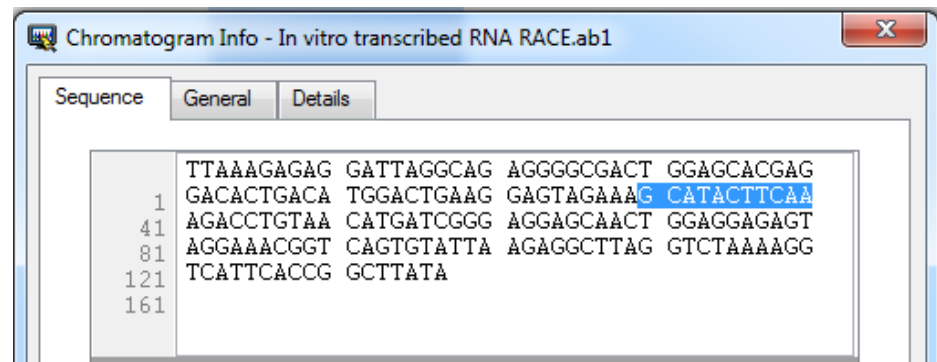
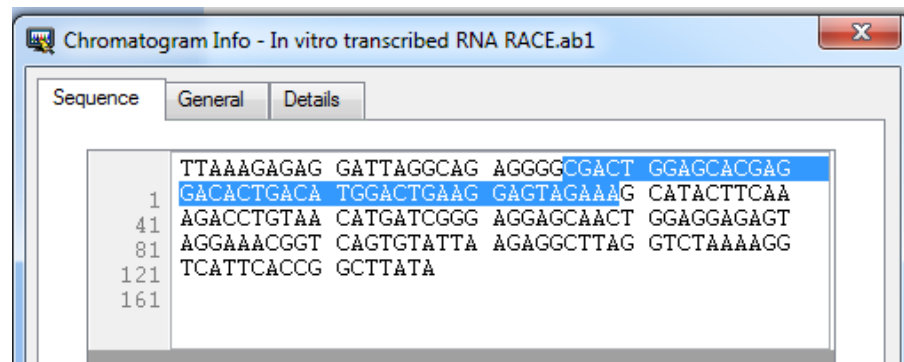
GP2.3.17 siRNA3



GP2.5.17.20

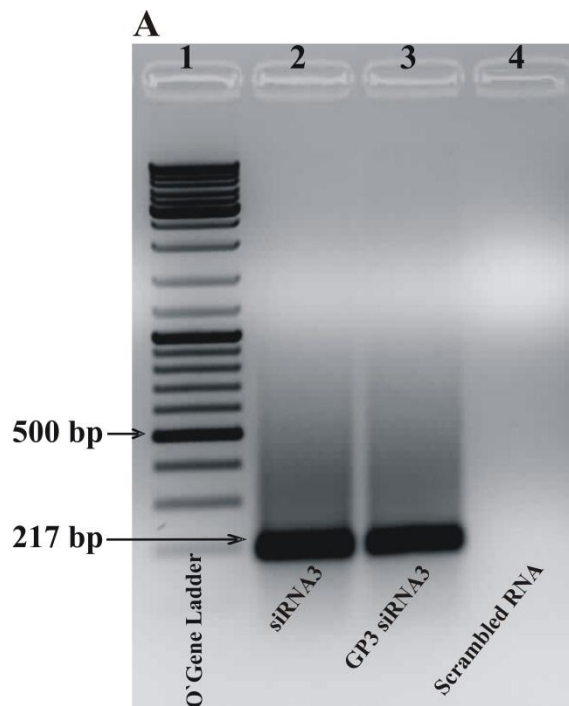


In vitro transcribed RNA (5' RACE positive control)



7.4. Detection of siRNA-mediated mRNA cleavage in mice by 5' RACE

7.4.1. Detection of cleavage product by 5' RACE-PCR and DNA sequencing:



B Sequence of GeneRacer™ RNA oligo

1. 5' -...**GACACUGACAUGGACUGAAGGAGUAGAAA**-3'

Target mRNA sequence

2. 5' -CGACCUUGAGG**CAUACUCAA**-3'

Positive 5' RACE PCR product

3. 5' -...**GACACTGACATGGACTGAAGGAGTAGAAA****CATACTTCAA**-3'

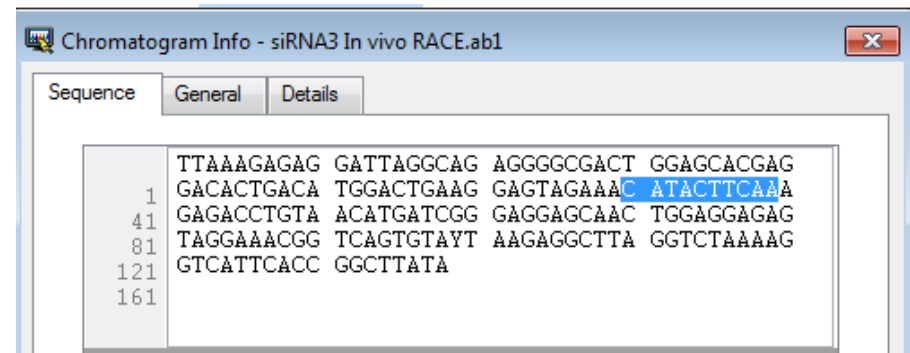
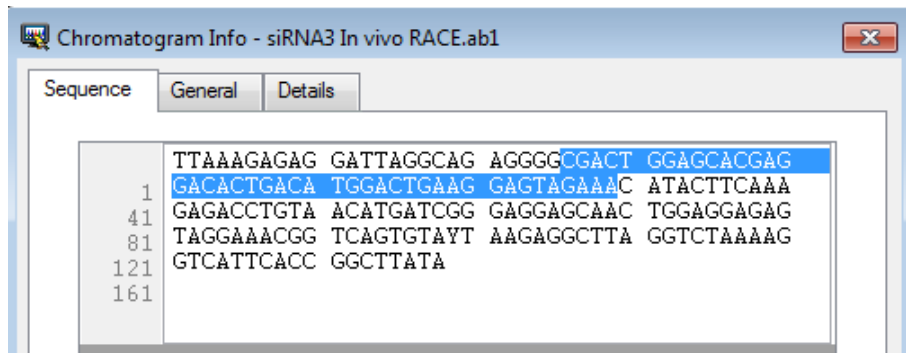
Figure 7.4.1. Detection of siRNA-mediated mRNA cleavage product *in vivo*

Agarose gel electrophoresis of amplified PCR products after reverse transcription of mRNA comprising the GeneRacer™ RNA oligo ligated to the 5' end of the target RNA (A). Sequences of the ligated GeneRacer™ RNA oligo (in red), mRNA cleavage product (in blue) and a positive 5' RACE product comprised of sequences derived from the RNA oligo and mRNA cleavage product (B).

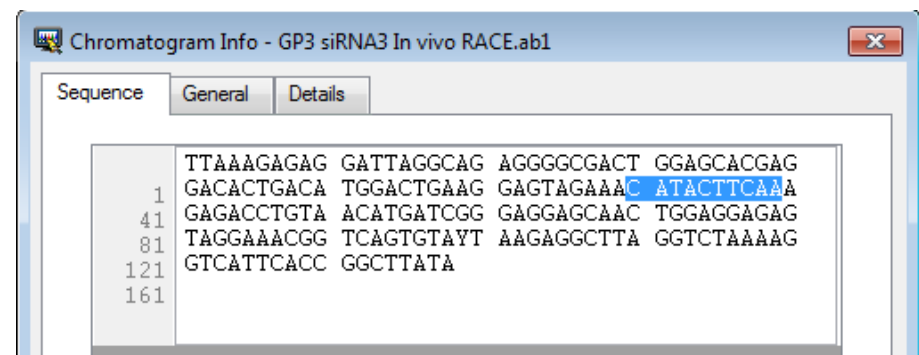
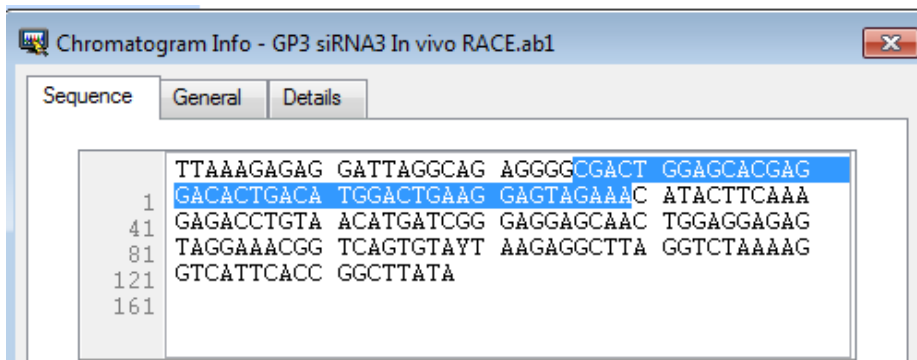
7.4.2. Representative sequencing data of siRNA samples used for 5' RACE experiment *in vivo*:

Sequences of ligated RNA oligo (left panel) and amplified cleavage product *in vivo* (right panel):

siRNA3



GP3 siRNA3



7.5. List of publications:

The following are additional published journal articles emanating from work presented in this thesis.



Synthesis of 2'-O-guanidinopropyl-modified nucleoside phosphoramidites and their incorporation into siRNAs targeting hepatitis B virus

Jolanta Brzezinska^a, Jennifer D'Onofrio^a, Maximilian C.R. Buff^a, Justin Hean^b, Abdullah Ely^b, Musa Marimani^b, Patrick Arbutnot^b, Joachim W. Engels^{a,*}

^aGoethe-University, Institute of Organic Chemistry & Chemical Biology, Max-von-Laue-Str. 7, 60438 Frankfurt am Main, Germany

^bAntiviral Gene Therapy Research Unit, School of Pathology, Health Sciences Faculty, University of the Witwatersrand, Private Bag 3, Wits 2050, Johannesburg, South Africa

ARTICLE INFO

Article history:

Received 1 November 2011

Revised 12 December 2011

Accepted 13 December 2011

Available online 21 December 2011

Keywords:

siRNA

RNA synthesis

2'-Modification

HBV

Guanidinopropyl

ABSTRACT

Synthetic RNAi activators have shown considerable potential for therapeutic application to silencing of pathology-causing genes. Typically these exogenous RNAi activators comprise duplex RNA of approximately 21 bp with 2 nt overhangs at the 3' ends. To improve efficacy of siRNAs, chemical modification at the 2'-OH group of ribose has been employed. Enhanced stability, gene silencing and attenuated immunostimulation have been demonstrated using this approach. Although promising, efficient and controlled delivery of highly negatively charged nucleic acid gene silencers remains problematic. To assess the potential utility of introducing positively charged groups at the 2' position, our investigations aimed at assessing efficacy of novel siRNAs containing 2'-O-guanidinopropyl (GP) moieties. We describe the formation of all four GP-modified nucleosides using the synthesis sequence of Michael addition with acrylonitrile followed by Raney-Ni reduction and guanidinylation. These precursors were used successfully to generate antihepatitis B virus (HBV) siRNAs. Testing in a cell culture model of viral replication demonstrated that the GP modifications improved silencing. Moreover, thermodynamic stability was not affected by the GP moieties and their introduction into each position of the seed region of the siRNA guide strand did not alter the silencing efficacy of the intended HBV target. These results demonstrate that modification of siRNAs with GP groups confers properties that may be useful for advancing therapeutic application of synthetic RNAi activators.

© 2011 Elsevier Ltd. All rights reserved.

1. Introduction

Use of synthetic small interfering RNAs (siRNAs) to trigger RNA interference- (RNAi-) mediated gene silencing has shown considerable potential for therapeutic application.^{1–3} Typically, siRNAs are synthetic mimics of natural Dicer products and comprise 21–25 nt duplexes with 2 nt 3' overhangs. Progress with use of synthetic siRNAs has profited from vast experience gained from developing antisense RNA molecules. Consequently advances have been rapid and improving siRNA efficacy has benefited from valuable biological and synthetic chemistry insights. Advantages of synthetic siRNAs over expressed RNAi activators are that they are amenable to chemical modification to improve stability, safety and specificity.^{4,5} Also, controlled large scale preparation necessary for clinical use is feasible with chemical synthetic procedures. Nevertheless, despite significant advances, the delivery of these polyanionic nucleic acids across lipid-rich cell membranes remains problematic. Vectors used to transport synthetic RNAi activators to target cells have included cationic lipid-containing lipoplexes,⁶ conjugations to peptides⁷ or

oligocationic compounds such as spermidine.⁸ However, success using these methods has been variable. To overcome difficulties of the excessive negative charge of nucleic acids, while at the same time improving thermal and serum stability, we previously investigated an approach that entailed 2'-modification of ribose with cationic groups.^{9,10} Initially we generated always 2'-O-aminoethyl-adenosine and 2'-O-aminoethyl uridine. Synthesis entailed initial alkylation by methyl bromoacetate, which was followed by a series of transformation reactions. Using a luciferase reporter assay to measure knockdown, it was demonstrated that the 2'-O-aminoethyl modifications were at least as efficient as 2'-OME siRNA modifications. An important property of the 2'-O-aminoethyl derivatives was their ability to rescue less active siRNAs when the chemical modifications were placed at the 3' end of the siRNA passenger strand.¹¹ Subsequently this approach was advanced by developing methods that enabled successful alkylation of all four ribonucleosides.¹² This was achieved using phalimidoethyltriflate as an alkylating agent and with this methodology all four phosphoramidites bearing 2'-O-aminoethyl side chains were formed. Although encouraging, a problem of using these siRNA reagents is that the yields of the multistep chemical synthesis are typically low. Moreover scaling up the synthesis reaction is difficult. To address these

* Corresponding author. Tel.: +49 69 798 29150; fax: +49 69 798 29148.

E-mail address: Joachim.Engels@chemie.uni-frankfurt.de (J.W. Engels).

concerns, we have investigated utility of an alternative 2'-*O*-guanidinopropyl (GP) nucleoside modification method. Using the novel approach reported here, we describe the formation of all four GP-modified nucleosides using the synthesis sequence of Michael addition with acrylonitrile^{13–15} followed by Raney-Ni reduction¹⁶ and guanidinylation. Efficiency of the GP siRNAs was assessed in a cell culture model of hepatitis B virus (HBV) replication using target sequences that have previously been shown to be suitable for RNAi-based inhibition of viral replication.^{17–20} Results demonstrate more effective silencing of markers of viral replication than unmodified counterparts. Moreover, the GP-modified siRNAs were more stable to serum conditions than the unmodified controls.

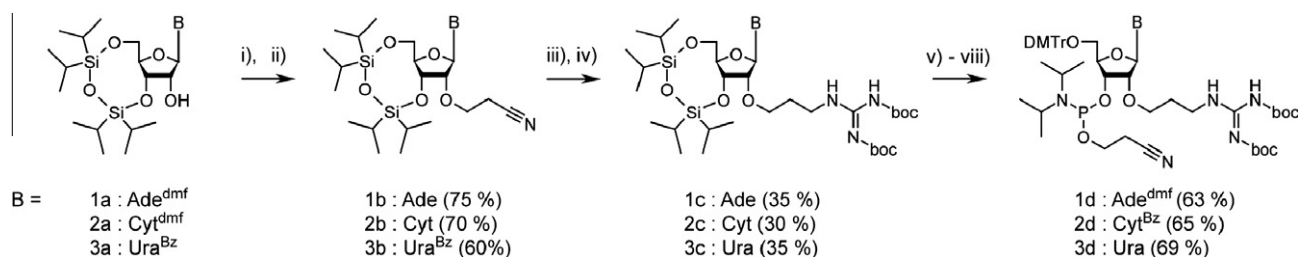
2. Results

2.1. Synthesis of the four 2'-*O*-guanidinopropyl-nucleoside-phosphoramidites

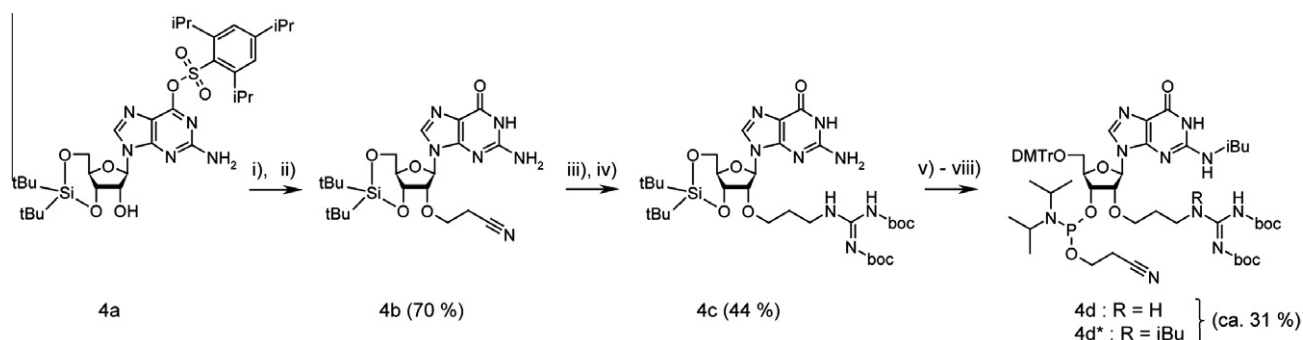
Each of the four 2'-*O*-guanidinopropyl-nucleoside phosphoramidites was synthesised using essentially analogous methodology. The synthesis of the adenosine (A), cytidine (C) and uridine (U) derivatives is depicted in Scheme 1. Since a different protecting group strategy was employed to synthesise the guanosine (G) derivative, it is shown in a separate scheme (Scheme 2). Each synthesis was initiated by simultaneous protection of 5'- and the 3'-OH-groups with 1,1,3,3-tetraisopropylidisiloxane-1,3-diyl (TIPS) (for A,C and U) or di-*tert*-butylsilylaniyadiyl (DTBS) for guanosine. DTBS was selected for protection of G as this group has been reported to improve selectivity for the subsequent 2,4,6-trisopropylbenzenesulfonyl (TPS) protection of *O*⁶-position of guanosine.²¹ The exocyclic amino functions of A and C were protected

with dimethylaminomethylene groups employing standard conditions and a benzoyl group was attached to *N*³-position of U using the two phase system reported by Sekine.²² The resulting nucleotide precursors (**1a–4a**) were then subjected to the first crucial step of the 2'-*O*-guanidinopropyl derivatisation. Employing the procedure reported by Sekine et al.,²³ a Michael addition under mild conditions (Cs₂CO₃, *tert*-butanol, room temperature) was performed using acrylonitrile to obtain the 2'-*O*-cyanoethyl derivatives. In a subsequent step the dimethylaminomethylene group of the A and C derivatives was removed with hydrazine to form the 2'-*O*-cyanoethyl derivatives **1b** and **2b**. This additional deprotection step was necessary to avoid formation of a mixture of dimethylaminomethylene protected and unprotected derivatives that result from proceeding directly to the next reduction step. For the uridine derivative **3b** no intermediate deprotection of the *N*³-benzoyl group was necessary. This is because the benzoyl group was completely removed under the ammonia conditions of the following step. The *O*⁶-TPS group of the guanosine derivative was removed without further purification of the Michael reaction product. This was achieved after filtration and evaporation of solvents using formic acid in a mixture of dioxane and water to yield the 2'-*O*-cyanoethyl-guanosine derivative **4b**.

In the next step, the 2'-*O*-cyanoethyl group was transformed into a 2'-*O*-aminopropyl group. Reduction with hydrogen (30 bar) with Raney-nickel as catalyst in ammonia and methanol was used to achieve this according to a procedure we previously described.²⁴ The hydrogenation step was sensitive to reaction conditions such as the ratio of amount of starting material to catalyst, the size of the autoclave employed and reaction time. Under optimised conditions, yields from reduction of each nucleotide derivative were moderate (about 50%). A loss of the desired product was also



Scheme 1. Synthesis of the 2'-*O*-guanidinopropyl adenosine-, cytidine- and uridine- phosphoramidites for oligoribonucleotide synthesis. (i) acrylonitrile, Cs₂CO₃, *tert*-butyl alcohol, rt; (ii) H₂N-NH₂·H₂O, methanol, rt (adenosine and cytidine derivative); no deprotection of the uridine derivative; (iii) H₂ (30 bar), NH₃, methanol, 30–60 min, rt; (iv) *N,N*-di-Boc-*N'*-triflylguanidine, Et₃N, CH₂Cl₂, 0 °C (30 min) to rt (30 min); (v) DMF-dimethyl diacetale, methanol, rt (adenosine derivative); benzoyl chloride, pyridine, 0 °C (30 min) to rt (30 min) (cytidine derivative); no protection group was applied to the uridine derivative; (vi) Et₃N·3HF, THF, rt; (vii) 4,4'-dimethoxytrityl chloride, pyridine, rt; (viii) 2-cyanoethyl *N,N,N,N*-tetraisopropyl phosphane, 4,5-dicyanoimidazole, CH₂Cl₂, rt.



Scheme 2. Synthesis of the 2'-*O*-guanidinopropyl guanosine phosphoramidite for oligoribonucleotide synthesis. (i) Acrylonitrile, Cs₂CO₃, *tert*-butyl alcohol, rt; (ii) formic acid (70%), dioxane/water; (iii) H₂ (30 bar), NH₃, methanol, 30–60 min, rt; (iv) *N,N*-di-Boc-*N'*-triflylguanidine, Et₃N, CH₂Cl₂, 0 °C (30 min) to rt (30 min); (v) isobutyryl chloride, pyridine, 0 °C (1 h) to rt (1 h); (vi) Et₃N·3HF, THF, rt; (vii) 4,4'-dimethoxytrityl chloride, pyridine, rt; (viii) 2-cyanoethyl *N,N,N,N*-tetraisopropyl phosphane, 4,5-dicyanoimidazole, CH₂Cl₂, rt.

Table 1
Synthesised GP modified oligonucleotides

Name	Sequence
GP2 siRNA3	5-UU _{GP} G AAG UAU GCC UCA AGG UCG-3'
GP3 siRNA3	5-UUG _{GP} AAG UAU GCC UCA AGG UCG-3'
GP4 siRNA3	5-UUG A _{GP} AG UAU GCC UCA AGG UCG-3'
GP5 siRNA3	5-UUG AA _{GP} G UAU GCC UCA AGG UCG-3'
GP6 siRNA3	5-UUG AAG _{GP} UAU GCC UCA AGG UCG-3'
GP7 siRNA3	5-UUG AAG U _{GP} AU GCC UCA AGG UCG-3'
GP8 siRNA3	5-UUG AAG UA _{GP} U GCC UCA AGG UCG-3'
GP13 siRNA3	5-UUG AAG UAU GCC U _{GP} CA AGG UCG-3'

Table 2
Effect of GP modification on duplex stability with complementary RNA (5'-GGCAU-ACUCAA-3')

Oligo	Sequence	T _m [°C]	ΔT _m [°C]
ON 1	5'-UUG AAG UAU GCC-3'	54.9	–
ON 2	5'-UUG _{GP} AAG UAU GCC-3'	54.5	–0.4
ON 3	5'-UUG AAG _{GP} UAU GCC-3'	52.5	–2.4
ON 4	5'-UUG AAG UAU _{GP} GCC-3'	54.4	–0.5
ON 5	5'-UUG _{GP} AAG _{GP} UAU GCC-3'	54.6	–0.3
ON 6	5'-UUG _{GP} AAG _{GP} UAU _{GP} GCC-3'	54.4	–0.5

confirmed by the observation that part of the amino compound was not released from the catalyst during filtration, despite being subjected to several washes with methanol. To minimise losses the crude unpurified 2'-O-aminopropyl compounds were used to introduce the guanidino groups. *N,N'*-di-Boc-*N''*-triflylguanidine was employed as guanidinylation agent. The procedure we employed was initially reported by Goodman et al. in 1998 and the reagent is now commercially available.²⁵ Our previous studies showed that the boc groups are cleaved under the repetitive deprotection conditions during oligonucleotide synthesis when employing the TBDMS-phosphoramidite method. Also, the guanidino group undergoes no side reaction during the solid phase synthesis.²⁶ The guanidinylation took place with good yields (70% for **1c** (A), 60% for **2c** (C), around 60% for **3c** (U) and approximately 90% for **4c** (G)).

After successful guanidinylation, established reaction conditions were applied to synthesize the desired phosphoramidites (**1d**–**4d**). This entailed use of protection groups that were suitable for the TBDMS method of oligoribonucleotide synthesis. The A derivative was protected with dimethylaminomethylene at the *N*⁶-position, and the exocyclic amino function of the C derivative was protected with a benzoyl group. The *N*²-position of the G derivative was protected with an isobutyryl group. However, under the reaction conditions we employed, a mixture of the desired G derivative product, as well as a compound with an additional isobutyryl group on the non-boc-protected nitrogen of the guanidino group, were obtained. It was very difficult to separate this double isobutyryl modified compound using chromatography. However, since it would be cleaved during the ammonia deprotection step at the completion of oligonucleotide synthesis, we utilised this mixture of **4d** and **4d*** for solid phase oligonucleotide synthesis. To synthesise U derivatives, no further protection was necessary. For synthesis of all of the 2'-O-guanidinopropyl phosphoramidites, removal of silyl protecting groups was achieved with Et₃N-3HF. The 5'-OH-group was protected with a 4,4'-dimethoxytrityl group and in a last step the 3'-OH group was converted to a phosphoramidite using 2-cyanoethyl *N,N,N,N'*-tetraisopropylamino phosphane and 4,5-dicyanoimidazole as activator. Starting with the adenosine, cytidine and guanosine nucleosides, synthesis of the 2'-O-guanidinopropyl phosphoramidites took place in 10 steps and provided overall yields of 15.4% (**1d**), 6.3% (**2d**) and 7.5% (**4d**). Synthesis of

the 2'-O-guanidinopropyl uridine phosphoramidite was performed in eight steps with an overall yield of 11.8% (**3d**).

The obtained phosphoramidites were used for synthesis of the GP-modified siRNA antisense strands depicted in Table 1 and the GP-modified oligonucleotides for melting point studies depicted in Table 2. For the modified phosphoramidites a prolonged coupling step of 25 min was used. To ensure complete cleavage of the boc groups, an additional deprotection step of 30 min with 3% trichloroacetic acid in dichloromethane was applied after completion of oligonucleotide synthesis. The boc group was chosen for protection of the guanidine moiety due to its compatibility concerning the protecting group strategy that was used for synthesis of the monomers. Although partial cleavage of the boc groups during RNA-synthesis is expected in consequence of the acidic deprotection step of each cycle, no side reaction of the free guanidino groups was observed. According to the anion-exchange chromatograms of the deprotected RNA (an exemplary chromatogram is shown in the Supplementary data), only one main product has formed. After purification the oligonucleotides were obtained with 10% to 40% yield (1 μmol synthesis scale).

2.2. Hybridization studies

The influence of GP-modified nucleosides on thermal stability of different RNA duplexes was examined. For this purpose, the G_{GP} and U_{GP} modified phosphoramidites were inserted into 12mer RNA (ON2–ON6) and the duplex melting point measured. As shown in Table 2, the presence of GP group in oligoribonucleotides did not significantly affect the stability of duplexes, although slightly destabilized them. Guanidinopropyl modified building blocks give almost the same T_m value for single, double and triple substituted oligonucleotides.

Interestingly, in the case when a GP modification of G was placed in a central position, the T_m decreased more significantly (ΔT_m = –2.4 °C).

The results indicate that the thermodynamic effect of GP group is more or less independent on the placement of the modification and modified nucleoside. While more modifications were incorporated, substitutions were not adjacent, additional destabilizing effect was not observed (ON5 and ON6, Table 2). Moreover, for the modified oligonucleotides bearing more than one GP residue, high binding affinity to the complementary strand was unaffected.

2.3. Inhibition of Firefly luciferase activity in transfected cells

Initially, to measure knockdown efficiency of GP-modified siRNAs in situ, HEK293 cells were co-transfected with RNAi activators together with a reporter gene plasmid (psiCHECK-*HBx*)²⁰ (Fig. 1). The siRNAs targeted a single sequence of the X open reading frame (ORF) of HBV (*HBx*) that has previously been shown to be an effective cognate for RNAi-based silencing.²⁷ Each of the siRNAs differed with respect to location of the GP modification, and these were within the seed region or at nucleotide 13 of the antisense strand of the siRNA duplex. siRNAs have been named according to the positioning of the GP modifications from the 5' end of the intended guide strand. In psiCHECK-*HBx*, the viral target sequence was located in the *Renilla* transcript but downstream of the reporter ORF (Fig. 1A). Expression of Firefly luciferase is constitutively active to enable correction for variations in transfection efficiency. The ratio of *Renilla* to Firefly luciferase activity was used to assess knockdown efficacy. Compared to a scrambled siRNA control, analysis showed that the Firefly luciferase activity was diminished by approximately 70% when co-transfected with the unmodified siRNA (Fig. 1B). There was some variation in the efficacy of the inhibition of reporter gene activity that was dependent on the position of the chemically modified siRNAs. Knockdown efficacy was weakest

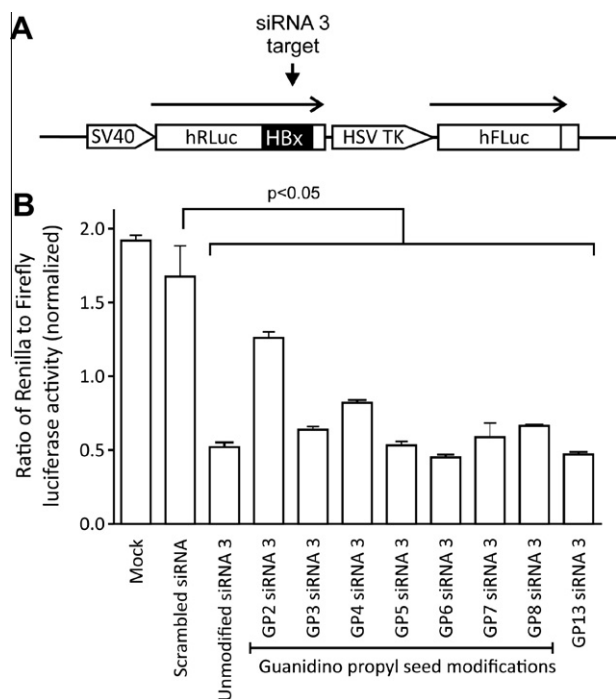


Figure 1. Dual luciferase assay to determine efficacy of GP antiHBV siRNAs. (A) Schematic illustration of dual luciferase reporter plasmid. The HBx target sequence was inserted downstream of the hRLuc ORF. *Renilla* luciferase activity was used as an indicator of target silencing and efficacy was determined relative to activity of constitutively expressed Firefly luciferase. (B) Ratio of *Renilla* to Firefly luciferase activity following cotransfection with indicated siRNAs together with dual luciferase reporter plasmid. Controls included a mock transfection in which inert plasmid DNA was substituted for siRNA as well as a scrambled siRNA that did not have complementary sequences to the HBx target. Data are represented as mean ratios of *Renilla* to Firefly luciferase activity (\pm SEM) and are normalized relative to the mock treated cells. Differences were considered statistically significant when the *p* value, determined according to the Student's 2 tailed paired *t*-test, was less than 0.05.

with GP2 siRNA3, when the GP modification was placed at nucleotide 2 of the siRNA antisense sequence. siRNAs with the modification at positions 5 and 6 (GP5 siRNA3 and GP6 siRNA3) achieved most effective knockdown of reporter gene expression which was similar to that of the unmodified siRNA. A siRNA with the GP modification placed outside of the seed region at nucleotide 13 also achieved knockdown of 75%. GP modifications in antiHBV siRNA sequences are therefore compatible with effective target silencing, but position within the seed of the antisense guide influences efficacy.

2.4. Inhibition of HBV surface antigen (HBsAg) secretion from transfected cells by GP-modified siRNAs

To assess efficacy against HBV replication *in vitro*, Huh7 liver-derived cells were co-transfected with siRNAs together with the pCH-9/3091 HBV replication competent target plasmid (Fig. 2A).²⁸ Compared to HBsAg concentration in the culture supernatant of cells treated with scrambled siRNA, knockdown of up to 85% of viral antigen secretion was achieved by GP-modified siRNAs (Fig. 2B). The unmodified siRNA was slightly less effective than the siRNAs containing GP moieties. Of the modified siRNAs, positioning of the GP residue at nucleotides 5 or 6 (GP5 siRNA3 and GP6 siRNA3) resulted in the most effective suppression of HBsAg secretion (approximately 90%). These data correlate with observations using the reporter gene knockdown assay. Interestingly, GP2 siRNA3 inhibited HBsAg secretion from transfected cells more effectively than it did *Renilla* luciferase activity. The reason for this difference

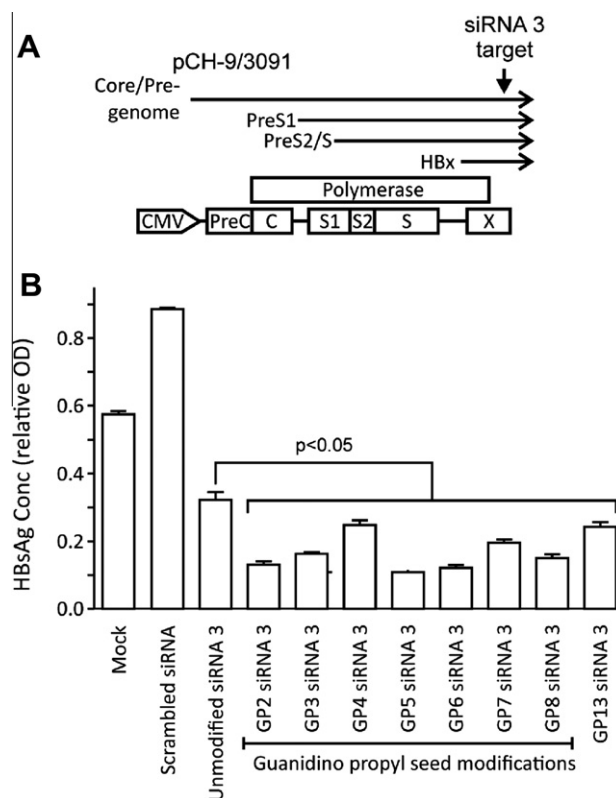


Figure 2. Inhibition of HBV replication by antiHBV siRNAs in cultured cells. A. Illustration of the HBV replication competent plasmid, pCH-9/3091, which was used to transfect liver-derived Huh7 cells in culture. (B) The concentration of HBsAg was measured in cell culture supernatants following co-transfection GP-modified siRNAs. Values are given as relative OD readings from the ELISA assay. Unmodified siRNA did not include GP residues. Controls included a mock transfection in which inert plasmid DNA was substituted for siRNA as well as a scrambled siRNA that did not have complementary sequences to the HBx target. Data are represented as mean ratios of *Renilla* to Firefly luciferase activity (\pm SEM) and are normalized relative to the mock treated cells. Differences were considered statistically significant when the *p* value, determined according to the Student's 2 tailed paired *t*-test, was less than 0.05.

is unclear but may result from better GP2 siRNA3 target accessibility in the context of the natural HBV transcripts. Overall, these data support the notion that seed region GP modifications are compatible with target silencing that is similar or more effective than unmodified siRNAs.

2.5. Stability of GP-modified siRNAs in 80% FCS

siRNAs containing GP modifications were incubated in the presence or absence of 80% foetal calf serum (FCS) for time intervals of 0–24 h to assess their stability (Fig. 3). siRNAs were detected using polyacrylamide gel electrophoresis and staining with ethidium bromide. Bands corresponding to siRNAs were quantified to determine stability and FCS resistance. Analysis revealed that unmodified siRNA3 was stable for 24 h when maintained in DMEM tissue culture medium that did not include FCS. However, rapid degradation of siRNA occurred in the presence of FCS, and approximately 10% of the input siRNA remained at 5 h. Analysis of stability of GP2 siRNA3, GP3 siRNA3, GP4 siRNA3, GP5 siRNA3 and GP6 siRNA3 showed a similar rapid degradation. When the GP modifications were placed further from the 5' end of the antisense strand of the siRNA (GP7 siRNA3, GP8 siRNA3 and GP13 siRNA3) slower degradation of the siRNAs was observed. With these siRNAs, at the time point of 5 h approximately 40% of the input siRNA remained intact. Stability is therefore improved by including GP

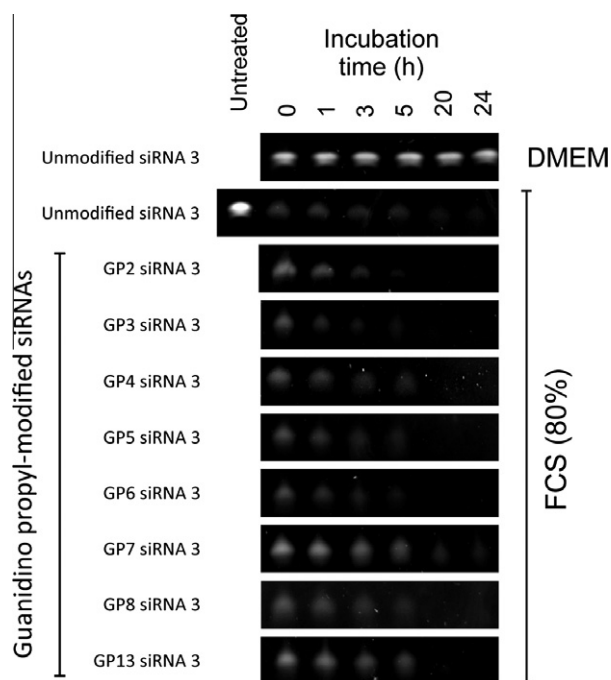


Figure 3. Assessment of stability of GP-modified siRNAs. The panel of GP-modified siRNAs was incubated with DMEM alone, or DMEM with 80% foetal calf serum, for times ranging from 0 to 24 h. Thereafter degradation of siRNAs was assessed using polyacrylamide gel electrophoresis with ethidium bromide staining.

modifications, but location of these moieties to central regions of the siRNAs is important to confer this property.

3. Discussion

Successful preparation of GP phosphoramidite nucleosides for incorporation into siRNAs presents a novel approach to utilising chemical modification for enhancement of efficacy of synthetic siRNAs. Ideally, for gene silencing sequences to be therapeutically applicable they should be stable, amenable to efficient delivery to target tissues, effective and specific to their targets. Alterations to siRNAs have typically involved 2'-OH modification of the ribose groups¹¹ and reviewed in Refs. 4,5). Changes at this site are useful for improving overall siRNA efficacy for several reasons. The 2'-OH may cause nucleophilic attack and removal of the hydroxyl group limits susceptibility of siRNAs to degradation. Alterations at the 2'-OH of ribose may also attenuate toxic innate immune responses of duplex RNA by preventing interaction with intracellular Toll Like Receptors (TLRs). Furthermore, 2'-OH modification may influence nucleotide stacking to enhance interaction of the siRNA guide with its target. Alterations to the 2'-OH that have been reported to date have included 2'-F, 2'-methoxy ribosyl (2'-OMe) and locked nucleic acid modifications.^{5,11} Recently a 2'-azido modification was reported, that not only replaces the 2'-OH group but can also be used for postsynthetic labelling of RNA.²⁹ Although improvements in siRNA stability, efficacy and immunostimulatory effects have been reported, difficulties with efficient regulation of nucleic acid delivery remain. The GP modification reported here presents a novel approach that has distinct properties that potentially have advantages over previously described 2'-OH modifications. The three amino groups of the GP moiety together with the three carbon atom propyl linker provide a flexible charge-neutralising group.

Chemical synthesis of GP-modified nucleosides is straightforward and comprises the following crucial steps. Cyanoethylation

based on Michael addition of suitably protected nucleosides with acrylonitrile. The following Raney-Ni reduction results in the propylamino derivatives that are finally guanidylated by triflylguanidine. Different chemical structures of each of the bases require that the protecting group strategies differ slightly between the four nucleosides. Standard phosphorylation provides the appropriate phosphoramidites **1d–4d**, which are ready for solid phase oligonucleotide synthesis (see Tables 1 and 2). Using this reaction sequence, this is the first time that a full set of phosphoramidites modified with guanidino groups at the 2' position is provided for incorporation in synthetic oligonucleotides. Synthesis of modified oligonucleotides was carried out under standard conditions of phosphoramidite chemistry. Moreover coupling efficiency of the GP-modified phosphoramidites was as good as for the unmodified phosphoramidites.

An additional advantage of the synthetic procedures described here is that it is possible to introduce diversification at the 2'-O-aminopropyl site of our compounds. With common peptide-coupling reagents, such as carbodiimides and 1-hydroxybenzotriazoles, the 2'-O-aminopropyl group can readily be modified with carboxylic acid derivatives. These include amino acids, fatty acids or carboxy-modified spermine to obtain more cationic or more lipophilic oligonucleotides.²⁴ Also, protection of the amino group with a trifluoroacetyl group during oligonucleotide solid phase synthesis would enable postsynthetic labelling with amino-reactive fluorophore derivatives (e.g., NHS-esters or isothiocyanates) or reaction with cross linkers to connect nucleic acids to carrier molecules, for example, cell penetrating peptides.

The melting behaviour of the duplex oligonucleotides showed that the melting temperature was independent of the placement and number of GP modifications (Table 2). For this analysis, we chose a 12-mer with a sequence that was identical to the seed sequence of our siRNA. This shorter sequence, with a T_m of approximately 55 °C, was better for demonstrating smaller changes in melting properties. The results concur with hybridization analysis of oligonucleotides containing 2'-O-aminopropyl (AP) groups.³⁰ Incorporation of one AP unit at the 3'-end or in the middle of an oligomer reduces the T_m of a RNA duplex. Duplex stabilization was observed in RNA containing AP groups at adjacent sites or within an entire strand. Molecular dynamic and NMR data indicate that no strong electrostatic interaction or hydrogen bonding is formed as a result of flexibility of aminoalkyl chains.³⁰ Another possibility that has been proposed is that some stabilizing effect might be conferred by hydration of the AP.^{31,32} For the guanidino group reported here, there are three nitrogen atoms in a plane which are protonated over a wide pH range. The individual contributions of GP-RNA to thermodynamic stability are not clear yet but nanosecond molecular modelling points to high flexibility in water. (Villa and Stock, unpublished)

When investigating the potential therapeutic utility of a new chemical modification to siRNAs, it is desirable to verify that silencing is maintained in a clinically relevant model. In this study, we assessed the efficacy in a model of HBV infection. Persistence of HBV is an important global cause of public health problems (reviewed in Ref. 33). Cirrhosis and liver cancer, which are potentially fatal complications of HBV persistence, occur frequently. There is a need to develop more effective antiHBV treatments to eliminate these problems and harnessing the RNAi pathway to counter the infection has shown promise.³⁴ To assess silencing by GP-modified siRNAs, a panel of silencing sequences was tested against a previously described susceptible HBV target.²⁷ Evidence from this study shows that incorporation of GP groups at the 2' ribose position enhances HBV silencing, while also improving stability. Interaction of sequences within the guide seed region and the target are critically important to effect silencing. Chemical modification in the guide seed potentially compromises the interaction of the guide with

its cognate. Our data demonstrate that silencing efficacy of the intended target is retained after incorporating the GP residues into each of the nucleotides comprising the guide strand seed. This observation is in accordance with previous reports showing minimal attenuation of intended target silencing caused by modification in the seed region.^{35,36} Complete base pair matching within the remainder of the siRNA guide and intended target compensates for disruption that may occur in the seed.

The novel 2'-GP modification that is described here potentially has several advantages for therapeutic application. Our data demonstrate that changes in single nucleotides achieve enhanced silencing efficacy and stability of siRNAs. Modification of more than one nucleotide in a siRNA is feasible and multiple PG moieties could further augment the efficacy of therapeutic sequences. Current investigations are addressing this as well as the role of GP modifications on off target seed interaction and improvement in *in vivo* delivery of GP-modified siRNA by non-viral vectors.

4. Experimental

4.1. Material and methods

All reagents were of analytical reagent grade, obtained from commercial resources and used without further purification. For synthesis, solvents with quality *pro analysis* were used. Dry solvents were kept over molecular sieve and for column chromatography technical solvents were distilled before use.

All NMR spectra were measured on Bruker AM250 (¹H: 250 MHz, ¹³C: 63 MHz), AV300 (¹H: 300 MHz, ¹³C: 75 MHz, ³¹P: 121 MHz) and AV400 (¹H: 400 MHz, ¹³C: 101 MHz, ³¹P: 162 MHz) instruments. Chemical shifts (δ) are reported in parts per million (ppm). The following annotations were used with peak multiplicity: s, singlet; d, doublet; t, triplet; q, quartet; m, multiplet; b, broadened. *J* values are given in Hz.

MALDI mass spectra were recorded on a Fisons VG Tofspec spectrometer and ESI mass spectra on a Fisons VG Plattform II spectrometer. High resolution mass spectra were acquired on a Thermo MALDI Orbitrap XL.

UV-melting curves were measured on a JASCO V-650 spectrophotometer. Melting profiles of the RNA duplexes were recorded in a phosphate buffer containing NaCl (100 mM, pH 7) at oligonucleotide concentrations 2 μ M for each strand at wavelength 260 nm. Each melting curve was determined triply. The temperature range was 5–95 °C with a heating rate 0.5 °C. The thermodynamic data were extracted from the melting curves by means of a two state model for the transition from duplex to single strands.

Statistical analysis: Data have been expressed as the mean \pm standard error of the mean. Statistical difference was considered significant when *P* < 0.05 and was determined according to the student's *t*-test and calculated with the GraphPad Prism software package (GraphPad Software Inc., CA, USA).

4.2. Chemistry

4.2.1. Synthesis of the 2'-O-guanidinopropyl adenosine phosphoramidite

3',5'-O-(Tetraisopropylidisiloxane-1,3-diyl)-N⁶-dimethylaminomethylene adenosine (**1a**) was synthesised as previously described.¹⁶

4.2.1.1. N⁶-Dimethylaminomethylene-2'-O-cyanoethyl-3',5'-O-(tetraisopropylidisiloxane-1,3-diyl)-adenosine (**1e**).

To a solution of compound **1a** (3.0 g, 5.31 mmol) in *tert*-butanol (25 mL), freshly distilled acrylonitrile (6.7 mL, 102 mmol) and cesium carbonate (1.6 g, 4.9 mmol) were added. The mixture was

stirred vigorously at room temperature for 3 h. The reaction mixture was filtered and the residue was washed with dichloromethane. The filtrate was evaporated and the residue was purified using column chromatography with ethyl acetate/methanol (99:1–95:5, v/v) to give 3.28 g (87%) of the product. ¹H NMR (400 MHz, DMSO-*d*₆) δ [ppm] 8.90 (s, 1H, admidine-H), 8.34 (s, 1H, H₂ or H₈), 8.32 (s, 1H, H₂ or H₈), 6.02–6.01 (m, 1H, H_{1'}), 5.05–5.01 (m, 1H, H_{3'}), 4.64–4.62 (m, 1H, H_{2'}), 4.08–3.84 (m, 5H, H_{4'}, 2 \times H_{5'}, O-CH₂-CH₂-CN), 3.20 (s, 3H, N-CH₃), 3.13 (s, 3H, N-CH₃), 2.83–2.80 (m, 2H, O-CH₂-CH₂-CN), 1.10–1.00 (m, 28H, tetraisopropyl-CH and -CH₃); MS (ESI) was calculated to be 618.3 for C₂₈H₄₈N₇O₅Si₂ (M+H⁺), and found to be 618.8.

4.2.1.2. 2'-O-Cyanoethyl-3',5'-O-(tetraisopropylidisiloxane-1,3-diyl)-adenosine (**1b**).

N⁶-Dimethylaminomethylene-2'-O-cyanoethyl-3',5'-O-(tetraisopropylidisiloxane-1,3-diyl)-adenosine (**1e**) (1.0 g, 1.62 mmol) was dissolved in methanol (20 mL) then hydrazine hydrate (H₂N-NH₂·H₂O; 500 μ L, 10.3 mmol) was added. The reaction solution was stirred at room temperature for 3 h. The solvents were evaporated and the residue was purified using a silica gel column with ethylacetate as eluent to give 773 mg (87%) of **1b**. ¹H NMR (400 MHz, DMSO-*d*₆) δ [ppm] 8.21 (s, 1H, H₂ or H₈), 8.07 (s, 1H, H₂ or H₈), 7.33 (bs, 2H, NH₂), 5.98–5.96 (m, 1H, H_{1'}), 5.03–4.99 (m, 1H, H_{3'}), 4.59–4.57 (m, 1H, H_{2'}), 4.08–3.83 (m, 5H, H_{4'}, 2 \times H_{5'}, O-CH₂-CH₂-CN), 2.84–2.80 (m, 2H, O-CH₂-CH₂-CN), 1.09–0.97 (m, 28H, tetraisopropyl-CH and -CH₃); ¹³C NMR (101 MHz, DMSO-*d*₆) δ [ppm] 156.01, 152.41 (C₂ or C₈), 148.46, 139.26 (C₂ or C₈), 119.20, 118.83, 87.47 (C_{1'}), 81.11 (C_{2'}), 80.45 (C_{4'}), 70.04 (C_{3'}), 65.62 (O-CH₂-CH₂-CN), 60.09 (C_{5'}), 18.38 (O-CH₂-CH₂-CN), {17.20, 17.06, 17.05, 17.01, 16.98, 16.85, 16.81, 16.71} (tetraisopropyl-CH₃), {12.60, 12.28, 12.09, 12.04} (tetraisopropyl-CH); MS (MALDI) was calculated to be 563.8 for C₂₅H₄₃N₆O₅Si₂ (M+H⁺) and found to be 564.0.

4.2.1.3. 2'-O-Aminopropyl-3',5'-O-(tetraisopropylidisiloxane-1,3-diyl)-adenosine (**1f**).

Compound **1b** (1.0 g, 1.78 mmol) was dissolved in 10 mL of methanol in a glass tube suitable for use in an autoclave. Approximately 0.5 mL of the Raney-nickel slurry was rinsed thoroughly with dry methanol and then washed into the glass tube with the solution of **1b**. After addition of 5 mL methanol saturated with ammonia, the mixture was stirred for 1 h at room temperature under a hydrogen atmosphere (30 bar). The reaction mixture was filtered and the catalyst was washed several times with methanol. The filtrate was evaporated and the residue was purified using column chromatography with ethyl acetate/methanol/triethylamine (70:25:5, v/v/v) to yield 503 mg (50%) of the desired compound. When this reaction was repeated, the crude product was used for the next step without further purification. ¹H NMR (400 MHz, DMSO-*d*₆) δ [ppm] 8.20 (s, 1H, H₂ or H₈), 8.07 (s, 1H, H₂ or H₈), 7.32 (bs, 2H, NH₂), 5.95–5.94 (m, 1H, H_{1'}), 4.95–4.90 (m, 1H, H_{3'}), 4.41–4.39 (m, 1H, H_{2'}), 4.08–3.90 (m, 3H, H_{4'}, 2 \times H_{5'}), 3.86–3.70 (m, 2H, O-CH₂-CH₂-CH₂-NH₂), 2.66–2.61 (m, 2H, O-CH₂-CH₂-CH₂-NH₂), 1.65–1.58 (m, 2H, O-CH₂-CH₂-CH₂-NH₂), 1.08–0.96 (m, 28H, tetraisopropyl-CH and -CH₃); MS (MALDI) was calculated to be 567.9 for C₂₅H₄₇N₆O₅Si₂ (M+H⁺), and found to be 567.9.

4.2.1.4. 2'-O-(N,N-Di-boc-guanidinopropyl)-3',5'-O-(tetraisopropylidisiloxane-1,3-diyl)-adenosine (**1c**).

N,N-Di-boc-N'-triflyl guanidine (280 mg, 0.72 mmol) was dissolved in 5 mL dichloromethane then triethylamine (100 μ L) was added. After cooling to 0 °C, 2'-O-aminopropyl-3',5'-O-(tetraisopropylidisiloxane-1,3-diyl)-adenosine (**1f**) (400 mg, 0.71 mmol) was added and the mixture was stirred for 1 h at 0 °C then for 1 h at room temperature. The reaction was diluted with dichloromethane and washed with saturated sodium bicarbonate solution and brine. The organic

layer was dried over Na₂SO₄ and the solvent was evaporated. The residue was purified using column chromatography with dichloromethane/methanol (98:2, v/v) to give a yield of 402 mg (70%) of **1c**. ¹H NMR (400 MHz, DMSO-*d*₆) δ [ppm] 11.50 (s, 1H, NH-boc), 8.45–8.41 (m, 1H, NH-CH₂-), 8.17 (s, 1H, H₂ or H₈), 8.06 (s, 1H, H₂ or H₈), 7.31 (bs, 2H, NH₂), 6.02–5.99 (m, 1H, H₁'), 4.96–4.91 (m, 1H, H₃'), 4.43–4.40 (m, 1H, H₂'), 4.06–3.70 (m, 5H, H₄', 2 × H₅', O-CH₂-CH₂-CH₂-NH-), 3.51–3.32 (m, 2H, O-CH₂-CH₂-CH₂-NH-), 1.84–1.78 (m, 2H, O-CH₂-CH₂-CH₂-NH-), 1.44 (s, 9H, C(CH₃)₃), 1.37 (s, 9H, C(CH₃)₃), 1.07–0.99 (m, 28H, tetraisopropyl-CH and -CH₃); ¹³C NMR (101 MHz, DMSO-*d*₆) δ [ppm] 163.00, 156.00, 155.07, 152.40 (C₂ or C₈), 151.96, 148.48, 139.04 (C₂ or C₈), 119.21, 87.69 (C₁'), 82.70, 81.26 (C₂'), 80.41 (C₄'), 77.87, 69.99 (C₃'), 69.63 (O-CH₂-CH₂-CH₂-NH-), 60.13 (C₅'), 38.41 (O-CH₂-CH₂-CH₂-NH-), 28.71 (O-CH₂-CH₂-CH₂-NH-), 27.85 (C(CH₃)₃), 27.44 (C(CH₃)₃), {17.19, 17.05, 17.03, 17.00, 16.95, 16.82, 16.74, 16.68} (tetraisopropyl-CH₃), {12.59, 12.28, 12.09, 12.01} (tetraisopropyl-CH); MS (MALDI) was calculated to be 810.1 for C₃₆H₆₅N₈O₉Si₂ (M+H⁺), and found to be 808.3.

4.2.1.5. N⁶-Dimethylaminomethylene-2'-O-(N,N'-di-boc-guanidinopropyl)-3',5'-O-(tetraisopropylidisiloxane-1,3-diyl)-adenosine (1g). Compound **1c** (500 mg, 0.61 mmol) was dissolved in methanol (5 mL) and *N,N*-dimethylformamide dimethyl acetal (500 μL, 3.7 mmol) was added. The reaction was stirred at room temperature overnight and the solvents were evaporated. The crude product was used for further reactions without purification.

4.2.1.6. N⁶-Dimethylaminomethylene-2'-O-(N,N'-di-boc-guanidinopropyl)-adenosine (1h). Compound **1g** (500 mg, 0.58 mmol) was dissolved in tetrahydrofuran (5 mL) and triethylammonium trihydrofluoride (Et₃N·3HF; 330 μL, 2.0 mmol) was added. The mixture was stirred at room temperature for 1.5 h, then the solvent was evaporated. The residue was purified by column chromatography with ethyl acetate/methanol (98:2–9:1, v/v) giving 300 mg (83%) of the desired product. ¹H NMR (400 MHz, DMSO-*d*₆) δ [ppm] 11.47 (s, 1H, NH-boc), 8.92 (s, 1H, N⁶ = CH-NMe₂), 8.50 (s, 1H, H₂ or H₈), 8.41 (s, 1H, H₂ or H₈), 8.33–8.29 (m, 1H, NH-CH₂-), 6.11–6.09 (m, 1H, H₁'), 5.28–5.24 (m, 1H, 5'-OH), 5.18–5.16 (m, 1H, 3'-OH), 4.46–4.43 (m, 1H, H₂'), 4.36–4.32 (m, 1H, H₃'), 4.01–3.98 (m, 1H, H₄'), 3.72–3.46 (4H, 2 × H₅', O-CH₂-CH₂-CH₂-NH-), 3.33–3.28 (m, 2H, O-CH₂-CH₂-CH₂-NH-), 3.20 (s, 3H, N-CH₃), 3.13 (s, 3H, N-CH₃), 1.74–1.68 (m, 2H, O-CH₂-CH₂-CH₂-NH-), 1.45 (s, 9H, C(CH₃)₃), 1.37 (s, 9H, C(CH₃)₃); ¹³C NMR (101 MHz, DMSO-*d*₆) δ [ppm] 162.97, 159.22, 157.97 (N⁶ = CH-NMe₂), 155.09, 151.89, 151.77 (C₂ or C₈), 151.00, 141.08 (C₂ or C₈), 125.70, 85.91 (C₁'), 85.74 (C₄'), 82.72, 81.02 (C₂'), 77.99, 68.72 (C₃'), 67.88 (O-CH₂-CH₂-CH₂-NH-), 61.04 (C₅'), 40.56 (N-CH₃), 37.86 (O-CH₂-CH₂-CH₂-NH-), 34.45 (N-CH₃), 28.57 (O-CH₂-CH₂-CH₂-NH-), 27.87 (C(CH₃)₃), 27.51 (C(CH₃)₃); MS (MALDI) was calculated to be 622.7 for C₂₇H₄₄N₉O₈ (M+H⁺), and found to be 624.6.

4.2.1.7. N⁶-Dimethylaminomethylene-2'-O-(N,N'-di-boc-guanidinopropyl)-5'-O-(4,4'-dimethoxytrityl)-adenosine (1i). Compound **1h** (1.0 g, 1.6 mmol) was dissolved in dry pyridine (20 mL). 4,4'-Dimethoxytrityl chloride (660 mg, 1.95 mmol) was added and the reaction was stirred at room temperature overnight. The solution was diluted with dichloromethane and washed with saturated sodium bicarbonate solution. After evaporation of the solvents the residue was purified on a silica gel column with dichloromethane/methanol (98:2, v/v) containing 0.5% triethylamine, and 1.32 g (90%) of the tritylated compound was obtained. ¹H NMR (400 MHz, DMSO-*d*₆) δ [ppm] 11.48 (s, 1H, NH-boc), 8.90 (s, 1H, N⁶ = CH-NMe₂), 8.38–8.34 (m, 3H, H₂, H₃, NH-CH₂-), 7.37–7.34 (m, 2H, DMTr), 7.27–7.17 (m, 7H, DMTr), 6.84–6.79

(m, 4H, DMTr), 6.14–6.13 (m, 1H, H₁'), 5.18–5.15 (m, 1H, 3'-OH), 4.57–4.54 (m, 1H, H₂'), 4.47–4.42 (m, 1H, H₃'), 4.14–4.08 (m, 1H, H₄'), 3.72–3.71 (m, 6H, 2 × OCH₃), 3.70–3.56 (m, 2H, O-CH₂-CH₂-NH-), 3.37–3.32 (m, 2H, O-CH₂-CH₂-CH₂-NH-), 3.24–3.21 (m, 2H, 2 × H₅'), 3.19 (s, 3H, N-CH₃), 3.12 (s, 3H, N-CH₃), 1.77–1.70 (m, 2H, O-CH₂-CH₂-CH₂-NH-), 1.44 (s, 9H, C(CH₃)₃), 1.35 (s, 9H, C(CH₃)₃); ¹³C NMR (101 MHz, DMSO-*d*₆) δ [ppm] 162.98, 159.15, 157.97, 157.94, 157.91, 157.85 (N⁶ = CH-NMe₂), 155.09, 151.88 (C₂ or C₈), 151.06, 144.73, 141.18 (C₂ or C₈), 135.44, 135.37, {129.60, 129.56, 127.64, 127.59, 126.53} (DMTr), 125.70, 112.99 (DMTr), 86.14 (C₁'), 85.34, 82.97 (C₄'), 82.70, 80.36 (C₂'), 77.96, 69.08 (C₃'), 68.21 (O-CH₂-CH₂-CH₂-NH-), 63.40 (C₅'), 54.88 (OCH₃), 40.54 (N-CH₃), 37.97 (O-CH₂-CH₂-CH₂-NH-), 34.44 (N-CH₃), 28.56 (O-CH₂-CH₂-CH₂-NH-), 27.84 (C(CH₃)₃), 27.50 (C(CH₃)₃); MS (MALDI) was calculated to be 925.1 for C₄₈H₆₂N₉O₁₀ (M+H⁺), and found to be 924.9.

4.2.1.8. N⁶-Dimethylaminomethylene-2'-O-(N,N'-di-boc-guanidinopropyl)-5'-O-(4,4'-dimethoxytrityl)-adenosine 3'-(cyanoethyl)-N,N-diisopropyl phosphoramidite (1d). N⁶-Dimethylaminomethylene-2'-O-(N,N'-di-boc-guanidinopropyl)-5'-O-(4,4'-dimethoxytrityl)-adenosine (**1i**) (320 mg, 346 μmol) was dissolved in dichloromethane (8 mL). 2-cyanoethyl *N,N,N'*-tetraisopropylamino phosphane (132 μL, 415 μmol) and 4,5-dicyanoimidazole (47 mg, 398 μmol) were added. The mixture was stirred at room temperature. After 3 h, TLC revealed that some starting material did not react. An additional 0.6 equiv of the phosphitylating agent as well as the catalyst were therefore added. After 4 h the reaction was complete. The mixture was diluted with dichloromethane, washed with saturated sodium bicarbonate solution and the organic layer was dried over MgSO₄. The solvent was evaporated and the residue dissolved in a small amount of dichloromethane (ca. 5 mL). This solution was added dropwise into a flask with hexane (500 mL) to form a white precipitate. Two thirds of the solvent were evaporated and the remaining solvent was decanted from the solid. The precipitated product was redissolved in benzene and lyophilised to give 329 mg (84%) of **1d** as a white powder. ¹H NMR (300 MHz, acetone-*d*₆) δ [ppm] 11.65 (s, 1H, NH-boc) 8.95–8.93 (m, 1H, N⁶ = CH-NMe₂), 8.42–8.27 (m, 3H, H₂, H₃, NH-CH₂-), 7.50–7.46 (m, 2H, DMTr), 7.38–7.17 (m, 7H, DMTr), 6.87–6.80 (m, 4H, DMTr), 6.28–6.26 (m, 1H, H₁'), 4.96–4.79 (m, 2H, H₂', H₃') 4.45–4.37 (m, 1H, H₄'), 4.05–3.35 (m, 16H), 3.25 (s, 3H, N-CH₃), 3.18 (s, 3H, N-CH₃), 2.85 (m, 1H, cyanoethyl), 2.64–2.60 (m, 1H, cyanoethyl), 1.90–1.82 (m, 2H, O-CH₂-CH₂-CH₂-NH-), 1.50–1.49 (m, 9H, C(CH₃)₃), 1.42–1.40 (m, 9H, C(CH₃)₃), 1.25–1.10 (m, 12H, *i*Pr-CH₃); ³¹P NMR (121 MHz, acetone-*d*₆) δ [ppm] 149.6, 149.3; MS (ESI) was calculated to be 1125.3 for C₅₇H₇₉N₁₁O₁₁P (M+H⁺), and found to be 1125.7.

4.2.2. Synthesis of the 2'-O-guanidinopropyl cytidine phosphoramidite

N⁴-Dimethylaminomethylene-3',5'-O-(tetraisopropylidisiloxane-1,3-diyl)-cytidine (**2a**) was synthesised according to a previously described procedure.³⁷

4.2.2.1. N⁴-Dimethylaminomethylene-2'-O-cyanoethyl-3',5'-O-(tetraisopropylidisiloxane-1,3-diyl)-cytidine (2e). Compound **2a** (4 g, 7.39 mmol) was dissolved in acrylonitrile (8 mL, 122 mmol) and *tert*-Butanol (35 mL). Cesium carbonate (1.8 g, 5.52 mmol) was added and the reaction was stirred for 2.5 h at room temperature. The mixture was filtered over celite, the solvents evaporated, and then the residue was purified using column chromatography. Ethyl acetate was initially used as solvent then changed to ethyl acetate/methanol (9:1, v/v) after the unpolar impurities had passed through the column. A yield of 3.78 g (86%) of the product were obtained. ¹H NMR (400 MHz,

DMSO- d_6) δ [ppm] 8.62 (s, 1H, $N^4 = CH-NMe_2$), 7.88 (d, 1H, $J = 7.3$ Hz, H6), 5.90 (d, 1H, $J = 7.3$ Hz, H5), 5.65 (s, 1H, H1'), 4.22–3.91 (m, 7H), 3.17 (s, 3H, N- CH_3), 3.04 (s, 3H, N- CH_3), 2.86–2.82 (m, 2H, O- CH_2-CH_2-CN), 1.07–0.96 (m, 28H, tetraisopropyl- CH and - CH_3); ^{13}C NMR (101 MHz, DMSO- d_6) δ [ppm] 171.21 (C4), 157.77 ($N^4 = CH-NMe_2$), 154.57 (C2), 140.61 (C6), 118.86 (O- CH_2-CH_2-CN), 101.14 (C5), 88.99 (C1'), 81.42, 80.69, 67.83, 65.22 (O- CH_2-CH_2-CN), 59.39 (C5'), 40.79 (N- CH_3), 34.71 (N- CH_3), 18.18 (O- CH_2-CH_2-CN), {17.22, 17.11, 17.04, 16.97, 16.84, 16.72, 16.69, 16.61} (tetraisopropyl- CH_3), {12.60, 12.20, 11.88} (tetraisopropyl- CH); MS (ESI) was calculated to be 594.9 for $C_{27}H_{48}N_5O_6Si_2$ ($M+H^+$) and found to be 594.9.

4.2.2.2. 2'-O-Cyanoethyl-3',5'-O-(tetraisopropylidisiloxane-1,3-diyl)-cytidine (2b).

N^4 -Dimethylaminomethylene-2'-O-cyanoethyl-3',5'-O-(tetraisopropylidisiloxane-1,3-diyl)-cytidine (2e) (1.0 g, 1.68 mmol) was dissolved in methanol (10 mL) and hydrazine hydrate (500 μ L, 10.3 mmol) was added. The mixture was stirred for 1 h at room temperature and then the solvents were evaporated. The residue was purified on a silica gel column with ethyl acetate/methanol (95:5, v/v) to give 745 mg (82%) of 2b. 1H NMR (400 MHz, DMSO- d_6) δ [ppm] 7.69 (d, 1H, $J = 7.4$ Hz, H6), 7.21 (s, 2H, NH_2), 5.69 (d, 1H, $J = 7.4$ Hz, H5), 5.61 (s, 1H, H1'), 4.19–3.90 (m, 7H), 2.90–2.76 (m, 2H, O- CH_2-CH_2-CN), 1.07–0.97 (m, 28 H, tetraisopropyl- CH and - CH_3); ^{13}C NMR (101 MHz, DMSO- d_6) δ [ppm] 165.70, 154.60, 139.36 (C6), 118.89, 93.30 (C5), 88.66 (C1'), 81.55 (C2'), 80.49, 67.92, 65.19 (O- CH_2-CH_2-CN), 59.44 (C5'), 18.20 (O- CH_2-CH_2-CN), {17.23, 17.11, 17.05, 16.98, 16.85, 16.73, 16.72, 16.63} (tetraisopropyl- CH_3), {12.62, 12.28, 12.21, 11.88} (tetraisopropyl- CH); MS (ESI) was calculated to be 539.8 for $C_{24}H_{43}N_4O_6Si_2$ ($M+H^+$) and found to be 540.0.

4.2.2.3. 2'-O-Aminopropyl-3',5'-O-(tetraisopropylidisiloxane-1,3-diyl)-cytidine (2f).

Compound 2b (500 mg, 928 μ mol) was dissolved in 10 mL of methanol in a glass tube. Approximately 0.5 mL of the Raney-nickel sediment was washed thoroughly with dry methanol and was rinsed into the glass tube with the solution of 2b. After addition of 5 mL methanol saturated with ammonia, the mixture was stirred for 1 h at room temperature under a hydrogen atmosphere (30 bar). The reaction mixture was filtered through celite and the catalyst was washed several times with methanol. The solvent was evaporated and the residue was purified on a silica gel column using ethyl acetate/methanol/triethylamine (60:35:5) to give 251 mg (50%) of the product. When this procedure was repeated, the crude material after filtration and evaporation was used in further reactions without purification. 1H NMR (400 MHz, DMSO- d_6) δ [ppm] 7.69 (d, 1H, $J = 7.2$ Hz, H6), 7.18 (bs, 2H, ar. NH_2), 5.68 (d, 1H, $J = 7.5$ Hz, H5), 5.60 (s, 1H, H1'), 4.18–3.76 (m, 7H), 2.70–2.66 (m, 2H, O- $CH_2-CH_2-CH_2-NH_2$), 1.68–1.61 (m, 2H, O- $CH_2-CH_2-CH_2-NH_2$), 1.07–0.95 (m, 28 H, tetraisopropyl- CH and - CH_3); MS (MALDI) was calculated to be 643.8 for $C_{24}H_{47}N_4O_6Si_2$ ($M+H^+$) and found to be 544.6.

4.2.2.4. 2'-O-(N,N -Di-boc-guanidinopropyl)-3',5'-O-(tetraisopropylidisiloxane-1,3-diyl)-cytidine (2c).

N,N -Di-boc- N' -triflyl guanidine (360 mg, 920 μ mol) was dissolved in 5 mL dichloromethane and triethylamine (125 μ L) then added. After cooling to 0 °C, compound 2f (500 mg, 922 μ mol) was added and the solution was stirred for 1 h at 0 °C and then 1 h at room temperature. The reaction was diluted with dichloromethane and washed with saturated sodium bicarbonate solution and brine. The combined organic layers were dried over Na_2SO_4 and after evaporating the solvent the residue was purified using column chromatography with dichloromethane/methanol (98:2–95:5, v/v) to give 434 mg (60%) of 2c. 1H NMR (400 MHz, DMSO- d_6) δ [ppm] 11.48 (s, 1H, NH -boc), 8.38–8.35 (m, 1H, $NH-CH_2-$), 7.67 (d, 1H, $J = 7.4$ Hz, H6),

7.19 (bs, 2H, NH_2), 5.68 (d, 1H, $J = 7.4$ Hz, H5), 5.63 (s, 1H, H1'), 4.17–3.78 (m, 7H), 3.49–3.33 (m, 2H, O- $CH_2-CH_2-CH_2-NH-$), 1.84–1.77 (m, 2H, O- $CH_2-CH_2-CH_2-NH-$), 1.45 (m, 9H, $C(CH_3)_3$), 1.38 (m, 9H, $C(CH_3)_3$), 1.06–0.96 (m, 28 H, tetraisopropyl- CH and - CH_3); ^{13}C NMR (101 MHz, DMSO- d_6) δ [ppm] 165.61, 162.99, 155.04, 154.52, 151.94, 139.45 (C6), 93.21 (C5), 88.97 (C1'), 82.66, 81.76 (C2'), 80.36 (C4'), 77.86, 69.11 (O- $CH_2-CH_2-CH_2-NH-$), 68.27 (C3'), 59.51 (C5'), 38.28 (O- $CH_2-CH_2-CH_2-NH-$), 28.61 (O- $CH_2-CH_2-CH_2-NH-$), 27.86 ($C(CH_3)_3$), 27.44 ($C(CH_3)_3$), {17.22, 17.10, 17.03, 16.96, 16.83, 16.70, 16.68, 16.60} (tetraisopropyl- CH_3), {12.59, 12.26, 12.21, 11.87} (tetraisopropyl- CH); MS (MALDI) was calculated to be 786.1 for $C_{35}H_{65}N_6O_{10}Si_2$ ($M+H^+$) and found to be 786.4.

4.2.2.5. N^4 -Benzoyl-2'-O-(N,N -di-boc-guanidinopropyl)-3',5'-O-(tetraisopropylidisiloxane-1,3-diyl)-cytidine (2g).

Compound 2c (1.0 g, 1.27 mmol) was dissolved in dry pyridine (10 mL) and the solution was cooled in an ice bath. Benzoyl chloride (240 μ L, 2.06 mmol) was added and the reaction solution was stirred at 0 °C for 1 h. The reaction was quenched with water and ammonia (25% in water; 3 mL) was added. The mixture was then stirred for 30 min at room temperature. The solvents were evaporated and the residue was dissolved in dichloromethane and washed with saturated sodium bicarbonate solution. The organic layer was dried over Na_2SO_4 and after evaporating the solvent, the residue was purified by column chromatography using dichloromethane/methanol (98:2, v/v) and 950 mg (84%) of the product were obtained. 1H NMR (400 MHz, DMSO- d_6) δ [ppm] 11.50 (s, 1H, NH), 11.31 (s, 1H, NH), 8.40–8.37 (m, 1H, $NH-CH_2-$), 8.15 (d, 1H, $J = 7.3$ Hz, H6), 8.03–7.99 (m, 2H, benzoyl), 7.65–7.60 (m, 1H, benzoyl), 7.53–7.49 (m, 2H, benzoyl), 7.38 (d, 1H, $J = 7.3$ Hz, H5), 5.73 (s, 1H, H1'), 4.24–4.13 (m, 3H, H3', H4', H5'), 4.02–4.03 (m, 1H, H2'), 3.97–3.92 (m, 1H, H5'), 3.87–3.83 (m, 2H, O- $CH_2-CH_2-CH_2-NH-$), 3.52–3.35 (m, 2H, O- $CH_2-CH_2-CH_2-NH-$), 1.87–1.80 (m, 2H, O- $CH_2-CH_2-CH_2-NH-$), 1.45 (m, 9H, $C(CH_3)_3$), 1.38 (m, 9H, $C(CH_3)_3$), 1.08–0.95 (m, 28H, tetraisopropyl- CH and - CH_3); ^{13}C NMR (101 MHz, DMSO- d_6) δ [ppm] 167.21, 163.14, 163.00, 155.06, 154.01, 151.97, 143.37 (C6), 132.97, 132.64, 128.31, 95.61 (C5), 89.46 (C1'), 82.67, 81.30 (C2'), 80.86 (C4'), 77.86, 69.26 (O- $CH_2-CH_2-CH_2-NH-$), 67.95 (C3'), 59.38 (C5'), 38.28 (O- $CH_2-CH_2-CH_2-NH-$), 28.62 (O- $CH_2-CH_2-CH_2-NH-$), 27.86 ($C(CH_3)_3$), 27.43 ($C(CH_3)_3$), {17.22, 17.11, 17.04, 16.97, 16.89, 16.73, 16.71, 16.66} (tetraisopropyl- CH_3), {12.56, 12.29, 12.22, 11.86} (tetraisopropyl- CH); MS (ESI) was calculated to be 890.2 for $C_{42}H_{69}N_6O_{11}Si_2$ ($M+H^+$), and found to be 890.4.

4.2.2.6. N^4 -Benzoyl-2'-O-(N,N -di-boc-guanidinopropyl)-cytidine (2h).

N^4 -Benzoyl-2'-O-(N,N -di-boc-guanidinopropyl)-3',5'-O-(tetraisopropylidisiloxane-1,3-diyl)-cytidine (2g) (900 mg, 1.01 mmol) was dissolved in tetrahydrofuran (20 mL). Triethylamine trihydrofluoride ($Et_3N \cdot 3HF$; 560 μ L, 3.54 mmol) was added and the solution was stirred at room temperature for 2 h. The solvent was evaporated and the residue was purified using column chromatography with dichloromethane/methanol (98:2–97:3, v/v) to give 607 mg (93%) of the product as a pale yellow foam. 1H NMR (300 MHz, DMSO- d_6) δ [ppm] 11.50 (s, 1H, NH), 11.28 (bs, 1H, NH), 8.57 (d, 1H, $J = 7.5$ Hz, H6), 8.40–8.35 (m, 1H, $NH-CH_2-$), 8.02–7.98 (m, 2H, benzoyl), 7.66–7.60 (m, 1H, benzoyl), 7.54–7.48 (m, 2H, benzoyl), 7.34 (d, 1H, $J = 7.2$ Hz, H5), 5.86–5.85 (m, 1H, H1'), 5.24 (t, 1H, $J = 5.0$ Hz, 5'-OH), 4.98 (d, 1H, $J = 6.8$ Hz, 3'-OH), 4.12–3.60 (m, 7H), 3.44–3.37 (m, 2H, O- $CH_2-CH_2-CH_2-NH-$), 1.85–1.76 (m, 2H, O- $CH_2-CH_2-CH_2-NH-$), 1.46 (m, 9H, $C(CH_3)_3$), 1.38 (m, 9H, $C(CH_3)_3$); ^{13}C NMR (75 MHz, acetone- d_6) δ [ppm] 169.22, 165.59, 164.82, 157.83, 156.15, 154.80, 147.10 (C6), 135.58, 134.60, 130.46, 130.05, 97.67 (C5), 91.39 (C1'), 86.19 (C4'), 84.69 ($C(CH_3)_3$), 84.62 (C2'), 79.88 ($C(CH_3)_3$), 70.71

(O-CH₂-CH₂-CH₂-NH-), 69.63 (C3'), 61.46 (C5'), 40.29 (O-CH₂-CH₂-CH₂-NH-), 30.86 (O-CH₂-CH₂-CH₂-NH-), 29.46 (C(CH₃)₃), 29.14 (C(CH₃)₃); HRMS (MALDI) was calculated to be 647.3035 for C₃₀H₄₃N₆O₁₀ (M+H⁺), and found to be 647.3031.

4.2.2.7. N⁴-Benzoyl-2'-O-(N,N'-di-boc-guanidinopropyl)-5'-O-(4,4'-dimethoxytrityl)-cytidine (2i).

N⁴-Benzoyl-2'-O-(N,N'-di-boc-guanidinopropyl)-cytidine (**2h**) (516 mg, 798 μmol) was dissolved in dry pyridine (20 mL) and the solution was cooled in an ice bath. 4,4'-Dimethoxytrityl chloride (515 mg, 1.52 mmol) was added and the mixture was stirred overnight while the bath came up to room temperature. The reaction was quenched with methanol (10 mL) and the solvents were evaporated. The residue was purified by column chromatography using dichloromethane/methanol (99:1–98:2, v/v). The column was packed with solvent containing 1% triethylamine to yield 715 mg (94%) of the product as a pale yellow foam. ¹H NMR (400 MHz, DMSO-*d*₆) δ [ppm] 11.50 (s, 1H, NH), 11.29 (bs, 1H, NH), 8.43–8.37 (m, 2H, H₆, NH-CH₂-), 8.02–7.99 (m, 2H, benzoyl), 7.65–7.60 (m, 1H, benzoyl), 7.54–7.50 (m, 2H, benzoyl), 7.43–7.25 (m, 9H, DMTr), 7.18–7.15 (m, 1H, H₅), 6.94–6.91 (m, 4H, DMTr), 5.88 (s, 1H, H1'), 5.04 (d, 1H, J = 7.3 Hz, 3'-OH), 4.34–4.28 (m, 1H, H3'), 4.13–4.10 (m, 1H, H4'), 3.94–3.87 (m, 2H, H2', 1 × O-CH₂-CH₂-CH₂-NH-), 3.76 (s, 6H, 2 × OCH₃), 3.76–3.70 (m, 1H, 1 × O-CH₂-CH₂-CH₂-NH-), 3.46–3.36 (m, 4H, 2 × H5', O-CH₂-CH₂-CH₂-NH-), 1.86–1.80 (m, 2H, O-CH₂-CH₂-CH₂-NH-), 1.42 (m, 9H, C(CH₃)₃), 1.36 (m, 9H, C(CH₃)₃); ¹³C NMR (75 MHz, DMSO-*d*₆) δ [ppm] 167.19, 163.02, 158.11, 158.08, 155.12, 154.07, 151.93, 144.24 (C6), 135.47, 135.11, 133.06, 132.62, 129.70, 129.55, 128.35, 127.85, 127.73, 126.78, 113.19, 95.93 (C5), 88.99 (C1'), 85.90, 82.67 (C(CH₃)₃), 81.93 (C2'), 81.44 (C4'), 77.94 (C(CH₃)₃), 68.44 (O-CH₂-CH₂-CH₂-NH-), 67.62 (C3'), 61.36 (C5'), 54.91 (OCH₃), 54.90 (OCH₃), 38.17 (O-CH₂-CH₂-CH₂-NH-), 28.59 (O-CH₂-CH₂-CH₂-NH-), 27.87 (C(CH₃)₃), 27.48 (C(CH₃)₃); HRMS (MALDI) was calculated to be 971.4161 for C₅₁H₆₀N₆O₁₂Na (M+Na⁺), and found to be 971.4181.

4.2.2.8. N⁴-Benzoyl-2'-O-(N,N'-di-boc-guanidinopropyl)-5'-O-(4,4'-dimethoxytrityl)-cytidine 3'-(cyanoethyl)-N,N'-diisopropyl phosphoramidite (2d).

Compound **2i** (683 mg, 720 μmol) was dissolved in dichloromethane (15 mL). 2-cyanoethyl N,N,N',N'-tetraisopropylamino phosphane (274 μL, 864 μmol) and 4,5-dicyanoimidazole (98 mg, 828 μmol) were added. After stirring at room temperature for 5 h, TLC revealed that some starting material had not reacted. Therefore 10 mg of 4,5-dicyanoimidazole and 30 μL of the phosphitylation agent were added and the reaction was stirred at room temperature overnight. The solution was diluted with dichloromethane and washed with saturated sodium bicarbonate solution. After drying the organic layer over MgSO₄ the solvent was evaporated and the residue was dissolved in a small amount (5 mL) of dichloromethane. This solution was dripped into a flask with hexane (500 mL) to form a white precipitate. Two thirds of the solvent was evaporated and the residual solvent was decanted carefully. The precipitate was redissolved in benzene and lyophilised to give 738 mg (89%) of **2d**. According to ³¹P NMR spectrum the product was still containing a small amount of the hydrolysed phosphitylation reagent but this did not interfere with the oligonucleotide synthesis. ¹H NMR (400 MHz, DMSO-*d*₆) δ [ppm] 11.50–11.48 (m, 1H, NH), 11.25 (bs, 1H, NH), 8.52–8.45 (m, 1H, H₆), 8.39–8.34 (m, 1H, NH-CH₂-), 8.01–7.98 (m, 2H, benzoyl), 7.66–7.61 (m, 1H, benzoyl), 7.53–7.49 (m, 2H, benzoyl), 7.45–7.25 (m, 9H, DMTr), 7.13–7.09 (m, 1H, H₅), 6.93–6.89 (m, 4H, DMTr), 5.95–5.92 (m, 1H, H1'), 4.56–4.38 (m, 1H, H3'), 4.31–4.28 (m, 1H, H4'), 4.07–3.29 (m, 17H), 2.90–2.57 (m, 2H, cyanoethyl), 1.86–1.78 (m, 2H, O-CH₂-CH₂-CH₂-NH-), 1.40–1.35 (m, 18H, 2 × C(CH₃)₃), 1.20–0.93 (m, 12H, *i*Pr-CH₃); ³¹P NMR (162 MHz, DMSO-*d*₆) δ [ppm] 148.4, 148.0

(The signal of the hydrolysed phosphitylation reagent appears at 13.9 ppm); HRMS (MALDI) was calculated to be 1149.5421 for C₆₀H₇₈N₈O₁₃P (M+H⁺), was found to be 1149.5447.

4.2.3. Synthesis of the 2'-O-guanidinopropyl uridine phosphoramidite

N³-Benzoyl-3',5'-O-(tetraisopropylidisiloxane-1,3-diyl)-uridine (**3a**) was synthesised according to a previously described procedure.²²

4.2.3.1. N³-Benzoyl-2'-O-cyanoethyl-3',5'-O-(tetraisopropylidisiloxane-1,3-diyl)-uridine (3b).

Compound **3a** (1.14 g, 1.93 mmol) was dissolved in 9.6 mL of *tert*-butanol. Freshly distilled acrylonitrile (2.5 mL, 38.6 mmol) was added. After addition of cesium carbonate (645 mg, 1.98 mmol) the reaction was stirred for 4 h at room temperature. The reaction solution was filtered over celite. The residue was washed with 100 mL of dichloromethane. The filtrate was evaporated in vacuum. Purification via column chromatography in dichloromethane/ethyl acetate (99:1–95:5, v/v) yielded 746 mg (60%) of the desired product as a white powder. ¹H NMR (250 MHz, acetone-*d*₆) δ [ppm] 8.03–7.99 (m, 3H, H₆, benzoyl), 7.79–7.72 (m, 1H, benzoyl), 7.61–7.55 (m, 2H, benzoyl), 5.80–5.74 (m, 2H, H₅, H1'), 4.50–3.94 (m, 7H), 2.80–2.75 (m, 2H, O-CH₂-CH₂-CN), 1.17–1.07 (m, 28H, tetraisopropyl-CH and -CH₃); ¹³C NMR (63 MHz, acetone-*d*₆) δ [ppm] 171.11, 163.78, 151.06, 141.48, 136.94, 133.92, 132.20, 131.13, 119.80, 102.75, 91.47, 84.05, 83.69, 70.65, 68.08, 61.60, 20.35, 18.92, 18.91, 18.75, 18.73, 18.64, 18.50, 18.46, 18.40, 15.23, 14.79, 14.72, 14.43; HRMS (XXX) was calculated to be 666.2637 for C₃₁H₄₅N₃O₈Si₂Na (M+Na⁺) and found to be 666.2647.

4.2.3.2. 2'-O-(Aminopropyl)-3',5'-O-(tetraisopropylidisiloxane-1,3-diyl)-uridine (3e).

Compound **3b** (500 mg, 0.78 mmol) was dissolved in 10 mL of methanol in a glass tube suitable for the applied autoclave. Approximately 0.5 mL of the Raney-nickel slurry was put on a glass filter, washed thoroughly with dry methanol and rinsed into the glass tube with the solution of **3b**. After addition of 5 mL methanol saturated with ammonia, the mixture was stirred for 1 h at room temperature in an autoclave under a hydrogen atmosphere (30 bar). The reaction solution was decanted from the catalyst into a glass filter. The catalyst was washed several times with methanol and the solvent was removed from the combined filtrates under reduced pressure. The product was purified on a silica gel column initially using dichloromethane/ethyl acetate (7:3–0:1, v/v) and thereafter ethyl acetate/methanol/triethylamine (6: 3.5: 0.5, v/v/v) to obtain 253 mg (60%) of a white powder. When we repeated the reduction we used the crude product after filtration and evaporation for further derivatisation. ¹H NMR (250 MHz, acetone-*d*₆) δ [ppm] 7.81 (d, 1H, J = 8.1 Hz, H₆), 5.71 (s, 1H, H1'), 5.53 (d, 1H, J = 8.1 Hz, H₅), 4.39–4.34 (m, 1H, H3'), 4.28–4.23 (m, 1H, H5'), 4.14–4.03 (m, 3H, H2', H4', H5'), 3.97–3.81 (m, 2H, O-CH₂-CH₂-CH₂-NH₂), 3.37–3.25 (m, 2H, O-CH₂-CH₂-CH₂-NH₂), 1.92–1.82 (m, 2H, O-CH₂-CH₂-CH₂-NH₂), 1.14–1.05 (m, 28H, tetraisopropyl-CH and -CH₃); ¹³C NMR (63 MHz, acetone-*d*₆) δ [ppm] 167.18, 164.59, 151.93, 141.033, 102.82, 91.15, 83.77, 83.50, 70.88, 70.85, 61.78, 49.36, 33.03, 18.91, 18.90, 18.74, 18.61, 18.49, 18.47, 18.40, 15.19, 14.82, 14.71, 14.41; HRMS (MALDI) was calculated to be 544.2869 for C₂₄H₄₆N₃O₇Si₂ (M+H⁺), and found to be 544.2880.

4.2.3.3. 2'-O-(N,N'-Di-boc-guanidinopropyl)-3',5'-O-(tetraisopropylidisiloxane-1,3-diyl)-uridine (3c). N,N'-Di-boc-N'-triflyl guanidine (320 mg, 0.82 mmol) was dissolved in 3.6 mL dichloromethane and triethylamine (150 μL) was added. The solution was cooled in an ice bath and 2'-O-(aminopropyl)-3',5'-O-(tetraisopropylidisiloxane-1,3-diyl)-uridine (**3e**) (490 mg, 0.9 mmol)

was added. After 15 min the reaction mixture was removed from the ice bath and stirred for 2.5 h at room temperature. The reaction solution was washed with saturated sodium bicarbonate solution and brine. After drying over Na_2SO_4 the solvent was evaporated in vacuum. The crude product was purified using column chromatography with dichloromethane/methanol (96:4–94:6, v/v). 410 mg (58%) of compound **3c** were obtained. ^1H NMR (400 MHz, $\text{DMSO}-d_6$) δ [ppm] 11.49 (s, 1H, NH), 11.37 (m, 1H, $\text{NH}_{\text{uridine}}$), 8.40–8.37 (m, 1H, $\text{NH}-\text{CH}_2-$), 7.64 (d, 1H, $J = 7.9$ Hz, H6), 5.64 (s, 1H, $\text{H}1'$), 5.53 (d, 1H, $J = 7.9$ Hz, H5), 4.25–4.22 ($\text{H}3'$), 4.13–4.09 (m, 1H, $\text{H}5'$), 4.06–4.05 (m, 1H, $\text{H}2'$), 4.03–4.00 (m, 1H, $\text{H}4'$), 3.93–3.89 (m, 1H, $\text{H}5'$), 3.84–3.70 (m, 2H, $\text{O}-\text{CH}_2-\text{CH}_2-\text{CH}_2-\text{NH}-$), 3.49–3.32 (m, 2H, $\text{O}-\text{CH}_2-\text{CH}_2-\text{CH}_2-\text{NH}-$), 1.83–1.77 (m, 2H, $\text{O}-\text{CH}_2-\text{CH}_2-\text{CH}_2-\text{NH}-$), 1.45 (s, 9H, $\text{C}(\text{CH}_3)_3$), 1.38 (s, 9H, $\text{C}(\text{CH}_3)_3$), 1.06–0.97 (m, 28H, tetraisopropyl-CH and - CH_3); HRMS (MALDI) was calculated to be 808.3955 for $\text{C}_{35}\text{H}_{63}\text{N}_5\text{O}_{11}\text{Si}_2\text{Na}$ ($\text{M}+\text{Na}^+$), and found to be 808.3991.

4.2.3.4. 2'-O-(N,N-Di-boc-guanidinopropyl)-uridine (3f). To a solution of compound **3c** (910 mg, 1.16 mmol) and triethylamine (240 μL) in 13 mL tetrahydrofuran $\text{NEt}_3\cdot 3\text{HF}$ (700 μL , 4.3 mmol) was added. The reaction mixture was stirred for 1 h at room temperature. The solvents were evaporated and the residue was purified on a silica gel column using dichloromethane/methanol (93:7–92:8, v/v) to give 629 mg (97%) of a white foam. ^1H NMR (250 MHz, acetone- d_6) δ [ppm] 11.67 (bs, 1H, NH), 10.03 (bs, 1H, NH), 8.46–8.41 (m, 1H, $\text{NH}-\text{CH}_2-$), 8.10 (d, 1H, $J = 8.2$ Hz, H6), 5.99–5.97 (m, 1H, $\text{H}1'$), 5.58 (d, 1H, $J = 8.2$ Hz, H5), 4.39–3.46 (m, 11H), 1.95–1.85 (m, 2H, $\text{O}-\text{CH}_2-\text{CH}_2-\text{CH}_2-\text{NH}-$), 1.51 (s, 9H, $\text{C}(\text{CH}_3)_3$), 1.43 (s, 9H, $\text{C}(\text{CH}_3)_3$); ^{13}C NMR (63 MHz, acetone- d_6) δ [ppm] 165.64, 164.59, 157.88, 154.86, 152.37, 142.33, 103.31, 89.82, 86.67, 84.77, 84.74, 84.39, 79.91, 70.73, 70.69, 62.45, 40.20, 30.96, 29.51, 29.19; MS (ESI) was calculated to be 566.2 for $\text{C}_{23}\text{H}_{37}\text{N}_5\text{O}_{10}\text{Na}$ ($\text{M}+\text{Na}^+$), and found to be 567.0.

4.2.3.5. 2'-O-(N,N'-Di-boc-guanidinopropyl)-5'-O-(4,4'-dimethoxytrityl)-uridine (3g). 2'-O-(N,N'-Di-boc-guanidinopropyl)-uridine (**3f**) (588 mg, 1.08 mmol) was dissolved in 11.4 mL of dry pyridine and 4,4'-dimethoxytrityl chloride (460 mg, 1.36 mmol) was added. The reaction solution was stirred at room temperature for 5 h. The reaction mixture was quenched with water and the solvents were evaporated. The residue was dissolved in dichloromethane, washed twice with saturated sodium bicarbonate solution (2×50 mL) and then twice with brine (2×50 mL). The organic layer was dried over Na_2SO_4 and the solvent was removed under reduced pressure. After purification using column chromatography with dichloromethane/methanol (97:3, v/v) containing 0.5% triethylamine, 785 mg (86%) of a yellow powder was obtained. The yellow impurity could not be separated on the column. ^1H NMR (250 MHz, $\text{DMSO}-d_6$) δ [ppm] 11.49 (s, 1H, NH), 11.37 (m, 1H, NH), 8.41–8.36 (m, 1H, $\text{NH}-\text{CH}_2-$), 7.75 (d, 1H, $J = 8.1$ Hz, H6), 7.40–7.23 (m, 9H, DMTr), 6.92–6.88 (m, 4H, DMTr), 5.83–5.82 (m, 1H, $\text{H}1'$), 5.29–5.25 (m, 1H, H5), 5.09–5.06 (m, 1H, 3'-OH), 4.23–3.88 (m, 3H), 3.74 (s, 6H, $2 \times \text{O}-\text{CH}_3$), 3.68–3.63 (m, 2H), 3.43–3.20 (m, 4H), 1.82–1.72 (m, 2H, $\text{O}-\text{CH}_2-\text{CH}_2-\text{CH}_2-\text{NH}-$), 1.44 (s, 9H, $\text{C}(\text{CH}_3)_3$), 1.37 (s, 9H, $\text{C}(\text{CH}_3)_3$); HRMS (MALDI) was calculated to be 846.3920 for $\text{C}_{44}\text{H}_{56}\text{N}_5\text{O}_{12}$ ($\text{M}+\text{H}^+$), and found to be 846.3946.

4.2.3.6. 2'-O-(N,N'-Di-boc-guanidinopropyl)-5'-O-(4,4'-dimethoxytrityl)-uridine 3'-(cyanoethyl)-N,N-diisopropyl phosphoramidite (3d). 2'-O-(N,N'-Di-boc-guanidinopropyl)-5'-O-(4,4'-dimethoxytrityl)-uridine (**3g**) (770 mg, 0.9 mmol) was dissolved in dichloromethane (11 mL). To this solution, 2-cyanoethyl $\text{N,N,N}'$ -tetraisopropylamino phosphane (400 μL , 1.26 mmol) and 4,5-dicyanoimidazole (130 mg, 1.1 mmol) were added. The reaction progress was observed with TLC (dichloromethane/ethyl

acetate 1:1 (v:v), containing 0.5% triethylamine). Because the reaction was not complete after 2 h, an additional 0.3 equiv of the reagents were added and the reaction was completed after additional 40 min. The resulting solution was washed twice with saturated sodium bicarbonate solution (2×100 mL) and once with brine (200 mL). After drying over Na_2SO_4 , the solvent was evaporated and the residue was purified on a silica gel column with dichloromethane/ethyl acetate (6:4–1:1, v/v) containing 0.5% triethylamine. The mixture of the two diastereomers was obtained as a light yellow foam (762 mg, 83%). ^1H NMR (400 MHz, $\text{DMSO}-d_6$) δ [ppm] 11.50–11.48 (m, 1H, NH), 11.35 (bs, 1H, NH), 8.39–8.33 (m, 1H, $\text{NH}-\text{CH}_2-$), 7.87–7.80 (m, 1H, H6), 7.41–7.22 (m, 9H, DMTr), 6.91–6.86 (m, 4H, DMTr), 5.86–5.84 (m, 1H, $\text{H}1'$), 5.23–5.18 (m, 1H, H5), 4.46–4.32 (m, 1H), 4.21–4.16 (m, 1H), 4.09–4.03 (m, 1H), 3.83–3.26 (m, 16H), 2.80–2.59 (m, 2H, $-\text{O}-\text{CH}_2-\text{CH}_2-\text{CN}$), 1.81–1.74 (m, 2H, $\text{O}-\text{CH}_2-\text{CH}_2-\text{CH}_2-\text{NH}-$), 1.42–1.36 (m, 18H, $\text{C}(\text{CH}_3)_3$), 1.13–0.94 (m, 12H, $i\text{Pr}-\text{CH}_3$); ^{31}P NMR (121 MHz, $\text{DMSO}-d_6$) δ [ppm] 150.0, 148.6; HRMS (MALDI) was calculated to be 1046.4999 for $\text{C}_{53}\text{H}_{73}\text{N}_7\text{O}_{13}\text{P}$ ($\text{M}+\text{H}^+$), and found to be 1046.5021.

4.2.4. Synthesis of the 2'-O-guanidinopropyl guanosine phosphoramidite

O^6 -(2,4,6-Triisopropylbenzenesulfonyl)-3',5'-O-di-*tert*-butylsilylanediyl guanosine (**4a**) was synthesised according to a previously described procedure.²¹

4.2.4.1. 2'-O-(2-Cyanoethyl)-3',5'-O-di-*tert*-butylsilylanediyl guanosine (4b). Compound **4a** (2.28 g, 3.3 mmol) was dissolved in *tert*-butanol (17 mL). Freshly distilled acrylonitrile (4.25 mL, 66 mmol) and cesium carbonate (1.16 g, 3.3 mmol) were added to the solution. After vigorous stirring at room temperature for 2–3 h, the mixture was filtered through celite. The solvent and excess reagents were removed in vacuum. The crude material was used for the next reaction without further purification. The residue was dissolved in 4 mL of a mixture of formic acid/dioxane/water (70:24:6, v/v/v). After stirring at room temperature for 1 h, water (150 mL) was added to the mixture and the solution extracted with dichloromethane. The organic layer was dried over Na_2SO_4 and the solvent was evaporated. The residue was purified using column chromatography with dichloromethane/methanol (9:1, v/v) to give 1.1 g (70% over two steps) of **4b** as a colourless foam. ^1H NMR (250 MHz, $\text{DMSO}-d_6$) δ [ppm] 10.71 (bs, 1H, NH), 7.89 (s, 1H, H8), 6.45 (bs, 2H, NH_2), 5.81 (s, 1H, $\text{H}1'$), 4.45–4.33 (m, 3H), 4.05–3.81 (m, 4H), 2.83–2.76 (m, 2H, $\text{O}-\text{CH}_2-\text{CH}_2-\text{CN}$), 1.06 (s, 9H, $\text{C}(\text{CH}_3)_3$), 1.01 (s, 9H, $\text{C}(\text{CH}_3)_3$); ^{13}C NMR (63 MHz, $\text{DMSO}-d_6$) δ [ppm] 156.51, 153.69, 150.50, 135.36, 118.71, 116.53, 87.25, 80.31, 76.35, 73.80, 66.64, 65.14, 27.12, 26.80, 22.07, 19.82, 18.29; MS (ESI) was calculated to be 477.2 for $\text{C}_{21}\text{H}_{33}\text{N}_6\text{O}_5\text{Si}$ ($\text{M}+\text{H}^+$), and found to be 477.5.

4.2.4.2. 2'-O-(2-Aminopropyl)-3',5'-O-di-*tert*-butylsilylanediyl guanosine (4e). Compound **4b** (500 mg, 1.06 mmol) was dissolved in dry methanol (5 mL). Raney nickel (ca. 0.5 mL of the methanol-washed sediment) and methanol (5 mL) saturated with ammonia were then added. The mixture was hydrogenated at 30 bar hydrogen-pressure for 1 h at room temperature. Thereafter the mixture was filtered through a glass filter and the catalyst was washed several times with methanol and a methanol/water mixture. The solvents were evaporated from the filtrate and the residue was used without further purification for the next reaction. MS (ESI) was calculated to be 481.3 for $\text{C}_{21}\text{H}_{37}\text{N}_6\text{O}_5\text{Si}$ ($\text{M}+\text{H}^+$), and found to be 481.8.

4.2.4.3. 2'-O-(N,N'-Di-boc-guanidinopropyl)-3',5'-O-di-*tert*-butylsilylanediyl guanosine (4c). $\text{N,N}'$ -Di-boc- N' -triflyl guanidine (163 mg, 0.415 mmol) was dissolved in dichloromethane (2.1 mL)

and triethylamine (54 μL) was then added. The solution was cooled in an ice bath and then 2'-O-(2-Aminopropyl)-3',5'-O-di-*tert*-butylsilyl-*di*yl guanosine (**4e**) (200 mg, 0.42 mmol) was added. After 30 min the reaction mixture was removed from the ice bath then stirred for an additional 30 min at room temperature. The reaction solution was washed with saturated sodium bicarbonate solution and brine. After drying over Na_2SO_4 the solvent was evaporated. The residue was purified by column chromatography using dichloromethane/methanol (9:1, v/v) to give 270 mg (89%) of **4c**. ^1H NMR (400 MHz, $\text{DMSO}-d_6$) δ [ppm] 11.49 (bs, 1H, NH), 10.66 (bs, 1H, NH), 8.56–8.53 (m, 1H, NH-CH₂-), 7.87 (s, 1H, H8), 6.39 (bs, 2H, NH₂), 5.86 (s, 1H, H1'), 4.42–4.38 (m, 1H, H3'), 4.30–4.27 (m, 2H, H2', H5'), 4.06–3.93 (m, 3H, H4', H5', $\frac{1}{2} \times \text{O}-\text{CH}_2-\text{CH}_2-\text{CH}_2-\text{NH}-$), 3.72–3.67 (m, 1H, $\frac{1}{2} \times \text{O}-\text{CH}_2-\text{CH}_2-\text{CH}_2-\text{NH}-$), 3.51–3.30 (m, 2H, O-CH₂-CH₂-CH₂-NH-), 1.84–1.77 (m, 2H, O-CH₂-CH₂-CH₂-NH-), 1.46 (s, 9H, -CO-C(CH₃)₃), 1.39 (s, 9H, -CO-C(CH₃)₃), 1.06 (s, 9H, -Si-C(CH₃)₃), 0.97 (s, 9H, -Si-C(CH₃)₃); HRMS (MALDI) was calculated to be 723.3856 for C₃₂H₅₅N₈O₉Si (M+H⁺), and found to be 723.3880.

4.2.4.4. N²-Isobutyryl-2'-O-(N,N'-di-boc-guanidinopropyl)-3',5'-O-di-*tert*-butylsilyl-*di*yl guanosine (4f**) and N²-Isobutyryl-2'-O-(N,N'-di-boc-N''-isobutyryl-guanidinopropyl)-3',5'-O-di-*tert*-butylsilyl-*di*yl guanosine (**4f***).** A solution of compound **4c** (400 mg, 0.55 mmol) in 3.6 mL of pyridine was cooled in an ice bath and isobutyryl chloride (145 μL , 1.37 mmol) was then added dropwise. The mixture was stirred at 0 °C for 1 h, then at room temperature for 1 h and evaporated to dryness. The residue was dissolved in 40 mL dichloromethane and washed twice with saturated sodium bicarbonate solution (2 \times 60 mL) and once with brine (60 mL). The organic phase was dried over Na_2SO_4 and the solvent was evaporated. The residue was purified by column chromatography using dichloromethane/methanol (95:5–90:10, v/v) to give 318 mg (ca. 70%) of a mixture of mono- and di-isobutyryl derivative. ^1H NMR (250 MHz, $\text{DMSO}-d_6$) δ [ppm] 12.12 (s, 1H, NH), 11.57–11.51 (m, NH, NH-boc), 10.53 (s, NH-boc*), 8.54–8.49 (m, 2'-O-CH₂-CH₂-CH₂-NH-), 8.25–8.22 (m, 1H, H8), 5.90–5.88 (m, 1H, H1'), 4.42–3.42 (m, 9H), 2.85–2.72 (m, 1.5H, -CH(CH₃)₂), 1.99–1.73 (m, 2H, 2'-O-CH₂-CH₂-CH₂-NH-), 1.47–1.33 (m, 18H, 2 \times -CO-C(CH₃)₃), 1.15–0.99 (m, 27H, 2 \times -Si-C(CH₃)₃, -CH(CH₃)₂, -CH(CH₃)₂*). As a result of the mixture comprising mono- and diisobutyryl derivatives, some of the integrals could not be given as whole numbers. Thus, signals that depend only on the diisobutyryl compound are marked with an asterisk. MS (ESI) was calculated to be 793.4 for C₃₆H₆₁N₈O₁₀Si (M+H⁺), and found to be 794.6.

4.2.4.5. N²-Isobutyryl-2'-O-(N,N'-di-boc-guanidinopropyl)-guanosine (4g**) and N²-Isobutyryl-2'-O-(N,N'-di-boc-N''-isobutyryl-guanidinopropyl)-guanosine (**4g***).** A mixture of N²-Isobutyryl-2'-O-(N,N'-di-boc-guanidinopropyl)-3',5'-O-di-*tert*-butylsilyl-*di*yl guanosine (**4f**) and N²-Isobutyryl-2'-O-(N,N'-di-boc-N''-isobutyryl-guanidinopropyl)-3',5'-O-di-*tert*-butylsilyl-*di*yl guanosine (**4f***) (490 mg, ca. 592 μmol) was dissolved in dry tetrahydrofuran (7 mL). Triethylamine (165 μL , 1.11 mmol) and Et₃N-3HF (352 μL , 2.16 mmol) were then added. After stirring at room temperature for 1 h the solvent was evaporated. The residue was purified using column chromatography with dichloromethane/methanol (9:1, v/v) to give 322 mg (ca. 79%) of a mixture of N²-isobutyryl-2'-O-(N,N'-di-boc-guanidinopropyl)-guanosine and N²-isobutyryl-2'-O-(N,N'-di-boc-N''-isobutyryl-guanidinopropyl)-guanosine as white foam. A small sample of the mixture was separated for NMR spectroscopy. NMR data is given for the mono-isobutyryl compound. ^1H NMR (400 MHz, $\text{DMSO}-d_6$) δ [ppm] 12.08 (s, 1H, NH), 11.65 (s, 1H, NH), 11.46 (s, 1H, NH), 8.29 (s, 1H, H8), 8.28–8.25 (m, 1H, NH-CH₂-), 5.91 (d, 1H, J = 6.0 Hz, H1'), 5.16 (d, 1H,

J = 4.8 Hz, 3'-OH), 5.06–5.03 (m, 1H, 5'-OH), 4.36–4.29 (m, 2H, H2', H3'), 3.95–3.93 (m, 1H, H4'), 3.67–3.46 (m, 4H, 2 \times H5', O-CH₂-CH₂-CH₂-NH-), 3.33–3.28 (m, 2H, O-CH₂-CH₂-CH₂-NH-), 2.77 (sep, 1H, J = 6.8 Hz, -CH(CH₃)₂), 1.75–1.67 (m, 2H, O-CH₂-CH₂-CH₂-NH-), 1.45 (s, 9H, -CO-C(CH₃)₃), 1.37 (s, 9H, -CO-C(CH₃)₃), 1.12 (d, 6H, J = 6.8 Hz, -CH(CH₃)₂); ^{13}C NMR (63 MHz, CDCl_3) δ [ppm] 178.72, 163.52, 156.12, 155.16, 153.39, 147.73, 147.05, 138.81, 122.49, 88.47, 86.74, 83.65, 82.28, 79.58, 70.69, 69.87, 62.66, 38.87, 36.39, 29.32, 28.28, 28.11, 18.96, 18.89; HRMS (MALDI) was calculated to be 653.3253 for C₂₈H₄₅N₈O₁₀ (M+H⁺), and found to be 653.3274.

4.2.4.6. N²-Isobutyryl-2'-O-(N,N'-di-boc-guanidinopropyl)-5'-O-(4,4'-dimethoxytrityl)-guanosine (4h**) and N²-Isobutyryl-2'-O-(N,N'-di-boc-N''-isobutyryl-guanidinopropyl)-5'-O-(4,4'-dimethoxytrityl)-guanosine (**4h***).** A mixture of N²-Isobutyryl-2'-O-(N,N'-di-boc-guanidinopropyl)-guanosine (**4g**) and N²-Isobutyryl-2'-O-(N,N'-di-boc-N''-isobutyryl-guanidinopropyl)-guanosine (**4g***) (400 mg, ca. 583 μmol) was dissolved in dry pyridine (11 mL). 4,4'-Dimethoxytrityl chloride (280 mg, 0.82 mmol) was added and the solution was stirred for 3 h at room temperature. TLC revealed that some starting material remained at this time and an additional 0.3 equiv of 4,4'-Dimethoxytrityl chloride were therefore added. When TLC demonstrated that the starting material had been consumed, the reaction was quenched with water and the solvents evaporated. The residue was purified by column chromatography using dichloromethane/methanol (98:2, v/v) containing 0.5% triethylamine to give 427 mg (ca. 74%) of the desired products. ^1H NMR (400 MHz, $\text{DMSO}-d_6$) δ [ppm] 12.09 (s, 1H, NH), 11.58 (s, 1H, NH), 11.47 (s, 0.5H, NH-boc), 10.50 (s, 0.5H, NH-boc*), 8.33–8.30 (m, 0.5H, 2'-O-CH₂-CH₂-CH₂-NH-), 8.15–8.12 (m, 1H, H8), 7.35–7.18 (m, 9H, DMTr), 6.84–6.80 (m, 4H, DMTr), 5.97–5.94 (m, 1H, H1'), 5.15–5.13 (m, 1H, 3'-OH), 4.42–4.37 (m, 1H, H2'), 4.35–4.30 (m, 1H, H3'), 4.09–4.03 (m, 1H, H4'), 3.72 (s, 6H, 2 \times O-CH₃), 3.69–3.47 (m, 2H, 2'-O-CH₂-CH₂-CH₂-NH-), 3.37–3.26 (m, 3H, 2'-O-CH₂-CH₂-CH₂-NH-, H5'), 3.17–3.13 (m, 1H, H5'), 2.79–2.73 (m, 1.5H, -CH(CH₃)₂), 1.77–1.67 (m, 2H, 2'-O-CH₂-CH₂-CH₂-NH-), 1.43–1.35 (m, 18H, 2 \times -CO-C(CH₃)₃), 1.13–1.10 (m, 6H, -CH(CH₃)₂), 1.00–0.98 (m, 3H, -CH(CH₃)₂*). As a result of the mixture comprising mono- and diisobutyryl derivatives, some of the integrals could not be given as whole numbers. Thus, signals that depend only on the diisobutyryl compound are marked with an asterisk. MS (ESI) was calculated to be 955.5 for C₄₉H₆₃N₈O₁₂ (M+H⁺), and found to be 956.5.

4.2.4.7. N²-Isobutyryl-2'-O-(N,N'-di-boc-guanidinopropyl)-5'-O-(4,4'-dimethoxytrityl)-guanosine 3'-(cyanoethyl)-N,N-diisopropyl phosphoramidite (4d**) and N²-Isobutyryl-2'-O-(N,N'-di-boc-N''-isobutyryl-guanidinopropyl)-5'-O-(4,4'-dimethoxytrityl)-guanosine 3'-(cyanoethyl)-N,N-diisopropyl phosphoramidite (**4d***).** A mixture of compounds **4h** and **4h*** (380 mg, ca. 384 μmol) was dissolved in dichloromethane (8 mL), then 2-cyanoethyl N,N,N',N'-tetraisopropylamino phosphane (160 μL , 0.52 mmol) and 4,5-dicyanoimidazole (57 mg, 0.5 mmol) were added. After 2 h TLC showed complete consumption of the starting material. The reaction solution was then washed twice with saturated sodium bicarbonate solution (2 \times 50 mL) and once with brine (100 mL). After drying over Na_2SO_4 the solvent was evaporated and the residue was purified using column chromatography with dichloromethane/ethyl acetate (8:2, v/v) containing 0.5% triethylamine to give 350 mg (ca. 76%) of the two diastereomers of **4d** and **4d***. ^1H NMR (400 MHz, $\text{DMSO}-d_6$) δ [ppm] 12.11 (bs, 1H, NH), 11.61–11.57 (m, 1H, NH), 11.46–11.44 (m, 0.5H, NH-boc), 10.50–10.46 (m, 0.5H, NH-boc*), 8.31–8.27 (m, 0.5H, 2'-O-CH₂-CH₂-CH₂-NH-), 8.18–8.14 (m, 1H, H8), 7.36–7.19 (m, 9H, DMTr), 6.85–6.80 (m, 4H, DMTr), 5.97–5.88 (m, 1H, H1'), 4.64–4.61 (m,

1H, H2'), 4.44–4.37 (m, 1H, H3'), 4.27–4.12 (m, 1H, H4'), 3.79–3.18 (m, 10H), 3.72 (s, 6H, 2 × OCH₃), 2.81–2.70 (m, 2.5H, –CH(CH₃)₂), 2.60–2.47 (m, 2H, –P–O–CH₂–CH₂–CN), 1.75–1.65 (m, 2H, 2'–O–CH₂–CH₂–CH₂–NH–), 1.41–1.34 (m, 18H, 2 × –CO–C(CH₃)₃), 1.15–1.10 (m, 18H, –N((CH(CH₃)₂)₂), –CO–CH(CH₃)₂), 1.00–0.96 (m, 3H, –CH(CH₃)₂^{*}): ³¹P NMR (162 MHz, DMSO-*d*₆) δ [ppm] 149.59, 149.44, 149.52, 149.19. As a result of the mixture comprising mono- and diisobutyryl derivatives, some of the integrals could not be given as whole numbers. Thus, signals that depend only on the diisobutyryl compound are marked with an asterisk. MS (ESI) was calculated to be 1155.6 for C₅₈H₈₀N₁₀O₁₃P (M+H⁺), and found to be 1157.3.

4.3. Oligonucleotide synthesis

Modified oligonucleotides were synthesised on 500 Å CPG material on an Expedite 8909 synthesiser using phosphoramidite chemistry. The GP modified nucleosides were inserted into the HBV antisense strand (intended guide, 5' UUG AAG UAU GCC UCA AGG UCG 3') at each of positions 2, 3, 4, 5, 6, 7 and 13 from the 5' end. The sense strand oligonucleotide (5' ACC UUG AAG CAU ACU UCA ATT 3') did not include modifications. The duplex HBV siRNA3 targeted HBV genotype A coordinates 1693 to 1711. Control siRNA with scrambled unmodified sequences comprised 5'-UAUUGGGUGUGCGGUCACGGT-3' (antisense) and 5'-CGU-GACCGCACACCAAUATT-3' (sense). 5-Ethylthio-1H-tetrazole (0.25 M in acetonitrile) was used as activator. Unmodified 2'-TBDMS-phosphoramidites were benzoyl- (A), isobutyryl- (G) or acetyl- (C) protected. Coupling time for the modified phosphoramidites was 25 min. After completion of synthesis, 30 min of deprotection in 3% trichloroacetic acid in dichloromethane was carried out to ensure complete cleavage of the boc groups. The RNA oligomers were cleaved from the controlled-pore-glass (CPG) support by incubation at 40 °C for 24 h using an ethanol:ammonia solution (1:3). The 2'-TBDMS groups were deprotected by incubation for 90 min at 65 °C with a triethylamine, *N*-methylpyrrolidinone and Et₃N·3HF mixture. RNA oligomers were precipitated with BuOH at 80 °C for 30 min and purified by anion exchange HPLC using a Dionex DNA-Pac 100 column (1 M LiCl, water, gradient: 0–70% LiCl solution in 40 min, flow: 1 mL/min). Oligonucleotides were desalted in a subsequent reverse phase HPLC step (column: *phenomenex* Jupiter 4u Proteo 90A 250 mm × 15 mm, 0.1 M triethylammonium acetate pH 7, acetonitrile, gradient: 0% acetonitrile for 2 min, 0–37% acetonitrile in 28 min). Identity was confirmed by mass spectroscopy on a Bruker micrOTOF-Q.

4.4. Biological experiments

4.4.1. Cell culture, transfection, dual luciferase assay and measurement of HBV surface antigen (HBsAg) concentrations

Huh7 and HEK293 cells were cultured in DMEM (Lonza, Basel, Switzerland) supplemented with 5% foetal calf serum (Gibco BRL, UK). Cells were seeded in 24-well plates at a confluency of 40% on the day before transfection, and were then maintained in antibiotic-free medium for at least an hour prior to transfection. To assess target knockdown when using the luciferase reporter assay, Lipofectamine 2000 (Invitrogen, Carlsbad, CA) was employed to transfect HEK293 cells with 100 ng psiCHECK-HBx²⁰ and 32.5 ng siRNA (5 nM final concentration) at ratios of 1:1 and 1:3 (ml:mg), respectively. The psiCHECK-HBx reporter vector contains the HBx target sequence downstream of the *Renilla* ORF within the psiCHECK 2.2 (Promega, WI, USA) and has been described previously.²⁰ Forty-eight hours after transfection, cells were assayed for luciferase activity using the Dual-Luciferase[®] Reporter Assay System (Promega, WI, USA) and the ratio of *Renilla* luciferase to Firefly luciferase activity was calculated. Similarly, to assess knock-

down of HBV replication in a liver-derived line, Huh7 cells were transfected with 100 ng pCH-9/3091²⁸ and 32.5 ng siRNA. Forty-eight hours after transfection, growth medium was harvested and HBsAg concentration was measured by ELISA using the MON-OLISA[®] HBs Ag ULTRA kit (Bio-Rad, CA, USA). Each experiment was repeated at least in triplicate.

4.4.2. siRNA serum stability assessment

Annealed siRNAs were diluted in 80% FCS to a final concentration of 5 μM and incubated at 37 °C. At time points ranging from 1 to 24 h, aliquots were removed and snap frozen using liquid nitrogen. Twenty picomoles of the samples were subjected to electrophoresis through a 10% denaturing polyacrylamide gel then stained with ethidium bromide.

Acknowledgments

Financial support for this work from the South African National Research Foundation, Poliomyelitis Research Foundation and Medical Research Council and from the German Research Foundation (DFG) is gratefully acknowledged.

We would like to thank Stefan Bernhardt for his valuable help with oligonucleotide synthesis and purification and Diana Knapp for scientific discussion about conception of the modified oligonucleotides.

Supplementary data

Supplementary data associated with this article can be found, in the online version, at doi:10.1016/j.bmc.2011.12.024.

References and notes

- Haussecker, D. *Hum. Gene Ther.* **2008**, *19*, 451.
- Tripp, R. A.; Tompkins, S. M. In *Methods in Molecular Biology*; Humana Press, 2009; Vol. 555, p 43.
- Bumcrot, D.; Manoharan, M.; Kotliansky, V.; Sah, D. W. Y. *Nat. Chem. Biol.* **2006**, *2*, 711.
- Behlke, M. A. *Mol. Ther.* **2006**, *13*, 644.
- Behlke, M. A. *Oligonucleotides* **2008**, *18*, 305.
- Li, J.; Huang, L. *Nanomedicine* **2010**, *5*, 1483.
- Moschos, S. A.; Jones, S. W.; Perry, M. M.; Williams, A. E.; Erjefalt, J. S.; Turner, J. J.; Barnes, P. J.; Sproat, B. S.; Gait, M. J.; Lindsay, M. A. *Bioconjugate Chem.* **2007**, *18*, 1450.
- Nothisen, M.; Kotera, M.; Voirin, E.; Remy, J.-S.; Behr, J.-P. *J. Am. Chem. Soc.* **2009**, *131*, 17730.
- Engels, J. W.; Odadzic, D.; Smicius, R.; Haas, J. In *Methods in Molecular Biology*; Humana Press, 2010; Vol. 623, p 155.
- Odadzic, D.; Bramsen, J. B.; Smicius, R.; Bus, C.; Kjemis, J.; Engels, J. W. *Bioorg. Med. Chem.* **2008**, *16*, 518.
- Bramsen, J. B.; Laursen, M. B.; Nielsen, A. F.; Hansen, T. B.; Bus, C.; Langkjær, N.; Babu, B. R.; Højland, T.; Abramov, M.; Van Aerschot, A.; Odadzic, D.; Smicius, R.; Haas, J.; Andree, C.; Barman, J.; Wenska, M.; Srivastava, P.; Zhou, C.; Honcharenko, D.; Hess, S.; Müller, E.; Bobkov, G. V.; Mikhailov, S. N.; Fava, E.; Meyer, T. F.; Chattopadhyaya, J.; Zerial, M.; Engels, J. W.; Herdewijn, P.; Wengel, J.; Kjemis, J. *Nucleic Acids Res.* **2009**, *37*, 2867.
- Smicius, R.; Engels, J. W. *J. Org. Chem.* **2008**, *73*, 4994.
- Sekine, T.; Kawashima, E.; Ishido, Y. *Nucleic Acids Symposium Series*; Oxford University Press, 1995. p 11.
- Sekine, M.; Satoh, T. *Nucleic Acids Symposium Series*; Oxford University Press: London, 1990. p 11.
- Sekine, M.; Nakanishi, T. *Nucleic Acids Symposium Series*; Oxford University Press: London, 1989. p 33.
- Haas, J.; Mueller-Kuller, T.; Klein, S.; Engels, J. W. *Nucleosides, Nucleotides Nucleic Acids* **2007**, *26*, 865.
- Carmona, S.; Ely, A.; Crowther, C.; Moolla, N.; Salazar, F. H.; Marion, P. L.; Ferry, N.; Weinberg, M. S.; Arbuthnot, P. *Mol. Ther.* **2006**, *13*, 411.
- Ely, A.; Naidoo, T.; Arbuthnot, P. *Nucleic Acids Res.* **2009**, *37*, e91.
- Ely, A.; Naidoo, T.; Mufamadi, S.; Crowther, C.; Arbuthnot, P. *Mol. Ther.* **2008**, *16*, 1105.
- Weinberg, M. S.; Ely, A.; Barichiev, S.; Crowther, C.; Mufamadi, S.; Carmona, S.; Arbuthnot, P. *Mol. Ther.* **2007**, *15*, 534.
- Mukobata, T.; Ochi, Y.; Ito, Y.; Wada, S.; Urata, H. *Bioorg. Med. Chem. Lett.* **2010**, *20*, 129.
- Sekine, M. *J. Org. Chem.* **1989**, *54*, 2321.
- Saneyoshi, H.; Seio, K.; Sekine, M. *J. Org. Chem.* **2005**, *70*, 10453.

24. Haas, J.; Engels, J. W. *Tetrahedron Lett.* **2007**, *48*, 8891.
25. Feichtinger, K.; Zapf, C.; Sings, H. L.; Goodman, M. J. *Org. Chem.* **1998**, *63*, 3804.
26. Odadzic, D. Ph.D. Thesis, Goethe-University at Frankfurt am Main, August **2009**.
27. Hean, J.; Crowther, C.; Ely, A.; ul Islam, R.; Barichiev, S.; Bloom, K.; Weinberg, M. S.; van Otterlo, W. A. L.; de Koning, C. B.; Salazar, F.; Marion, P.; Roesch, E. B.; LeMaitre, M.; Herdewijn, P.; Arbuthnot, P. *Artif. DNA: PNA XNA* **2010**, *1*, 17.
28. Nassal, M. J. *J. Virol.* **1992**, *66*, 4107.
29. Aigner, M.; Hartl, M.; Fauster, K.; Steger, J.; Bister, K.; Micura, R. *ChemBioChem* **2011**, *12*, 47.
30. Griffey, R. H.; Monia, B. P.; Cummins, L. L.; Freier, S.; Greig, M. J.; Guinosso, C. J.; Lesnik, E.; Manalili, S. M.; Mohan, V.; Owens, S.; Ross, B. R.; Sasmor, H.; Wancewicz, E.; Weiler, K.; Wheeler, P. D.; Cook, P. D. *J. Med. Chem.* **1996**, *39*, 5100.
31. Prakash, T. P.; Manoharan, M.; Fraser, A. S.; Kawasaki, A. M.; Lesnik, E. A.; Owens, S. R. *Tetrahedron Lett.* **2000**, *41*, 4855.
32. Teplova, M.; Wallace, S. T.; Tereshko, V.; Minasov, G.; Symons, A. M.; Cook, P. D.; Manoharan, M.; Egli, M. *Proc. Natl. Acad. Sci.* **1999**, *96*, 14240.
33. Arbuthnot, P.; Kew, M. J. *Exp. Pathol.* **2001**, *82*, 77.
34. Ivacic, D.; Ely, A.; Arbuthnot, P. *Rev. Med. Virol.* **2011**. doi:10.1002/rmv.705.
35. Jackson, A. L.; Burchard, J.; Schelter, J.; Chau, B. N.; Cleary, M.; Lim, L.; Linsley, P. S. *RNA* **2006**, *12*, 1179.
36. Dua, P.; Yoo, J. W.; Kim, S.; Lee, D. *Mol. Ther.* **2011**, *19*, 1676.
37. Matthews, D. P.; Persichetti, R. A.; Sabol, J. S.; Stewart, K. T.; McCarthy, J. R. *Nucleosides Nucleotides* **1993**, *12*, 115.

Synthesis of 2'-O-guanidinopropyl-modified nucleoside phosphoramidites and their incorporation into siRNAs targeting hepatitis B virus

Supplementary Information

Jolanta Brzezinska^a, Jennifer D'Onofrio^a, Maximilian C. R. Buff^a, Justin Hean^b, Abdullah Ely^b, Musa Marimani^b, Patrick Arbuthnot^b and Joachim W. Engels^{a}*

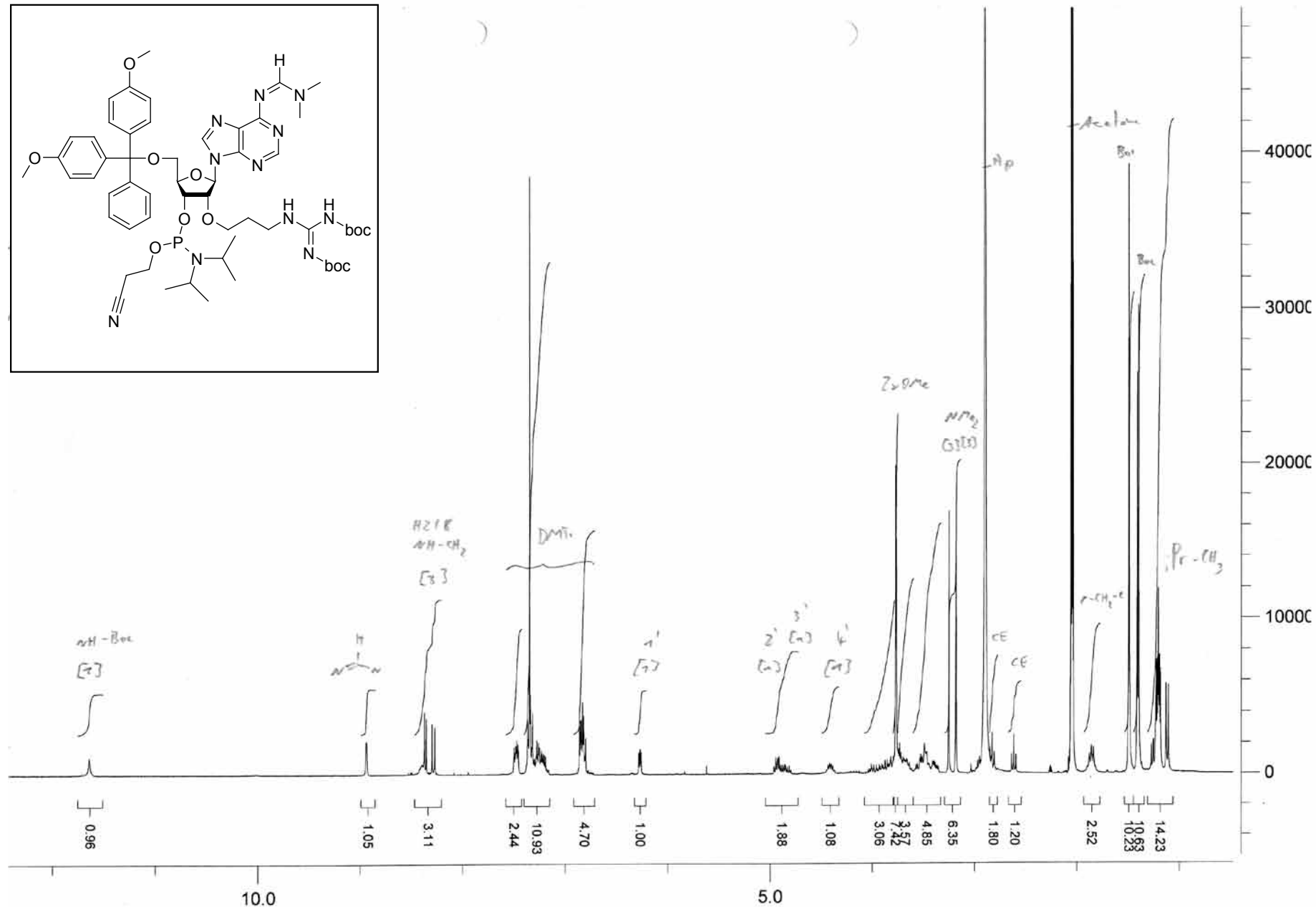
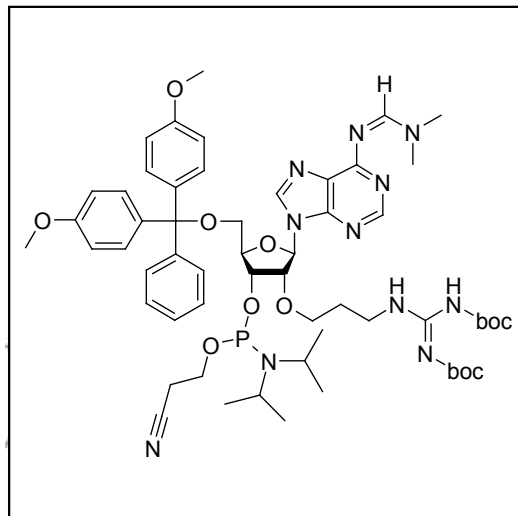
^aGoethe-University, Institute of Organic Chemistry & Chemical Biology, Max-von-Laue-Str. 7, 60438 Frankfurt am Main, Germany

^bAntiviral Gene Therapy Research Unit, School of Pathology, Health Sciences Faculty, University of the Witwatersrand, Private Bag 3, WITS 2050, Johannesburg, SOUTH AFRICA

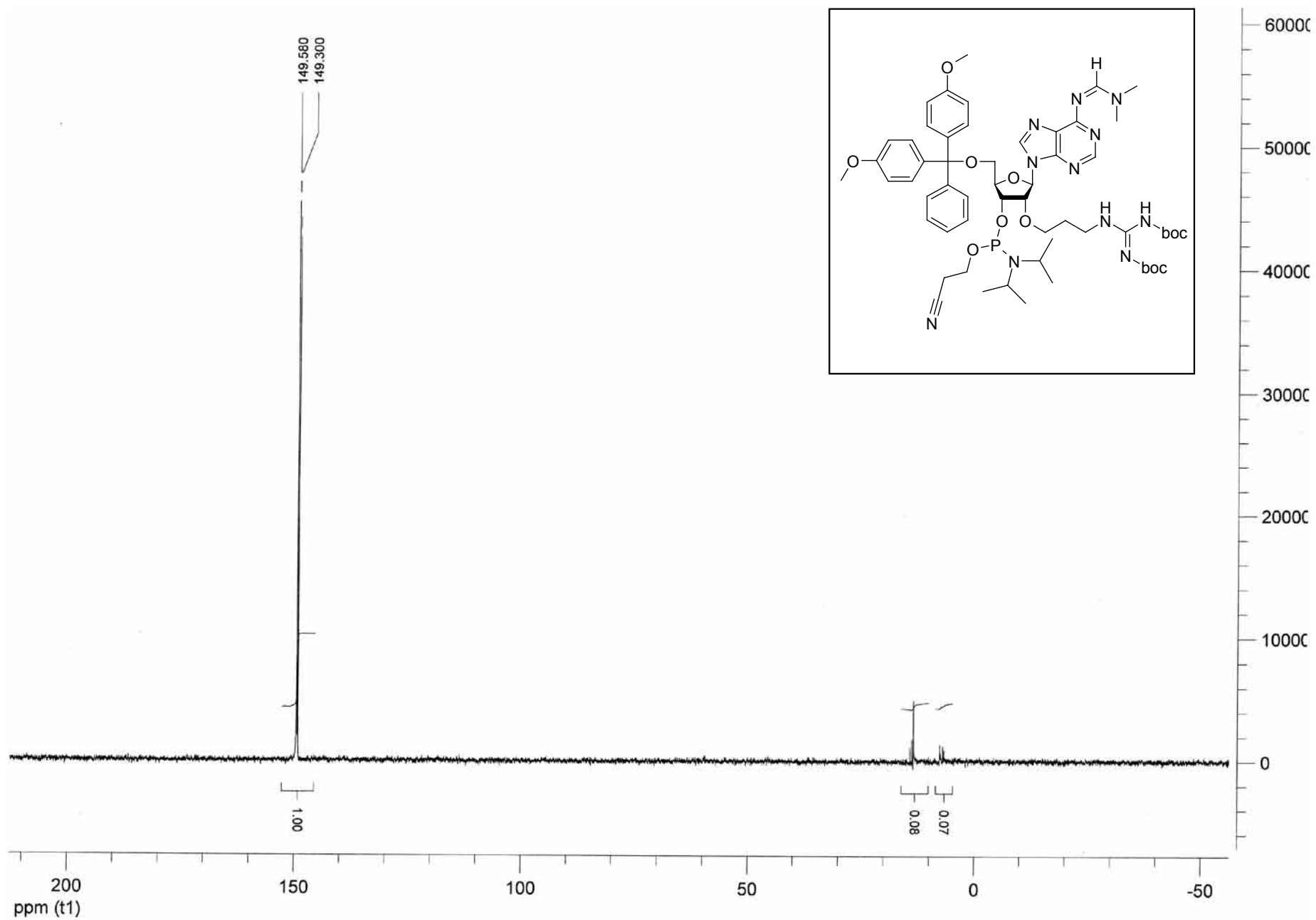
* To whom correspondence should be addressed: Joachim W. Engels. Tel.: +49-69-798-29150; fax: +49-69-798-29148; e-mail: Joachim.Engels@chemie.uni-frankfurt.de

¹ H NMR of 1d	S3
³¹ P NMR of 1d	S4
¹ H NMR of N⁶-Dimethylaminomethylene-2'-O-(N,N'-di-boc-guanidinopropyl)-adenosine	S5
¹³ C NMR of N⁶-Dimethylaminomethylene-2'-O-(N,N'-di-boc-guanidinopropyl)-adenosine	S6
¹ H NMR of 2d	S7
³¹ P NMR of 2d	S8
¹ H NMR of N⁴-Benzoyl-2'-O-(N,N'-di-boc-guanidinopropyl)-cytidine	S9
¹³ C NMR of N⁴-Benzoyl-2'-O-(N,N'-di-boc-guanidinopropyl)-cytidine	S10
¹ H NMR of 3d	S11
³¹ P NMR of 3d	S12
¹ H NMR of 2'-O-(N,N'-Di-boc-guanidinopropyl)-uridine	S13
¹³ C NMR of 2'-O-(N,N'-Di-boc-guanidinopropyl)-uridine	S14
¹ H NMR of 4d (+4d*)	S15
³¹ P NMR of 4d (+4d*)	S16
¹ H NMR of N²-Isobutyryl-2'-O-(N,N'-di-boc-guanidinopropyl)-guanosine	S17
¹³ C NMR of N²-Isobutyryl-2'-O-(N,N'-di-boc-guanidinopropyl)-guanosine	S18
Exemplary chromatogram of crude RNA after deprotection	S19
Organisation of the hepatitis B virus genome	S20

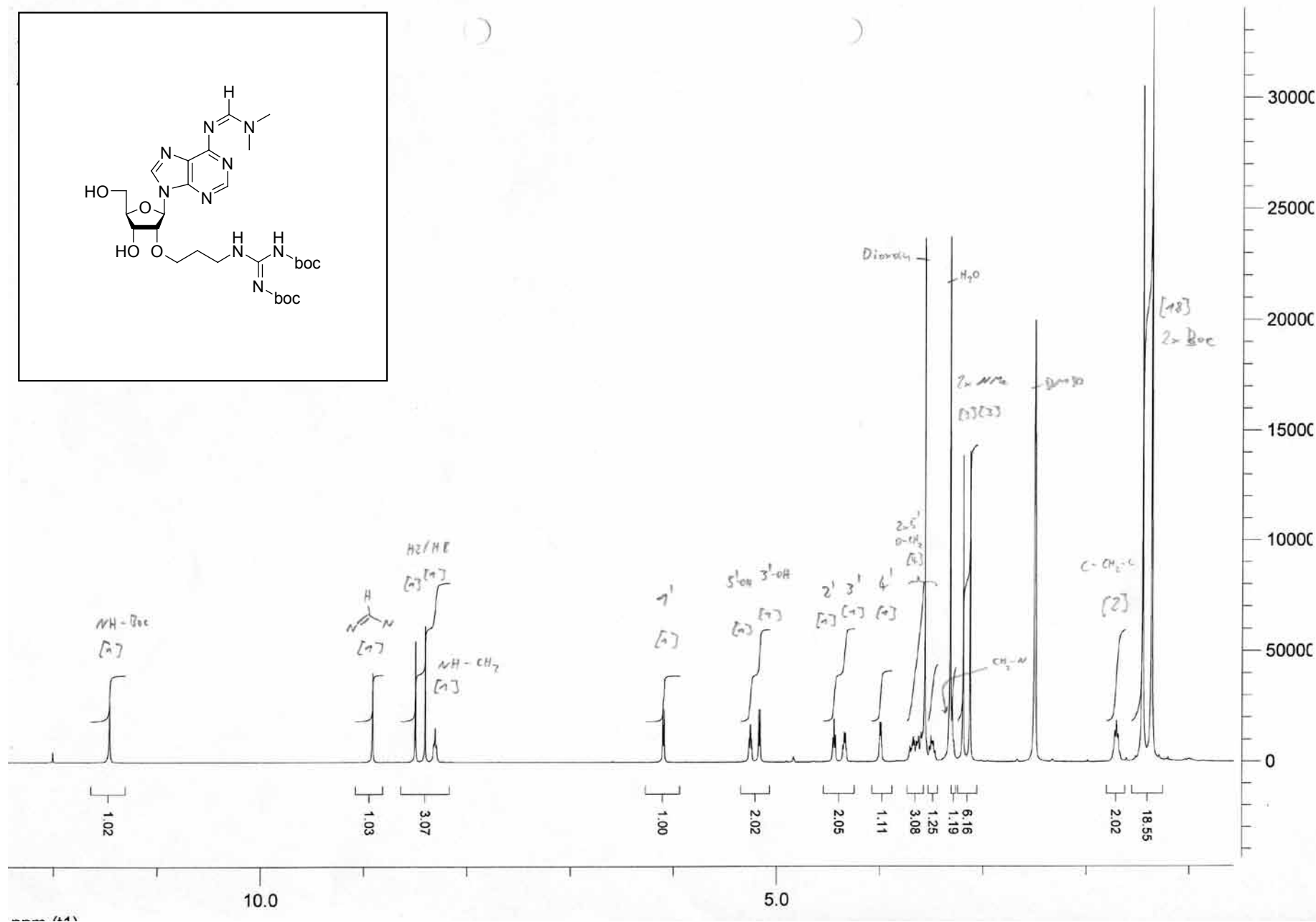
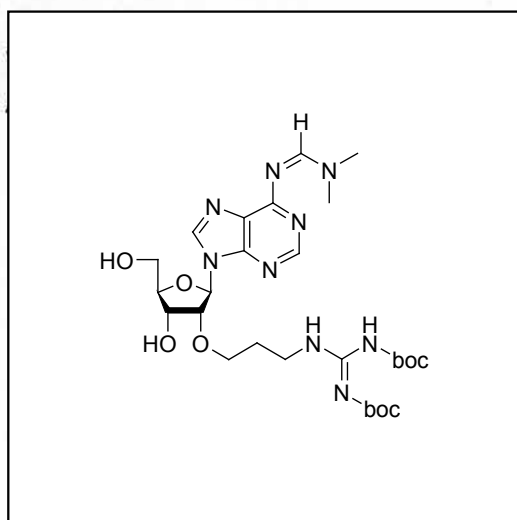
¹H NMR (300 MHz) in acetone-d₆



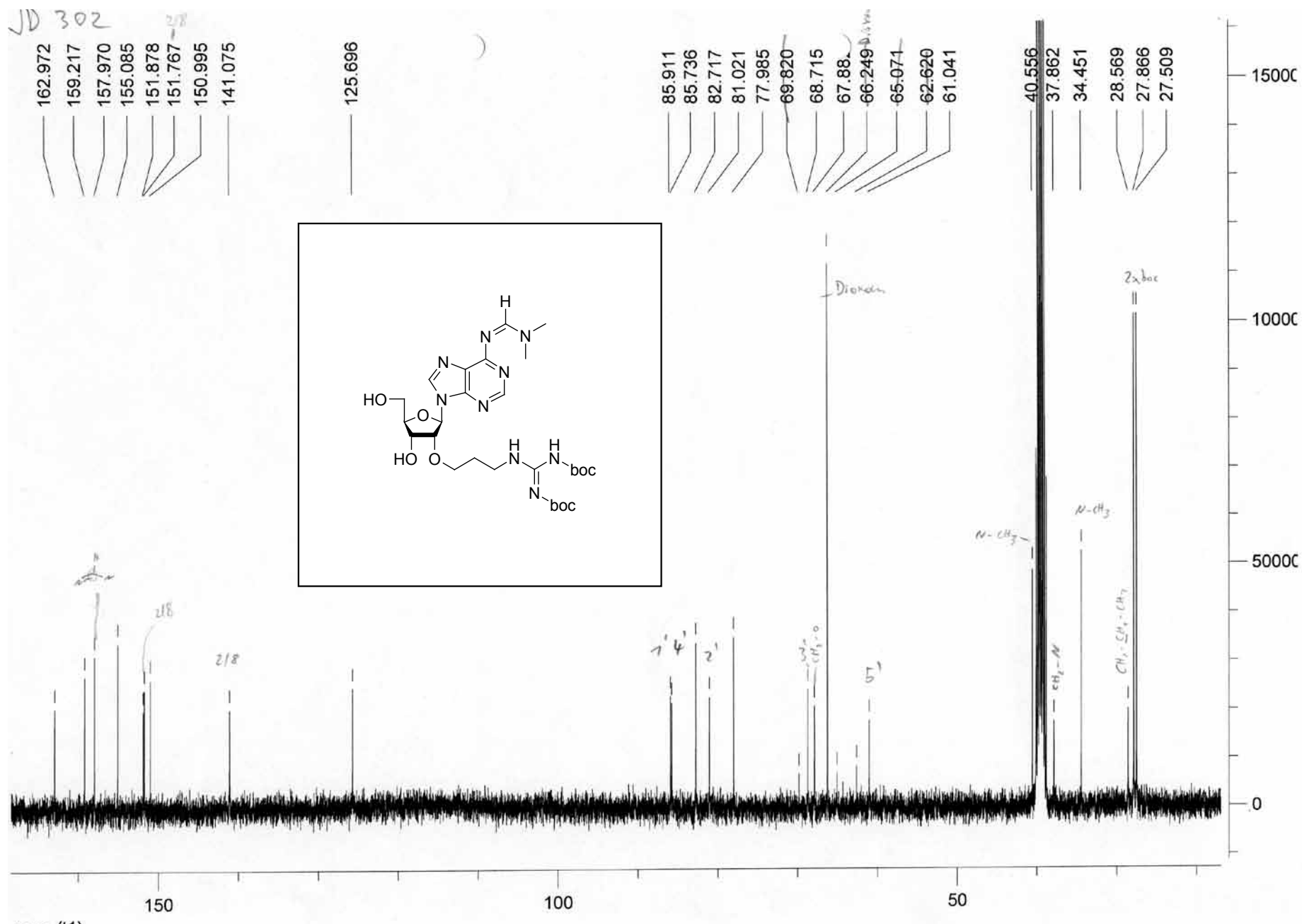
^{31}P NMR (121 MHz) in acetone- d_6



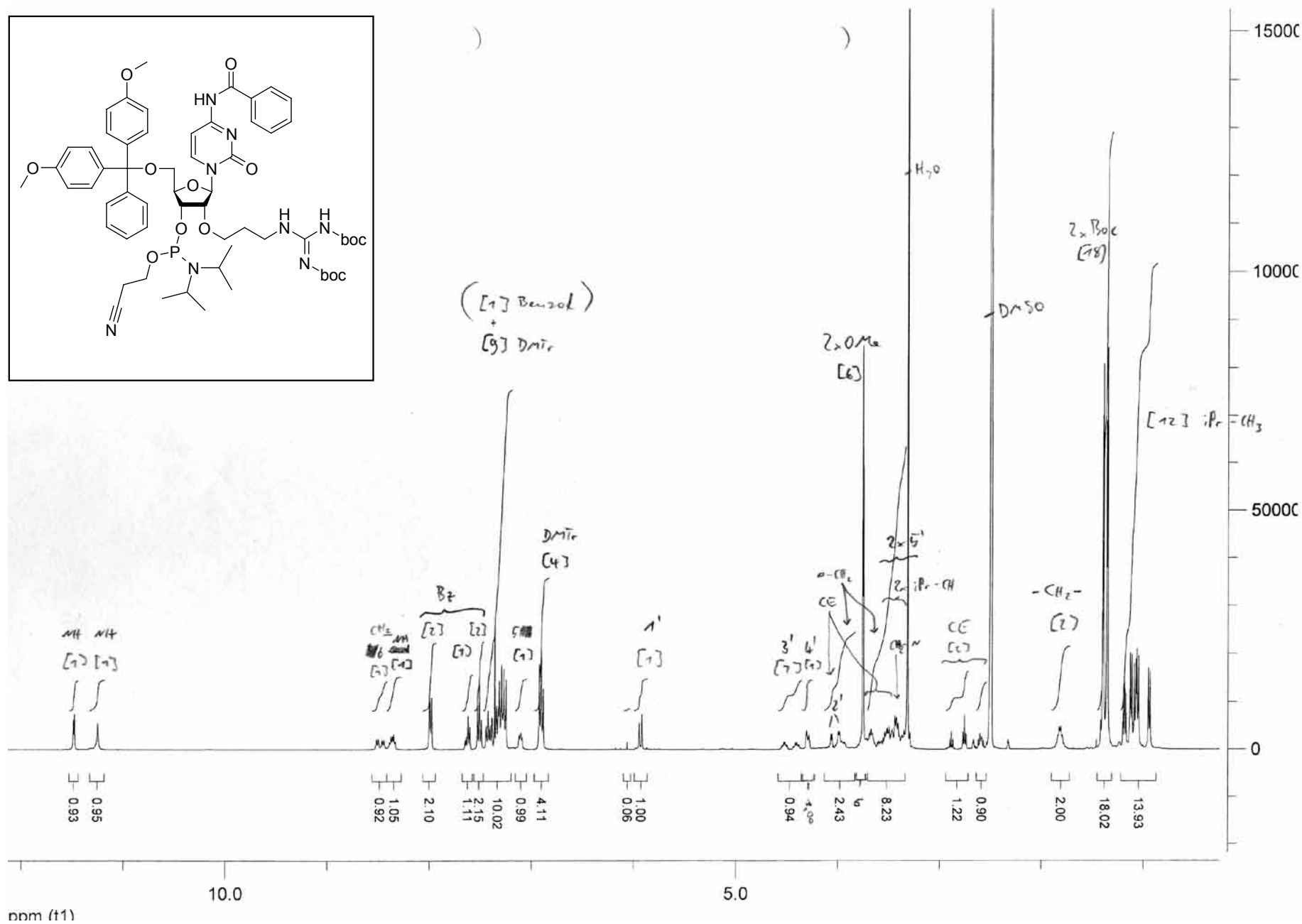
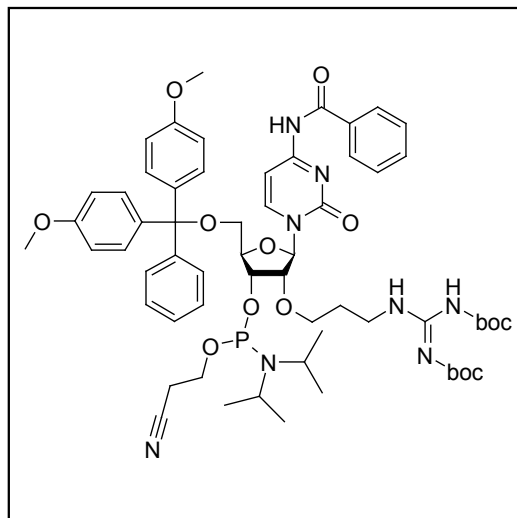
^1H NMR (400 MHz) in DMSO-d_6



^{13}C NMR (101 MHz) in DMSO-d_6



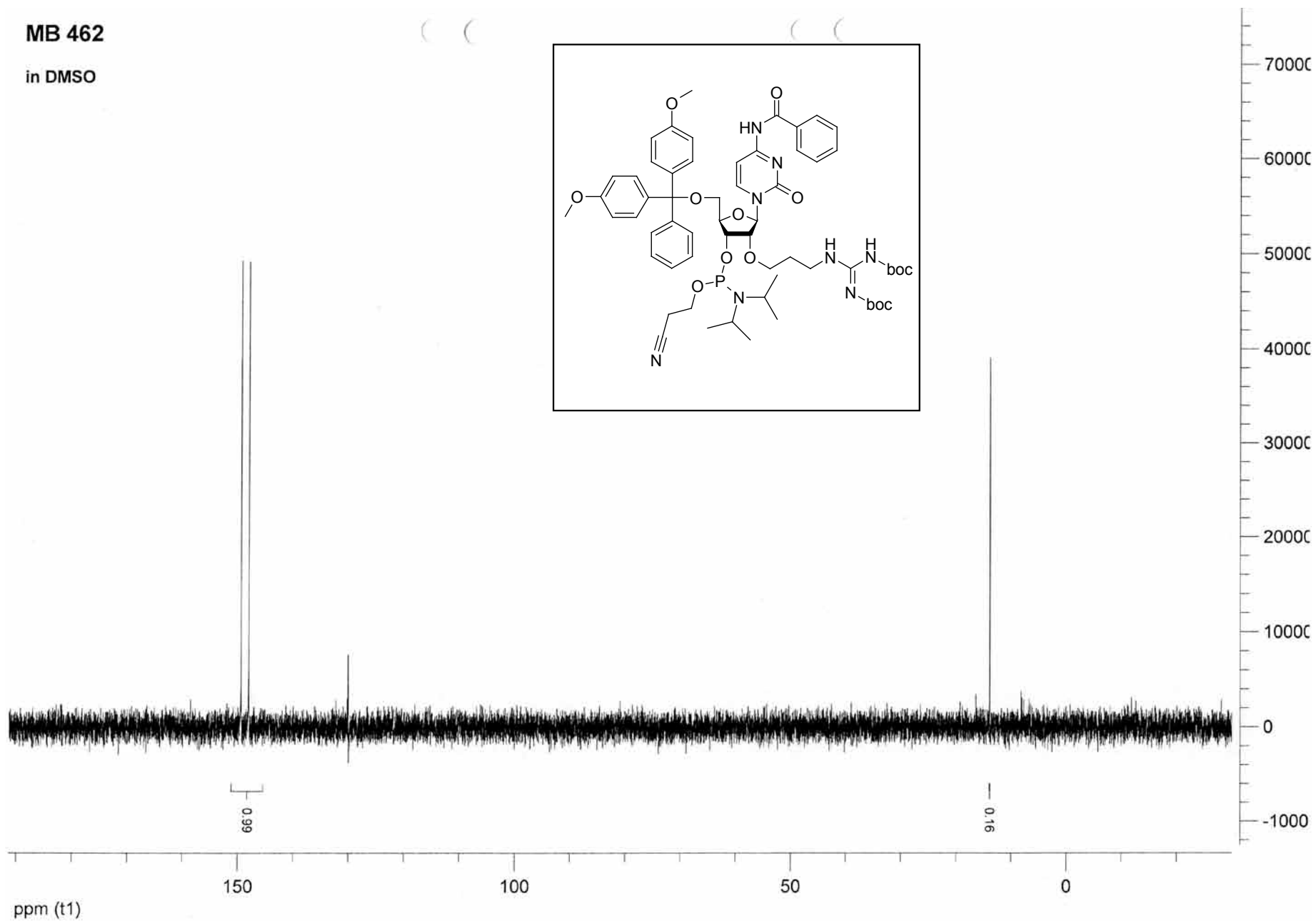
^1H NMR (400 MHz) in DMSO-d_6



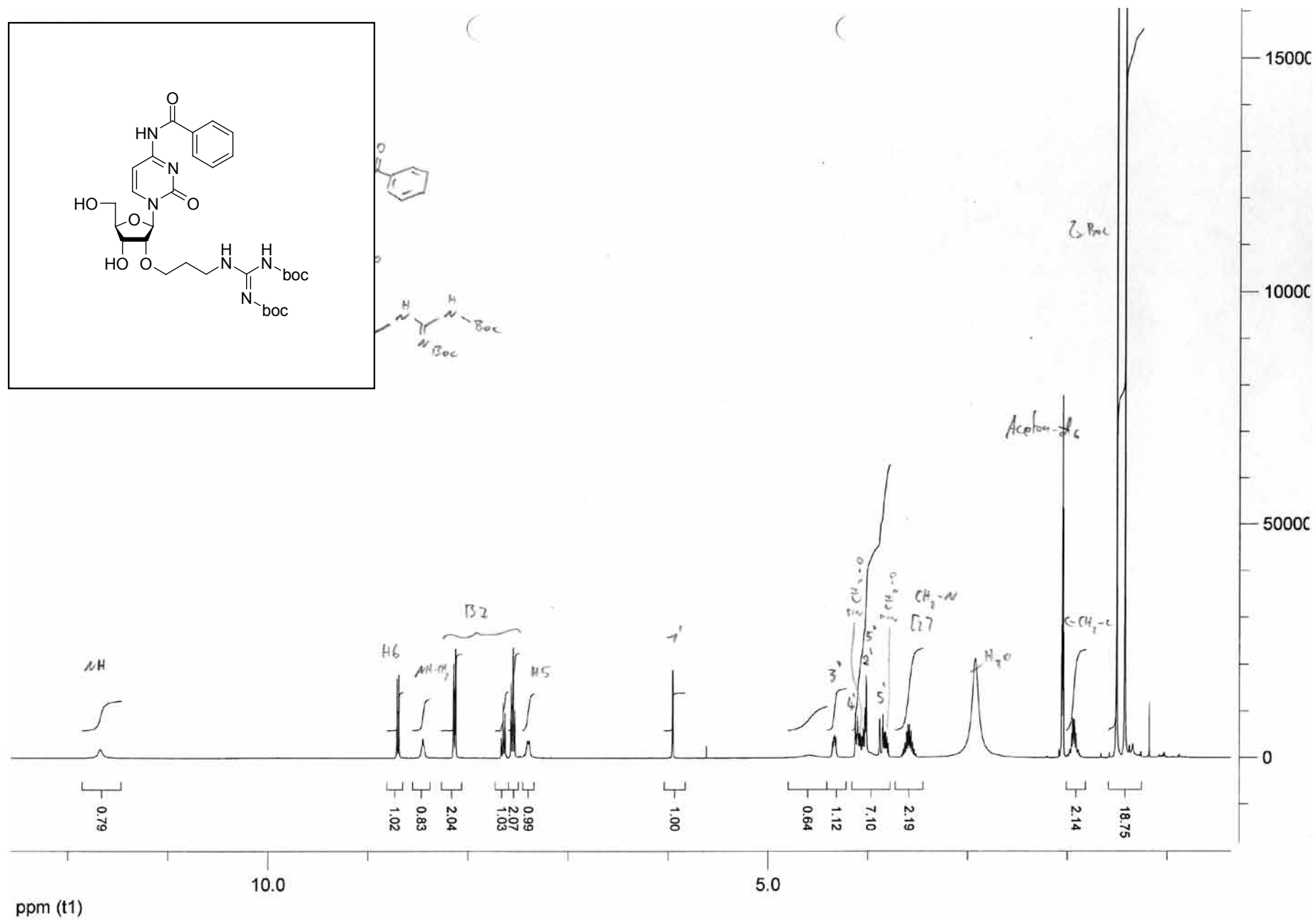
^{31}P NMR (162 MHz) in DMSO-d_6

MB 462

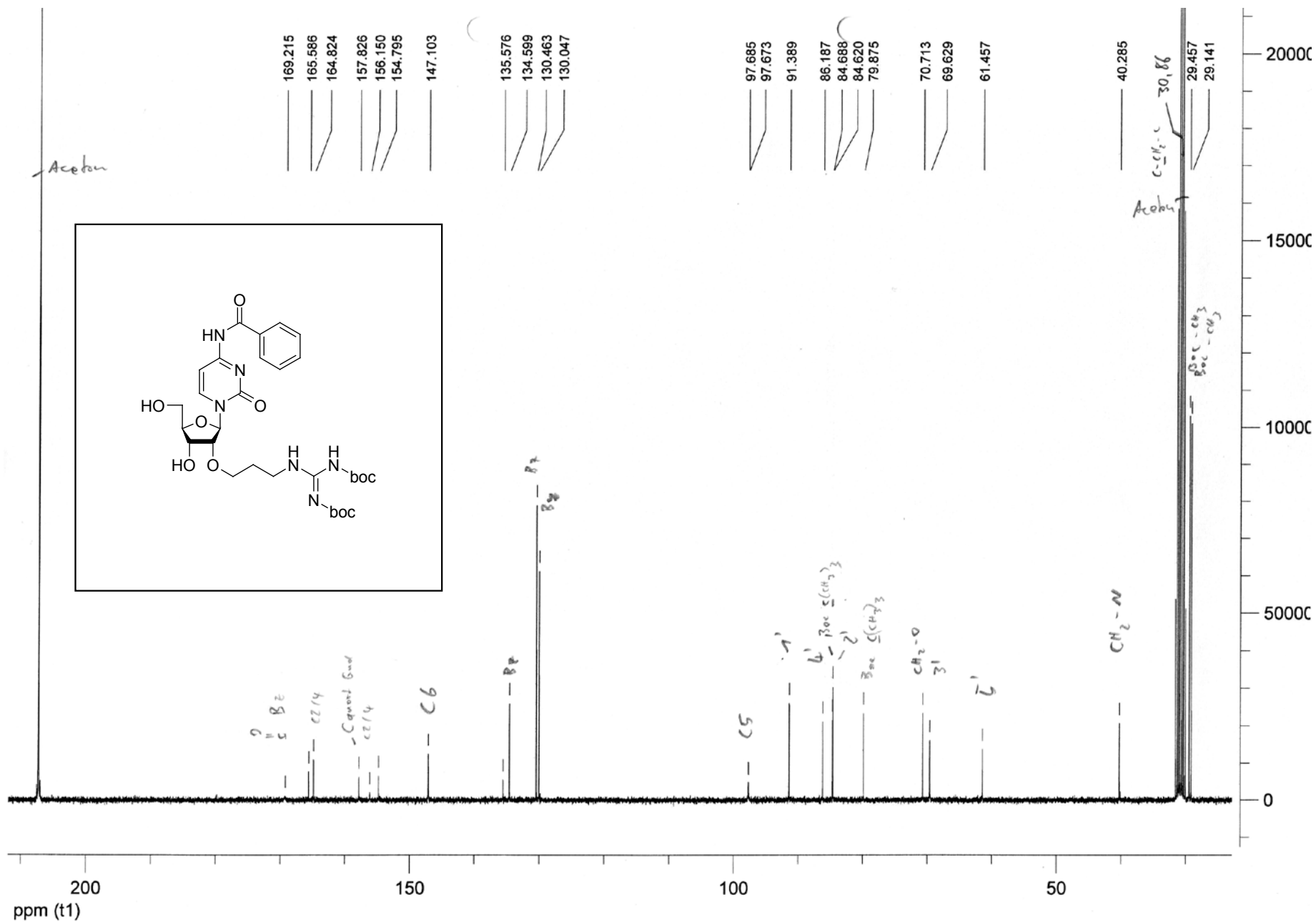
in DMSO



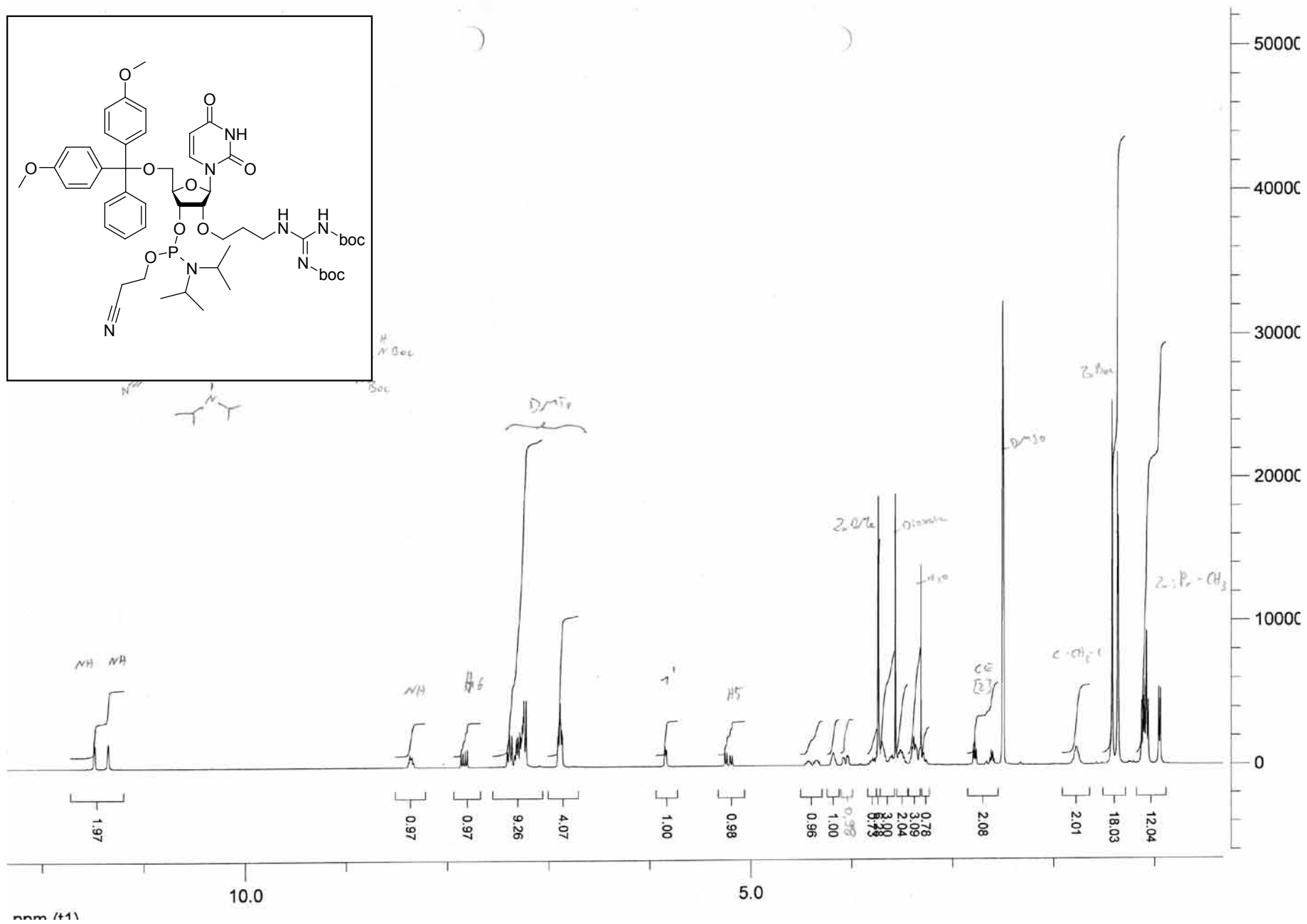
^1H NMR (300 MHz) in DMSO-d_6



^{13}C NMR (75 MHz) in acetone- d_6



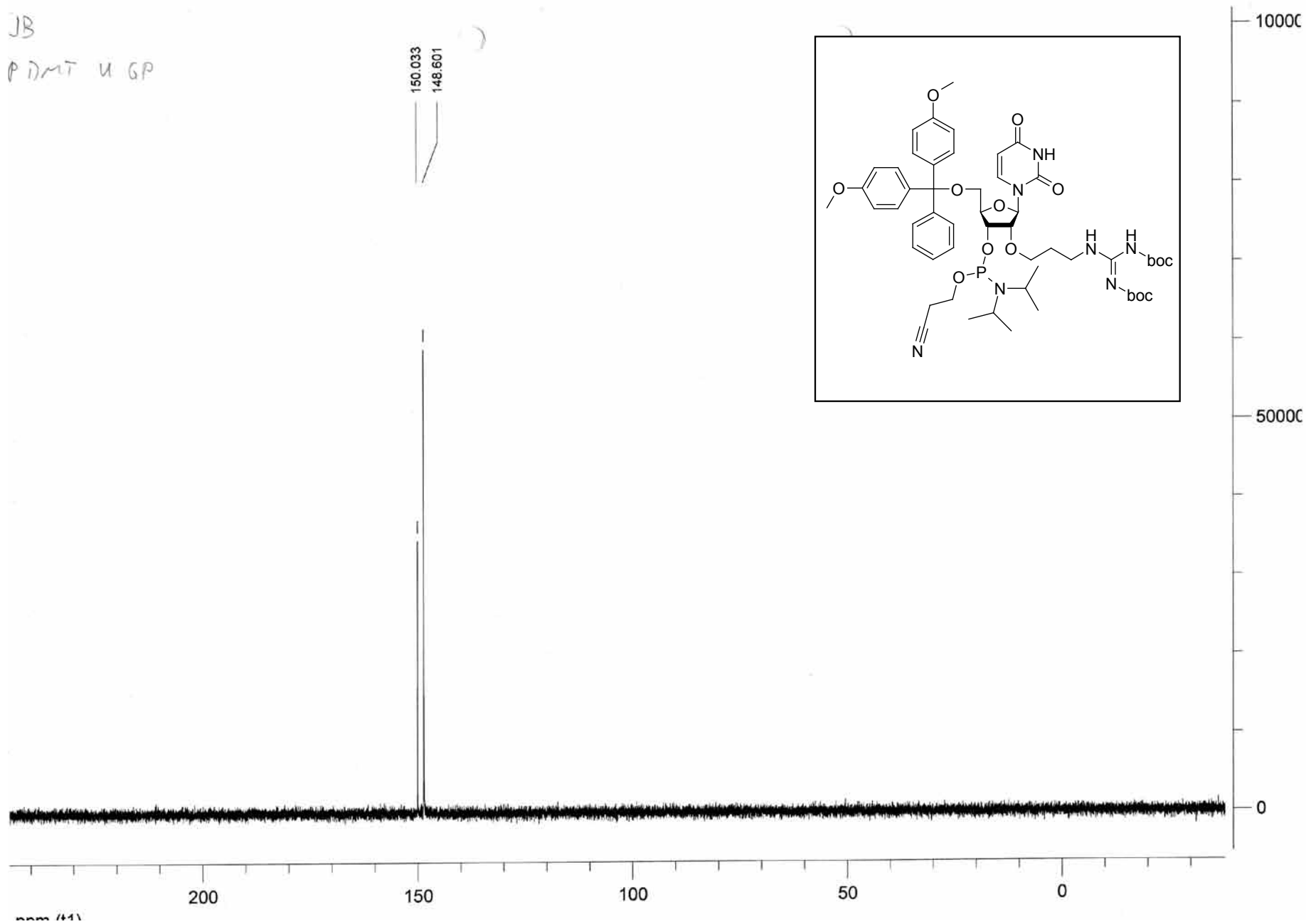
^1H NMR (400 MHz) in DMSO-d_6



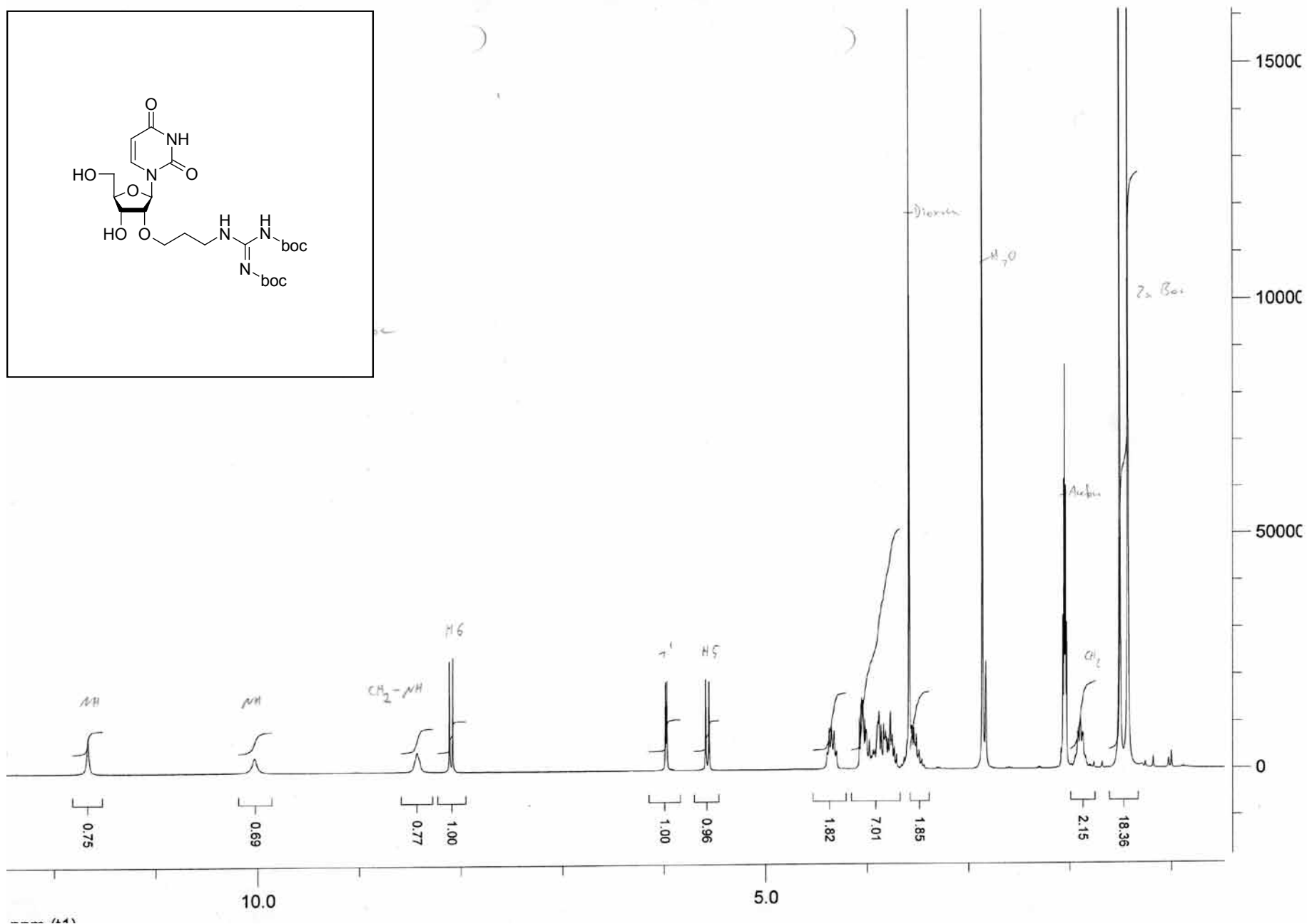
³¹P NMR (121 MHz) in DMSO-d₆

JB

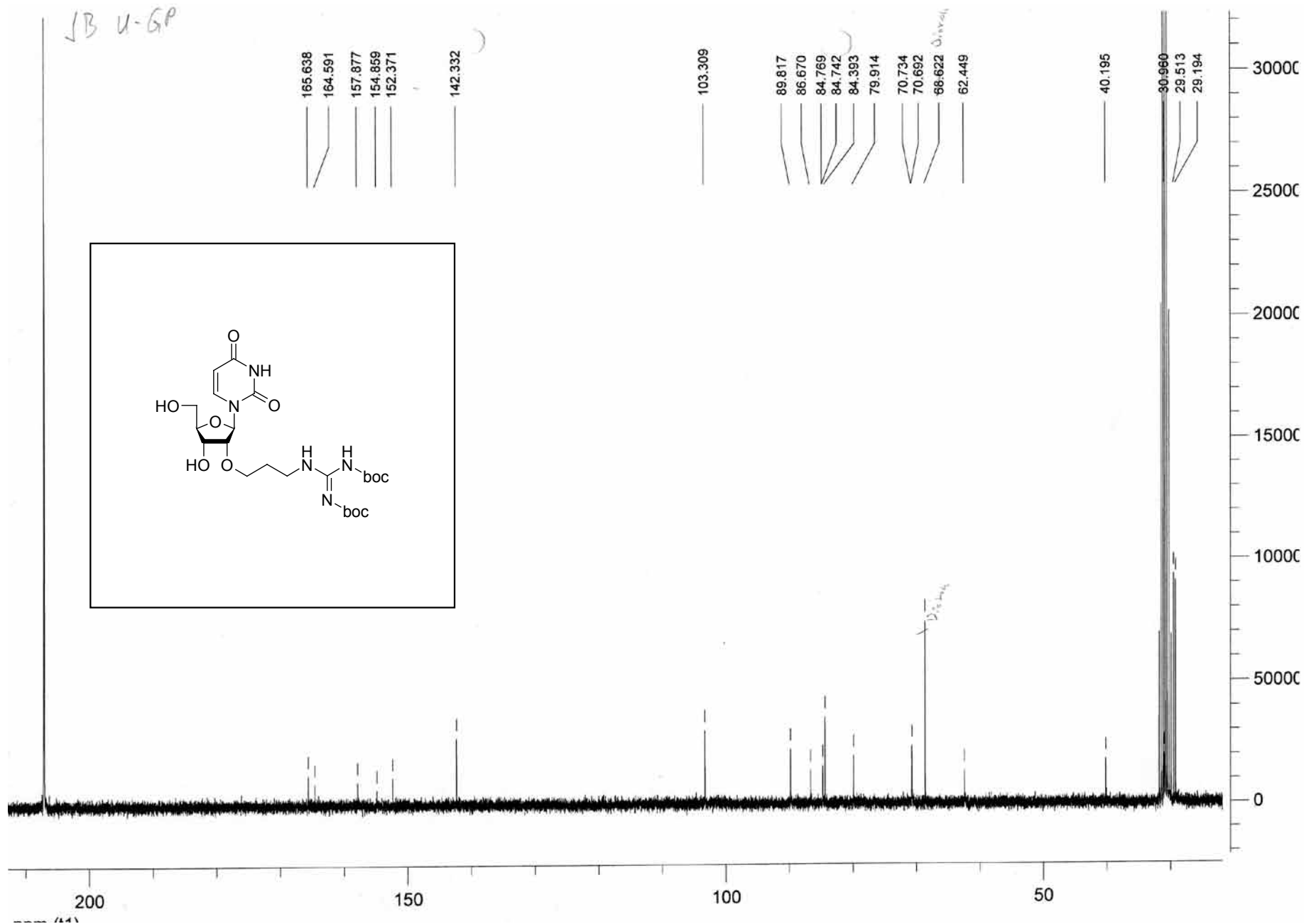
PDMT u GP



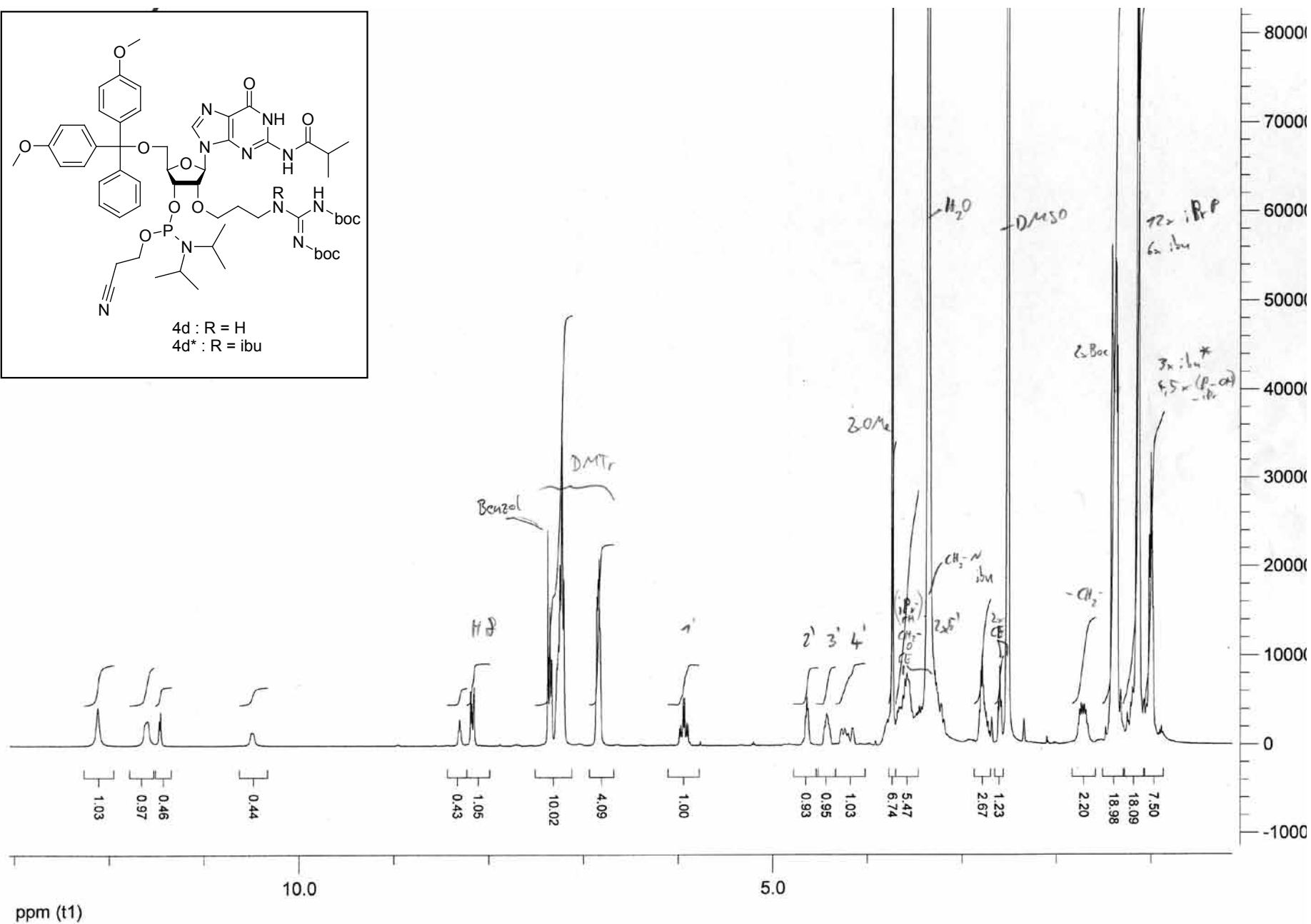
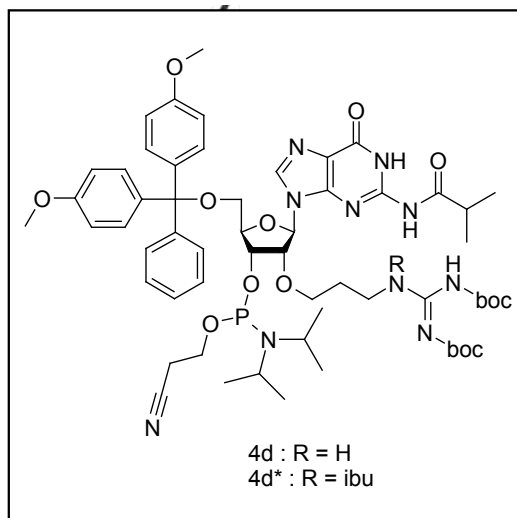
^1H NMR (250 MHz) in acetone- d_6



^{13}C NMR (63 MHz) in acetone- d_6

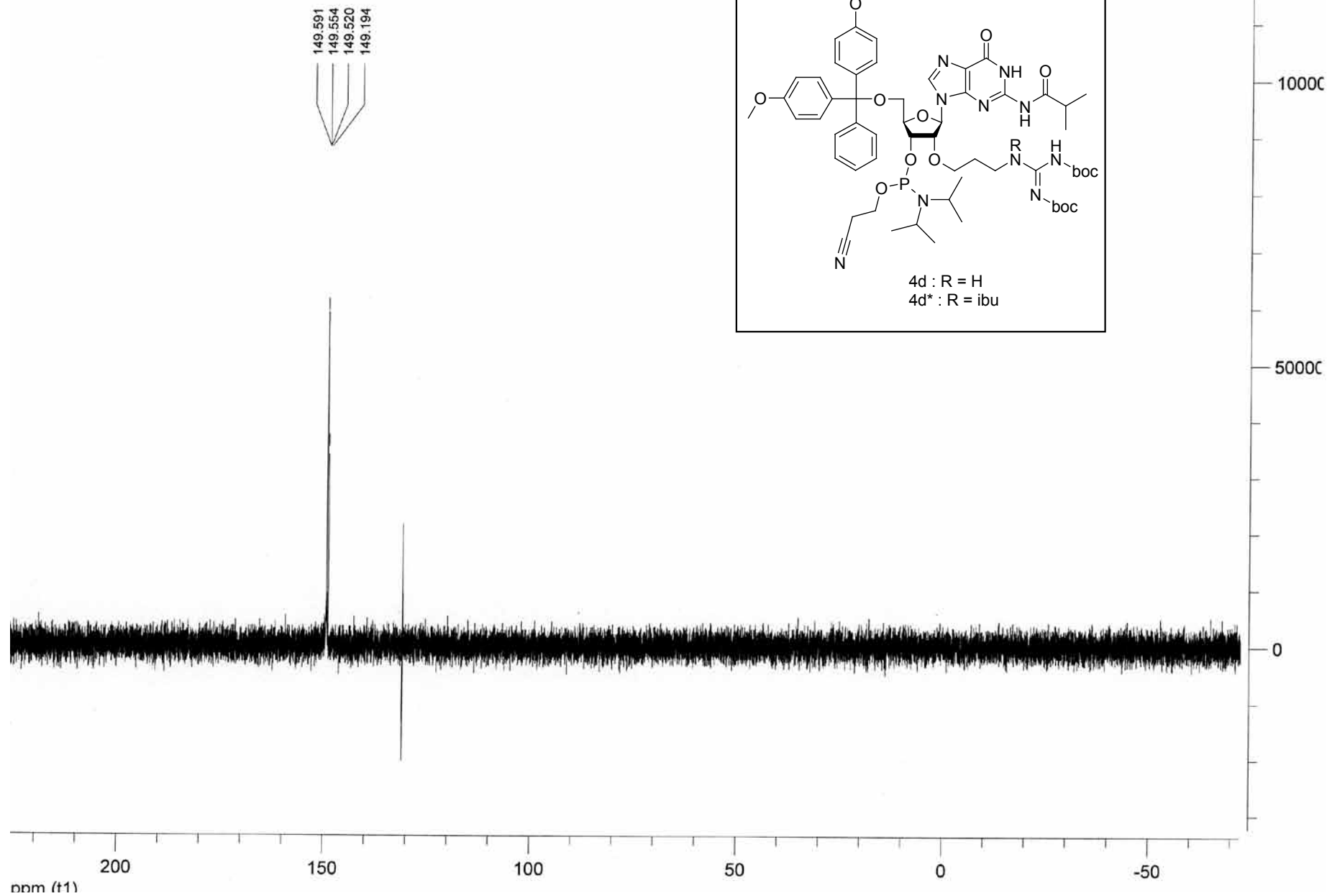


^1H NMR (400 MHz) in DMSO-d_6

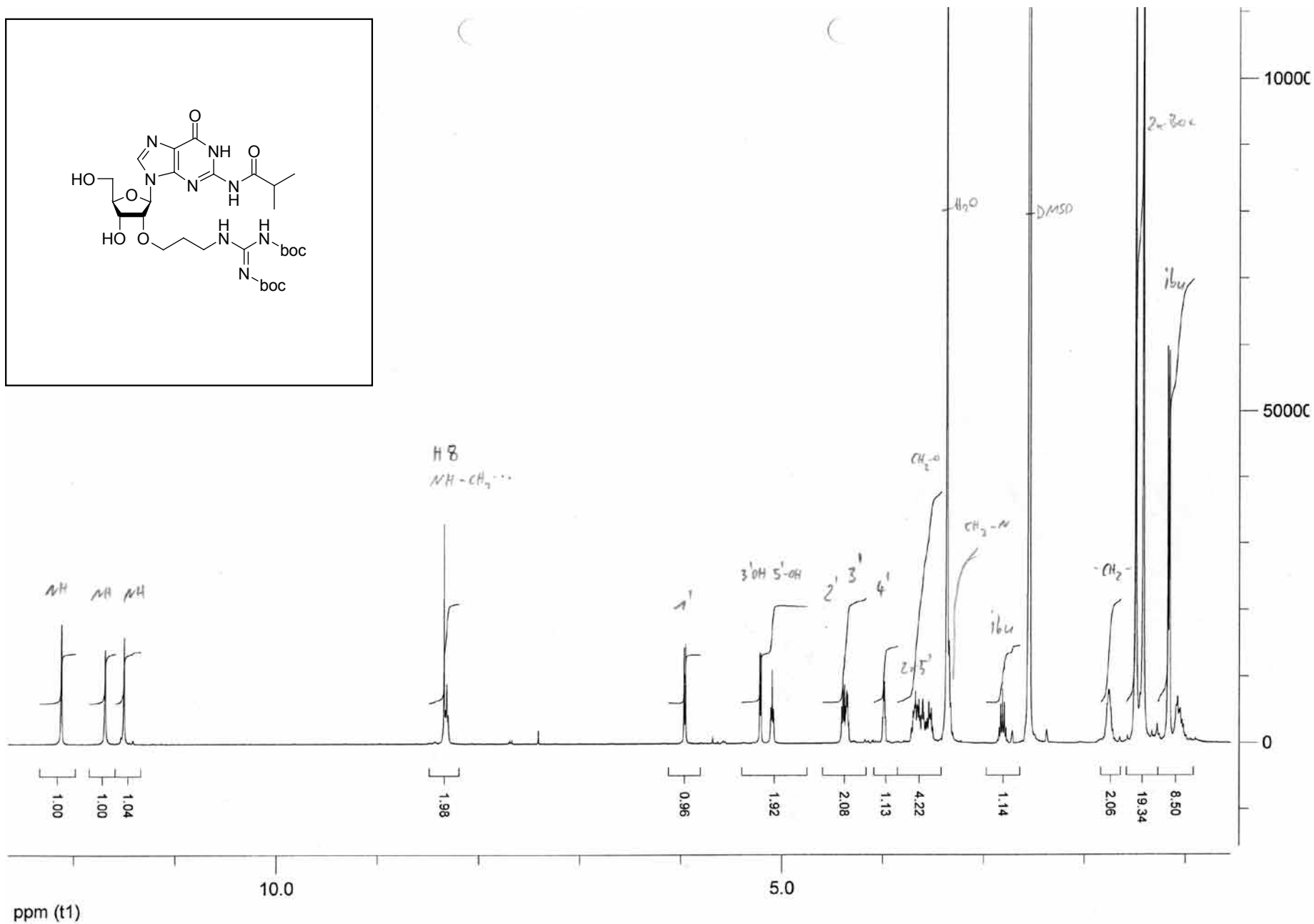
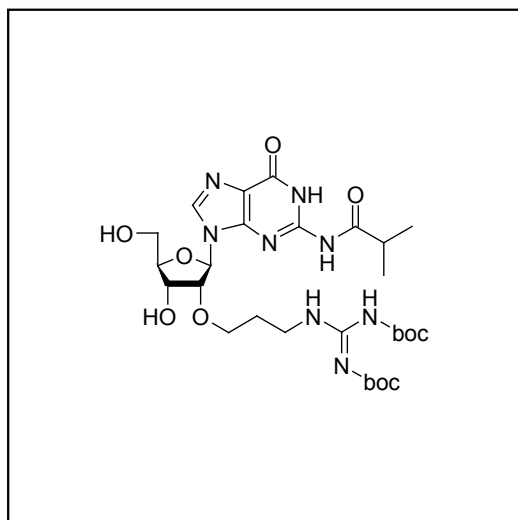


^{31}P NMR (162 MHz) in DMSO-d_6

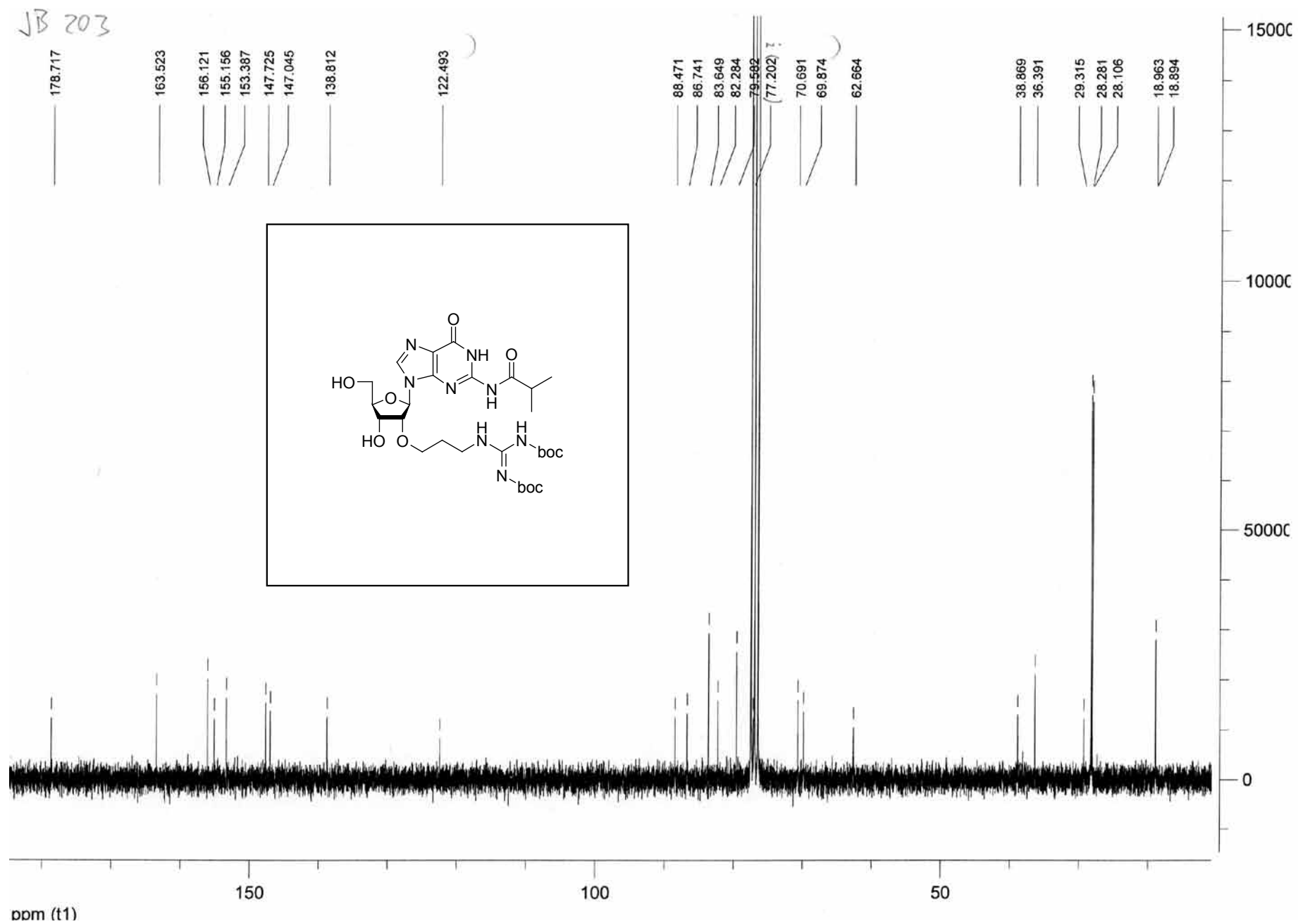
10 JB x 006 G



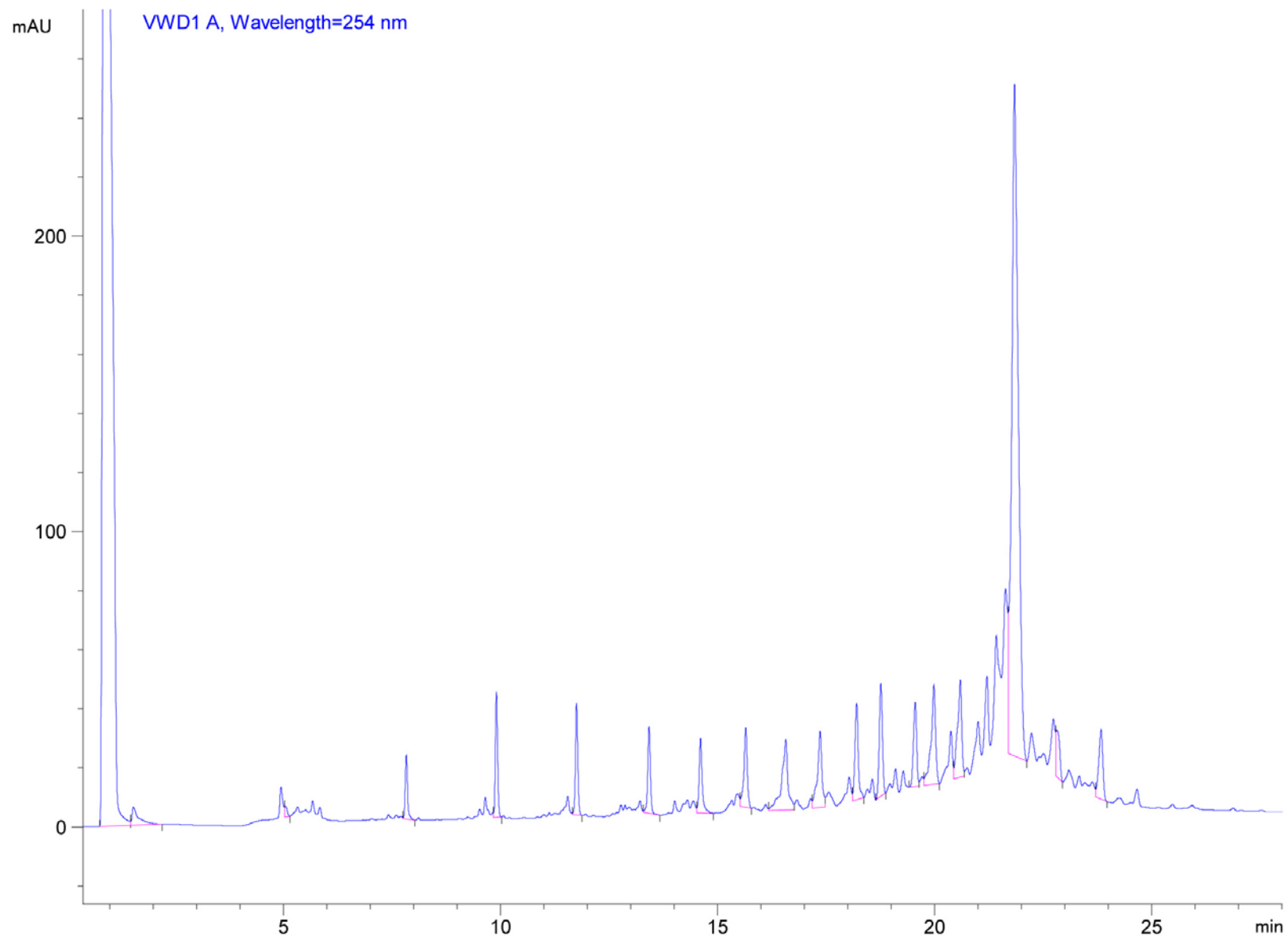
^1H NMR (400 MHz) in DMSO-d_6



^{13}C NMR (63 MHz) in CDCl_3

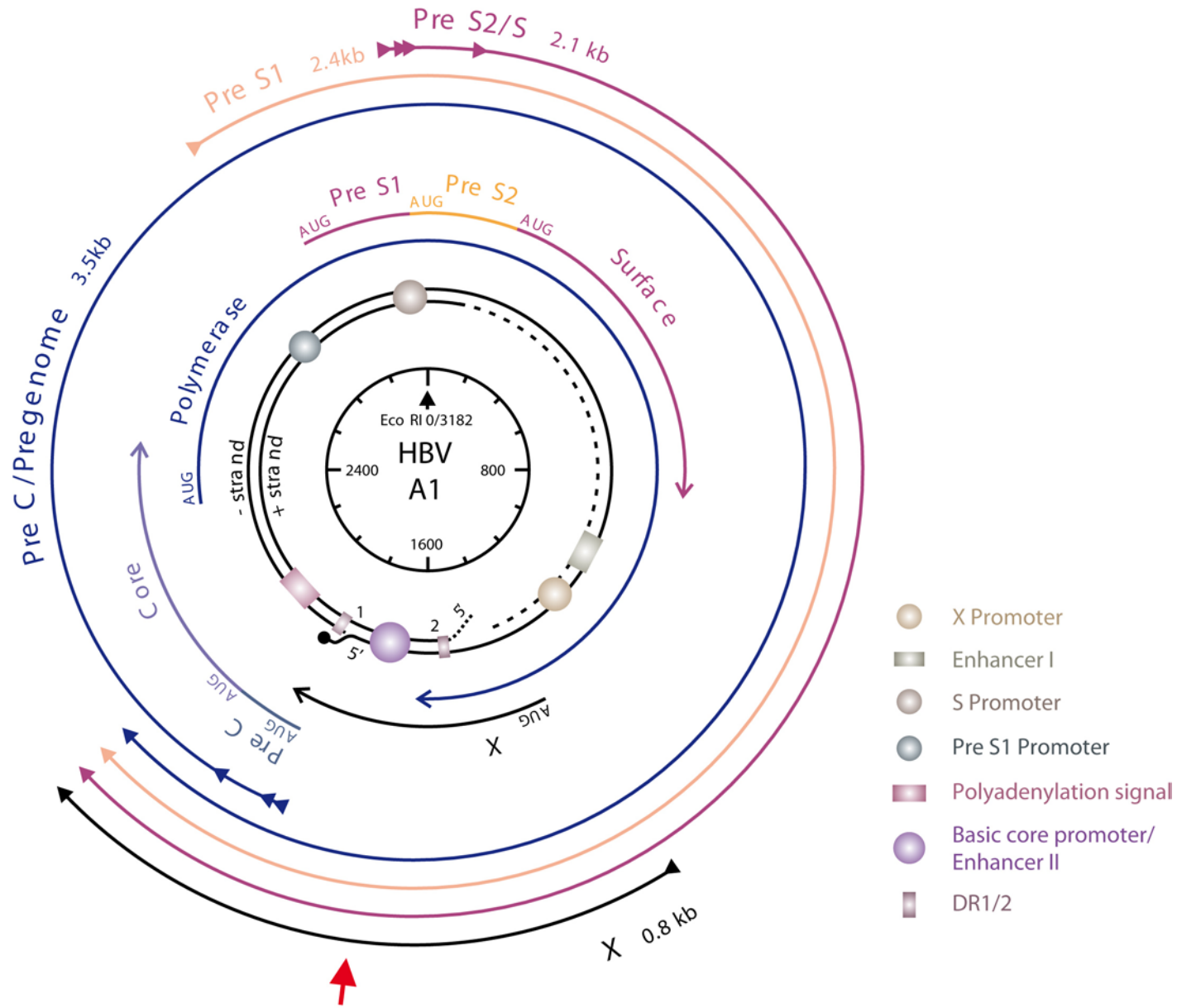


GP8 siRNA3 5- UUG AAG UA_{GP} U GCC UCA AGG UCG -3'



Exemplary anionexchange-chromatogram of the crude RNA (GP8 siRNA3) after basic deprotection (NH_3/EtOH 3:1, 40°C, 24h) and cleavage of TBDMS groups (triethylamine/*N*-methylpyrrolidinone/ $\text{Et}_3\text{N}\cdot 3\text{HF}$ 3 : 6 : 4, 65°C, 90 min) using a *Dionex* DNA-Pac 100 column (4 x 250 mm) (0.5 M NaClO_4 in 20 mM Tris-HCl pH = 8, 20 mM Tris-HCl pH = 8, gradient: 0 % to 75 % NaClO_4 solution in 38 minutes, flow: 1.5 mL/min, column was heated to 80°C).

Organisation of the hepatitis B virus genome



HBV siRNA 3
Targeted region 1693-1711

Use of Guanidinopropyl-Modified siRNAs to Silence Gene Expression

Maximilian C.R. Buff, Stefan Bernhardt, Musa D. Marimani, Abdullah Ely, Joachim W. Engels, and Patrick Arbuthnot

Abstract

Silencing gene expression by harnessing the RNA interference (RNAi) pathway with short interfering RNAs (siRNAs) has useful analytical and potentially therapeutic application. To augment silencing efficacy of siRNAs, chemical modification has been employed to improve stability, target specificity, and delivery to target tissues. siRNAs incorporating guanidinopropyl (GP) moieties have demonstrated enhanced target gene silencing in cell culture and in vivo models of hepatitis B virus replication. Here we describe the synthesis of GP-modified siRNAs and use of 5' rapid amplification of cDNA ends (5' RACE) to verify an RNAi-mediated mechanism of action of these novel chemically modified siRNAs.

Key words siRNA, RNAi, RNA, Oligonucleotide synthesis, Guanidinopropyl, HBV, 5' RACE

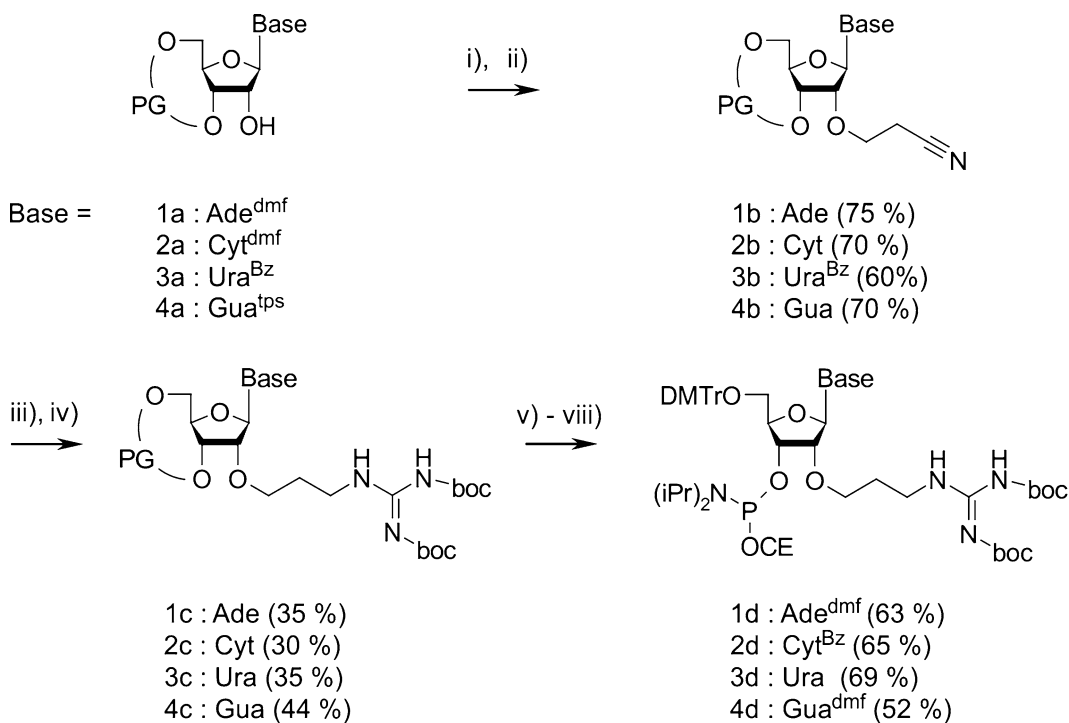
1 Introduction

Since discovery of the RNA interference (RNAi) pathway, there has been widespread interest in using exogenous sequences to silence a variety of gene targets. RNAi naturally occurs in cells of a variety of organisms, which include mammals, fungi, and plants (reviewed in [1]). The pathway typically involves expression and processing of RNA comprising hairpin motifs that are processed to form short duplex microRNAs (miRNAs) that comprise approximately 23 base pairs. One of the two strands of the mature miRNA is selected to serve as a guide sequence for mRNA inactivation by the RNA-Induced Silencing Complex (RISC). Complete pairing between the guide and target leads to Ago2-mediated cleavage of the mRNA (*see* Chapter 1). However partial complementarity between the seed region of miRNA guide strands and their targets naturally occurs more commonly to cause mRNA destabilization and translational suppression [2].

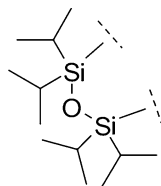
Exogenous RNA sequences used to reprogramme RNAi simulate intermediates of the pathway, and their guide strands are often designed to mediate silencing by causing cleavage of completely complementary target mRNA [3]. Synthetic short interfering RNAs (siRNAs), which mimic mature miRNAs, as well as DNA cassettes that express artificial pri-miRNAs and pre-miRNAs have been used widely to silence target gene expression. Since siRNAs are considerably smaller than pri-miRNA- or pre-miRNA-encoding DNA cassettes, delivery to target cells and better dose regulation are easier to achieve. Nevertheless, susceptibility of siRNAs to degradation, nonspecific gene silencing, and inadequate delivery to target cells remain problematic. Chemical modification of siRNAs offers the means of addressing these difficulties [4]. Several different approaches have been employed, which include addition of various groups to the 2' and 4' carbons of ribose, changes to the phosphodiester linkage and substitution of ribose with other sugars [5, 6].

In earlier studies, our groups have shown that incorporating 2'-*O*-guanidinopropyl (GP) moieties can be used successfully to improve stability, efficacy, and specificity of siRNAs that target the *HBx* open reading frame of hepatitis B virus (HBV) [7, 8]. Detailed analysis, which entailed incorporation of GP substitutions at positions 2 to 21 of the intended siRNA guide, demonstrated that modifications to nucleotides in the seed region limited off target silencing. Melting point analysis showed that the GP modifications caused only minimal destabilization of the duplexes. An added potential benefit of introducing a positive charge within the GP residue is that the overall neutralization of the negative charge of the siRNAs facilitates their delivery to target cells. Using murine hydrodynamic tail vein injection to administer siRNAs resulted in highly effective knock down of viral replication markers in vivo. Collectively these positive features indicate that GP modification of siRNAs has potential utility for gene silencing.

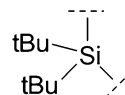
Here we describe our improved and now standard synthesis procedures for the generation of GP-modified nucleosides and their incorporation into siRNAs. Importantly, one of the changes involved replacing the isobutyryl group to a dimethylformamidino group at the N²-position of guanosine, thus avoiding formation of a mixture of mono- and di-isobutyryl substituted compounds during the synthesis. This alteration in procedure improved the product yields considerably. Production of each of the adenosine (A), cytidine (C), and uridine (U) derivatives follows an analogous chemical protecting scheme, while the protecting groups of the guanosine (G) derivative was changed slightly to improve yields and purity (Scheme 1). Each synthesis started with simultaneous protection of 5'- and 3'-OH-groups with either 1,1,3,3-tetraisopropylidisiloxane-1,3-diyl (TIPS) for adenosine (**1**), cytidine (**2**), and uridine (**3**) or di-*tert*-butylsilylaniyadiyl (DTBS) for



PG (protecting group) for A, C and U:



for G:



Scheme 1 Synthesis of the 2'-*O*-guanidinopropyl adenosine-, cytidine- uridine- and guanosine-phosphoramidites for oligoribonucleotide synthesis. (i) acrylonitrile, CsCO₃, *tert*-butyl alcohol, rt; (ii) H₂N-NH₂·H₂O, methanol, rt (adenosine and cytidine derivative); formic acid (70 %), dioxane/water (guanosine derivative); no deprotection of the uridine derivative; (iii) H₂ (30 bar), Raney-Nickel, NH₃, methanol, 30–60 min, rt; (iv) *N,N'*-di-Boc-*N''*-triflylguanidine, Et₃N, CH₂Cl₂, 0 °C (30 min) to rt (30 min); (v) DMF-dimethyl diacetale, methanol, rt (adenosine and guanosine derivative); benzoyl chloride, pyridine, 0 °C (30 min) to rt (30 min) (cytidine derivative); no protection group was applied to the uridine derivative; (vi) Et₃N·3HF, THF, rt; (vii) 4,4'-dimethoxytrityl chloride, pyridine, rt; (viii) 2-cyanoethyl *N,N,N',N'*-tetraisopropylphosphane, 4,5-dicyanoimidazole, CH₂Cl₂, rt

guanosine (**4**). The latter was chosen to improve the reported selectivity for the subsequent 2,4,6-triisopropylbenzenesulfonyl (TPS) protection at the *O*⁶-position of guanosine (**4a**) [9]. The exocyclic amino functions of A and C were protected with dimethylaminomethylene groups employing standard conditions and a benzoyl group was attached to *N*³-position of U [10]. The first key step follows Michael addition of acrylonitrile in *tert*-butanol

with Cs_2CO_3 as base to 2'-*O*-cyanoethyl [11]. Deprotection of dimethylaminomethylene groups of the A and C with hydrazine yielded **1b** and **2b**. This additional deprotection step was necessary to avoid formation of mixtures of dimethylaminomethylene-protected and unprotected derivatives. The TPS-group from the O⁶-position of the guanosine derivative was cleaved with a mixture of formic acid (70 %), dioxane, and water (**4b**). For production of the uridine derivative, this extra step was not necessary. In the next key step, the nitrile to amine transformation was achieved by reduction with hydrogen (30 bar) and using Raney-nickel in ammonia and methanol as catalyst [12]. The hydrogenation step was found to be sensitive to subtle variations in the reaction conditions, which include the mass ratio of starting material to catalyst, the size of the autoclave and the reaction time. Under optimal conditions we were able to produce yields of about 50 % for each nucleoside. Despite intensive washings with methanol, critical loss of the desired amino compound occurred as a result of adsorption onto the catalyst. To minimize this, we introduced the guanidino groups directly. Thus *N,N'*-di-Boc-*N''*-triflylguanidine, now commercially available [13], was added as guanidinylation agent. Our previous studies showed that two boc groups are sufficient in RNA solid phase synthesis, although they are cleaved after repetitive acid deprotection using TBDMS-phosphoramidite protocols. The guanidino group does not seem to undergo side reactions during the solid phase synthesis. Yields after guanidinylation were 70 % for **1c** (A), 60 % for **2c** (C), around 60 % for **3c** (U) and approximately 90 % for **4c** (G).

Established standard reaction conditions were applied to synthesize the desired phosphoramidites (**1d** – **4d**). The A and G derivatives were protected with dimethylaminomethylene at the N⁶- or N²-positions, and the exocyclic amino function of the C derivative was protected with a benzoyl group. For U derivative, no further protection of the base was necessary. Finally we accomplished the synthesis of all four 2'-*O*-guanidinopropyl phosphoramidites by removal of silyl protecting groups with $\text{Et}_3\text{N} \cdot 3\text{HF}$. Then the 5'-OH-group was protected with a 4,4'-dimethoxytrityl group and in a last step the 3'-OH group was converted to a phosphoramidite using 2-cyanoethyl *N,N,N',N'*-tetraisopropylaminophosphane and 4,5-dicyanoimidazole as activator. Starting with the adenosine, cytidine, uridine, and guanosine nucleosides, synthesis of the 2'-*O*-guanidinopropyl phosphoramidites took place in 6–8 steps and routinely provided overall yields of 16–17 % (**1d**), 13–14 % (**2d**), 14–15 % (**3d**) and 16–17 % (**4d**).

To incorporate GP-containing nucleotides into the oligonucleotides constituting the siRNAs, standard phosphoramidite synthetic procedures with a prolonged coupling time of 30 min were employed. Control siRNA3 without GP moieties, referred to in

this study as being unmodified, were also synthesized. The siRNAs contain the classical two dT residues at the 3' end of the sense strand to improve stability. In addition to the detailed description of the methods for synthesis of GP-modified siRNAs, procedures for verifying Ago2-mediated target HBV mRNA cleavage by GP-modified siRNAs, using 5' rapid amplification of cDNA ends (RACE), are presented.

2 Materials

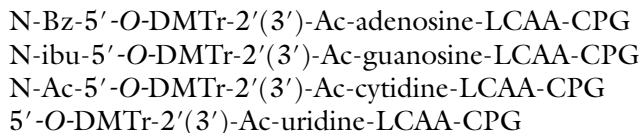
2.1 Synthesis of 2'-O-GP-Modified Nucleotide Precursors

The syntheses of the GP-modified phosphoramidites are performed with standard chemicals and solvents suitable for chemical synthesis. Chemicals were purchased from *Sigma-Aldrich*, *TCI*, *Acros Organics*, and *ChemGenes* among other suppliers.

1. Chemicals and solvents for syntheses: adenosine, cytidine, uridine, guanosine, 1,3-dichloro-1,1,3,3-tetraisopropylidisiloxane, di-*tert*-butylsilyl ditriflate, *tert*-butanol, acrylonitrile (freshly distilled), cesium carbonate, hydrazine hydrate ($\text{H}_2\text{N}-\text{NH}_2 \cdot \text{H}_2\text{O}$), Raney-Nickel (activated nickel catalyst), methanol saturated with ammonia, hydrogen (H_2 , compressed in a steel cylinder), triethylamine, *N,N'*-di-boc-*N''*-triflyl guanidine, *N,N*-dimethylformamide dimethylacetale, triethylammonium trihydrofluoride ($\text{Et}_3\text{N} \cdot 3\text{HF}$), 4,4'-dimethoxytrityl chloride, 2-cyanoethyl-*N,N,N',N'*-tetraisopropylamino phosphane, 4,5-dicyanoimidazole, benzoyl chloride, ammonium hydroxide solution (25–33 % in water), sodium carbonate, tetrabutylammonium bromide, 4-(*N,N*-dimethylamino)pyridine (DMAP), 2,4,6-triisopropylbenzenesulfonyl chloride, formic acid, dioxane, ethanol, acetone, benzene, pyridine, toluene.
2. Water-free solvents for syntheses (bottled with septum and molecular sieve): dichloromethane, dimethylformamide, methanol, pyridine, tetrahydrofuran.
3. Solutions and desiccants for workup: saturated sodium bicarbonate solution, saturated sodium chloride solution (brine), anhydrous magnesium sulfate, or sodium sulfate, celite.
4. Solvents for extractions and column chromatography: dichloromethane, ethyl acetate, hexane, methanol. (We used technical grade solvents that were redistilled before usage to avoid contamination of the purified products with nonvolatile impurities of the solvents.)
5. Solid-phase material for column chromatography: silica gel 60 with grain size of 0.04–0.063 mm (e.g. from *Merck KGaA* or *Macherey-Nagel GmbH & Co. KG*), TLC plates: silica gel 60 on aluminum foil with fluorescence indicator (254 nm).

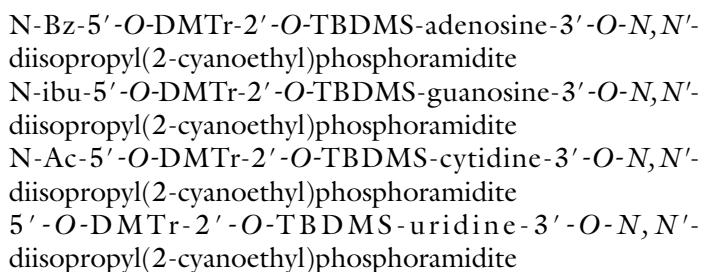
2.2 Solid-Phase Oligonucleotide Synthesis

1. Empty synthesis columns fitting to your synthesizer (e.g. from *Glen Research* or *ChemGenes*)
2. Ribonucleoside functionalized solid support (LCAA-support, 500 Å, e.g. from *ChemGenes*):



Commercially available prepacked synthesis columns may also be used.

3. Ribonucleoside phosphoramidites for unmodified positions (e.g. from *SAFC/Proligo* or *ChemGenes* or *Glen Research*):



4. Reagents and solvents required for the synthesizer (e.g. from *SAFC/Proligo*): anhydrous acetonitrile, deblock solution (3 % trichloroacetic acid in dichloromethane), activator (0.35 M 5-ethylthiotetrazole (ETT) in acetonitrile (*see Note 1*)), Cap A (acetic anhydride/tetrahydrofuran 9.1/90.9 (v/v)), Cap B (Tetrahydrofuran/N-Methylimidazole/Pyridine 8/1/1 (v/v/v)), oxidizer (0.1 M iodine in tetrahydrofuran/pyridine/water (75:20:2 v/v/v))
5. Amidite diluent: anhydrous acetonitrile (100 mL, bottled with septum, e.g. from *SAFC/Proligo*)

2.3 Workup, Purification, and Analytics of 2'-O-GP-Modified Oligonucleotides

1. Oligonucleotide cleavage: For cleavage from solid support and removal of the cyanoethyl groups and exocyclic amino protecting groups of the bases we use a 3:1 mixture of ammonium hydroxide solution (25–33 % in water) and ethanol.
2. Cleavage of the 2'-O-TBDMS-groups: Et₃N · 3HF/1-methyl-2-pyrrolidone/Et₃N (6:3:4, v/v/v)
3. DEPC-water: Diethylpyrocarbonate (DEPC) is dissolved in distilled or deionized water (0.1 % DEPC). The solution is kept overnight at room temperature and then autoclaved at 120 °C for 20 min to deactivate the DEPC.
4. For RNA-precipitation: n-Butanol
5. LiCl-Buffer: 1 M lithium chloride in DEPC-water, adjusted to pH 8.
6. Triethylammonium acetate buffer: 0.1 M triethylammonium acetate in DEPC-water. We prepare a 1 M solution of triethylammonium

acetate and dilute it 1:9 with DEPC-water before usage. For the 1 M solution acetic acid (60.05 g, 57.2 mL, 1 mol) is dissolved in 700 mL DEPC-water. Triethylamine (101.2 g, 138.6 mL, 1 mol) is added in small portions while the solution is stirred vigorously. Caution: As a result of the enthalpy of the neutralization reaction, the solution heats up, so cooling may be required. After the solution has cooled down to room temperature, the volume is adjusted to 1,000 mL with DEPC-water and the pH is adjusted to pH 7 with acetic acid or triethylamine.

7. Anion-exchange HPLC-column: *Dionex* DNA Pac PA-100 (9 mm × 250 mm)
8. Reverse-phase HPLC-column: *Phenomenex* Jupiter 4u Proteo 90 Å 250 mm × 15 mm.
9. Chemicals: acetic acid, triethylamine, lithium chloride, 1-methyl-2-pyrrolidone.

2.4 Analysis of RNAi-Mediated Target Cleavage by GP-Modified siRNAs Using 5' RACE

- 1 Stock solutions of target and reporter plasmids (100 ng/μL) prepared using anion-exchange resins (e.g. Qiagen Plasmid Maxi Kit, MD, USA): pCH-9/3091¹⁴, pCI-neo-eGFP¹⁵ (*see Note 2*).
- 2 Lipofectamine®-2000 and Opti MEM® (Invitrogen, CA, USA).
- 3 Tri Reagent® (Sigma, MO, USA).
- 4 Diethyl pyrocarbonate-treated water (*see above*).
- 5 GeneRacer™ Kit (Invitrogen, CA, USA).
- 6 Thermocycler (e.g. T100™ Instrument from BioRad, CA, USA)
- 7 MinElute Gel Extraction kit (Qiagen, MD, USA)
- 8 Reverse transcriptase gene-specific primers: HBx RT 5'-AGGGTCGATGTCCATGCCCC-3' (Integrated DNA Technologies, IA, USA) (*see Note 3*).

3 Methods

Syntheses of the GP-modified phosphoramidites have previously been described for A, C, and U⁷ and separately for G⁸. Since many reagents are sensitive to hydrolysis, it is highly recommended to work under inert gas atmosphere (nitrogen or argon) and use anhydrous solvents for the reactions (*see Note 4*).

3.1 Synthesis of the 2'-O-GP-Modified Adenosine-phosphoramidite (1d)

1. Synthesis of N⁶-Dimethylaminomethylene-2'-O-cyanoethyl-3', 5'-O-(tetraisopropylidisiloxane-1,3-diyl)-adenosine (**1e**). To a solution of N⁶-Dimethylaminomethylene-3',5'-O-(tetraisopropylidisiloxane-1,3-diyl)-adenosine (**1a**) (3.0 g, 5.31 mmol) in *tert*-butanol (25 mL), freshly distilled acrylonitrile (6.7 mL, 102 mmol) and cesium carbonate (1.6 g, 4.9 mmol) are added.

The mixture is stirred vigorously at room temperature for 3 h. The reaction mixture is filtered and the residue is washed with dichloromethane. The filtrate is evaporated and the residue is purified using column chromatography with ethyl acetate/methanol (99:1–95:5, v/v) to give 3.28 g (87 %) of N⁶-Dimethylaminomethylene-2'-O-cyanoethyl-3', 5'-O-(tetraisopropylidisiloxane-1,3-diyl)-adenosine (**1e**). ¹H NMR (400 MHz, DMSO-*d*₆) δ [ppm] 8.90 (s, 1H, amidine-H), 8.34 (s, 1H, *H2* or *H8*), 8.32 (s, 1H, *H2*, or *H8*), 6.02–6.01 (m, 1H, *H1'*), 5.05–5.01 (m, 1H, *H3'*), 4.64–4.62 (m, 1H, *H2'*), 4.08–3.84 (m, 5H, *H4'*, 2× *H5'*, O-CH₂-CH₂-CN), 3.20 (s, 3H, N-CH₃), 3.13 (s, 3H, N-CH₃), 2.83–2.80 (m, 2H, O-CH₂-CH₂-CN), 1.10–1.00 (m, 28H, tetraisopropyl-CH and -CH₃); MS (ESI) was calculated to be 618.3 for C₂₈H₄₈N₇O₅Si₂ (M + H⁺), and found to be 618.8.

- Synthesis of 2'-O-cyanoethyl-3', 5'-O-(tetraisopropylidisiloxane-1, 3-diyl)-adenosine (**1b**). N⁶-Dimethylaminomethylene-2'-O-cyanoethyl-3', 5'-O-(tetraisopropylidisiloxane-1,3-diyl)-adenosine (**1e**) (1.0 g, 1.62 mmol) is dissolved in methanol (20 mL) then hydrazine hydrate (H₂N-NH₂·H₂O; 500 μL, 10.3 mmol) is added. The reaction solution is stirred at room temperature for 3 h. The solvents are evaporated and the residue is purified using a silica gel column with ethyl acetate as eluent to give 773 mg (87 %) 2'-O-cyanoethyl-3', 5'-O-(tetraisopropylidisiloxane-1,3-diyl)-adenosine (**1b**). ¹H NMR (400 MHz, DMSO-*d*₆) δ [ppm] 8.21 (s, 1H, *H2*, or *H8*), 8.07 (s, 1H, *H2*, or *H8*), 7.33 (bs, 2H, NH₂), 5.98–5.96 (m, 1H, *H1'*), 5.03–4.99 (m, 1H, *H3'*), 4.59–4.57 (m, 1H, *H2'*), 4.08–3.83 (m, 5H, *H4'*, 2× *H5'*, O-CH₂-CH₂-CN), 2.84–2.80 (m, 2H, O-CH₂-CH₂-CN), 1.09–0.97 (m, 28H, tetraisopropyl-CH and -CH₃); MS (MALDI) was calculated to be 563.8 for C₂₅H₄₃N₆O₅Si₂ (M + H⁺) and found to be 564.0.
- Synthesis of 2'-O-Aminopropyl-3', 5'-O-(tetraisopropylidisiloxane-1,3-diyl)-adenosine (**1f**) (*see* **Notes 5** and **6**). 2'-O-cyanoethyl-3', 5'-O-(tetraisopropylidisiloxane-1,3-diyl)-adenosine (**1b**) (1.0 g, 1.78 mmol) is dissolved in 10 mL of methanol in a glass tube suitable for use in an autoclave. Approximately 0.5 mL of Raney-nickel slurry are rinsed thoroughly on a glass filter (*see* **Note 7**) with dry methanol and then washed into the glass tube containing the solution of 2'-O-cyanoethyl-3', 5'-O-(tetraisopropylidisiloxane-1,3-diyl)-adenosine (**1b**). After addition of 5 mL methanol saturated with ammonia, the mixture is stirred for 1 h at room temperature under a hydrogen atmosphere (30 bar). The reaction mixture is filtered and the catalyst is washed three times with methanol. The filtrate is evaporated and the residue is purified using column chromatography with ethyl acetate/methanol/triethylamine (70:25:5, v/v/v) to yield

503 mg (50 %) of 2'-*O*-Aminopropyl-3',5'-*O*-(tetraisopropylidisiloxane-1,3-diyl)-adenosine (**1f**). If no NMR or MS analysis is needed, the crude product can be used for the next step without chromatographic purification. ¹H NMR (400 MHz, DMSO-*d*₆) δ [ppm] 8.20 (s, 1H, *H*2, or *H*8), 8.07 (s, 1H, *H*2, or *H*8), 7.32 (bs, 2H, *NH*₂), 5.95–5.94 (m, 1H, *H*1'), 4.95–4.90 (m, 1H, *H*3'), 4.41–4.39 (m, 1H, *H*2'), 4.08–3.90 (m, 3H, *H*4', 2× *H*5'), 3.86–3.70 (m, 2H, O-CH₂-CH₂-CH₂-NH₂), 2.66–2.61 (m, 2H, O-CH₂-CH₂-CH₂-NH₂), 1.65–1.58 (m, 2H, O-CH₂-CH₂-CH₂-NH₂), 1.08–0.96 (m, 28H, tetraisopropyl-CH and -CH₃); MS (MALDI) was calculated to be 567.9 for C₂₅H₄₇N₆O₅Si₂ (M+H⁺), and found to be 567.9.

4. Synthesis of 2'-*O*-(*N,N'*-Di-boc-guanidinopropyl)-3',5'-*O*-(tetraisopropylidisiloxane-1,3-diyl)-adenosine (**1c**). *N,N'*-Di-boc-*N''*-triflyl guanidine (280 mg, 0.72 mmol) is dissolved in 5 mL dichloromethane then triethylamine (100 μL) is added. After cooling to 0 °C, 2'-*O*-aminopropyl-3',5'-*O*-(tetraisopropylidisiloxane-1,3-diyl)-adenosine (**1f**) (400 mg, 0.71 mmol) is added and the mixture is stirred for 1 h at 0 °C then for 1 h at room temperature. The reaction is diluted with dichloromethane and washed with saturated sodium bicarbonate solution and brine. The organic layer is dried over Na₂SO₄ and the solvent is evaporated. The residue is purified using column chromatography with dichloromethane/methanol (98:2, v/v) to give a yield of 402 mg (70 %) of 2'-*O*-(*N,N'*-Di-boc-guanidinopropyl)-3',5'-*O*-(tetraisopropylidisiloxane-1,3-diyl)-adenosine (**1c**). ¹H NMR (400 MHz, DMSO-*d*₆) δ [ppm] 11.50 (s, 1H, *NH*-boc), 8.45–8.41 (m, 1H, *NH*-CH₂-), 8.17 (s, 1H, *H*2, or *H*8), 8.06 (s, 1H, *H*2 or *H*8), 7.31 (bs, 2H, *NH*₂), 6.02–5.99 (m, 1H, *H*1'), 4.96–4.91 (m, 1H, *H*3'), 4.43–4.40 (m, 1H, *H*2'), 4.06–3.70 (m, 5H, *H*4', 2× *H*5', O-CH₂-CH₂-CH₂-NH-), 3.51–3.32 (m, 2H, O-CH₂-CH₂-CH₂-NH-), 1.84–1.78 (m, 2H, O-CH₂-CH₂-CH₂-NH-), 1.44 (s, 9H, C(CH₃)₃), 1.37 (s, 9H, C(CH₃)₃), 1.07–0.99 (m, 28H, tetraisopropyl-CH and -CH₃); MS (MALDI) was calculated to be 810.1 for C₃₆H₆₅N₈O₉Si₂ (M+H⁺), and found to be 808.3.
5. Synthesis of *N*⁶-Dimethylaminomethylene-2'-*O*-(*N,N'*-di-boc-guanidinopropyl)-3',5'-*O*-(tetraisopropylidisiloxane-1,3-diyl)-adenosine (**1g**). 2'-*O*-(*N,N'*-Di-boc-guanidinopropyl)-3',5'-*O*-(tetraisopropylidisiloxane-1,3-diyl)-adenosine (**1c**) (500 mg, 0.61 mmol) is dissolved in methanol (5 mL) and *N,N*-dimethylformamide dimethyl acetal (500 μL, 3.7 mmol) is added. The reaction is stirred at room temperature overnight and the solvents are evaporated. The crude product is used for further reactions without purification.

6. Synthesis of N⁶-Dimethylaminomethylene-2'-O-(N,N'-di-boc-guanidinopropyl)-adenosine (**1h**). N⁶-Dimethylaminomethylene-2'-O-(N,N'-di-boc-guanidinopropyl)-3',5'-O-(tetraiso-propylidisiloxane-1,3-diyl)-adenosine (**1g**) (500 mg, 0.58 mmol) is dissolved in tetrahydrofuran (5 mL) and triethylammonium trihydrofluoride (Et₃N·3HF; 330 μL, 2.0 mmol) is added. The mixture is stirred at room temperature for 1.5 h, and then the solvent is evaporated. The residue is purified by column chromatography with ethyl acetate/methanol (98:2–9:1, v/v) giving 300 mg (83 %) of N⁶-Dimethylaminomethylene-2'-O-(N,N'-di-boc-guanidinopropyl)-adenosine (**1h**). ¹H NMR (400 MHz, DMSO-*d*₆) δ [ppm] 11.47 (s, 1H, NH-boc), 8.92 (s, 1H, N⁶=CH-NMe₂), 8.50 (s, 1H, H₂, or H₈), 8.41 (s, 1H, H₂, or H₈), 8.33–8.29 (m, 1H, NH-CH₂-), 6.11–6.09 (m, 1H, H1'), 5.28–5.24 (m, 1H, 5'-OH), 5.18–5.16 (m, 1H, 3'-OH), 4.46–4.43 (m, 1H, H₂'), 4.36–4.32 (m, 1H, H₃'), 4.01–3.98 (m, 1H, H₄'), 3.72–3.46 (4H, 2× H₅', O-CH₂-CH₂-CH₂-NH-), 3.33–3.28 (m, 2H, O-CH₂-CH₂-CH₂-NH-), 3.20 (s, 3H, N-CH₃), 3.13 (s, 3H, N-CH₃), 1.74–1.68 (m, 2H, O-CH₂-CH₂-CH₂-NH-), 1.45 (s, 9H, C(CH₃)₃), 1.37 (s, 9H, C(CH₃)₃); MS (MALDI) was calculated to be 622.7 for C₂₇H₄₄N₉O₈ (M+H⁺), and found to be 624.6.
7. Synthesis of N⁶-Dimethylaminomethylene-2'-O-(N,N'-di-boc-guanidinopropyl)-5'-O-(4,4'-dimethoxytrityl)-adenosine (**1i**). N⁶-Dimethylaminomethylene-2'-O-(N,N'-di-boc-guanidinopropyl)-adenosine (**1g**) (1.0 g, 1.6 mmol) is dissolved in dry pyridine (20 mL). 4,4'-Dimethoxytrityl chloride (660 mg, 1.95 mmol) is added and the reaction is stirred at room temperature overnight. The solution is diluted with dichloromethane and washed with saturated sodium bicarbonate solution. After evaporation of the solvents the residue is purified on a silica gel column with dichloromethane/methanol (98:2, v/v) containing 0.5 % triethylamine (*see* Note 8), and 1.32 g (90 %) of N⁶-Dimethylaminomethylene-2'-O-(N,N'-di-boc-guanidinopropyl)-5'-O-(4,4'-dimethoxytrityl)-adenosine (**1i**) can be obtained. ¹H NMR (400 MHz, DMSO-*d*₆) δ [ppm] 11.48 (s, 1H, NH-boc), 8.90 (s, 1H, N⁶=CH-NMe₂), 8.38–8.34 (m, 3H, H₂, H₃, NH-CH₂-), 7.37–7.34 (m, 2H, DMTr), 7.27–7.17 (m, 7H, DMTr), 6.84–6.79 (m, 4H, DMTr), 6.14–6.13 (m, 1H, H1'), 5.18–5.15 (m, 1H, 3'-OH), 4.57–4.54 (m, 1H, H₂'), 4.47–4.42 (m, 1H, H₃'), 4.14–4.08 (m, 1H, H₄'), 3.72–3.71 (m, 6H, 2× OCH₃), 3.70–3.56 (m, 2H, O-CH₂-CH₂-CH₂-NH-), 3.37–3.32 (m, 2H, O-CH₂-CH₂-CH₂-NH-), 3.24–3.21 (m, 2H, 2× H₅'), 3.19 (s, 3H, N-CH₃), 3.12 (s, 3H, N-CH₃), 1.77–1.70 (m, 2H, O-CH₂-CH₂-CH₂-NH-), 1.44 (s, 9H, C(CH₃)₃), 1.35 (s, 9H, C(CH₃)₃); MS (MALDI) was calculated to be 925.1 for C₄₈H₆₂N₉O₁₀ (M+H⁺), and found to be 924.9.

8. Synthesis of N^6 -Dimethylaminomethylene-2'-*O*-(*N,N'*-di-boc-guanidinopropyl)-5'-*O*-(4,4'-dimethoxytrityl)-adenosine 3'-(cyanoethyl)-*N,N*-diisopropyl phosphoramidite (**1d**). N^6 -Dimethylaminomethylene-2'-*O*-(*N,N'*-di-boc-guanidinopropyl)-5'-*O*-(4,4'-dimethoxytrityl)-adenosine (**1i**) (320 mg, 346 μmol) is dissolved in dichloromethane (8 mL). 2-cyanoethyl *N,N,N',N'*-tetraisopropylamino phosphane (132 μL , 415 μmol) and 4,5-dicyanoimidazole (47 mg, 398 μmol) are added. The mixture is stirred at room temperature. After 3 h, TLC checks completion of the reaction. In the event that some starting material did not react, an additional 0.6 equivalents of the phosphitylating agent as well as the catalyst are added and the reaction is stirred at room temperature for additional 4 h. After completion of the reaction, the mixture is diluted with dichloromethane, washed with saturated sodium bicarbonate solution and the organic layer is dried over MgSO_4 . The solvent is evaporated and the residue dissolved in a small amount of dichloromethane (ca. 5 mL). This solution is added drop wise into a flask with hexane (500 mL) to form a white precipitate. Two thirds of the solvent is evaporated and the remaining solvent is decanted from the solid (*see Note 9*). The precipitated product is redissolved in benzene and lyophilized (*see Note 10*) to give 329 mg (84%) of N^6 -Dimethylaminomethylene-2'-*O*-(*N,N'*-di-boc-guanidinopropyl)-5'-*O*-(4,4'-dimethoxytrityl)-adenosine 3'-(cyanoethyl)-*N,N*-diisopropyl phosphoramidite (**1d**) as a white powder (*see Note 11*). ^1H NMR (300 MHz, acetone- d_6) δ [ppm] 11.65 (s, 1H, *NH*-boc) 8.95–8.93 (m, 1H, $N^6 = \text{CH}-\text{NMe}_2$), 8.42–8.27 (m, 3H, *H2*, *H3*, *NH-CH}_2^-*), 7.50–7.46 (m, 2H, DMTr), 7.38–7.17 (m, 7H, DMTr), 6.87–6.80 (m, 4H, DMTr), 6.28–6.26 (m, 1H, *H1'*), 4.96–4.79 (m, 2H, *H2'*, *H3'*) 4.45–4.37 (m, 1H, *H4'*), 4.05–3.35 (m, 16H), 3.25 (s, 3H, $\text{N}-\text{CH}_3$), 3.18 (s, 3H, $\text{N}-\text{CH}_3$), 2.85 (m, 1H, cyanoethyl), 2.64–2.60 (m, 1H, cyanoethyl), 1.90–1.82 (m, 2H, $\text{O}-\text{CH}_2-\text{CH}_2-\text{CH}_2-\text{NH}-$), 1.50–1.49 (m, 9H, $\text{C}(\text{CH}_3)_3$), 1.42–1.40 (m, 9H, $\text{C}(\text{CH}_3)_3$), 1.25–1.10 (m, 12H, *iPr-CH}_3*); ^{31}P NMR (121 MHz, acetone- d_6) δ [ppm] 149.6, 149.3; MS (ESI) was calculated to be 1,125.3 for $\text{C}_{57}\text{H}_{79}\text{N}_{11}\text{O}_{11}\text{P}$ ($\text{M} + \text{H}^+$), and found to be 1,125.7.

3.2 Synthesis of the 2'-*O*-GP-Modified Cytidine-phosphoramidite (**2d**)

1. Synthesis of N^4 -Dimethylaminomethylene-2'-*O*-cyanoethyl-3', 5'-*O*-(tetraisopropylidisiloxane-1,3-diyl)-cytidine (**2e**). N^4 -Dimethylaminomethylene-3', 5'-*O*-(tetraisopropylidisiloxane-1,3-diyl)-cytidine (**2a**) (4 g, 7.39 mmol) is dissolved in acrylonitrile (8 mL, 122 mmol) and *tert*-Butanol (35 mL). Cesium carbonate (1.8 g, 5.52 mmol) is added and the reaction is stirred for 2.5 h at room temperature. The mixture is filtered over celite, the solvents are evaporated and the residue is purified using column chromatography. Ethyl acetate is ini-

tially used as solvent then changed to ethyl acetate/methanol (9:1, v/v) after the nonpolar impurities have passed through the column. A yield of 3.78 g (86%) of N^4 -Dimethylaminomethylene-2'-*O*-cyanoethyl-3',5'-*O*-(tetraisopropylidisiloxane-1,3-diyl)-cytidine (**2e**) can be obtained. $^1\text{H NMR}$ (400 MHz, $\text{DMSO-}d_6$) δ [ppm] 8.62 (s, 1H, $N^4 = \text{CH-NMe}_2$), 7.88 (d, 1H, $J = 7.3$ Hz, *H*6), 5.90 (d, 1H, $J = 7.3$ Hz, *H*5), 5.65 (s, 1H, *H*1'), 4.22–3.91 (m, 7H), 3.17 (s, 3H, N-CH_3), 3.04 (s, 3H, N-CH_3), 2.86–2.82 (m, 2H, $\text{O-CH}_2\text{-CH}_2\text{-CN}$), 1.07–0.96 (m, 28H, tetraisopropyl-CH and -CH_3); MS (ESI) was calculated to be 594.9 for $\text{C}_{27}\text{H}_{48}\text{N}_5\text{O}_6\text{Si}_2$ ($\text{M} + \text{H}^+$) and found to be 594.9.

- Synthesis of 2'-*O*-cyanoethyl-3',5'-*O*-(tetraisopropylidisiloxane-1,3-diyl)-cytidine (**2b**). N^4 -Dimethylaminomethylene-2'-*O*-cyanoethyl-3',5'-*O*-(tetraisopropylidisiloxane-1,3-diyl)-cytidine (**2e**) (1.0 g, 1.68 mmol) is dissolved in methanol (10 mL) and hydrazine hydrate (500 μL , 10.3 mmol) is added. The mixture is stirred for 1 h at room temperature and then the solvents are evaporated. The residue is purified on a silica gel column with ethyl acetate/methanol (95:5, v/v) to give 745 mg (82 %) of 2'-*O*-cyanoethyl-3',5'-*O*-(tetraisopropylidisiloxane-1,3-diyl)-cytidine (**2b**). $^1\text{H NMR}$ (400 MHz, $\text{DMSO-}d_6$) δ [ppm] 7.69 (d, 1H, $J = 7.4$ Hz, *H*6), 7.21 (s, 2H, NH_2), 5.69 (d, 1H, $J = 7.4$ Hz, *H*5), 5.61 (s, 1H, *H*1'); 4.19–3.90 (m, 7H), 2.90–2.76 (m, 2H, $\text{O-CH}_2\text{-CH}_2\text{-CN}$), 1.07–0.97 (m, 28 H, tetraisopropyl-CH and -CH_3); MS (ESI) was calculated to be 539.8 for $\text{C}_{24}\text{H}_{43}\text{N}_4\text{O}_6\text{Si}_2$ ($\text{M} + \text{H}^+$) and found to be 540.0.
- Synthesis of 2'-*O*-Aminopropyl-3',5'-*O*-(tetraisopropylidisiloxane-1,3-diyl)-cytidine (**2f**) (*see* Notes 5 and 6). 2'-*O*-cyanoethyl-3',5'-*O*-(tetraisopropylidisiloxane-1,3-diyl)-cytidine (**2b**) (500 mg, 928 μmol) is dissolved in 10 mL of methanol in a glass tube. Approximately 0.5 mL of Raney-nickel sediment is washed thoroughly with dry methanol on a glass filter (*see* Note 7) and is rinsed with methanol into the glass tube containing the solution of 2'-*O*-cyanoethyl-3',5'-*O*-(tetraisopropylidisiloxane-1,3-diyl)-cytidine (**2b**). After addition of 5 mL methanol saturated with ammonia, the mixture is stirred for 1 h at room temperature under a hydrogen atmosphere (30 bar). The reaction mixture is then filtered through celite and the catalyst is washed several times with methanol. The solvent is evaporated and the residue is purified on a silica gel column using ethyl acetate/methanol/triethylamine (60:35:5) to give 251 mg (50 %) of 2'-*O*-Aminopropyl-3',5'-*O*-(tetraisopropylidisiloxane-1,3-diyl)-cytidine (**2f**). If no NMR or MS analysis is needed, the crude product can be used for the next step without chromatographic purification. $^1\text{H NMR}$ (400 MHz, $\text{DMSO-}d_6$) δ [ppm] 7.69 (d, 1H, $J = 7.2$ Hz, *H*6), 7.18 (bs, 2H, ar. NH_2), 5.68 (d, 1H, $J = 7.5$ Hz, *H*5), 5.60 (s, 1H, *H*1'), 4.18–3.76 (m, 7H),

2.70–2.66 (m, 2H, O–CH₂–CH₂–CH₂–NH₂), 1.68–1.61 (m, 2H, O–CH₂–CH₂–CH₂–NH₂), 1.07–0.95 (m, 28 H, tetraisopropyl-CH and -CH₃); MS (MALDI) was calculated to be 543.8 for C₂₄H₄₇N₄O₆Si₂ (M + H⁺) and found to be 544.6.

4. Synthesis of 2'-O-(*N,N'*-Di-boc-guanidinopropyl)-3',5'-O-(tetraisopropylidisiloxane-1,3-diyl)-cytidine (**2c**). *N,N'*-Di-boc-*N''*-triflyl guanidine (360 mg, 920 μmol) is dissolved in 5 mL dichloromethane and triethylamine (125 μL) is then added. After cooling to 0 °C, 2'-O-Aminopropyl-3',5'-O-(tetraisopropylidisiloxane-1,3-diyl)-cytidine (**2f**) (500 mg, 922 μmol) is added and the solution is stirred for 1 h at 0 °C and then 1 h at room temperature. The reaction is diluted with dichloromethane and washed with saturated sodium bicarbonate solution and brine. The combined organic layers are dried over Na₂SO₄ and after evaporating the solvent the residue is purified using column chromatography with dichloromethane/methanol (98:2–95:5, v/v) to give 434 mg (60 %) 2'-O-(*N,N'*-Di-boc-guanidinopropyl)-3',5'-O-(tetraisopropylidisiloxane-1,3-diyl)-cytidine (**2c**). ¹H NMR (400 MHz, DMSO-*d*₆) δ [ppm] 11.48 (s, 1H, NH-boc), 8.38–8.35 (m, 1H, NH-CH₂-), 7.67 (d, 1H, J = 7.4 Hz, H₆), 7.19 (bs, 2H, NH₂), 5.68 (d, 1H, J = 7.4 Hz, H₅), 5.63 (s, 1H, H_{1'}), 4.17–3.78 (m, 7H), 3.49–3.33 (m, 2H, O–CH₂–CH₂–CH₂–NH-), 1.84–1.77 (m, 2H, O–CH₂–CH₂–CH₂–NH-), 1.45 (m, 9H, C(CH₃)₃), 1.38 (m, 9H, C(CH₃)₃), 1.06–0.96 (m, 28 H, tetraisopropyl-CH and -CH₃); MS (MALDI) was calculated to be 786.1 for C₃₅H₆₅N₆O₁₀Si₂ (M + H⁺) and found to be 786.4.
5. Synthesis of N⁴-Benzoyl-2'-O-(*N,N'*-di-boc-guanidinopropyl)-3',5'-O-(tetraisopropylidisiloxane-1,3-diyl)-cytidine (**2g**). 2'-O-(*N,N'*-Di-boc-guanidinopropyl)-3',5'-O-(tetraisopropylidisiloxane-1,3-diyl)-cytidine (**2c**) (1.0 g, 1.27 mmol) is dissolved in dry pyridine (10 mL) and the solution is cooled in an ice bath. Benzoyl chloride (240 μL, 2.06 mmol) is added and the reaction solution is stirred at 0 °C for 1 h. The reaction is quenched with water, and then ammonia (25 % in water; 3 mL) is added. The mixture is stirred for 30 min at room temperature. The solvents are evaporated and the residue is dissolved in dichloromethane and washed with saturated sodium bicarbonate solution. The organic layer is dried over Na₂SO₄ and after evaporating the solvent, the residue is purified by column chromatography using dichloromethane/methanol (98:2, v/v) and 950 mg (84 %) of N⁴-Benzoyl-2'-O-(*N,N'*-di-boc-guanidinopropyl)-3',5'-O-(tetraisopropylidisiloxane-1,3-diyl)-cytidine (**2g**) can be obtained. ¹H NMR (400 MHz, DMSO-*d*₆) δ [ppm] 11.50 (s, 1H, NH), 11.31 (s, 1H, NH), 8.40–8.37 (m, 1H, NH-CH₂-), 8.15 (d, 1H, J = 7.3 Hz, H₆), 8.03–7.99 (m, 2H, benzoyl), 7.65–7.60 (m, 1H, benzoyl), 7.53–7.49

- (m, 2H, benzoyl), 7.38 (d, 1H, $J=7.3$ Hz, H_5), 5.73 (s, 1H, $H_{1'}$), 4.24–4.13 (m, 3H, $H_{3'}$, $H_{4'}$, $H_{5'}$), 4.02–4.03 (m, 1H, $H_{2'}$), 3.97–3.92 (m, 1H, $H_{5'}$), 3.87–3.83 (m, 2H, O–CH₂–CH₂–CH₂–NH–), 3.52–3.35 (m, 2H, O–CH₂–CH₂–CH₂–NH–), 1.87–1.80 (m, 2H, O–CH₂–CH₂–CH₂–NH–), 1.45 (m, 9H, C(CH₃)₃), 1.38 (m, 9H, C(CH₃)₃), 1.08–0.95 (m, 28H, tetraisopropyl–CH and –CH₃); MS (ESI) was calculated to be 890.2 for C₄₂H₆₉N₆O₁₁Si₂ (M + H⁺), and found to be 890.4.
6. Synthesis of N⁴-Benzoyl-2'-O-(N,N'-di-boc-guanidinopropyl)-cytidine (**2h**). N⁴-Benzoyl-2'-O-(N,N'-di-boc-guanidinopropyl)-3',5'-O-(tetraisopropylsiloxane-1,3-diyl)-cytidine (**2g**) (900 mg, 1.01 mmol) is dissolved in tetrahydrofuran (20 mL). Triethylamine trihydrofluoride (Et₃N·3HF; 560 μL, 3.54 mmol) is added and the solution is stirred at room temperature for 2 h. The solvent is evaporated and the residue is purified using column chromatography with dichloromethane/methanol (98:2–97:3, v/v) to give 607 mg (93 %) of N⁴-Benzoyl-2'-O-(N,N'-di-boc-guanidinopropyl)-cytidine (**2h**) as a pale yellow foam. ¹H NMR (300 MHz, DMSO-*d*₆) δ [ppm] 11.50 (s, 1H, NH), 11.28 (bs, 1H, NH), 8.57 (d, 1H, $J=7.5$ Hz, H_6), 8.40–8.35 (m, 1H, NH–CH₂–), 8.02–7.98 (m, 2H, benzoyl), 7.66–7.60 (m, 1H, benzoyl), 7.54–7.48 (m, 2H, benzoyl), 7.34 (d, 1H, $J=7.2$ Hz, H_5), 5.86–5.85 (m, 1H, $H_{1'}$), 5.24 (t, 1H, $J=5.0$ Hz, 5'–OH), 4.98 (d, 1H, $J=6.8$ Hz, 3'–OH), 4.12–3.60 (m, 7H), 3.44–3.37 (m, 2H, O–CH₂–CH₂–CH₂–NH–), 1.85–1.76 (m, 2H, O–CH₂–CH₂–CH₂–NH–), 1.46 (m, 9H, C(CH₃)₃), 1.38 (m, 9H, C(CH₃)₃); HRMS (MALDI) was calculated to be 647.3035 for C₃₀H₄₃N₆O₁₀ (M + H⁺), and found to be 647.3031.
7. Synthesis of N⁴-Benzoyl-2'-O-(N,N'-di-boc-guanidinopropyl)-5'-O-(4,4'-dimethoxytrityl)-cytidine (**2i**). N⁴-Benzoyl-2'-O-(N,N'-di-boc-guanidinopropyl)-cytidine (**2h**) (516 mg, 798 μmol) is dissolved in dry pyridine (20 mL) and the solution is cooled in an ice bath. 4,4'-Dimethoxytrityl chloride (515 mg, 1.52 mmol) is added and the mixture is stirred overnight while the bath comes up to room temperature. The reaction is quenched with methanol (10 mL) and the solvents are evaporated. The residue is purified by column chromatography using dichloromethane/methanol (99:1–98:2, v/v) (The column is packed with solvent containing 1 % triethylamine (*see* **Note 8**)) to yield 715 mg (94 %) N⁴-Benzoyl-2'-O-(N,N'-di-boc-guanidinopropyl)-5'-O-(4,4'-dimethoxytrityl)-cytidine (**2i**) as a pale yellow foam. ¹H NMR (400 MHz, DMSO-*d*₆) δ [ppm] 11.50 (s, 1H, NH), 11.29 (bs, 1H, NH), 8.43–8.37 (m, 2H, H_6 , NH–CH₂–), 8.02–7.99 (m, 2H, benzoyl), 7.65–7.60 (m, 1H, benzoyl), 7.54–7.50 (m, 2H, benzoyl), 7.43–7.25 (m, 9H, DMTr), 7.18–7.15 (m, 1H, H_5), 6.94–6.91 (m, 4H, DMTr), 5.88 (s, 1H, $H_{1'}$), 5.04 (d, 1H, $J=7.3$ Hz,

3'-OH), 4.34–4.28 (m, 1H, $H3'$), 4.13–4.10 (m, 1H, $H4'$), 3.94–3.87 (m, 2H, $H2'$, 1× O-CH₂-CH₂-CH₂-NH-), 3.76 (s, 6H, 2× OCH₃), 3.76–3.70 (m, 1H, 1× O-CH₂-CH₂-CH₂-NH-), 3.46–3.36 (m, 4H, 2× $H5'$, O-CH₂-CH₂-CH₂-NH-), 1.86–1.80 (m, 2H, O-CH₂-CH₂-CH₂-NH-), 1.42 (m, 9H, C(CH₃)₃), 1.36 (m, 9H, C(CH₃)₃); HRMS (MALDI) was calculated to be 971.4161 for C₅₁H₆₀N₆O₁₂Na (M+Na⁺), and found to be 971.4181.

8. Synthesis of N⁴-Benzoyl-2'-O-(*N,N'*-di-boc-guanidinopropyl)-5'-O-(4,4'-dimethoxytrityl)-cytidine 3'-(cyanoethyl)-*N,N'*-diisopropyl phosphoramidite (**2d**). N⁴-Benzoyl-2'-O-(*N,N'*-di-boc-guanidinopropyl)-5'-O-(4,4'-dimethoxytrityl)-cytidine (**2i**) (683 mg, 720 μmol) is dissolved in dichloromethane (15 mL). 2-cyanoethyl *N,N,N',N'*-tetraisopropylamino phosphane (274 μL, 864 μmol) and 4,5-dicyanoimidazole (98 mg, 828 μmol) are added. After stirring at room temperature for 5 h, completion of the reaction is checked by TLC. In the event that some starting material did not react, an additional 0.5 equivalents of the phosphitylating agent as well as the catalyst are added and the reaction is stirred at room temperature for additional 4 h. After completion of the reaction the solution is diluted with dichloromethane and washed with saturated sodium bicarbonate solution. After drying the organic layer over MgSO₄ the solvent is evaporated and the residue is dissolved in a small amount (5 mL) of dichloromethane. This solution is added dropwise into a flask with hexane (500 mL) to form a white precipitate. Two thirds of the solvent is evaporated and the residual solvent is decanted carefully (*see Note 9*). The precipitate is redissolved in benzene and lyophilized (*see Note 10*) to give 738 mg (89 %) of N⁴-Benzoyl-2'-O-(*N,N'*-di-boc-guanidinopropyl)-5'-O-(4,4'-dimethoxytrityl)-cytidine 3'-(cyanoethyl)-*N,N'*-diisopropyl phosphoramidite (**2d**) (*see Note 11*). ¹H NMR (400 MHz, DMSO-*d*₆) δ [ppm] 11.50–11.48 (m, 1H, NH), 11.25 (bs, 1H, NH), 8.52–8.45 (m, 1H, $H6$), 8.39–8.34 (m, 1H, NH-CH₂-), 8.01–7.98 (m, 2H, benzoyl), 7.66–7.61 (m, 1H, benzoyl), 7.53–7.49 (m, 2H, benzoyl), 7.45–7.25 (m, 9H, DMTr), 7.13–7.09 (m, 1H, $H5$), 6.93–6.89 (m, 4H, DMTr), 5.95–5.92 (m, 1H, $H1'$), 4.56–4.38 (m, 1H, $H3'$), 4.31–4.28 (m, 1H, $H4'$), 4.07–3.29 (m, 17H), 2.90–2.57 (m, 2H, cyanoethyl), 1.86–1.78 (m, 2H, O-CH₂-CH₂-CH₂-NH-), 1.40–1.35 (m, 18H, 2× C(CH₃)₃), 1.20–0.93 (m, 12H, *i*Pr-CH₃); ³¹P NMR (162 MHz, DMSO-*d*₆) δ [ppm] 148.4, 148.0 (The signal of the hydrolyzed phosphitylation reagent appears at 13.9 ppm); HRMS (MALDI) was calculated to be 1,149.5421 for C₆₀H₇₈N₈O₁₃P (M+H⁺), was found to be 1,149.5447.

3.3 Synthesis of the 2'-O-GP-Modified Uridine-phosphoramidite (3d)

1. Synthesis of N³-Benzoyl-2'-O-cyanoethyl-3',5'-O-(tetraisopropylidisiloxane-1,3-diyl)-uridine (**3b**). N³-Benzoyl-3',5'-O-(tetraisopropylidisiloxane-1,3-diyl)-uridine (**3a**) (1.14 g, 1.93 mmol) is dissolved in 9.6 mL of *tert*-butanol. Freshly distilled acrylonitrile (2.5 mL, 38.6 mmol) is added. After addition of cesium carbonate (645 mg, 1.98 mmol) the reaction is stirred for 4 h at room temperature. The reaction solution is filtered over celite. The residue is washed with 100 mL of dichloromethane. The filtrate is evaporated in a vacuum. Purification via column chromatography in dichloromethane/ethyl acetate (99:1–95:5, v/v) yields 746 mg (60 %) of N³-Benzoyl-2'-O-cyanoethyl-3',5'-O-(tetraisopropylidisiloxane-1,3-diyl)-uridine (**3b**) as a white powder. ¹H NMR (250 MHz, acetone-*d*₆) δ [ppm] 8.03–7.99 (m, 3H, *H*₆, benzoyl), 7.79–7.72 (m, 1H, benzoyl), 7.61–7.55 (m, 2H, benzoyl), 5.80–5.74 (m, 2H, *H*₅, *H*_{1'}), 4.50–3.94 (m, 7H), 2.80–2.75 (m, 2H, O–CH₂–CH₂–CN), 1.17–1.07 (m, 28H, tetraisopropyl-CH and –CH₃); HRMS (MALDI) was calculated to be 666.2637 for C₃₁H₄₅N₃O₈Si₂Na (M + Na⁺) and found to be 666.2647.
2. Synthesis of 2'-O-(Aminopropyl)-3',5'-O-(tetraisopropylidisiloxane-1,3-diyl)-uridine (**3e**) (*see* Notes 5 and 6). N³-Benzoyl-2'-O-cyanoethyl-3',5'-O-(tetraisopropylidisiloxane-1,3-diyl)-uridine (**3b**) (500 mg, 0.78 mmol) is dissolved in 10 mL of methanol in a glass tube suitable for the applied autoclave. Approximately 0.5 mL of Raney-nickel slurry is put on a glass filter, washed thoroughly with dry methanol (*see* Note 7) and rinsed into the glass tube containing the solution of N³-Benzoyl-2'-O-cyanoethyl-3',5'-O-(tetraisopropylidisiloxane-1,3-diyl)-uridine (**3b**). After addition of 5 mL methanol saturated with ammonia, the mixture is stirred for 1 h at room temperature in an autoclave under a hydrogen atmosphere (30 bar). The reaction solution is decanted from the catalyst into a glass filter. The catalyst is washed several times with methanol and the solvent is removed from the combined filtrates under reduced pressure. The product is purified on a silica gel column initially using dichloromethane/ethyl acetate (7:3–0:1, v/v) and thereafter ethyl acetate/methanol/triethylamine (6:3.5:0.5, v/v/v) to obtain 253 mg (60 %) of 2'-O-(Aminopropyl)-3',5'-O-(tetraisopropylidisiloxane-1,3-diyl)-uridine (**3e**) as a white powder. If no NMR or MS analysis is needed, the crude product can be used for the next step without chromatographic purification. ¹H NMR (250 MHz, acetone-*d*₆) δ [ppm] 7.81 (d, 1H, J=8.1 Hz, *H*₆), 5.71 (s, 1H, *H*_{1'}), 5.53 (d, 1H, J=8.1 Hz, *H*₅), 4.39–4.34 (m, 1H, *H*_{3'}), 4.28–4.23 (m, 1H, *H*_{5'}), 4.14–4.03 (m, 3H, *H*_{2'}, *H*_{4'}, *H*_{5'}), 3.97–3.81 (m, 2H, O–CH₂–CH₂–CH₂–NH₂), 3.37–3.25 (m, 2H, O–CH₂–CH₂–CH₂–NH₂), 1.92–1.82 (m, 2H,

O-CH₂-CH₂-CH₂-NH₂), 1.14–1.05 (m, 28H, tetraisopropyl-CH and -CH₃); HRMS (MALDI) was calculated to be 544.2869 for C₂₄H₄₆N₃O₇Si₂ (M + H⁺), and found to be 544.2880.

- Synthesis of 2'-O-(*N,N'*-Di-boc-guanidinopropyl)-3',5'-O-(tetraisopropylidisiloxane-1,3-diyl)-uridine (**3c**). *N,N'*-Di-boc-*N''*-triflyl guanidine (320 mg, 0.82 mmol) is dissolved in 3.6 mL dichloromethane and triethylamine (150 μL) is added. The solution is cooled in an ice bath and 2'-O-(Aminopropyl)-3',5'-O-(tetraisopropylidisiloxane-1,3-diyl)-uridine (**3e**) (490 mg, 0.9 mmol) is added. After 15 min the reaction mixture is removed from the ice bath and is stirred for 2.5 h at room temperature. The reaction solution is washed with saturated sodium bicarbonate solution and brine. After drying over Na₂SO₄ the solvent is evaporated. The crude product is purified using column chromatography with dichloromethane/methanol (96:4–94:6, v/v). A yield of 410 mg (58 %) of 2'-O-(*N,N'*-Di-boc-guanidinopropyl)-3',5'-O-(tetraisopropylidisiloxane-1,3-diyl)-uridine (**3c**) can be obtained. ¹H NMR (400 MHz, DMSO-*d*₆) δ [ppm] 11.49 (s, 1H, NH), 11.37 (m, 1H, NH_{uridine}), 8.40–8.37 (m, 1H, NH-CH₂-), 7.64 (d, 1H, J = 7.9 Hz, H6), 5.64 (s, 1H, H1'), 5.53 (d, 1H, J = 7.9 Hz, H5), 4.25–4.22 (H3'), 4.13–4.09 (m, 1H, H5'), 4.06–4.05 (m, 1H, H2'), 4.03–4.00 (m, 1H, H4'), 3.93–3.89 (m, 1H, H5'), 3.84–3.70 (m, 2H, O-CH₂-CH₂-CH₂-NH-), 3.49–3.32 (m, 2H, O-CH₂-CH₂-CH₂-NH-), 1.83–1.77 (m, 2H, O-CH₂-CH₂-CH₂-NH-), 1.45 (s, 9H, C(CH₃)₃), 1.38 (s, 9H, C(CH₃)₃), 1.06–0.97 (m, 28H, tetraisopropyl-CH and -CH₃); HRMS (MALDI) was calculated to be 808.3955 for C₃₅H₆₃N₅O₁₁Si₂Na (M + Na⁺), and found to be 808.3991.
- Synthesis of 2'-O-(*N,N'*-Di-boc-guanidinopropyl)-uridine (**3f**). To a solution of 2'-O-(*N,N'*-Di-boc-guanidinopropyl)-3',5'-O-(tetraisopropylidisiloxane-1,3-diyl)-uridine (**3c**) (910 mg, 1.16 mmol) and triethylamine (240 μL) in 13 mL tetrahydrofuran, NEt₃·3HF (700 μL, 4.3 mmol) is added. The reaction mixture is stirred for 1 h at room temperature. The solvents are evaporated and the residue is purified on a silica gel column using dichloromethane/methanol (93:7–92:8, v/v) to give 629 mg (97%) 2'-O-(*N,N'*-Di-boc-guanidinopropyl)-uridine (**3f**) as a white foam. ¹H NMR (250 MHz, acetone-*d*₆) δ [ppm] 11.67 (bs, 1H, NH), 10.03 (bs, 1H, NH), 8.46–8.41 (m, 1H, NH-CH₂-), 8.10 (d, 1H, J = 8.2 Hz, H6), 5.99–5.97 (m, 1H, H1'), 5.58 (d, 1H, J = 8.2 Hz, H5), 4.39–3.46 (m, 11H), 1.95–1.85 (m, 2H, O-CH₂-CH₂-CH₂-NH-), 1.51 (s, 9H, C(CH₃)₃), 1.43 (s, 9H, C(CH₃)₃); MS (ESI) was calculated to be 566.2 for C₂₃H₃₇N₅O₁₀Na (M + Na⁺), and found to be 567.0.

5. Synthesis of 2'-O-(*N,N'*-Di-boc-guanidinopropyl)-5'-O-(4,4'-dimethoxytrityl)-uridine (**3g**). 2'-O-(*N,N'*-Di-boc-guanidinopropyl)-uridine (**3f**) (588 mg, 1.08 mmol) is dissolved in 11.4 mL of dry pyridine and 4,4'-Dimethoxytrityl chloride (460 mg, 1.36 mmol) is added. The reaction solution is stirred at room temperature for 5 h. The reaction mixture is quenched with water and the solvents are evaporated. The residue is dissolved in dichloromethane, washed twice with saturated sodium bicarbonate solution (2 × 50 mL) and then twice with brine (2 × 50 mL). The organic layer is dried over Na₂SO₄ and the solvent is removed under reduced pressure. After purification using column chromatography with dichloromethane/methanol (97:3, v/v) containing 0.5 % triethylamine (*see Note 8*), 785 mg (86 %) of 2'-O-(*N,N'*-Di-boc-guanidinopropyl)-5'-O-(4,4'-dimethoxytrityl)-uridine (**3g**) (yellow powder) can be obtained. There may be a yellow impurity that cannot be separated on the column. ¹H NMR (250 MHz, DMSO-*d*₆) δ [ppm] 11.49 (s, 1H, NH), 11.37 (m, 1H, NH), 8.41–8.36 (m, 1H, NH-CH₂-), 7.75 (d, 1H, J=8.1 Hz, H₆), 7.40–7.23 (m, 9H, DMTr), 6.92–6.88 (m, 4H, DMTr), 5.83–5.82 (m, 1H, H1'), 5.29–5.25 (m, 1H, H5), 5.09–5.06 (m, 1H, 3'-OH), 4.23–3.88 (m, 3H), 3.74 (s, 6H, 2 × O-CH₃), 3.68–3.63 (m, 2H), 3.43–3.20 (m, 4H), 1.82–1.72 (m, 2H, O-CH₂-CH₂-CH₂-NH-), 1.44 (s, 9H, C(CH₃)₃), 1.37 (s, 9H, C(CH₃)₃); HRMS (MALDI) was calculated to be 846.3920 for C₄₄H₅₆N₅O₁₂ (M+H⁺), and found to be 846.3946.
6. Synthesis of 2'-O-(*N,N'*-Di-boc-guanidinopropyl)-5'-O-(4,4'-dimethoxytrityl)-uridine 3'-(cyanoethyl)-*N,N*-diisopropyl phosphoramidite (**3d**). 2'-O-(*N,N'*-Di-boc-guanidinopropyl)-5'-O-(4,4'-dimethoxytrityl)-uridine (**3g**) (770 mg, 0.9 mmol) is dissolved in dichloromethane (11 mL). To this solution, 2-cyanoethyl *N,N,N',N'*-tetraisopropylamino phosphane (400 μL, 1.26 mmol) and 4,5-dicyanoimidazole (130 mg, 1.1 mmol) are added. The reaction progress is observed with TLC (dichloromethane/ethyl acetate 1:1 (v:v), containing 0.5 % triethylamine). In the event that after 2 h some starting material did not react, an additional 0.3 equivalents of the phosphitylating agent as well as the catalyst are added and the reaction is stirred at room temperature for additional 2 h. After completion of the reaction the reaction mixture is washed twice with saturated sodium bicarbonate solution (2 × 100 mL) and once with brine (200 mL). After drying over Na₂SO₄, the solvent is evaporated and the residue is purified on a silica gel column with dichloromethane/ethyl acetate (6:4–1:1, v/v) containing 0.5 % triethylamine (*see Note 8*). 2'-O-(*N,N'*-Di-boc-guanidinopropyl)-5'-O-(4,4'-dimethoxytrityl)-uridine 3'-(cyanoethyl)-*N,N*-diisopropyl phosphoramidite (**3d**) is obtained as a light yellow foam (762 mg, 83 %). ¹H NMR

(400 MHz, DMSO- d_6) δ [ppm] 11.50–11.48 (m, 1H, NH), 11.35 (bs, 1H, NH), 8.39–8.33 (m, 1H, NH-CH₂-), 7.87–7.80 (m, 1H, H6), 7.41–7.22 (m, 9H, DMTr), 6.91–6.86 (m, 4H, DMTr), 5.86–5.84 (m, 1H, H1'), 5.23–5.18 (m, 1H, H5), 4.46–4.32 (m, 1H), 4.21–4.16 (m, 1H), 4.09–4.03 (m, 1H), 3.83–3.26 (m, 16H), 2.80–2.59 (m, 2H, -O-CH₂-CH₂-CN), 1.81–1.74 (m, 2H, O-CH₂-CH₂-CH₂-NH-), 1.42–1.36 (m, 18H, C(CH₃)₃), 1.13–0.94 (m, 12H, *i*Pr-CH₃); ³¹P NMR (121 MHz, DMSO- d_6) δ [ppm] 150.0, 148.6; HRMS (MALDI) was calculated to be 1,046.4999 for C₅₃H₇₃N₇O₁₃P (M + H⁺), and found to be 10,046.5021.

3.4 Synthesis of the 2'-O-GP-Modified Guanosine-phosphoramidite

1. Synthesis of 2'-O-(2-cyanoethyl)-3',5'-O-di-*tert*-butylsilanediylguanosine (**4b**). *O*⁶-(2,4,6-Triisopropylbenzenesulfonyl)-3',5'-O-di-*tert*-butylsilanediylguanosine (**4a**) (2.28 g, 3.3 mmol) is dissolved in *tert*-butanol (17 mL). Freshly distilled acrylonitrile (4.25 mL, 66 mmol) and cesium carbonate (1.16 g, 3.3 mmol) are added to the solution. After vigorous stirring at room temperature for 2–3 h, the mixture is filtered through celite. The solvent and excess reagents are removed in vacuo. The crude material is used for the next reaction without further purification: The residue is dissolved in 4 mL of a mixture of formic acid/dioxane/water (70:24:6, v/v/v). After stirring at room temperature for 1 h, water (150 mL) is added to the mixture and the solution is extracted with dichloromethane. The organic layer is dried over Na₂SO₄ and the solvent is evaporated. The residue is purified using silica gel column chromatography with dichloromethane/methanol (9:1, v/v) to give 1.1 g (70 % over 2 steps) of 2'-O-(2-cyanoethyl)-3',5'-O-di-*tert*-butylsilanediylguanosine (**4b**) as a colorless foam. ¹H NMR (250 MHz, DMSO- d_6) δ [ppm] 10.71 (bs, 1H, NH), 7.89 (s, 1H, H8), 6.45 (bs, 2H, NH₂), 5.81 (s, 1H, H1'), 4.45–4.33 (m, 3H), 4.05–3.81 (m, 4H), 2.83–2.76 (m, 2H, O-CH₂-CH₂-CN), 1.06 (s, 9H, C(CH₃)₃), 1.01 (s, 9H, C(CH₃)₃); MS (ESI) was calculated to be 477.2 for C₂₁H₃₃N₆O₅Si (M + H⁺), and found to be 477.5.
2. Synthesis of 2'-O-(2-Aminopropyl)-3',5'-O-di-*tert*-butylsilanediylguanosine (**4e**) (*see* Notes 5 and 6). 2'-O-(2-cyanoethyl)-3',5'-O-di-*tert*-butylsilanediylguanosine (**4b**) (500 mg, 1.06 mmol) is dissolved in dry methanol (5 mL). Raney nickel (ca. 0.5 mL of the methanol-washed sediment (*see* Note 7)) and methanol (5 mL) saturated with ammonia are then added. The mixture is hydrogenated at 30 bar hydrogen-pressure for 1 h at room temperature. Thereafter the mixture is filtered through a glass filter and the catalyst is washed several times with methanol and a methanol/water mixture. The solvents are evaporated from the filtrate and the residue is used without further purification for the next reaction. MS (ESI) was calculated to be 481.3 for C₂₁H₃₇N₆O₅Si (M + H⁺), and found to be 481.8.

3. Synthesis of 2'-O-(*N,N'*-Di-*tert*-butoxycarbonylguanidinopropyl)-3',5'-O-di-*tert*-butylsilanediylguanosine (**4c**). *N,N'*-Di-boc-*N''*-triflylguanidine (163 mg, 0.415 mmol) is dissolved in dichloromethane (2.1 mL) and triethylamine (54 μ L) is then added. The solution is cooled in an ice bath and 2'-O-(2-Aminopropyl)-3',5'-O-di-*tert*-butylsilanediylguanosine (**4e**) (200 mg, 0.42 mmol) is added. After 30 min the reaction mixture is removed from the ice bath and stirred for additional 30 min at room temperature. The reaction solution is washed with saturated sodium bicarbonate solution and brine. After drying over Na₂SO₄ the solvent is evaporated. The residue is purified by column chromatography using dichloromethane/methanol (9:1, v/v) to give 270 mg (89 %) of 2'-O-(*N,N'*-Di-*tert*-butoxycarbonylguanidinopropyl)-3',5'-O-di-*tert*-butylsilanediylguanosine (**4c**). ¹H NMR (400 MHz, DMSO-*d*₆) δ [ppm] 11.49 (bs, 1H, NH), 10.66 (bs, 1H, NH), 8.56–8.53 (m, 1H, NH-CH₂-), 7.87 (s, 1H, H8), 6.39 (bs, 2H, NH₂), 5.86 (s, 1H, H1'), 4.42–4.38 (m, 1H, H3'), 4.30–4.27 (m, 2H, H2', H5'), 4.06–3.93 (m, 3H, H4', H5', $\frac{1}{2} \times$ O-CH₂-CH₂-CH₂-NH-), 3.72–3.67 (m, 1H, $\frac{1}{2} \times$ O-CH₂-CH₂-CH₂-NH-), 3.51–3.30 (m, 2H, O-CH₂-CH₂-CH₂-NH-), 1.84–1.77 (m, 2H, O-CH₂-CH₂-CH₂-NH-), 1.46 (s, 9H, -CO-C(CH₃)₃), 1.39 (s, 9H, -CO-C(CH₃)₃), 1.06 (s, 9H, -Si-C(CH₃)₃), 0.97 (s, 9H, -Si-C(CH₃)₃); HRMS (MALDI) was calculated to be 723.3856 for C₃₂H₅₅N₈O₉Si (M + H⁺), and found to be 723.3880.
4. Synthesis of *N*²-Dimethylformamidine-2'-O-(*N,N'*-di-*tert*-butoxycarbonylguanidinopropyl)-3',5'-O-di-*tert*-butylsilanediylguanosine (**4f**). 2'-O-(*N,N'*-Di-*tert*-butoxycarbonylguanidinopropyl)-3',5'-O-di-*tert*-butylsilanediylguanosine (**4c**) (1.12 g, 1.55 mmol) is dissolved in 25 mL dry methanol. *N,N*-dimethylformamide dimethyl acetal (1.0 mL, 7.76 mmol) is added and the solution is stirred at room temperature overnight. After a reaction time of 12 h the solvents are removed in vacuo and the residue is purified by silica gel column chromatography using dichloromethane/methanol (19:1, v/v) to give 1.14 g (94 %) of *N*²-Dimethylformamidine-2'-O-(*N,N'*-di-*tert*-butoxycarbonylguanidinopropyl)-3',5'-O-di-*tert*-butylsilanediylguanosine (**4f**). ¹H NMR (400 MHz, DMSO-*d*₆) δ [ppm] 11.51 (s, 1H, N¹H), 11.40 (s, 1H, NH-boc), 8.54 (s, 1H, -N=CH-N(CH₃)₂), 8.47 (m, 1H, 2'-O-CH₂-CH₂-CH₂-NH-), 7.99 (s, 1H, H-8), 5.98 (s, 1H, H1'), 4.48–4.45 (m, 1H, H5'), 4.41–4.39 (m, 1H, H2'), 4.33–4.30 (m, 1H, H5'), 4.07–3.99 (m, 2H, H3' und H4'), 3.98–3.77 (m, 2H, 2'-O-CH₂-CH₂-CH₂-NH-), 3.48–3.37 (m, 2H, 2'-O-CH₂-CH₂-CH₂-NH-), 3.14 (s, 3H, N-CH₃), 3.04 (s, 3H, N-CH₃), 1.87–1.78 (m, 2H, 2'-O-CH₂-CH₂-CH₂-NH-), 1.47

(s, 9H, $-\text{CO}-\text{C}(\text{CH}_3)_3$), 1.37 (s, 9H, $-\text{CO}-\text{C}(\text{CH}_3)_3$), 1.06 (s, 9H, $-\text{Si}-\text{C}(\text{CH}_3)_3$), 1.00 ppm (s, 9H, $-\text{Si}-\text{C}(\text{CH}_3)_3$); HRMS (MALDI) was calculated to be 800.4097 for $\text{C}_{35}\text{H}_{59}\text{N}_9\text{O}_9\text{SiNa}$ ($\text{M}+\text{Na}^+$), and found to be 800.4124.

5. Synthesis of *N*²-Dimethylformamidine-2'-*O*-(*N,N'*-di-*tert*-butoxycarbonylguanidinopropyl)-guanosine (**4g**). *N*²-Dimethylformamidine-2'-*O*-(*N,N'*-di-*tert*-butoxycarbonylguanidinopropyl)-3',5'-*O*-di-*tert*-butylsilanediylguanosine (**4f**) (1.24 g, 1.59 mmol) is dissolved in dry tetrahydrofuran (17 mL). Triethylamine (470 μL , 3.18 mmol) and $\text{Et}_3\text{N}\cdot 3\text{HF}$ (943 μL , 5.79 mmol) are then added. After stirring at room temperature for 1 h the solvent is evaporated. The residue is purified using silica gel column chromatography with dichloromethane/methanol (9:1, v/v) to give 840 mg (83 %) of *N*²-Dimethylformamidine-2'-*O*-(*N,N'*-di-*tert*-butoxycarbonylguanidinopropyl)-guanosine (**4g**) as a white foam. ¹H NMR (400 MHz, $\text{DMSO}-d_6$) δ [ppm] 11.50 (s, 1H, *N*¹*H*), 11.34 (s, 1H, *NH*-*boc*), 8.54 (s, 1H, $-\text{N}=\text{CH}-\text{N}(\text{CH}_3)_2$), 8.35 (m, 1H, 2'-*O*- $\text{CH}_2-\text{CH}_2-\text{CH}_2-\text{NH}-$), 8.10 (s, 1H, *H*8), 5.95–5.94 (m, 1H, *H*1'), 5.14–5.12 (m, 1H, 3'-*OH*), 5.08–5.05 (m, 1H, 5'-*OH*), 4.31–4.30 (m, 2H, *H*2', *H*3'), 3.95–3.93 (m, 1H, *H*4'), 3.67–3.56 (m, 4H, 2 \times *H*5', $\text{O}-\text{CH}_2-\text{CH}_2-\text{CH}_2-\text{NH}-$), 3.36–3.33 (m, 2H, $\text{O}-\text{CH}_2-\text{CH}_2-\text{CH}_2-\text{NH}-$), 3.16 (s, 3H, *N*- CH_3), 3.04 (s, 3H, *N*- CH_3), 1.77–1.74 (m, 2H, $\text{O}-\text{CH}_2-\text{CH}_2-\text{CH}_2-\text{NH}-$), 1.47 (s, 9H, $-\text{CO}-\text{C}(\text{CH}_3)_3$), 1.37 (s, 9H, $-\text{CO}-\text{C}(\text{CH}_3)_3$); HRMS (MALDI) was calculated to be 660.3076 for $\text{C}_{27}\text{H}_{43}\text{N}_9\text{O}_9\text{Na}$ ($\text{M}+\text{Na}^+$), and found to be 660.3087.
6. Synthesis of *N*²-Dimethylformamidine-2'-*O*-(*N,N'*-di-*tert*-butoxycarbonylguanidinopropyl)-5'-*O*-(4,4'-dimethoxytrityl)-guanosine (**4h**). *N*²-Dimethylformamidine-2'-*O*-(*N,N'*-di-*tert*-butoxycarbonylguanidinopropyl)-guanosine (**4g**) (840 mg, 1.32 mmol) is dissolved in dry pyridine (30 mL). 4,4'-Dimethoxytrityl chloride (670 mg, 1.98 mmol) is added and the solution is stirred for 3 h at room temperature. After the reaction is complete as assessed by TLC, the reaction is quenched with methanol and the solvents are evaporated. The residue is purified by silica gel column chromatography using dichloromethane/methanol (100:0 \rightarrow 95:5, v/v; the column is packed with dichloromethane containing 0.5 % triethylamine (*see* **Note 8**)) to give 1.08 g (87 %) of *N*²-Dimethylformamidine-2'-*O*-(*N,N'*-di-*tert*-butoxycarbonylguanidinopropyl)-5'-*O*-(4,4'-dimethoxytrityl)-guanosine (**4h**). ¹H NMR (400 MHz, $\text{DMSO}-d_6$) δ [ppm] 11.51 (s, 1H, *N*¹*H*), 11.38 (s, 1H, *NH*-*boc*), 8.50 (s, 1H, $-\text{N}=\text{CH}-\text{N}(\text{CH}_3)_2$), 8.40 (m, 1H, 2'-*O*- $\text{CH}_2-\text{CH}_2-\text{CH}_2-\text{NH}-$), 7.94 (s, 1H, *H*8), 7.38–7.20 (m, 9H,

DMTr), 6.86–6.82 (m, 4H, DMTr), 6.01–6.00 (m, 1H, $H1'$), 5.16–5.13 (m, 1H, $3'-OH$), 4.35–4.30 (m, 2H, $H2'$, $H3'$), 4.08–4.05 (m, 1H, $H4'$), 3.73 (s, 6H, $2 \times O-CH_3$), 3.71–3.61 (m, 2H, $2'-O-CH_2-CH_2-CH_2-NH-$), 3.40–3.35 (m, 2H, $2'-O-CH_2-CH_2-CH_2-NH-$), 3.28–3.16 (m, 2H, $2 \times H5'$), 3.09 (s, 3H, $N-CH_3$), 3.02 (s, 3H, $N-CH_3$), 1.80–1.74 (m, 2H, $2'-O-CH_2-CH_2-CH_2-NH-$), 1.44 (s, 9H, $-CO-C(CH_3)_3$), 1.34 (s, 9H, $-CO-C(CH_3)_3$); HRMS (MALDI) was calculated to be 962.4383 for $C_{48}H_{61}N_9O_{11}Na$ ($M+Na^+$), and found to be 962.4408.

7. Synthesis of N^2 -Dimethylformamidine-2'-*O*-(N,N' -di-*tert*-butoxycarbonylguanidinopropyl)-5'-*O*-(4,4'-dimethoxytrityl)-guanosine 3'-(cyanoethyl)- N,N -diisopropylphosphoramidite (**4d**). N^2 -Dimethylformamidine-2'-*O*-(N,N' -di-*tert*-butoxycarbonylguanidinopropyl)-5'-*O*-(4,4'-dimethoxytrityl)-guanosine (**4h**) (1.08 g, 1.15 mmol) is dissolved in dichloromethane (25 mL), then 2-cyanoethyl- N,N,N',N' -tetraisopropylaminophosphane (590 μ L, 1.76 mmol) and 4,5-dicyanoimidazole (199 mg, 1.69 mmol) are added. After 4 h the reaction progress is checked by TLC. In the event that some starting material did not react, an additional 0.3 equivalents of the phosphitylating agent as well as the catalyst are added and the reaction is stirred at room temperature for additional 4 h. After completion of the reaction the reaction solution is washed twice with saturated sodium bicarbonate solution and once with brine. After drying over Na_2SO_4 the solvent is evaporated and the residue is purified using silica gel column chromatography with dichloromethane/acetone/methanol (4:0:1 \rightarrow 3:0:2 \rightarrow 2:1:2 \rightarrow 2:2:1, v/v, the column is packed with eluent containing 0.5 % triethylamine (*see Note 8*)). The residue is dissolved in a small amount (5 mL) of dichloromethane. This solution is added dropwise into a flask with hexane (500 mL) to form a white precipitate. Two thirds of the solvent is evaporated and the residual solvent decanted carefully (*see Note 9*). The precipitate is redissolved in benzene and lyophilized (*see Note 10*) to give 1.01 g (77 %) of N^2 -Dimethylformamidine-2'-*O*-(N,N' -di-*tert*-butoxycarbonylguanidinopropyl)-5'-*O*-(4,4'-dimethoxytrityl)-guanosine 3'-(cyanoethyl)- N,N -diisopropylphosphoramidite (**4d**) (*see Note 11*). 1H NMR (400 MHz, $DMSO-d_6$) δ [ppm] 11.50–11.48 (m, 1H, NH), 11.39 (s, 1H, NH), 8.44–8.42 (m, 1H, $-N=CH-N(CH_3)_2$), 8.39–8.34 (m, 1H, $2'-O-CH_2-CH_2-CH_2-NH-$), 7.96 (s, 1H, $H8$), 7.37–7.19 (m, 9H, DMTr), 6.85–6.78 (m, 4H, DMTr), 6.07–6.05 (m, 1H, $H1'$), 4.64–4.58 (m, 1H, $H3'$), 4.48–4.44 (m, 1H, $H2'$), 4.26–4.19 (m, 1H, $H4'$), 3.80–3.23 (m, 10H), 3.73–3.70 (m, 6H, $2 \times OCH_3$), 3.07 (s, 3H, $N-CH_3$), 3.02 (s, 3H, $N-CH_3$), 2.77–2.74 (m, 1H, $-P-O-CH_2-CH_2-CN$), 2.55–2.52 (m, 1H,

$-P-O-CH_2-CH_2-CN$), 1.80–1.72 (m, 2H, $2'-O-CH_2-CH_2-CH_2-NH-$), 1.44–1.34 (m, 18H, $2 \times -CO-C(CH_3)_3$), 1.20–0.93 (m, 12H, $-N((CH(CH_3)_2)_2)$); ^{31}P NMR (121 MHz, DMSO- d_6) δ [ppm] 149.21, 148.93.

3.5 Automated Solid-Phase Synthesis of GP-Modified Oligonucleotides

The solid-phase syntheses of the GP-modified oligonucleotides are carried out according to the phosphoramidite method. We used an EXPEDITE Perceptive Biosystems 8909 synthesizer for the synthesis of our GP-modified oligonucleotides and performed our syntheses in a 1 μ mol scale. A more comprehensive description of the synthesis of $2'-O$ -modified oligonucleotides has previously been reported [16].

1. Check your synthesizer: Refill all reagent bottles and required solvents or replace empty bottles, check Argon supply, check waste.
2. Dissolve the applied phosphoramidites with amidite diluent (anhydrous acetonitrile) and attach them to the synthesizer according to manufacturer's information.
3. Program your synthesizer as specified by the manufacturer. Use the standard RNA cycle for unmodified nucleotides. Use a prolonged coupling time of 25 min for GP-modified phosphoramidites. After synthesis is completed, an additional deprotection step with deblock solution (3 % trichloroacetic acid in dichloromethane) for 20 min has to be applied (*see Note 12*).
4. Fill the synthesis column with an appropriate amount of solid-phase material and attach the column to your synthesizer (or use prefilled synthesis columns).
5. Start synthesis.
6. (optional, see **step 3**): If an additional deprotection step with deblock solution after completion of the synthesis cannot be programmed, it is necessary to apply this step by manual operation of the synthesizer (*see Note 12*): When the synthesis is finished, flush the synthesis column with deblock solution and let it act on the column for 20 min. Then thoroughly purge the synthesis column with acetonitrile and dry it with the applied inert gas.

3.6 Deprotection of GP-Modified Oligonucleotides

After deprotection, the RNA is sensitive to RNase degradation. Therefore it is recommended to work under RNase-free conditions from then on (*see Note 13*).

1. The solid-phase material is transferred to an appropriate vial.
2. To the solid-phase material 1 mL of a 3:1 mixture of ammonium hydroxide solution (25–33 %) and ethanol is added and the mixture is kept at 40 °C for 24 h. This cleaves the RNA

from the solid support and also removes the cyanoethyl groups and the protecting groups of the exocyclic amino functions.

3. The supernatant is transferred into a 4 mL vial. The solid-phase material is washed with an additional 0.5 mL of the ammonia/ethanol mixture. After sedimentation the supernatant is again transferred into the new vial and the RNA-solution is dried in a centrifugal evaporator.
4. The dried RNA is treated with 300 μL of a mixture from $\text{Et}_3\text{N} \cdot 3\text{HF}/1\text{-methyl-2-pyrrolidone}/\text{Et}_3\text{N}$ (6:3:4, v/v/v) and incubated at 60 °C for 90 min. This step removes the 2'-O-TBDMS-groups.
5. RNA-precipitation: After cooling to room temperature *n*-butanol (1.4 mL) is added and the solution is cooled to -80 °C for 60 min to facilitate precipitation.
6. The solution is centrifuged at 0 °C for 30 min.
7. The supernatant is discarded and the RNA-pellet is kept for further purification.

3.7 Purification and Analytics of GP-Modified Oligonucleotides

For a more comprehensive description of purification and analytics of 2'-O-modified oligonucleotides we refer again to a previously published article [16].

1. Anion-exchange HPLC: The pellet of the deprotected RNA (from 3.6) is dissolved in 1-methyl-2-pyrrolidone (200 μL) and DEPC-water (200 μL) and purified by AE-HPLC using a *Dionex* DNA-Pac 100 column (9 mm \times 250 mm) (1 M LiCl-buffer, DEPC-water, gradient: 0–70 % LiCl-solution in 40 min, flow: 5 mL/min, column oven: 80 °C). The fraction of the desired RNA-oligomer is collected and dried in a centrifugal evaporator (*see Note 14*).
2. Reverse-phase HPLC: The dried RNA fraction is dissolved in DEPC-water (1.5 mL) and purified by RP-HPLC using a *Phenomenex* Jupiter 4u Proteo 90 Å (15 mm \times 250 mm) (0.1 M triethylammonium acetate pH 7, acetonitrile, gradient: 0 % acetonitrile for 2 min, 0–37 % acetonitrile in 28 min, flow: 6 mL/min). The fraction with the purified RNA is collected and dried in a centrifugal evaporator. The RNA is redissolved in DEPC-water (500 μL) and dried again, to remove any traces of triethylammonium acetate.
3. Quantification: The RNA is dissolved in a specific volume of DEPC-water. The OD (optical density) is measured in a conventional UV spectrophotometer or with a NanoDrop Instrument at 260 nm. For appropriate values of the OD, the RNA-solution may need to be diluted. The concentration of the RNA-solution is calculated by the formula: $c = \text{OD}_{260} / \epsilon \times d$, where ϵ is the extinction coefficient of the oligonucleotide and

d is the length of the light path through the sample. The extinction coefficient of the RNA oligonucleotides was calculated using the nearest neighbor method.

4. Identity of the RNA was confirmed by mass spectrometry. We used *Bruker* micrOTOF-Q II. Four hundred picomoles of RNA was diluted with DEPC-water to a sample volume of 20 μL . The sample was applied to the mass spectrometer by the use of an attached HPLC-system. The measuring procedure included an integrated desalting step on a short RP-column previous to injection into the ion source.

3.8 Analysis of RNAi-Mediated Target Cleavage by GP-Modified siRNAs Using 5' RACE

Procedures to define the exact site of cleavage by a siRNA that is perfectly matched to its target cognate are illustrated schematically in Fig. 1.

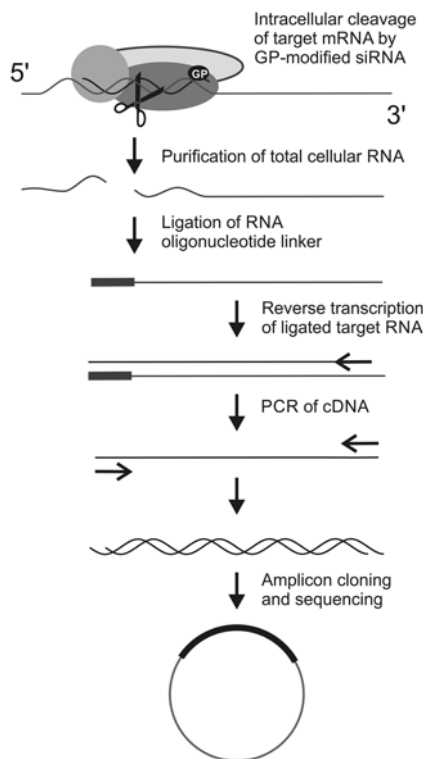


Fig. 1 Schematic illustration of the 5' RACE protocol. After transfection of cells with siRNA sequences, total RNA is isolated approximately two days later. Ligation of the RNA oligonucleotide to the 5' end of the cleaved target is followed by reverse transcription using a gene specific reverse primer. The cDNA is then used as template for PCR amplification with a primer specific to the ligated RNA oligonucleotide-derived sequence and a reverse gene specific primer. The amplicons are then inserted into a plasmid and a representative number of positive clones, approximately 10, subjected to sequencing analysis

3.8.1 Cell Culture, Transfection, and RNA Extraction

A day before transfection, seed Huh7 cells in 24-well plates at a confluency of 40 %. Cells should be cultured in Dulbecco's modified essential medium (DMEM, Lonza, Basel, Switzerland) supplemented with 10 % FCS (Gibco BRL, UK). Incubation is in a humidified atmosphere at 37 °C with 5 % CO₂. siRNAs are transfected at a final concentration of 10 nM. For a single well of a 24-well plate prepare transfection mixes as follows: mix 100 ng of target plasmid (pCH-9/3091), 100 ng of marker plasmid (pCI-neo-eGFP) and 20 pmol of the respective siRNA duplex (approximately 32.5 ng) and add Opti MEM[®] up to a volume of 50 µL. Dilute 0.3 µL of Lipofectamine[®] 2000 in 50 µL of Opti MEM[®]. The ratio of Lipofectamine to plasmid DNA is 1:1 (mL:mg), while that of Lipofectamine to siRNAs is 3:1 (mL:mg). Mix the nucleic acid/Opti MEM[®] and the Lipofectamine/Opti MEM[®] by vortexing and incubate at room temperature for 5 min. Add 50 µL of the Lipofectamine/Opti MEM[®] solution to 50 µL of the nucleic acid/Opti MEM[®], briefly vortex and incubate at room temperature for 35 min. Transfections are typically carried out in triplicate and transfection mixes are scaled-up accordingly. For transfection, dispense 100 µL of the transfection mix to each well. Gently mix by shaking and incubate for 48 h. For all studies, include unmodified and scrambled siRNAs as positive and negative controls, respectively.

3.8.2 Ligation of RNA to GeneRacer[™] RNA Oligo

Perform the 5' RACE technique using reagents from the GeneRacer[™] kit (Invitrogen, CA, USA) and procedures described by the supplier. Add 7 µL of total RNA (100 ng/µL) to a tube containing the aliquot of lyophilized GeneRacer[™] RNA Oligo (0.25 µg), mix thoroughly, collect the solution by brief centrifugation and incubate at 65 °C for 5 min. Thereafter, place on ice for 2 min, add 1 µL of Ligase Buffer (10×), 1 µL ATP (10 mM), 1 µL RNaseOut[™] (40 U/µL), 1 µL of T4 RNA ligase (5 U/µL) and incubate at 37 °C for 1 h.

After incubation, add 90 µL of nuclease-free water, 100 µL phenol-chloroform and mix vigorously by vortexing for 30 s. Centrifuge the mixture at 15,000×g for 5 min at room temperature. Transfer the upper aqueous phase (about 100 µL) to a fresh tube. Add 2 µL of mussel glycogen (10 mg/mL) and 10 µL 3 M sodium acetate (pH 5.2) and mix gently. Add 220 µL of 95 % ethanol, mix and incubate overnight at -20 °C. Collect the RNA by centrifugation at 15,000×g for 20 min at 4 °C and discard the supernatant. Wash the pellet with 500 µL of 70 % ethanol and centrifuge at 15,000×g for 2 min. Gently remove the ethanol, air-dry the pellet at room temperature for 2 min, resuspend the ligated RNA in 10 µL nuclease-free water and keep at -70 °C until required.

3.8.3 Reverse Transcription of Ligated RNA

Unless otherwise indicated all reagents were supplied with the GeneRacer[™] kit (Invitrogen, CA, USA). To tubes containing 10 µL of ligated RNA add 1 µL of the reverse gene specific primer

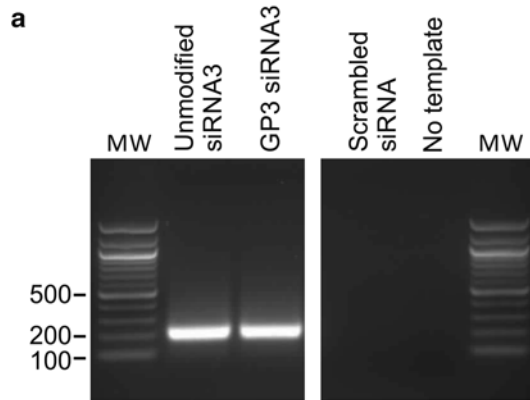
(10 μM , 5'-AGGGTCGATGTCCATGCCCC-3', Integrated DNA Technologies, Iowa, USA (*see* **Note 3**), 1 μL dNTP mix (at 10 mM each) and 1 μL of nuclease-free water. Incubate the mixture at 65 $^{\circ}\text{C}$ for 5 min then place on ice for 2 min. Subsequently, add 4 μL of First Strand Buffer (5 \times), 1 μL (0.1 M DTT), 1 μL RNaseOutTM (40 U/ μL) and 1 μL SuperScriptTM III RT (200 U/ μL) and incubate at 55 $^{\circ}\text{C}$ for 1 h. Inactivate the reaction by incubating at 70 $^{\circ}\text{C}$ for 15 min then place on ice for 2 min. Add 1 μL of RNase H (2 U) and incubate at 37 $^{\circ}\text{C}$ for 20 min. Prepare 10 μL aliquots of each cDNA sample and store at -20 $^{\circ}\text{C}$ until required for use.

3.8.4 Amplification of cDNA by 5' RACE-PCR

Amplify the cDNA template using Platinum[®] *Taq* High Fidelity DNA Polymerase (Invitrogen, CA, USA). Make up the reaction mix in a total volume of 25 μL comprising 2.5 μL High Fidelity PCR Buffer (10 \times), 0.5 μL dNTP solution (at 10 mM each), 1.5 μL of the forward GeneRacerTM primer (10 μM , 5'-CGACTGGA GCACGAGGACACTGA-3'), 0.5 μL of the reverse gene specific PCR primer (10 μM , 5'-CAAGAGATGATTAGGCAGAGGTG-3', Integrated DNA Technologies, Iowa, USA), 0.25 μL Platinum[®] *Taq* High Fidelity DNA Polymerase (5 U/ μL), 1.25 μL cDNA and 18.5 μL of nuclease-free water. Perform amplification reactions using a PCR thermocycler (T100TM Thermal Cycler, BIORAD, CA, USA) with the following cycling conditions: one cycle of 94 $^{\circ}\text{C}$ for 3 min (initial denaturation), 35 cycles of 94 $^{\circ}\text{C}$ for 30 s (denaturation), 63 $^{\circ}\text{C}$ for 30 s (annealing) and 72 $^{\circ}\text{C}$ for 1 min (extension). Perform the final extension step at 72 $^{\circ}\text{C}$ for 10 min (*see* **Note 15**). Electrophorese 10 μL of the samples on a 2 % agarose gel at 100 V for approximately 30 min and visualize the amplified PCR products under UV transillumination (Syngene G:Box, SYNGENE, UK) (Fig. 2).

3.8.5 Gel Extraction of PCR Products and Inserting Them into the pTZ57R/T Plasmid

Purification of the PCR products is carried out according to procedures recommended by the supplier of the MinElute Gel Extraction kit (Qiagen, MD, USA) with minor modifications. Briefly, cut the band containing the PCR product from the gel using a clean sharp blade. Weigh the gel slice and add 3 volumes of QG buffer. Melt the agarose by incubating the tube at 55 $^{\circ}\text{C}$ for approximately 5 min. Add an equal gel volume of isopropanol, mix and apply to the spin column. Centrifuge for 1 min at room temperature then discard the flow through. Apply 500 μL of QG buffer to the column and centrifuge at 10,000 $\times g$. Discard the flow through and then wash with 750 μL of PE buffer. After discarding the flow through, recentrifuge for 1 min at 10,000 $\times g$. Place the column in a fresh 1.7 mL tube and add 50 μL of water to the column matrix. Incubate for 2 min at room temperature then elute the DNA by centrifugation.



b

Target mRNA sequence

5' ..GACUCUCAGCAAUGUCAACGAC *CGACCUUGAGGCAUACUUC*AAAGACUGUUUGUUUAAAAG.. 3'

Ligated RNA oligonucleotide sequence

5' GACACUGACAUGGACUGAAGGAGUAG 3'

Sequence of cDNA

5' GACACTGACATGGACTGAAGGAGTAG *AGGCATACTTC*AAAGACTGTTTGTTTAAAG.. 3'

Fig. 2 Representative data from 5' RACE analysis of RNA targeted by siRNA modified with a GP residue in position 3 from the 5' end of the guide strand GP3 siRNA3. The GP3 siRNA3 targeted a sequence within the *HBx* region of HBV. **(a)** Agarose gel resolution of DNA amplified after reverse transcription of RNA comprising the RNA linker oligonucleotide ligated to the downstream target RNA. The reverse primer was specific to the HBV target sequence and the forward primer hybridized to complementary sequences of the oligonucleotide linker. Controls to verify specificity of the reaction included RNA extracted from cells that had been transfected with unmodified siRNA3 targeting the HBV sequence, a scrambled siRNA that did not target any known gene and no template cDNA. **(b)** Sequence of the HBV target region with sequence complementary to GP3 siRNA3 indicated in *italic font*. Sequence of the RNA oligonucleotide and amplicon are indicated *below*. The junction of the oligonucleotide and target sequence indicates the site of cleavage mediated by GP3 siRNA3

Ligate the purified PCR products to the pTZ57R/T plasmid (Thermo Scientific, MA, USA) in a total reaction volume of 30 μ L comprising 6 μ L Ligation Buffer (5 \times), 1 μ L T4 DNA ligase (Thermo Scientific, MA, USA) (5 U/ μ L), 3 μ L of pTZ57R/T plasmid (0.17 pmol ends), 5 μ L of purified 5' RACE PCR product and 15 μ L nuclease-free water. Incubate overnight at 14 $^{\circ}$ C. Transform 100 μ L of chemically competent bacteria (e.g. DH5 α , Invitrogen, CA, USA) with 10 μ L of ligation reaction and spread on ampicillin-containing Luria Bertani agar plates impregnated with 5-bromo-4-chloro-3-indolyl- β -D-galactopyranoside (X-gal) (US BIOLOGICAL Life Sciences, MA, USA) and Isopropyl β -D-1-thiogalactopyranoside (IPTG) (Sigma, MO, USA). Incubate

overnight at 37 °C then pick ten individual white colonies using sterile procedures. Inoculate each into 10 mL of ampicillin-containing Luria Bertani broth and incubate overnight at 37 °C with shaking. Perform standard mini preparations of each cloned plasmid.

3.8.6 Screening for Positive Clones Using *Apa*LI

Screen for positive clones by digesting with *Apa*LI restriction enzyme (*see* **Note 16**) in a total reaction volume of 20 μ L comprising 2 μ L of Fast Digest Buffer (10 \times), 2 μ L Fast Digest *Apa*LI (1 U/ μ L) (Thermo Scientific, MA, USA), 5 μ L of plasmid DNA (200 ng/ μ L) and 11 μ L of water. Incubate the samples at 37 °C for about 30 min. Electrophorese 10 μ L of each sample on a 2 % agarose gel at 100 V for approximately 30 min and visualize under UV transillumination (Syngene G:Box, SYNGENE, UK). Presence of two DNA fragments of 1,859 bp and 1,246 bp indicates successful cloning of the PCR products into pTZ57R/T (*see* **Note 16**). Select the positive plasmid clones for automated sequencing. Presence of sequences derived from both the ligated GeneRacerTM RNA oligonucleotide and predicted mRNA cleavage product indicates specific RNAi-mediated cleavage of the target by GP-containing siRNAs (*see* example shown in Fig. 2).

4 Notes

1. We purchased solid 5-ethylthiotetrazole (e.g. from *Azco Biotech Inc.*) to be able to make our own solution with a particular concentration of 0.35 M. There are also ready-to-use solutions available with a 5-ethylthiotetrazole concentration of 0.25 M. These solutions can also be used, maybe with slightly less coupling efficiency for the modified phosphoramidites.
2. Plasmids are selected according to the specific requirements of the assay. In the example here we used an HBV replication-competent target plasmid (pCH-9/3091) [14] in conjunction with a GFP reporter plasmid [15] to verify transfection efficiency.
3. Gene-specific primers should be designed according to the sequence of the gene under investigation. They should complement a sequence at least 200 bases downstream of the intended siRNA cleavage site and the T_m suitable for use during reverse transcription at 42 °C. Short primers of 16–20 bases are typically preferred.
4. For the chemical syntheses it is necessary to use anhydrous solvents and to work with an inert gas atmosphere, because many of the reagents are sensitive to hydrolysis.
5. Reduction with activated Ni-catalyst and hydrogen. The hydrogenation step is sensitive to reaction conditions such as

the ratio of amount of starting material to catalyst, the size of the employed autoclave and reaction time. Under optimized conditions, yields for reduction of each nucleotide derivative were moderate (about 50 %). A loss of the desired product was also confirmed by the observation that part of the amino compound was not released from the catalyst during filtration, despite being subjected to several washes with methanol. To minimize losses the crude unpurified 2'-*O*-aminopropyl compounds were used to introduce the guanidino groups in the next synthesis step.

6. There might be an alternative way of reducing the 2'-*O*-cyanoethyl groups, if there is no autoclave available or to avoid the application of hazardous H₂ and the pyrophoric nickel catalyst. The original procedure was published here [17, 18]. We tested this reaction only with the guanosine derivative and with 2'-*O*-cyanomethyl-3',5'-*O*-(tetraisopropylidisiloxane-1,3-diyl)-uridine but it may also work with the other nucleosides. The yield was only moderate (ca. 30 %). Typical procedure: To obtain dry nickel(II)chloride, NiCl₂·6H₂O was placed in a round bottom flask and was heated carefully under reduced pressure with a heat gun until the solid turns golden yellow. The nucleoside (3 mmol) was dissolved in anhydrous ethanol under inert gas atmosphere and the solution was cooled to 0 °C. To the stirred solution dry NiCl₂ (3 mmol) was added and the sodium borohydride (9 mmol) was added in small portions. A black precipitate is formed. After 1 h the progress of the reaction is monitored by TLC and if the conversion is not complete, some more sodium borohydride is added. The reaction is stopped by addition of diethylenetriamine (30 mmol) and is stirred for another 30 min. The solvent is evaporated and the residue is dissolved in ethylacetate, washed twice with saturated sodium bicarbonate solution (2×80 mL). The organic phase is dried over magnesium sulfate, evaporated and the residue is purified by silica gel column chromatography with dichloromethane/methanol (5:1 (v/v)).
7. When the activated nickel catalyst (Raney-Nickel) is washed with methanol, it is important that the catalyst does not completely dry, because of its pyrophoric properties. Also, take great care when opening the autoclave because of the adsorbed H₂ in the catalyst.
8. The slightly acidic reaction of silica gel may cause a partial deprotection of the DMTr-group during purification. To circumvent this problem the addition of 0.5 % triethylamine to the eluent is recommended. If eluent with 0.5 % triethylamine is used for purification of phosphoramidites it is very important to completely remove the triethylamine from the purified product, because residual triethylamine will deprotonate the

5-ethylthiotetrazole in the activator solution of the synthesizer and will thereby reduce or completely extinguish coupling efficiency of your phosphoramidite. We only use 0.5 % triethylamine in the solvent used for packing the column while elution is performed without triethylamine.

9. The forming precipitate will largely adhere to the glass wall of the used flask or vessel, so decanting is easy. You have to make sure to thoroughly redissolve the entire adhering product for purification.
10. Lyophilization can be performed by dissolving the phosphoramidite in a round bottom flask, freezing the solution by dipping and slightly rotating the flask in liquid nitrogen. Finally the flask is connected to a vacuum pump with an interconnected cooling trap. To avoid the use of benzene, it is also possible to use dioxane for lyophilization. The dioxane must be checked for contamination with peroxides before use, because peroxides will oxidize the phosphoramidite to a phosphoramidate.
11. In some cases after precipitation (and even after column chromatography) the phosphoroamidite still contains some traces of hydrolysed phosphorylation agent (H-phosphonate). According to our experience, this does not interfere with solid-phase synthesis. The amount of the impurity can be reduced by several consecutive precipitations but this will slightly reduce yield. The signal of the H-phosphonate can be observed in ^{31}P -NMR at approximately 14 ppm.
12. The function of the additional deprotection step is the cleavage of the boc-protecting groups (*tert*-butoxycarbonyl-) from the guanidino moiety. This is especially required, if the GP-modification is introduced at the very end of the oligonucleotide and only few or no consecutive synthesis cycles including deprotection will follow.
13. After cleavage from solid support and removal of protecting groups, the RNA is sensitive to RNase digestion. To prevent the RNA from degradation it is recommended to wear gloves and to use RNase-free labware. DEPC-water and RNase-free reagents and solutions should be used. For long term storage the RNA-solution should be kept at $-80\text{ }^{\circ}\text{C}$. Alternatively the RNA can be precipitated or lyophilized again.
14. If a complete 1 μmol synthesis batch of siRNA is purified with a *Dionex* DNA-Pac 100 column (9 mm \times 250 mm), the signals will suffer significant signal broadening due to column overload. To avoid this problem the siRNA can be purified in smaller portions or a bigger column can be used.
15. Thermal cycling conditions vary according to the specific properties of the sequences to be analyzed. Importantly, the

primers should form stable and specific pairs with their cognates under the cycling conditions that are selected. Protocols giving advice on optimizing PCR conditions are widely available and a detailed discussion is beyond the scope of this article.

16. Selection of appropriate restriction enzymes for screening of plasmid clones should be made according to how the positions of their recognition sites relative to the inserted sequence will be most informative. The sizes of the electrophoretically resolved bands will also be dependent on the positions of the restriction sites of the cloned plasmids.

Acknowledgements

We gratefully acknowledge financial assistance from the Ernst & Ethel Eriksen Trust, National Research Foundation of South Africa (NRF), Medical Research Council, the Poliomyelitis Research Foundation (PRF) and from the German Research Foundation (DFG). We also thankfully acknowledge the helpful assistance of Corvin Steidinger, Christian Schuch, and Timo Weinrich in the synthesis of the GP-modified monomers.

References

1. Kim VN, Han J, Siomi MC (2009) Biogenesis of small RNAs in animals. *Nat Rev Mol Cell Biol* 10:126–139
2. Guo H, Ingolia NT, Weissman JS, Bartel DP (2010) Mammalian microRNAs predominantly act to decrease target mRNA levels. *Nature* 466:835–840
3. Kim D, Rossi J (2008) RNAi mechanisms and applications. *Biotechniques* 44:613–616
4. Behlke MA (2008) Chemical modification of siRNAs for in vivo use. *Oligonucleotides* 18:305–319
5. Fisher M, Abramov M, Van Aerschot A, Rozenski J, Dixit V, Juliano RL, Herdewijn P (2009) Biological effects of hexitol and alditol-modified siRNAs targeting B-Raf. *Eur J Pharmacol* 606:38–44
6. Hean J, Crowther C, Ely A, Ul Islam R, Barichievy S, Bloom K, Weinberg MS, van Otterlo WA, de Koning CB, Salazar F, Marion P, Roesch EB, Lemaitre M, Herdewijn P, Arbuthnot P (2010) Inhibition of hepatitis B virus replication in vivo using lipoplexes containing alditol-modified antiviral siRNAs. *Artif DNA PNA XNA* 1:17–26
7. Brzezinska J, D'Onofrio J, Buff MC, Hean J, Ely A, Marimani M, Arbuthnot P, Engels JW (2012) Synthesis of 2'-O-guanidinopropyl-modified nucleoside phosphoramidites and their incorporation into siRNAs targeting hepatitis B virus. *Bioorg Med Chem* 20:1594–1606
8. Marimani MD, Ely A, Buff MC, Bernhardt S, Engels JW, Arbuthnot P (2013) Inhibition of hepatitis B virus replication in cultured cells and in vivo using 2'-O-guanidinopropyl modified siRNAs. *Bioorg Med Chem* 21:6145–6155
9. Mukobata T, Ochi Y, Ito Y, Wada S, Urata H (2010) Facile and efficient approach for the synthesis of N(2)-dimethylaminomethylene-2'-O-methylguanosine. *Bioorg Med Chem Lett* 20:129–131
10. Sekine M (1989) General method for the preparation of N3- and O4-substituted uridine derivatives by phase-transfer reactions. *J Org Chem* 54:2321–2326
11. Saneyoshi H, Scio K, Sekine M (2005) A general method for the synthesis of 2'-O-cyanoethylated oligoribonucleotides having promising hybridization affinity for DNA and RNA and enhanced nuclease resistance. *J Org Chem* 70:10453–10460
12. Haas J, Engels J (2007) A novel entry to 2'-O-aminopropyl modified nucleosides amenable for further modifications. *Tetrahedron Lett* 48:8891–8894

13. Feichtinger K, Zapf C, Singe HL, Goodman M (1998) Diprotected triflylguanidines: a new class of guanidinylation reagents. *J Org Chem* 63:3804–3805
14. Nassal M (1992) The arginine-rich domain of the hepatitis B virus core protein is required for pregenome encapsidation and productive viral positive-strand DNA synthesis but not for virus assembly. *J Virol* 66:4107–4116
15. Passman M, Weinberg M, Kew M, Arbuthnot P (2000) In situ demonstration of inhibitory effects of hammerhead ribozymes that are targeted to the hepatitis Bx sequence in cultured cells. *Biochem Biophys Res Commun* 268:728–733
16. Engels JW, Odadzic D, Smicius R, Haas J (2010) Chemical synthesis of 2'-O-alkylated siRNAs. *Methods Mol Biol* 623:155–170
17. Caddick S, Judd DB, Lewis AKdK, Reich MT, Williams MR (2003) A generic approach for the catalytic reduction of nitriles. *Tetrahedron* 59:5417–5423
18. Khurana JM, Kukreja G (2002) Rapid reduction of nitriles to primary amines with Nickel Boride at ambient temperature [1]. *Synth Commun* 32:1265–1269

SUPPLEMENTARY METHODS:

7.5.1. Detection of siRNA-mediated HBV cleavage by 5' RACE

7.5.1.1. Generation of positive control for 5' RACE

The *in vitro* transcribed RNA was designed to have the same sequence as that of the predicted cleaved mRNA product *in vitro* and served as a positive control for 5' RACE analysis (Fig. 7.5A). The template for *in vitro* transcription was designed to contain the T7 promoter immediately upstream of the predicted siRNA3-mediated cleavage product. *In vitro* transcription using T7 RNA polymerase would therefore generate the predicted cleavage product. All reagents used for PCR were from Thermo Scientific (Thermo Scientific, MA, USA), unless otherwise stated. The *in vitro* transcribed template was prepared by amplifying the target region within pCH-9/3091 (100 ng/μl) with 10 pmol each of the following primer pair (Integrated DNA Technologies, IA, USA): forward siRNA3 TF 5'-GCTAGCTAATACGACTCACTATAGGGAGGCATACTTCAAAGACTGTTTGTT-3' and reverse siRNA3 TR 5'-GCGGCCGCAGGGTTCGATGTCCATGCCCCA-3'.

All PCR amplifications were performed in a PCR thermocycler comprised of the following cycling conditions: one cycle of 94°C for 3 minutes (initial denaturation), 35 cycles of 94°C for 30 seconds (denaturation), 63°C for 30 seconds (annealing) and 72°C for 1 minute (extension). The final extension step was performed at 72°C for 10 minutes. Amplified PCR products of about 257 bp were subjected to electrophoresis on a 2% agarose gel at 100 volts for 45 minutes and visualised under UV transillumination. The PCR products were subjected to MinElute Gel Extraction and subsequent cloning into pTZ57R/T plasmid, as described in **Supplementary Methods Section 5.4.3**. Positive clones were identified after digesting

plasmids (1 µg) with *PvuII* (40 U, Thermo Scientific, MA, USA) and *NotI* (10 U, Thermo Scientific, MA, USA) (Fig. 7.5A). Samples were incubated at 37°C for 2 hours and subjected to electrophoresis on a 2% agarose gel at 100 volts for 45 minutes and visualised under UV transillumination. Generation of three DNA fragments (of approximately 2513 bp, 375 bp and 257 bp) indicated successful cloning of PCR products into pTZ57R/T. Sequences of positive clones were confirmed by DNA sequencing using the M13 primer pair (Inqaba Biotech Industries, South Africa): forward 5'-GTAAAACGACGGCCAGT-3' and reverse 5'-CAGGAAACAGCTATGAC-3'.

7.5.1.2. Preparation of *in vitro* transcribed RNA

ScaI and *HindIII* (Thermo Scientific, MA, USA) digestion was performed to produce the template for *in vitro* transcription (Fig. 7.5B). This reaction was performed using DNA (1 µg), *HindIII* (40 U) and *ScaI* (20 U). Samples were incubated for 2 hours at 37°C, resolved on a 2% agarose gel at 100 volts for about 45 minutes and visualised under UV transillumination. Digestion with *HindIII* and *ScaI* produced two DNA fragments of about 1759 bp and 1386 bp. Thereafter, the smaller fragment of approximately 1386 bp was purified using the MinElute Gel Extraction as described in **Supplementary Methods Section 5.4.3**.

Samples were subjected to *in vitro* transcription using the TranscriptAid T7 High Yield Transcription Kit (Thermo Scientific, MA, USA) (Fig. 7.5B). This was conducted using NTPs (100 mM each), TranScriptAid™ Enzyme Mix and DNA template (1 µg). The reaction mixture was briefly centrifuged at 12 000 × g at 4°C for 20 seconds. The sample was resolved on a 2% agarose gel at 80 volts for 30 minutes and visualised under UV

transillumination. The generated RNA transcripts were purified using the phenol-chloroform extraction method as described in **Supplementary Methods Section 5.4.1**.

7.5.1.3. Detection of siRNA-mediated mRNA cleavage product *in vitro* by 5' RACE

The 5'-RLM-RACE technique was employed to specifically detect the cleaved mRNA product in cells transfected with unmodified or GP-modified siRNAs. For this experiment, Huh7 cells were maintained, seeded and co-transfected with 100 ng of pCH-9/3091 target plasmid, 100 ng pCI-eGFP and 10 nM siRNA (32.5 ng), as described in **Supplementary Methods Section 4.1**. A combination of siRNAs containing a single, double, triple or quadruplicate number of GP residues were employed and included: unmodified siRNA3, GP3 siRNA3, GP4 siRNA3, GP5 siRNA3, GP2.3 siRNA3, GP2.3.17 siRNA3, GP2.5.17.20 siRNA3 and scrambled siRNA (Table 7.1). The different combinations of GP modifications were employed to investigate whether the position or number of GP residues within the siRNA would alter the mRNA cleavage site. Total RNA extraction was performed using Tri Reagent[®] at 24-hours post-transfection as described in **Supplementary Methods Section 4.2**. Subsequently, ligation and reverse transcription were performed as described in **Supplementary Methods Section 5.4.1-5.4.2**.

Table 7.1: The siRNAs employed for 5' RACE analysis *in vitro*

Name of siRNA	Antisense siRNA sequence
Unmodified siRNA3	5'-UUG AAG UAU GCC UCA AGG UCG-3'
GP3 siRNA3	5'-UUG _{GP} AAG UAU GCC UCA AGG UCG-3'
GP4 siRNA3	5'-UUG A _{GP} AG UAU GCC UCA AGG UCG-3'
GP5 siRNA3	5'-UUG AA _{GP} G UAU GCC UCA AGG UCG-3'
GP2.3 siRNA3	5'-UU _{GP} G _{GP} AAG UAU GCC UCA AGG UCG-3'
GP2.3.17 siRNA3	5'-UU _{GP} G _{GP} AAG UAU GCC UCA AG _{GP} G UCG-3'
GP2.5.17.20 siRNA3	5'-UU _{GP} G AA _{GP} G UAU GCC UCA AG _{GP} G UC _{GP} G-3'
Scrambled siRNA	5'-GCG AAG UGA CCA GCG AAU AC dT-3'

7.5.1.4. Amplification of cDNA by 5' RACE-PCR, cloning and DNA sequencing

The generated cDNA template was amplified by 5' RACE-PCR using the Platinum[®] *Taq* DNA Polymerase High Fidelity kit (Life Technologies, CA, USA). The PCR was performed using dNTP solution (10 mM each), 10 pmol each of the forward GeneRacer[™] 5' primer (5'-CGACTGGAGCACGAGGACACTGA-3'; Life Technologies, CA, USA), reverse gene-specific PCR primer (5'-CAAGAGATGATTAGGCAGAGGTG-3'; Integrated DNA Technologies, IA, USA), 0.25 µl Platinum[®] *Taq* DNA Polymerase High Fidelity (5 U/µl) and 1.25 µl cDNA template (100 ng/µl). All PCR amplification reactions were performed in a thermocycler using the following cycling conditions: one cycle of 94°C for 3 minutes (initial denaturation), 35 cycles of denaturation at 94°C for 30 seconds, annealing at 63°C for 30 seconds and extension at 72°C for 1 minute. The final extension step was performed at 72°C

for 10 minutes. Amplified PCR products were subjected to electrophoresis on a 2% agarose gel at 100 volts for 30 minutes and visualised under UV transillumination (Appendix 7.3.1) [223]. This was followed by purification of PCR products, cloning into pTZ57R/T plasmid and DNA sequencing using the M13 reverse primer, as described in **Supplementary Methods Section 5.4.3**. The positive 5' RACE product was verified by the presence of sequences derived from the ligated GeneRacerTM RNA oligonucleotide and predicted mRNA cleavage product (Appendix 7.3.2) [223]. Diagrammatic illustration of the 5' RACE protocol is shown in a study conducted by Buff et al., 2015 [223].

Generation of 5' RACE positive control:

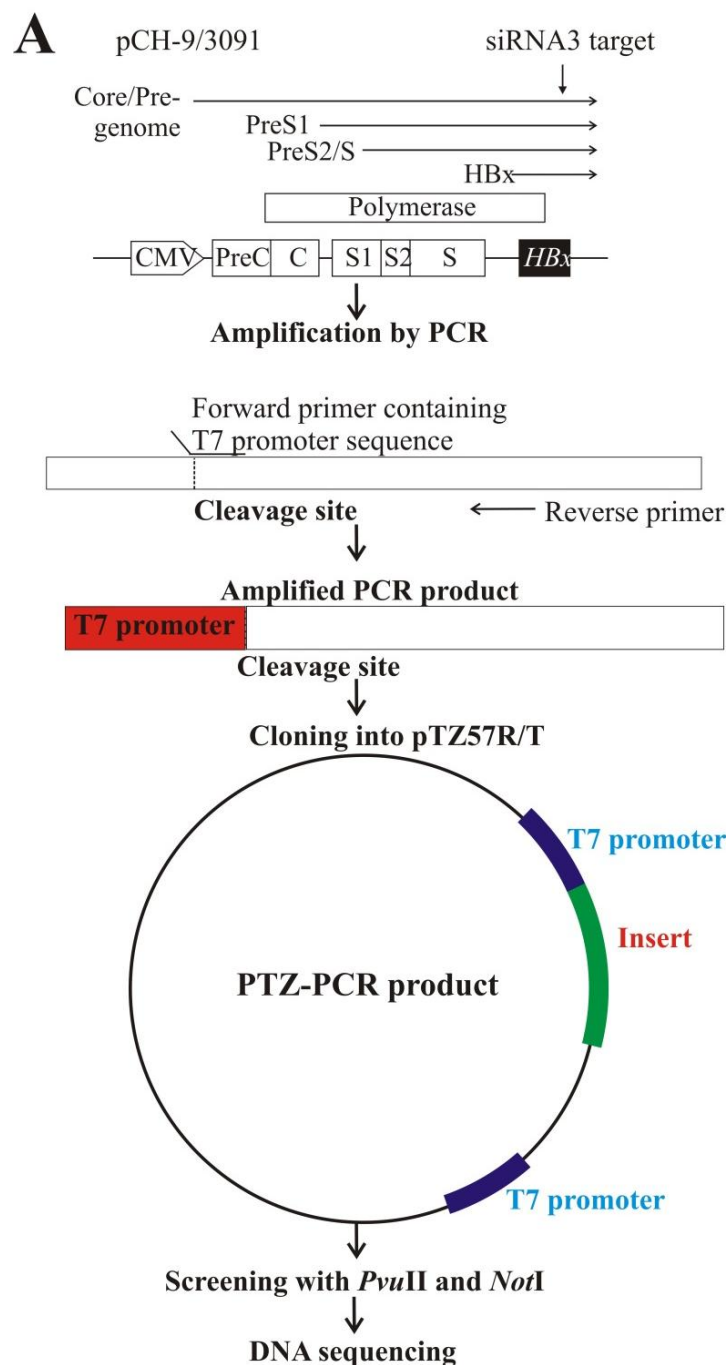


Figure 7.5A. Generation of positive control for 5' RACE

The 5' RACE positive control was generated by amplifying the region of pCH-9/3091 where siRNA-mediated cleavage was predicted to occur. After PCR amplification, the products were cloned into pTZ57R/T, followed by screening with *PvuII* and *NotI* and positive clones confirmed by DNA sequencing.

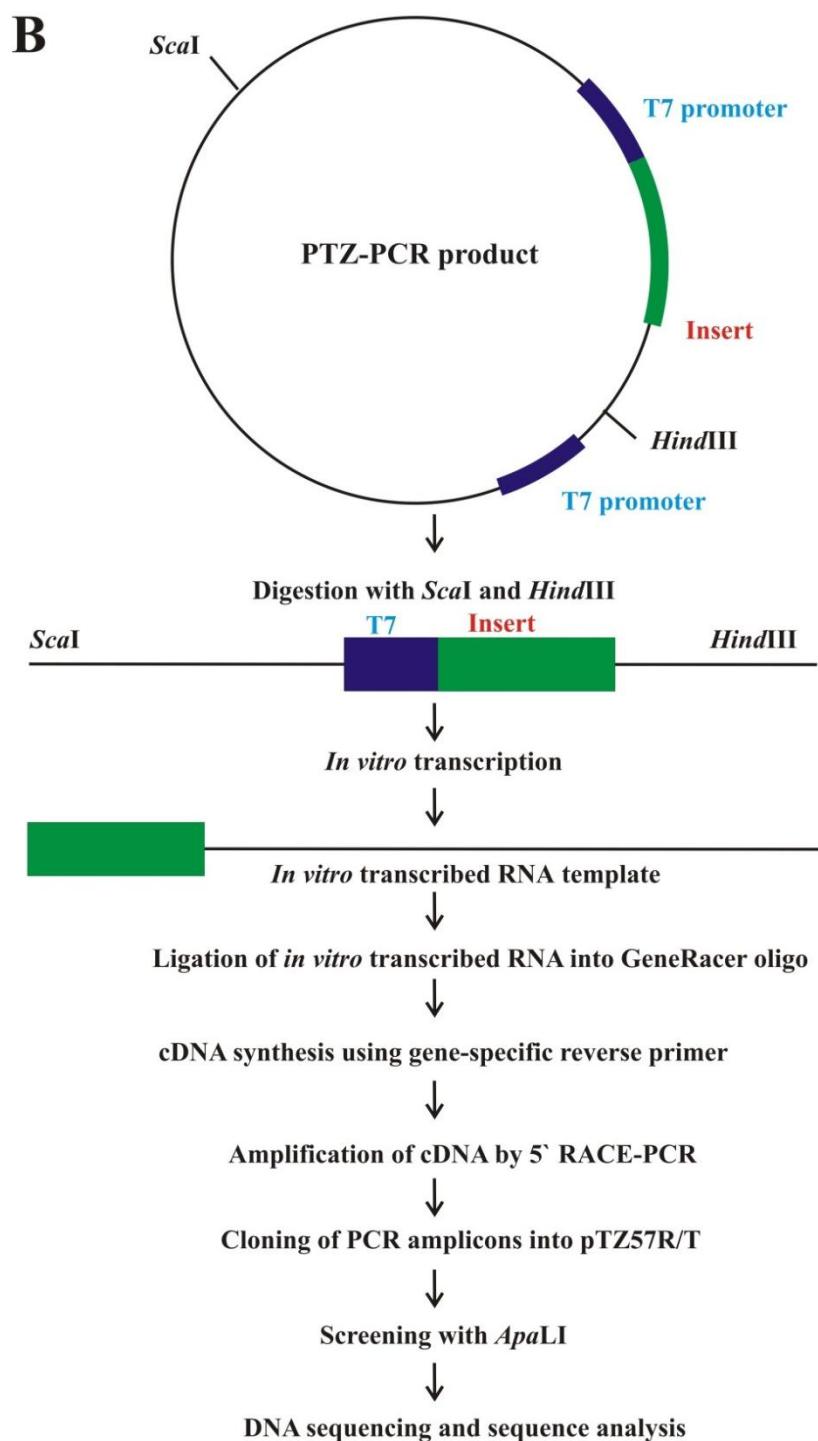


Figure 7.5B. Preparation of *in vitro* transcribed RNA

Following cloning into pTZ57R/T, screening with *PvuII* and *NotI*, and DNA sequencing, positive clones were digested with *ScaI* and *HindIII* to produce the template for *in vitro* transcription. Subsequently, samples were subjected to *in vitro* transcription to generate an RNA template possessing the same sequence as that of the predicted mRNA cleavage product for use as a positive control for 5' RACE analysis.

Chapter 8: References

1. Gust, I.D., et al., *Taxonomic classification of human hepatitis B virus*. Intervirology, 1986. **25**(1): p. 14-29.
2. Evans, A.A., et al., *Geographic variation in viral load among hepatitis B carriers with differing risks of hepatocellular carcinoma*. Cancer Epidemiol Biomarkers Prev, 1998. **7**(7): p. 559-65.
3. Redeker, A.G., *Viral hepatitis: clinical aspects*. Am J Med Sci, 1975. **270**(1): p. 9-16.
4. Zuckerman, A.J. and P.E. Taylor, *Persistence of the serum hepatitis (SH-Australia) antigen for many years*. Nature, 1969. **223**(5201): p. 81-2.
5. Summers, J., J.M. Smolec, and R. Snyder, *A virus similar to human hepatitis B virus associated with hepatitis and hepatoma in woodchucks*. Proc Natl Acad Sci U S A, 1978. **75**(9): p. 4533-7.
6. Lanford, R.E., et al., *Isolation of a hepadnavirus from the woolly monkey, a New World primate*. Proc Natl Acad Sci U S A, 1998. **95**(10): p. 5757-61.
7. Testut, P., et al., *A new hepadnavirus endemic in arctic ground squirrels in Alaska*. J Virol, 1996. **70**(7): p. 4210-9.
8. Mason, W.S., G. Seal, and J. Summers, *Virus of Pekin ducks with structural and biological relatedness to human hepatitis B virus*. J Virol, 1980. **36**(3): p. 829-36.
9. Sprengel, R., E.F. Kaleta, and H. Will, *Isolation and characterization of a hepatitis B virus endemic in herons*. J Virol, 1988. **62**(10): p. 3832-9.

10. Nayersina, R., et al., *HLA A2 restricted cytotoxic T lymphocyte responses to multiple hepatitis B surface antigen epitopes during hepatitis B virus infection*. J Immunol, 1993. **150**(10): p. 4659-71.
11. Penna, A., et al., *Cytotoxic T lymphocytes recognize an HLA-A2-restricted epitope within the hepatitis B virus nucleocapsid antigen*. J Exp Med, 1991. **174**(6): p. 1565-70.
12. Rehermann, B., et al., *The cytotoxic T lymphocyte response to multiple hepatitis B virus polymerase epitopes during and after acute viral hepatitis*. J Exp Med, 1995. **181**(3): p. 1047-58.
13. Rehermann, B., et al., *The hepatitis B virus persists for decades after patients' recovery from acute viral hepatitis despite active maintenance of a cytotoxic T-lymphocyte response*. Nat Med, 1996. **2**(10): p. 1104-8.
14. Bertoletti, A., et al., *Cytotoxic T lymphocyte response to a wild type hepatitis B virus epitope in patients chronically infected by variant viruses carrying substitutions within the epitope*. J Exp Med, 1994. **180**(3): p. 933-43.
15. Kew, M.C., et al., *Increased hepatocarcinogenic potential of hepatitis B virus genotype A in Bantu-speaking sub-saharan Africans*. J Med Virol, 2005. **75**(4): p. 513-21.
16. Chang, M.H., et al., *The significance of spontaneous hepatitis B e antigen seroconversion in childhood: with special emphasis on the clearance of hepatitis B e antigen before 3 years of age*. Hepatology, 1995. **22**(5): p. 1387-92.

17. Chang, M.H., et al., *Prevention of hepatocellular carcinoma by universal vaccination against hepatitis B virus: the effect and problems*. Clin Cancer Res, 2005. **11**(21): p. 7953-7.
18. Perz, J.F., et al., *The contributions of hepatitis B virus and hepatitis C virus infections to cirrhosis and primary liver cancer worldwide*. J Hepatol, 2006. **45**(4): p. 529-38.
19. Benvegnu, L., et al., *Concurrent hepatitis B and C virus infection and risk of hepatocellular carcinoma in cirrhosis. A prospective study*. Cancer, 1994. **74**(9): p. 2442-8.
20. Botha, J.F., et al., *Hepatitis B virus carrier state in black children in Ovamboland: role of perinatal and horizontal infection*. Lancet, 1984. **1**(8388): p. 1210-2.
21. Beasley, R.P. and L.Y. Hwang, *Hepatocellular carcinoma and hepatitis B virus*. Semin Liver Dis, 1984. **4**(2): p. 113-21.
22. Gitlin, N., *Hepatitis B: diagnosis, prevention, and treatment*. Clin Chem, 1997. **43**(8 Pt 2): p. 1500-6.
23. Kim, W.R., et al., *Serum activity of alanine aminotransferase (ALT) as an indicator of health and disease*. Hepatology, 2008. **47**(4): p. 1363-70.
24. Zuckerman, A.J., *Perinatal transmission of hepatitis B*. Arch Dis Child, 1984. **59**(11): p. 1007-9.
25. Tabor, E., et al., *Horizontal transmission of hepatitis B virus among children and adults in five rural villages in Zambia*. J Med Virol, 1985. **15**(2): p. 113-20.
26. Scott, R.M., et al., *Experimental transmission of hepatitis B virus by semen and saliva*. J Infect Dis, 1980. **142**(1): p. 67-71.

27. Hadchouel, M., et al., *Presence of HBV DNA in spermatozoa: a possible vertical transmission of HBV via the germ line*. J Med Virol, 1985. **16**(1): p. 61-6.
28. Kramvis, A. and M.C. Kew, *Epidemiology of hepatitis B virus in Africa, its genotypes and clinical associations of genotypes*. Hepatol Res, 2007. **37**(s1): p. S9-S19.
29. Sunbul, M., *Hepatitis B virus genotypes: global distribution and clinical importance*. World J Gastroenterol, 2014. **20**(18): p. 5427-34.
30. Kramvis, A., *Genotypes and genetic variability of hepatitis B virus*. Intervirology, 2014. **57**(3-4): p. 141-50.
31. Olinger, C.M., et al., *Phylogenetic analysis of the precore/core gene of hepatitis B virus genotypes E and A in West Africa: new subtypes, mixed infections and recombinations*. J Gen Virol, 2006. **87**(Pt 5): p. 1163-73.
32. Tuttleman, J.S., C. Pourcel, and J. Summers, *Formation of the pool of covalently closed circular viral DNA in hepadnavirus-infected cells*. Cell, 1986. **47**(3): p. 451-60.
33. Nassal, M., M. Junker-Niepmann, and H. Schaller, *Translational inactivation of RNA function: discrimination against a subset of genomic transcripts during HBV nucleocapsid assembly*. Cell, 1990. **63**(6): p. 1357-63.
34. Cummings, I.W., et al., *Isolation, characterization, and comparison of recombinant DNAs derived from genomes of human hepatitis B virus and woodchuck hepatitis virus*. Proc Natl Acad Sci U S A, 1980. **77**(4): p. 1842-6.

35. Weiser, B., et al., *Closed circular viral DNA and asymmetrical heterogeneous forms in livers from animals infected with ground squirrel hepatitis virus*. J Virol, 1983. **48**(1): p. 1-9.
36. Sohn, J.A., S. Litwin, and C. Seeger, *Mechanism for CCC DNA synthesis in hepadnaviruses*. PLoS One, 2009. **4**(11): p. e8093.
37. Newbold, J.E., et al., *The covalently closed duplex form of the hepadnavirus genome exists in situ as a heterogeneous population of viral minichromosomes*. J Virol, 1995. **69**(6): p. 3350-7.
38. Chen, M. and J.H. Ou, *Cell type-dependent regulation of the activity of the negative regulatory element of the hepatitis B virus core promoter*. Virology, 1995. **214**(1): p. 198-206.
39. Antonucci, T.K. and W.J. Rutter, *Hepatitis B virus (HBV) promoters are regulated by the HBV enhancer in a tissue-specific manner*. J Virol, 1989. **63**(2): p. 579-83.
40. Guo, W.T., K.D. Bell, and J.H. Ou, *Characterization of the hepatitis B virus EnhI enhancer and X promoter complex*. J Virol, 1991. **65**(12): p. 6686-92.
41. Su, H. and J.K. Yee, *Regulation of hepatitis B virus gene expression by its two enhancers*. Proc Natl Acad Sci U S A, 1992. **89**(7): p. 2708-12.
42. Yaginuma, K., et al., *Hepatitis B virus (HBV) particles are produced in a cell culture system by transient expression of transfected HBV DNA*. Proc Natl Acad Sci U S A, 1987. **84**(9): p. 2678-82.
43. Gunther, S., et al., *Type, prevalence, and significance of core promoter/enhancer II mutations in hepatitis B viruses from immunosuppressed patients with severe liver disease*. J Virol, 1996. **70**(12): p. 8318-31.

44. Magnius, L.O. and J.A. Espmark, *New specificities in Australia antigen positive sera distinct from the Le Bouvier determinants*. J Immunol, 1972. **109**(5): p. 1017-21.
45. Schodel, F., et al., *Structure of hepatitis B virus core and e-antigen. A single precore amino acid prevents nucleocapsid assembly*. J Biol Chem, 1993. **268**(2): p. 1332-7.
46. Ou, J.H., O. Laub, and W.J. Rutter, *Hepatitis B virus gene function: the precore region targets the core antigen to cellular membranes and causes the secretion of the e antigen*. Proc Natl Acad Sci U S A, 1986. **83**(6): p. 1578-82.
47. McLachlan, A., et al., *Expression of hepatitis B virus surface and core antigens: influences of pre-S and precore sequences*. J Virol, 1987. **61**(3): p. 683-92.
48. Lee, T.H., et al., *Hepatitis B virus transactivator X protein is not tumorigenic in transgenic mice*. J Virol, 1990. **64**(12): p. 5939-47.
49. Gearhart, T.L. and M.J. Bouchard, *The hepatitis B virus HBx protein modulates cell cycle regulatory proteins in cultured primary human hepatocytes*. Virus Res, 2011. **155**(1): p. 363-7.
50. Tang, H., et al., *The transcriptional transactivation function of HBx protein is important for its augmentation role in hepatitis B virus replication*. J Virol, 2005. **79**(9): p. 5548-56.
51. Heermann, K.H., et al., *Large surface proteins of hepatitis B virus containing the pre-s sequence*. J Virol, 1984. **52**(2): p. 396-402.
52. Moolla, N., M. Kew, and P. Arbuthnot, *Regulatory elements of hepatitis B virus transcription*. J Viral Hepat, 2002. **9**(5): p. 323-31.

53. Klingmuller, U. and H. Schaller, *Hepadnavirus infection requires interaction between the viral pre-S domain and a specific hepatocellular receptor*. J Virol, 1993. **67**(12): p. 7414-22.
54. Le Seyec, J., et al., *Infection process of the hepatitis B virus depends on the presence of a defined sequence in the pre-S1 domain*. J Virol, 1999. **73**(3): p. 2052-7.
55. Neurath, A.R., et al., *Identification and chemical synthesis of a host cell receptor binding site on hepatitis B virus*. Cell, 1986. **46**(3): p. 429-36.
56. Urban, S., et al., *Avian hepatitis B virus infection is initiated by the interaction of a distinct pre-S subdomain with the cellular receptor gp180*. J Virol, 1998. **72**(10): p. 8089-97.
57. Schulze, A., P. Gripon, and S. Urban, *Hepatitis B virus infection initiates with a large surface protein-dependent binding to heparan sulfate proteoglycans*. Hepatology, 2007. **46**(6): p. 1759-68.
58. Yan, H., et al., *Sodium taurocholate cotransporting polypeptide is a functional receptor for human hepatitis B and D virus*. Elife, 2012. **1**: p. e00049.
59. Zhong, G., et al., *Sodium taurocholate cotransporting polypeptide mediates woolly monkey hepatitis B virus infection of Tupaia hepatocytes*. J Virol, 2013. **87**(12): p. 7176-84.
60. Huang, H.C., et al., *Entry of hepatitis B virus into immortalized human primary hepatocytes by clathrin-dependent endocytosis*. J Virol, 2012. **86**(17): p. 9443-53.

61. Cooper, A. and Y. Shaul, *Clathrin-mediated endocytosis and lysosomal cleavage of hepatitis B virus capsid-like core particles*. J Biol Chem, 2006. **281**(24): p. 16563-9.
62. Schmitz, A., et al., *Nucleoporin 153 arrests the nuclear import of hepatitis B virus capsids in the nuclear basket*. PLoS Pathog, 2010. **6**(1): p. e1000741.
63. Bartenschlager, R., M. Junker-Niepmann, and H. Schaller, *The P gene product of hepatitis B virus is required as a structural component for genomic RNA encapsidation*. J Virol, 1990. **64**(11): p. 5324-32.
64. Bartenschlager, R. and H. Schaller, *Hepadnaviral assembly is initiated by polymerase binding to the encapsidation signal in the viral RNA genome*. EMBO J, 1992. **11**(9): p. 3413-20.
65. Will, H., et al., *Replication strategy of human hepatitis B virus*. J Virol, 1987. **61**(3): p. 904-11.
66. Wang, G.H. and C. Seeger, *The reverse transcriptase of hepatitis B virus acts as a protein primer for viral DNA synthesis*. Cell, 1992. **71**(4): p. 663-70.
67. Zoulim, F., *New insight on hepatitis B virus persistence from the study of intrahepatic viral cccDNA*. J Hepatol, 2005. **42**(3): p. 302-8.
68. Margolis, H.S., *Hepatitis B virus infection*. Bull World Health Organ, 1998. **76 Suppl 2**: p. 152-3.
69. Beasley, R.P., et al., *Prevention of perinatally transmitted hepatitis B virus infections with hepatitis B immune globulin and hepatitis B vaccine*. Lancet, 1983. **2**(8359): p. 1099-102.

70. Doong, S.L., et al., *Inhibition of the replication of hepatitis B virus in vitro by 2',3'-dideoxy-3'-thiacytidine and related analogues*. Proc Natl Acad Sci U S A, 1991. **88**(19): p. 8495-9.
71. *EASL Clinical Practice Guidelines: management of chronic hepatitis B*. J Hepatol, 2009. **50**(2): p. 227-42.
72. Zoulim, F. and S. Locarnini, *Management of treatment failure in chronic hepatitis B*. J Hepatol, 2012. **56 Suppl 1**: p. S112-22.
73. Heathcote, E.J., et al., *Three-year efficacy and safety of tenofovir disoproxil fumarate treatment for chronic hepatitis B*. Gastroenterology, 2011. **140**(1): p. 132-43.
74. Gish, R.G., et al., *Loss of HBsAg antigen during treatment with entecavir or lamivudine in nucleoside-naïve HBeAg-positive patients with chronic hepatitis B*. J Viral Hepat, 2010. **17**(1): p. 16-22.
75. Liaw, Y.F., et al., *Effects of extended lamivudine therapy in Asian patients with chronic hepatitis B*. Asia Hepatitis Lamivudine Study Group. Gastroenterology, 2000. **119**(1): p. 172-80.
76. Chen, J.D., et al., *Carriers of inactive hepatitis B virus are still at risk for hepatocellular carcinoma and liver-related death*. Gastroenterology, 2010. **138**(5): p. 1747-54.
77. Dienstag, J.L., et al., *Histological outcome during long-term lamivudine therapy*. Gastroenterology, 2003. **124**(1): p. 105-17.
78. Lai, C.L., et al., *A one-year trial of lamivudine for chronic hepatitis B*. Asia Hepatitis Lamivudine Study Group. N Engl J Med, 1998. **339**(2): p. 61-8.

79. Yuen, M.F., et al., *Effect of lamivudine therapy on the serum covalently closed-circular (ccc) DNA of chronic hepatitis B infection*. *Am J Gastroenterol*, 2005. **100**(5): p. 1099-103.
80. Liaw, Y.F., R.N. Chien, and C.T. Yeh, *No benefit to continue lamivudine therapy after emergence of YMDD mutations*. *Antivir Ther*, 2004. **9**(2): p. 257-62.
81. Marcellin, P., et al., *Long-term efficacy and safety of adefovir dipivoxil for the treatment of hepatitis B e antigen-positive chronic hepatitis B*. *Hepatology*, 2008. **48**(3): p. 750-8.
82. Lee, J.M., et al., *Rescue monotherapy in lamivudine-resistant hepatitis B e antigen-positive chronic hepatitis B: adefovir versus entecavir*. *Antivir Ther*, 2009. **14**(5): p. 705-12.
83. Ono-Nita, S.K., et al., *Susceptibility of lamivudine-resistant hepatitis B virus to other reverse transcriptase inhibitors*. *J Clin Invest*, 1999. **103**(12): p. 1635-40.
84. Hadziyannis, S.J., et al., *Long-term therapy with adefovir dipivoxil for HBeAg-negative chronic hepatitis B*. *N Engl J Med*, 2005. **352**(26): p. 2673-81.
85. Chang, T.T., et al., *A comparison of entecavir and lamivudine for HBeAg-positive chronic hepatitis B*. *N Engl J Med*, 2006. **354**(10): p. 1001-10.
86. Lai, C.L., et al., *Entecavir versus lamivudine for patients with HBeAg-negative chronic hepatitis B*. *N Engl J Med*, 2006. **354**(10): p. 1011-20.
87. Chang, T.T., et al., *Entecavir treatment for up to 5 years in patients with hepatitis B e antigen-positive chronic hepatitis B*. *Hepatology*, 2010. **51**(2): p. 422-30.

88. Hosaka, T., et al., *Long-term entecavir treatment reduces hepatocellular carcinoma incidence in patients with hepatitis B virus infection*. Hepatology, 2013. **58**(1): p. 98-107.
89. Tenney, D.J., et al., *Long-term monitoring shows hepatitis B virus resistance to entecavir in nucleoside-naïve patients is rare through 5 years of therapy*. Hepatology, 2009. **49**(5): p. 1503-14.
90. Delaney, W.E.t., et al., *Intracellular metabolism and in vitro activity of tenofovir against hepatitis B virus*. Antimicrob Agents Chemother, 2006. **50**(7): p. 2471-7.
91. Osborn, M.K., *Safety and efficacy of telbivudine for the treatment of chronic hepatitis B*. Ther Clin Risk Manag, 2009. **5**: p. 789-98.
92. Low, E., et al., *Telbivudine has activity against HIV-1*. AIDS, 2009. **23**(4): p. 546-7.
93. Soriano, V., et al., *Care of patients with chronic hepatitis B and HIV co-infection: recommendations from an HIV-HBV International Panel*. AIDS, 2005. **19**(3): p. 221-40.
94. Hou, J., et al., *Telbivudine versus lamivudine in Chinese patients with chronic hepatitis B: Results at 1 year of a randomized, double-blind trial*. Hepatology, 2008. **47**(2): p. 447-54.
95. Lai, C.L., et al., *Telbivudine versus lamivudine in patients with chronic hepatitis B*. N Engl J Med, 2007. **357**(25): p. 2576-88.
96. Chan, H.L., et al., *Treatment of hepatitis B e antigen positive chronic hepatitis with telbivudine or adefovir: a randomized trial*. Ann Intern Med, 2007. **147**(11): p. 745-54.

97. Gane, E.J., et al., *Efficacy and safety of prolonged 3-year telbivudine treatment in patients with chronic hepatitis B*. *Liver Int*, 2011. **31**(5): p. 676-84.
98. Zhang, X.S., et al., *Clinical features of adverse reactions associated with telbivudine*. *World J Gastroenterol*, 2008. **14**(22): p. 3549-53.
99. Wiens, A., et al., *Comparative efficacy of oral nucleoside or nucleotide analog monotherapy used in chronic hepatitis B: a mixed-treatment comparison meta-analysis*. *Pharmacotherapy*, 2013. **33**(2): p. 144-51.
100. Cooksley, W.G., et al., *Peginterferon alpha-2a (40 kDa): an advance in the treatment of hepatitis B e antigen-positive chronic hepatitis B*. *J Viral Hepat*, 2003. **10**(4): p. 298-305.
101. Marcellin, P., et al., *Peginterferon alfa-2a alone, lamivudine alone, and the two in combination in patients with HBeAg-negative chronic hepatitis B*. *N Engl J Med*, 2004. **351**(12): p. 1206-17.
102. Perrillo, R.P., et al., *A randomized, controlled trial of interferon alfa-2b alone and after prednisone withdrawal for the treatment of chronic hepatitis B*. *The Hepatitis Interventional Therapy Group*. *N Engl J Med*, 1990. **323**(5): p. 295-301.
103. Wong, D.K., et al., *Effect of alpha-interferon treatment in patients with hepatitis B e antigen-positive chronic hepatitis B. A meta-analysis*. *Ann Intern Med*, 1993. **119**(4): p. 312-23.
104. Erhardt, A., et al., *Mutations of the core promoter and response to interferon treatment in chronic replicative hepatitis B*. *Hepatology*, 2000. **31**(3): p. 716-25.

105. Janssen, H.L., et al., *Pegylated interferon alfa-2b alone or in combination with lamivudine for HBeAg-positive chronic hepatitis B: a randomised trial*. *Lancet*, 2005. **365**(9454): p. 123-9.
106. Zhang, X., et al., *Analysis of hepatitis B virus genotypes and pre-core region variability during interferon treatment of HBe antigen negative chronic hepatitis B*. *J Med Virol*, 1996. **48**(1): p. 8-16.
107. Krastev, Z.A., *The "return" of hepatitis B*. *World J Gastroenterol*, 2006. **12**(44): p. 7081-6.
108. Gota, C. and L. Calabrese, *Induction of clinical autoimmune disease by therapeutic interferon-alpha*. *Autoimmunity*, 2003. **36**(8): p. 511-8.
109. Ngo, H., et al., *Double-stranded RNA induces mRNA degradation in Trypanosoma brucei*. *Proc Natl Acad Sci U S A*, 1998. **95**(25): p. 14687-92.
110. Lohmann, J.U., I. Endl, and T.C. Bosch, *Silencing of developmental genes in Hydra*. *Dev Biol*, 1999. **214**(1): p. 211-4.
111. Kennerdell, J.R. and R.W. Carthew, *Use of dsRNA-mediated genetic interference to demonstrate that frizzled and frizzled 2 act in the wingless pathway*. *Cell*, 1998. **95**(7): p. 1017-26.
112. Wargelius, A., S. Ellingsen, and A. Fjose, *Double-stranded RNA induces specific developmental defects in zebrafish embryos*. *Biochem Biophys Res Commun*, 1999. **263**(1): p. 156-61.
113. Oelgeschlager, M., et al., *The evolutionarily conserved BMP-binding protein Twisted gastrulation promotes BMP signalling*. *Nature*, 2000. **405**(6788): p. 757-63.

114. Lee, Y., et al., *MicroRNA maturation: stepwise processing and subcellular localization*. EMBO J, 2002. **21**(17): p. 4663-70.
115. Zangi, L., et al., *Modified mRNA directs the fate of heart progenitor cells and induces vascular regeneration after myocardial infarction*. Nat Biotechnol, 2013. **31**(10): p. 898-907.
116. McCaffrey, A.P., et al., *Inhibition of hepatitis B virus in mice by RNA interference*. Nat Biotechnol, 2003. **21**(6): p. 639-44.
117. Choi, J.G., et al., *Multiplexing seven miRNA-Based shRNAs to suppress HIV replication*. Mol Ther, 2015. **23**(2): p. 310-20.
118. Ivacik, D., et al., *Sustained inhibition of hepatitis B virus replication in vivo using RNAi-activating lentiviruses*. Gene Ther, 2015. **22**(2): p. 163-71.
119. Novina, C.D., et al., *siRNA-directed inhibition of HIV-1 infection*. Nat Med, 2002. **8**(7): p. 681-6.
120. Zhang, X.N., et al., *siRNA-mediated inhibition of HBV replication and expression*. World J Gastroenterol, 2004. **10**(20): p. 2967-71.
121. Ely, A., et al., *Expressed anti-HBV primary microRNA shuttles inhibit viral replication efficiently in vitro and in vivo*. Mol Ther, 2008. **16**(6): p. 1105-12.
122. Mowa, M.B., et al., *Inhibition of hepatitis B virus replication by helper dependent adenoviral vectors expressing artificial anti-HBV pri-miRs from a liver-specific promoter*. Biomed Res Int, 2014. **2014**: p. 718743.
123. Sun, C.P., et al., *Studies of efficacy and liver toxicity related to adeno-associated virus-mediated RNA interference*. Hum Gene Ther, 2013. **24**(8): p. 739-50.

124. Hean, J., et al., *Inhibition of hepatitis B virus replication in vivo using lipoplexes containing altritol-modified antiviral siRNAs*. *Artif DNA PNA XNA*, 2010. **1**(1): p. 17-26.
125. Ebert, G., et al., *5' Triphosphorylated small interfering RNAs control replication of hepatitis B virus and induce an interferon response in human liver cells and mice*. *Gastroenterology*, 2011. **141**(2): p. 696-706, 706 e1-3.
126. Li, G., et al., *siRNA combinations mediate greater suppression of hepatitis B virus replication in mice*. *Cell Biochem Biophys*, 2014. **69**(3): p. 641-7.
127. Li, G., et al., *Inhibition of hepatitis B virus cccDNA by siRNA in transgenic mice*. *Cell Biochem Biophys*, 2014. **69**(3): p. 649-54.
128. Arbuthnot, P., *Harnessing RNA interference for the treatment of viral infections*. *Drug News Perspect*, 2010. **23**(6): p. 341-50.
129. Carmona, S., et al., *Effective inhibition of HBV replication in vivo by anti-HBx short hairpin RNAs*. *Mol Ther*, 2006. **13**(2): p. 411-21.
130. Chen, Y. and R.I. Mahato, *siRNA pool targeting different sites of human hepatitis B surface antigen efficiently inhibits HBV infection*. *J Drug Target*, 2008. **16**(2): p. 140-8.
131. Snyder, L.L., I. Ahmed, and L.F. Steel, *RNA polymerase III can drive polycistronic expression of functional interfering RNAs designed to resemble microRNAs*. *Nucleic Acids Res*, 2009. **37**(19): p. e127.
132. Giering, J.C., et al., *Expression of shRNA from a tissue-specific pol II promoter is an effective and safe RNAi therapeutic*. *Mol Ther*, 2008. **16**(9): p. 1630-6.

133. Grimm, D., et al., *Fatality in mice due to oversaturation of cellular microRNA/short hairpin RNA pathways*. Nature, 2006. **441**(7092): p. 537-41.
134. van de Wetering, M., et al., *Specific inhibition of gene expression using a stably integrated, inducible small-interfering-RNA vector*. EMBO Rep, 2003. **4**(6): p. 609-15.
135. Tiscornia, G., et al., *CRE recombinase-inducible RNA interference mediated by lentiviral vectors*. Proc Natl Acad Sci U S A, 2004. **101**(19): p. 7347-51.
136. Wiznerowicz, M., J. Szulc, and D. Trono, *Tuning silence: conditional systems for RNA interference*. Nat Methods, 2006. **3**(9): p. 682-8.
137. Czauderna, F., et al., *Inducible shRNA expression for application in a prostate cancer mouse model*. Nucleic Acids Res, 2003. **31**(21): p. e127.
138. Gupta, S., et al., *Inducible, reversible, and stable RNA interference in mammalian cells*. Proc Natl Acad Sci U S A, 2004. **101**(7): p. 1927-32.
139. Wu, R.H., et al., *A tightly regulated and reversibly inducible siRNA expression system for conditional RNAi-mediated gene silencing in mammalian cells*. J Gene Med, 2007. **9**(7): p. 620-34.
140. Ren, G.L., et al., *The short hairpin RNA driven by polymerase II suppresses both wild-type and lamivudine-resistant hepatitis B virus strains*. Antivir Ther, 2007. **12**(6): p. 865-76.
141. Snyder, L.L., et al., *Vector design for liver-specific expression of multiple interfering RNAs that target hepatitis B virus transcripts*. Antiviral Res, 2008. **80**(1): p. 36-44.

142. Ely, A., T. Naidoo, and P. Arbuthnot, *Efficient silencing of gene expression with modular trimeric Pol II expression cassettes comprising microRNA shuttles*. Nucleic Acids Res, 2009. **37**(13): p. e91.
143. Brunetti-Pierri, N., et al., *Efficient, long-term hepatic gene transfer using clinically relevant HDAd doses by balloon occlusion catheter delivery in nonhuman primates*. Mol Ther, 2009. **17**(2): p. 327-33.
144. Klein, C., et al., *Inhibition of hepatitis B virus replication in vivo by nucleoside analogues and siRNA*. Gastroenterology, 2003. **125**(1): p. 9-18.
145. Konishi, M., C.H. Wu, and G.Y. Wu, *Inhibition of HBV replication by siRNA in a stable HBV-producing cell line*. Hepatology, 2003. **38**(4): p. 842-50.
146. Qian, Z.K., et al., *Cost-effective method of siRNA preparation and its application to inhibit hepatitis B virus replication in HepG2 cells*. World J Gastroenterol, 2005. **11**(9): p. 1297-302.
147. Hamasaki, K., et al., *Short interfering RNA-directed inhibition of hepatitis B virus replication*. FEBS Lett, 2003. **543**(1-3): p. 51-4.
148. Elbashir, S.M., et al., *Duplexes of 21-nucleotide RNAs mediate RNA interference in cultured mammalian cells*. Nature, 2001. **411**(6836): p. 494-8.
149. Chiu, Y.L. and T.M. Rana, *siRNA function in RNAi: a chemical modification analysis*. RNA, 2003. **9**(9): p. 1034-48.
150. Choung, S., et al., *Chemical modification of siRNAs to improve serum stability without loss of efficacy*. Biochem Biophys Res Commun, 2006. **342**(3): p. 919-27.
151. Jackson, A.L., et al., *Expression profiling reveals off-target gene regulation by RNAi*. Nat Biotechnol, 2003. **21**(6): p. 635-7.

152. Robbins, M., et al., *Misinterpreting the therapeutic effects of small interfering RNA caused by immune stimulation*. Hum Gene Ther, 2008. **19**(10): p. 991-9.
153. Han, Q., et al., *Involvement of activation of PKR in HBx-siRNA-mediated innate immune effects on HBV inhibition*. PLoS One, 2011. **6**(12): p. e27931.
154. Hoerter, J.A. and N.G. Walter, *Chemical modification resolves the asymmetry of siRNA strand degradation in human blood serum*. RNA, 2007. **13**(11): p. 1887-93.
155. Jackson, A.L., et al., *Widespread siRNA "off-target" transcript silencing mediated by seed region sequence complementarity*. RNA, 2006. **12**(7): p. 1179-87.
156. Jackson, A.L., et al., *Position-specific chemical modification of siRNAs reduces "off-target" transcript silencing*. RNA, 2006. **12**(7): p. 1197-205.
157. Robbins, M., et al., *2'-O-methyl-modified RNAs act as TLR7 antagonists*. Mol Ther, 2007. **15**(9): p. 1663-9.
158. Morrissey, D.V., et al., *Activity of stabilized short interfering RNA in a mouse model of hepatitis B virus replication*. Hepatology, 2005. **41**(6): p. 1349-56.
159. Morrissey, D.V., et al., *Potent and persistent in vivo anti-HBV activity of chemically modified siRNAs*. Nat Biotechnol, 2005. **23**(8): p. 1002-7.
160. Monia, B.P., et al., *Evaluation of 2'-modified oligonucleotides containing 2'-deoxy gaps as antisense inhibitors of gene expression*. J Biol Chem, 1993. **268**(19): p. 14514-22.
161. Lubini, P., W. Zurcher, and M. Egli, *Stabilizing effects of the RNA 2'-substituent: crystal structure of an oligodeoxynucleotide duplex containing 2'-O-methylated adenosines*. Chem Biol, 1994. **1**(1): p. 39-45.

162. Adamiak, D.A., et al., *The 1.19 Å X-ray structure of 2'-O-Me(CGCGCG)(2) duplex shows dehydrated RNA with 2-methyl-2,4-pentanediol in the minor groove.* Nucleic Acids Res, 2001. **29**(20): p. 4144-53.
163. Inoue, H., et al., *Synthesis and hybridization studies on two complementary nona(2'-O-methyl)ribonucleotides.* Nucleic Acids Res, 1987. **15**(15): p. 6131-48.
164. Bramsen, J.B., et al., *A screen of chemical modifications identifies position-specific modification by UNA to most potently reduce siRNA off-target effects.* Nucleic Acids Res, 2010. **38**(17): p. 5761-73.
165. Kenski, D.M., et al., *siRNA-optimized Modifications for Enhanced In Vivo Activity.* Mol Ther Nucleic Acids, 2012. **1**: p. e5.
166. Bramsen, J.B., et al., *A large-scale chemical modification screen identifies design rules to generate siRNAs with high activity, high stability and low toxicity.* Nucleic Acids Res, 2009. **37**(9): p. 2867-81.
167. Khvorova, A., A. Reynolds, and S.D. Jayasena, *Functional siRNAs and miRNAs exhibit strand bias.* Cell, 2003. **115**(2): p. 209-16.
168. Schwarz, D.S., et al., *Asymmetry in the assembly of the RNAi enzyme complex.* Cell, 2003. **115**(2): p. 199-208.
169. Ge, Q., et al., *Effects of chemical modification on the potency, serum stability, and immunostimulatory properties of short shRNAs.* RNA, 2010. **16**(1): p. 118-30.
170. Judge, A.D., et al., *Design of noninflammatory synthetic siRNA mediating potent gene silencing in vivo.* Mol Ther, 2006. **13**(3): p. 494-505.
171. Fisher, M., et al., *Inhibition of MDR1 expression with altritol-modified siRNAs.* Nucleic Acids Res, 2007. **35**(4): p. 1064-74.

172. Fisher, M., et al., *Biological effects of hexitol and altritol-modified siRNAs targeting B-Raf*. Eur J Pharmacol, 2009. **606**(1-3): p. 38-44.
173. Hall, A.H., et al., *RNA interference using boranophosphate siRNAs: structure-activity relationships*. Nucleic Acids Res, 2004. **32**(20): p. 5991-6000.
174. Bouard, D., D. Alazard-Dany, and F.L. Cosset, *Viral vectors: from virology to transgene expression*. Br J Pharmacol, 2009. **157**(2): p. 153-65.
175. Aiuti, A., et al., *Progress and prospects: gene therapy clinical trials (part 2)*. Gene Ther, 2007. **14**(22): p. 1555-63.
176. Alexander, B.L., et al., *Progress and prospects: gene therapy clinical trials (part 1)*. Gene Ther, 2007. **14**(20): p. 1439-47.
177. Zhang, Y., et al., *Acute cytokine response to systemic adenoviral vectors in mice is mediated by dendritic cells and macrophages*. Mol Ther, 2001. **3**(5 Pt 1): p. 697-707.
178. Cotter, M.J., A.K. Zaiss, and D.A. Muruve, *Neutrophils interact with adenovirus vectors via Fc receptors and complement receptor 1*. J Virol, 2005. **79**(23): p. 14622-31.
179. Raper, S.E., et al., *Fatal systemic inflammatory response syndrome in a ornithine transcarbamylase deficient patient following adenoviral gene transfer*. Mol Genet Metab, 2003. **80**(1-2): p. 148-58.
180. Hurlbut, G.D., et al., *Preexisting immunity and low expression in primates highlight translational challenges for liver-directed AAV8-mediated gene therapy*. Mol Ther, 2010. **18**(11): p. 1983-94.

181. Yang, Y., H.C. Ertl, and J.M. Wilson, *MHC class I-restricted cytotoxic T lymphocytes to viral antigens destroy hepatocytes in mice infected with E1-deleted recombinant adenoviruses*. *Immunity*, 1994. **1**(5): p. 433-42.
182. Nault, J.C., et al., *Recurrent AAV2-related insertional mutagenesis in human hepatocellular carcinomas*. *Nat Genet*, 2015. **47**(10): p. 1187-93.
183. Kim, S.I., et al., *Systemic and specific delivery of small interfering RNAs to the liver mediated by apolipoprotein A-I*. *Mol Ther*, 2007. **15**(6): p. 1145-52.
184. Leng, Q., et al., *Buffering capacity and size of siRNA polyplexes influence cytokine levels*. *Mol Ther*, 2012. **20**(12): p. 2282-90.
185. Rozema, D.B., et al., *Dynamic PolyConjugates for targeted in vivo delivery of siRNA to hepatocytes*. *Proc Natl Acad Sci U S A*, 2007. **104**(32): p. 12982-7.
186. Wooddell, C.I., et al., *Hepatocyte-targeted RNAi therapeutics for the treatment of chronic hepatitis B virus infection*. *Mol Ther*, 2013. **21**(5): p. 973-85.
187. Nascimento, T.L., et al., *Supramolecular Organization and siRNA Binding of Hyaluronic Acid-Coated Lipoplexes for Targeted Delivery to the CD44 Receptor*. *Langmuir*, 2015. **31**(41): p. 11186-94.
188. Kim, H.K., et al., *Enhanced siRNA delivery using cationic liposomes with new polyarginine-conjugated PEG-lipid*. *Int J Pharm*, 2010. **392**(1-2): p. 141-7.
189. Xia, Y., J. Sun, and D. Liang, *Aggregation, fusion, and leakage of liposomes induced by peptides*. *Langmuir*, 2014. **30**(25): p. 7334-42.
190. Papahadjopoulos, D., et al., *Sterically stabilized liposomes: improvements in pharmacokinetics and antitumor therapeutic efficacy*. *Proc Natl Acad Sci U S A*, 1991. **88**(24): p. 11460-4.

191. Torchilin, V.P., et al., *Poly(ethylene glycol) on the liposome surface: on the mechanism of polymer-coated liposome longevity*. Biochim Biophys Acta, 1994. **1195**(1): p. 11-20.
192. Ewe, A., et al., *Storage stability of optimal liposome-polyethylenimine complexes (lipopolyplexes) for DNA or siRNA delivery*. Acta Biomater, 2014. **10**(6): p. 2663-73.
193. Xu, Y. and F.C. Szoka, Jr., *Mechanism of DNA release from cationic liposome/DNA complexes used in cell transfection*. Biochemistry, 1996. **35**(18): p. 5616-23.
194. Pelisek, J., et al., *Optimized lipopolyplex formulations for gene transfer to human colon carcinoma cells under in vitro conditions*. J Gene Med, 2006. **8**(2): p. 186-97.
195. Semple, S.C., et al., *Rational design of cationic lipids for siRNA delivery*. Nat Biotechnol, 2010. **28**(2): p. 172-6.
196. Farhood, H., N. Serbina, and L. Huang, *The role of dioleoyl phosphatidylethanolamine in cationic liposome mediated gene transfer*. Biochim Biophys Acta, 1995. **1235**(2): p. 289-95.
197. Maitani, Y., et al., *Cationic liposome (DC-Chol/DOPE=1:2) and a modified ethanol injection method to prepare liposomes, increased gene expression*. Int J Pharm, 2007. **342**(1-2): p. 33-9.
198. Vangala, A., et al., *Comparison of vesicle based antigen delivery systems for delivery of hepatitis B surface antigen*. J Control Release, 2007. **119**(1): p. 102-10.
199. Gregoriadis, G., R. Saffie, and J.B. de Souza, *Liposome-mediated DNA vaccination*. FEBS Lett, 1997. **402**(2-3): p. 107-10.

200. Kang, S.S., H.A. Cho, and J.S. Kim, *Biodistribution and improved anticancer effect of NIK-siRNA in combination with 5-FU for hepatocellular carcinoma*. Arch Pharm Res, 2011. **34**(1): p. 79-86.
201. Kim, D., et al., *Production of antibodies with peptide-CpG-DNA-liposome complex without carriers*. BMC Immunol, 2011. **12**: p. 29.
202. Rozema, D.B., et al., *Endosomolysis by masking of a membrane-active agent (EMMA) for cytoplasmic release of macromolecules*. Bioconjug Chem, 2003. **14**(1): p. 51-7.
203. Akinc, A., et al., *Targeted delivery of RNAi therapeutics with endogenous and exogenous ligand-based mechanisms*. Mol Ther, 2010. **18**(7): p. 1357-64.
204. Tagalakis, A.D., et al., *Receptor-targeted liposome-peptide nanocomplexes for siRNA delivery*. Biomaterials, 2011. **32**(26): p. 6302-15.
205. Yang, T., et al., *Co-delivery of doxorubicin and Bmi1 siRNA by folate receptor targeted liposomes exhibits enhanced anti-tumor effects in vitro and in vivo*. Theranostics, 2014. **4**(11): p. 1096-111.
206. Nishikawa, M., et al., *Galactosylated proteins are recognized by the liver according to the surface density of galactose moieties*. Am J Physiol, 1995. **268**(5 Pt 1): p. G849-56.
207. Ishihara, H., et al., *Preparation of asialofetuin-labeled liposomes with encapsulated human interferon-gamma and their uptake by isolated rat hepatocytes*. Pharm Res, 1990. **7**(5): p. 542-6.

208. Rejman, J., A. Bragonzi, and M. Conese, *Role of clathrin- and caveolae-mediated endocytosis in gene transfer mediated by lipo- and polyplexes*. *Mol Ther*, 2005. **12**(3): p. 468-74.
209. Simoes, S., et al., *Gene delivery by negatively charged ternary complexes of DNA, cationic liposomes and transferrin or fusogenic peptides*. *Gene Ther*, 1998. **5**(7): p. 955-64.
210. Simoes, S., et al., *Mechanisms of gene transfer mediated by lipoplexes associated with targeting ligands or pH-sensitive peptides*. *Gene Ther*, 1999. **6**(11): p. 1798-807.
211. Yamauchi, J., et al., *Comparison between a multifunctional envelope-type nano device and lipoplex for delivery to the liver*. *Biol Pharm Bull*, 2010. **33**(5): p. 926-9.
212. Hatakeyama, H., et al., *A pH-sensitive fusogenic peptide facilitates endosomal escape and greatly enhances the gene silencing of siRNA-containing nanoparticles in vitro and in vivo*. *J Control Release*, 2009. **139**(2): p. 127-32.
213. Midoux, P., et al., *Polymer-based gene delivery: a current review on the uptake and intracellular trafficking of polyplexes*. *Curr Gene Ther*, 2008. **8**(5): p. 335-52.
214. Boussif, O., et al., *A versatile vector for gene and oligonucleotide transfer into cells in culture and in vivo: polyethylenimine*. *Proc Natl Acad Sci U S A*, 1995. **92**(16): p. 7297-301.
215. Thomas, M. and A.M. Klibanov, *Enhancing polyethylenimine's delivery of plasmid DNA into mammalian cells*. *Proc Natl Acad Sci U S A*, 2002. **99**(23): p. 14640-5.

216. Sonawane, N.D., F.C. Szoka, Jr., and A.S. Verkman, *Chloride accumulation and swelling in endosomes enhances DNA transfer by polyamine-DNA polyplexes*. J Biol Chem, 2003. **278**(45): p. 44826-31.
217. Brzezinska, J., et al., *Synthesis of 2'-O-guanidinopropyl-modified nucleoside phosphoramidites and their incorporation into siRNAs targeting hepatitis B virus*. Bioorg Med Chem, 2012. **20**(4): p. 1594-606.
218. Smicius, R. and J.W. Engels, *Preparation of zwitterionic ribonucleoside phosphoramidites for solid-phase siRNA synthesis*. J Org Chem, 2008. **73**(13): p. 4994-5002.
219. Guidotti, L.G., et al., *High-level hepatitis B virus replication in transgenic mice*. J Virol, 1995. **69**(10): p. 6158-69.
220. Marimani, M.D., et al., *Inhibition of replication of hepatitis B virus in transgenic mice following administration of hepatotropic lipoplexes containing guanidinopropyl-modified siRNAs*. J Control Release, 2015. **209**: p. 198-206.
221. Marimani, M.D., et al., *Inhibition of hepatitis B virus replication in cultured cells and in vivo using 2'-O-guanidinopropyl modified siRNAs*. Bioorg Med Chem, 2013. **21**(20): p. 6145-55.
222. Cummins, L.L., et al., *Characterization of fully 2'-modified oligoribonucleotide hetero- and homoduplex hybridization and nuclease sensitivity*. Nucleic Acids Res, 1995. **23**(11): p. 2019-24.
223. Buff, M.C., et al., *Use of guanidinopropyl-modified siRNAs to silence gene expression*. Methods Mol Biol, 2015. **1218**: p. 217-49.

224. Aleman, L.M., J. Doench, and P.A. Sharp, *Comparison of siRNA-induced off-target RNA and protein effects*. RNA, 2007. **13**(3): p. 385-95.
225. Denise, H., et al., *Deep Sequencing Insights in Therapeutic shRNA Processing and siRNA Target Cleavage Precision*. Mol Ther Nucleic Acids, 2014. **3**: p. e145.
226. Meuleman, P., et al., *Morphological and biochemical characterization of a human liver in a uPA-SCID mouse chimera*. Hepatology, 2005. **41**(4): p. 847-56.
227. Cradick, T.J., et al., *Zinc-finger nucleases as a novel therapeutic strategy for targeting hepatitis B virus DNAs*. Mol Ther, 2010. **18**(5): p. 947-54.
228. Bloom, K., et al., *Inactivation of hepatitis B virus replication in cultured cells and in vivo with engineered transcription activator-like effector nucleases*. Mol Ther, 2013. **21**(10): p. 1889-97.
229. Chen, J., et al., *An efficient antiviral strategy for targeting hepatitis B virus genome using transcription activator-like effector nucleases*. Mol Ther, 2014. **22**(2): p. 303-11.
230. Lin, S.R., et al., *The CRISPR/Cas9 System Facilitates Clearance of the Intrahepatic HBV Templates In Vivo*. Mol Ther Nucleic Acids, 2014. **3**: p. e186.
231. Dong, C., et al., *Targeting hepatitis B virus cccDNA by CRISPR/Cas9 nuclease efficiently inhibits viral replication*. Antiviral Res, 2015. **118**: p. 110-7.
232. Zhen, S., et al., *Harnessing the clustered regularly interspaced short palindromic repeat (CRISPR)/CRISPR-associated Cas9 system to disrupt the hepatitis B virus*. Gene Ther, 2015. **22**(5): p. 404-12.

233. Takata, M., et al., *Homologous recombination and non-homologous end-joining pathways of DNA double-strand break repair have overlapping roles in the maintenance of chromosomal integrity in vertebrate cells*. EMBO J, 1998. **17**(18): p. 5497-508.
234. Christian, M., et al., *Targeting DNA double-strand breaks with TAL effector nucleases*. Genetics, 2010. **186**(2): p. 757-61.
235. Hockemeyer, D., et al., *Genetic engineering of human pluripotent cells using TALE nucleases*. Nat Biotechnol, 2011. **29**(8): p. 731-4.
236. Li, T., et al., *TAL nucleases (TALNs): hybrid proteins composed of TAL effectors and FokI DNA-cleavage domain*. Nucleic Acids Res, 2011. **39**(1): p. 359-72.
237. Schiffer, J.T., et al., *Predictors of hepatitis B cure using gene therapy to deliver DNA cleavage enzymes: a mathematical modeling approach*. PLoS Comput Biol, 2013. **9**(7): p. e1003131.

Internet source:

World Health Organization

<http://www.who.int/mediacentre/factsheets/fs204/en/> (last accessed on 12 May 2016).